U.S. Department
of Commerce

Volume 115
Number 1
January 2017

Fishery Bulletin

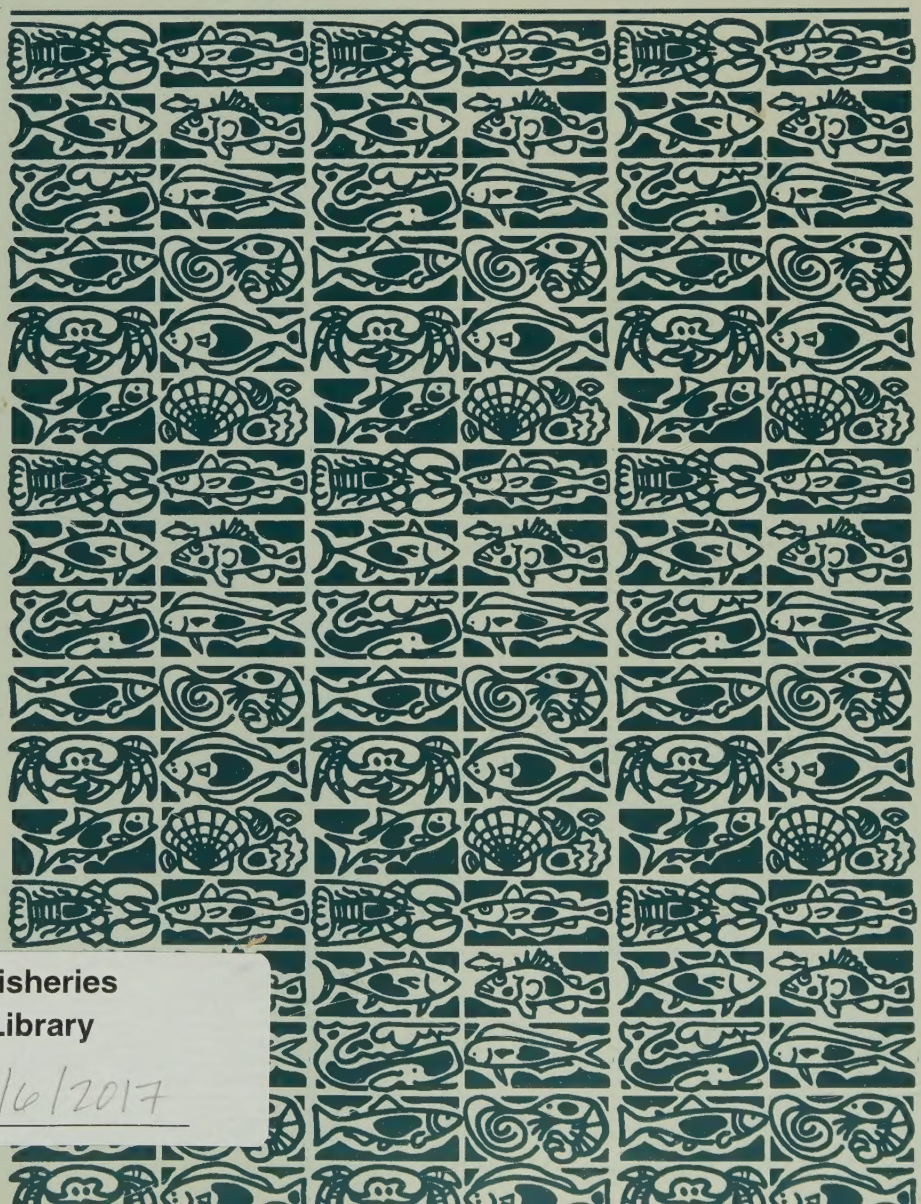

Pacific Islands Fisheries
Science Center Library

Received on: 11/6/2017

U.S. Department of Commerce
Penny S. Pritzker
Secretary

National Oceanic and Atmospheric Administration
Kathryn D. Sullivan
NOAA Administrator

National Marine Fisheries Service
Eileen Sobeck
Assistant Administrator for Fisheries

The *Fishery Bulletin* (ISSN 0090-0656) is published quarterly by the Scientific Publications Office, National Marine Fisheries Service, NOAA, 7600 Sand Point Way NE, Seattle, WA 98115-0070.

Although the contents of this publication have not been copyrighted and may be reprinted entirely, reference to source is appreciated.

The Secretary of Commerce has determined that the publication of this periodical is necessary according to law for the transaction of public business of this Department. Use of funds for printing of this periodical has been approved by the Director of the Office of Management and Budget.

For Sale by the Superintendent of Documents, U.S. Government Printing Office, Washington, DC 20402. Subscription price per year: $32.00 domestic and $44.80 foreign. Cost per single issue: $19.00 domestic and $26.60 foreign. **See back for order form.**

Fishery Bulletin

Scientific Editor
Richard Langton

National Marine Fisheries Service
Northeast Fisheries Science Center
Maine Field Station
17 Godfrey Drive, Suite 1
Orono, ME 04473

Managing Editor
Sharyn Matriotti

National Marine Fisheries Service
Scientific Publications Office
7600 Sand Point Way NE
Seattle, Washington 98115-0070

Associate Editor
Kathryn Dennis

National Marine Fisheries Service
Office of Science and Technology
1845 Wasp Blvd., Bldg. 176
Honolulu, Hawaii 96818

Editorial Committee

Richard Brodeur	National Marine Fisheries Service, Newport, Oregon
John Carlson	National Marine Fisheries Service, Panama City, Florida
Kevin Craig	National Marine Fisheries Service, Beaufort, North Carolina
John Graves	Virginia Institute of Marine Science, Gloucester Point, Virginia
Rich McBride	National Marine Fisheries Service, Woods Hole, Massachusetts
Rick Methot	National Marine Fisheries Service, Seattle, Washington
Bruce Mundy	National Marine Fisheries Service, Honolulu, Hawaii
David Sampson	Oregon State University, Newport, Oregon
Michael Simpkins	National Marine Fisheries Service, Woods Hole, Massachusetts
Dave Somerton	National Marine Fisheries Service, Seattle, Washington
Mary Yoklavich	National Marine Fisheries Service, Santa Cruz, California

***Fishery Bulletin* web site: www.fisherybulletin.noaa.gov**

The *Fishery Bulletin* carries original research reports on investigations in fishery science, engineering, and economics. It began as the Bulletin of the United States Fish Commission in 1881; it became the Bulletin of the Bureau of Fisheries in 1904 and the *Fishery Bulletin* of the Fish and Wildlife Service in 1941. Separates were issued as documents through volume 46; the last document was no. 1103. Beginning with volume 47 in 1931 and continuing through volume 62 in 1963, each separate appeared as a numbered bulletin. A new system began in 1963 with volume 63 in which papers are bound together in a single issue. Beginning with volume 70, number 1, January 1972, *Fishery Bulletin* became a periodical, issued quarterly. In this form, it is available by subscription from the Superintendent of Documents, U.S. Government Printing Office, Washington, DC 20402. It is also available free in limited numbers to libraries, research institutions, state and federal agencies, and in exchange for other scientific publications.

U.S. Department of Commerce
Seattle, Washington

Volume 115
Number 1
January 2017

Fishery Bulletin

Contents

Articles

1–12 **Steinhorst, Kirk, Timothy Copeland, Michael W. Ackerman, William C. Schrader, and Eric C. Anderson**

Abundance estimates and confidence intervals for the run composition of returning salmonids

13–26 **Lopez Quintero, Freddy Omar, Javier E. Contreras-Reyes, Rodrigo Wiff, and Reinaldo B. Arellano-Valle**

Flexible Bayesian analysis of the von Bertalanffy growth function with the use of a log-skew-*t* distribution

27–41 **Dapp, Derek R., Charlie Huveneers, Terence I. Walker, John Mandelman, David W. Kerstetter, and Richard D. Reina**

Using logbook data to determine the immediate mortality of blue sharks (*Prionace glauca*) and tiger sharks (*Galeocerdo cuvier*) caught in the commercial U.S. pelagic longline fishery

Short contribution

42–49 **Kilada, Raouf, Joel B. Webb, Kevin W. McNeel, Laura M. Slater, Quinn Smith, and Jayde Ferguson**

Preliminary assessment of a direct age-determination method for 3 commercially important crustaceans from Alaska

Articles

50–59 **Driggers III, William B., Matthew D. Campbell, Kristin M. Hannan, Eric. R. Hoffmayer, Christian M. Jones, Lisa M. Jones, and Adam G. Pollack**

Influence of bait type on catch rates of predatory fish species on bottom longline gear in the northern Gulf of Mexico

The National Marine Fisheries Service (NMFS) does not approve, recommend, or endorse any proprietary product or proprietary material mentioned in this publication. No reference shall be made to NMFS, or to this publication furnished by NMFS, in any advertising or sales promotion which would indicate or imply that NMFS approves, recommends, or endorses any proprietary product or proprietary material mentioned herein, or which has as its purpose an intent to cause directly or indirectly the advertised product to be used or purchased because of this NMFS publication.

The NMFS Scientific Publications Office is not responsible for the contents of the articles.

60–73 **Colmenero, Ana I., Víctor M. Tuset, and Pilar Sánchez**

Reproductive strategy of white anglerfish (*Lophius piscatorius*) in Mediterranean waters: implications for management

74–88 **Mace III, Marvin M., and Lawrence P. Rozas**

Population dynamics and secondary production of juvenile white shrimp (*Litopenaeus setiferus*) along an estuarine salinity gradient

89–100 **Dell'Apa, Andrea, Maria Grazia Pennino, and Christopher Bonzek**

Modeling the habitat distribution of spiny dogfish (*Squalus acanthias*), by sex, in coastal waters of the northeastern United States

101–116 **Hueter, Robert E., John P. Tyminski, John J. Morris, Alexei Ruiz Abierno, and Jorge Angulo Valdes**

Horizontal and vertical movements of longfin makos (*Isurus paucus*) tracked with satellite-linked tags in the northwestern Atlantic Ocean

Short contribution

117–124 **Ortega-Garcia, Sofia, Chugey Sepulveda, Scott Aalbers, Ulianov Jakes-Cota, and Ruben Rodriguez-Sanchez**

Age, growth, and length–weight relationship of roosterfish (*Nematistius pectoralis*) in the eastern Pacific Ocean

125–128 **Guidelines for authors**

National Marine Fisheries Service
NOAA

Fishery Bulletin
established in 1881

Spencer F. Baird
First U.S. Commissioner of Fisheries and founder of *Fishery Bulletin*

Abundance estimates and confidence intervals for the run composition of returning salmonids

Kirk Steinhorst[1]
Timothy Copeland (contact author)[2]
Michael W. Ackerman[3]
William C. Schrader[2]
Eric C. Anderson[4]

Email address for contact author: tim.copeland@idfg.idaho.gov

[1] Department of Statistical Science
University of Idaho 415A Brink Hall
875 Perimeter Drive
Moscow, Idaho 83844-1104

[2] Idaho Department of Fish and Game
1414 East Locust Lane
Nampa, Idaho 83686

[3] Eagle Fish Genetics Laboratory
Idaho Department of Fish and Game
Pacific States Marine Fisheries Commission
1800 Trout Road
Eagle, Idaho 83616

[4] Fisheries Ecology Division
National Marine Fisheries Service
Southwest Fisheries Science Center, NOAA
110 Shaffer Road
Santa Cruz, California 95060

Abstract—In 2-stage fishery sampling, abundance is often estimated by using a primary sampling gear and total abundance is then partitioned into groups of interest by applying data on composition derived from a secondary sampling gear. However, the literature is sparse on statistical properties of estimates of run composition. We examined the accuracy and precision of estimators of composition of wild steelhead (*Oncorhynchus mykiss*) in the Snake River, in the Pacific Northwest. We simulated estimators, using pooled and time-stratified data. We compared confidence intervals (CIs) determined on the basis of asymptotical normality or a 2-stage bootstrap method. Stratified estimators were unbiased, except in a few cases. Joint CIs (all groups considered simultaneously) had coverages near nominal. Conversely, pooled estimators performed poorly; the proportion of biased estimates increased as the number of groups estimated increased. Using empirical data, we show that CIs met precision goals for most groups. Half-widths of CIs decreased and stabilized as the number sampled and group abundance increased. In complex scenarios, estimates of small groups will yield poor precision and some may be biased, but a stratified estimate with a conservative joint CI can be of practical use. The 2-step bootstrap approach is flexible and can incorporate other sources of variability or sampling constraints.

Manuscripts submitted 22 December 2015.
Manuscripts accepted 25 August 2016.
Fish. Bull. 115:1–12 (2017).
Online publication date: 18 October 2016.
doi: 10.7755/FB.115.1.1

The views and opinions expressed or implied in this article are those of the author (or authors) and do not necessarily reflect the position of the National Marine Fisheries Service, NOAA.

In 2-stage sampling for fisheries monitoring and research, abundance is estimated with a primary sampling gear and then partitioned into groups of management interest by applying compositional data (e.g., species, stock, sex, age, and size) derived from a secondary sampling gear. For example, biological samples obtained from gillnetting or electrofishing can be used to allocate abundance estimates from hydroacoustic counts to species (e.g., Tarbox and Thorne, 1996; Pritt et al., 2013; Rudstam et al., 2013; Hughes and Hightower, 2015). Alternatively, a more highly controlled sampling regime can be instituted by counting fish as they move past barriers (e.g., weirs or dams) and by collecting biological samples or data from some portion of the fish in order to partition counts (e.g., Wagner, 2007; Campbell et al., 2012). However, the complexities of fishery sampling programs and the relevant groups into which the fish are parsed present difficulties for estimating precision of the generated point estimates.

Steelhead (*Oncorhynchus mykiss*) are an important cultural, economic, and recreational resource in the Pacific Northwest of the United States. After the construction of hydroelectric dams on the Columbia and Snake rivers during the late 1960s and early 1970s, the abundance and survival of steelhead in the Snake River decreased (Raymond, 1988). In response, steelhead within the Snake River basin were listed as threatened under the Endangered Species Act in 1997. In recent years, abundances have increased slightly. However, the increase has been dominated by fish produced in hatcheries (intended to mitigate for reduced harvest opportunities and to supplement natural populations), while the returns of steelhead born in the natural environment remain critically low (Ford, 2011). Fishery biologists need to know how many wild versus hatchery-produced steelhead return in order to manage fisheries effectively, as well as to assess the conservation status of wild populations. Further, for wild fish, we need to know the numbers of fish returning by sex, age, and stock to inform viability analyses.

We collected data on the run composition of adult steelhead as they migrated past Lower Granite Dam (LGD) on the Snake River, 695 km from the ocean. Adults returning from the Pacific Ocean to spawn in tributaries of the Snake River must ascend fish ladders at 8 dams during their migration; Lower Granite Dam is the final dam they encounter before dispersing to spawn. An observation window on the LGD fish ladder (the primary sampling "gear") allows the enumeration of fish by species as they migrate upstream. A trapping facility (a diversion gate in the fish ladder with chutes leading to a holding tank) located above the observation window (the secondary sampling gear) allows the interception of fish and the collection of biological data (Harmon, 2003). Counting and sampling returning adult steelhead at the dam provide the data for calculating run composition (Schrader et al.[1]). Surprisingly, the primary literature is sparse on the statistical properties of estimates derived with current methods and applied to run composition.

In our study, we examined the properties of estimators of fish composition and confidence intervals (CIs) derived from weightings of counts of fish at the observation window, data on origin (wild versus hatchery) obtained from the samples taken at the trapping facility, and compositional data (sex, age, and genetically defined stock) collected from wild fish subsampled at the trapping facility. We considered counts at the observational window to provide a census of fish passing the dam. Initially, we assumed trapping rates (proportion of time the trap was open) could be precisely controlled to obtain a constant proportion of the fish throughout the run and, therefore, that data could be pooled across time to estimate abundance. However, logistical issues that affected trapping rates through time led us to investigate temporally stratified estimators. Individual CIs (for each group considered independently) and joint CIs (for all groups within a variable of interest considered simultaneously) were derived 1) by using closed-form asymptotically normal equations or 2) a 2-step bootstrap sampling method, by origin (hatchery or wild) of the fish, by using compositional data collected from wild fish. Using simulations, we compared the options for developing accurate estimates of abundance and CIs with good coverage; we then applied the preferred method from the simulations to empirical data to develop guidance for sampling and interpreting fisheries data on fish composition.

Materials and methods

We used data to describe the abundance and composition of wild adult steelhead migrating past LGD to spawn in the Snake River during spring 2011. Spawning year (SY) 2011 is defined as the year when adult steelhead migrate past LGD between 1 July 2010 and 30 June 2011. Although all steelhead in the Snake River basin spawn in the spring, the majority migrate past LGD during the previous fall, and a smaller portion migrates during the spring just before spawning. Later in this section, we describe the data set and estimation procedures and the simulations developed to test the bias of the estimators and the coverage of the associated CIs. A complete description of the collection methods and data used in this study is given by Schrader et al.[1]

Data collection

Primary sampling stage (counts from the observation window) Adult steelhead were counted as they passed a viewing window located in the LGD fish ladder, which they must ascend to migrate upriver. Counts of fish observed from the window were conducted during a majority of the year and occurred daily at 0400–2000 Pacific Time. Counts from videos were used in lieu of counts from the window in November, December, and March and occurred at 0600–1600. Most fish pass the window during the 10–16 h of daylight when counts are made. The ladder is drained and closed in January and February, and, as a result, adult steelhead cannot migrate upriver during those months. Count data were downloaded from the U.S. Army Corps of Engineers website (website). The steelhead count consists of all fish >30 cm in fork length identified as *O. mykiss*. Daily counts were aggregated on a weekly basis. We further combined weeks into longer time periods (up to 2 months) if few fish (<75 individuals) were passing the window during a week—a level observed typically early and late in the migration season.

Secondary sampling stage (trapping rates) Trapping rates were determined by a committee of co-managers balancing sampling requirements for multiple projects with fish handling concerns. The trap is operational 24 h/day and the trapping rate determines how long a trap gate remains open 4 times/h, such that a daily systematic sample (by time) is taken from the fish ascending the fish ladder. Thus, the trapping rate (proportion of an hour that the trap gate is open) approximates the desired proportion of the population to be sampled. Trapping rates are typically 10–20%; for the majority of the SY2011 run, it was set at 10%.

Trapped fish were anesthetized and examined to determine whether they were of hatchery or wild origin. In the Snake River basin, most hatchery-origin steelhead have a clipped adipose fin; however, some are released with an intact adipose fin to supplement natural populations. Therefore, unclipped steelhead were examined for the presence of dorsal or ventral fin erosion, which often occurs in hatchery-reared fish (Latremouille, 2003). Unclipped hatchery fish may also be identified by the presence of a coded wire tag, by

[1] Schrader, W. C., M. P. Corsi, P. Kennedy, M. W. Ackerman, M. R. Campbell, K. K. Wright, and T. Copeland. 2013. Wild adult steelhead and Chinook salmon abundance and composition at Lower Granite Dam, spawn year 2011. 2011 annual report. Idaho Dep. Fish Game, IDFG Rep. 13-15, 89 p. [Available at website.]

parentage determined genetically (Steele et al., 2013), or by a ventral-fin clip. Genotyping procedures for parentage were conducted after the trapping season and gives accuracy rates approaching 100% (Steele et al., 2013). Fish not determined to be of hatchery origin were treated as wild fish.

Subsampling of trapped wild steelhead Scale and tissue samples were then taken from a systematic subsample of trapped fish deemed wild. Percentages of the wild steelhead that were subsampled averaged around 50% during this study. Scale samples were used to determine age on the basis of visual examination of scale annuli. Age data collected at LGD were used to assign returning adults back to a brood year (BY, the year in which their parents spawned).

Tissue samples from the anal fin were used to determine sex and the stock of origin. Stock composition was determined by using individual assignment, a method of genetic stock identification (Pella and Milner, 1987; Shaklee et al., 1999) based on single nucleotide polymorphisms (SNPs). Adults were screened at 187 SNPs and with a sex-specific allelic discrimination assay (Campbell et al., 2012). Only individuals that were genotyped at >90% of SNPs were included. We used the maximum likelihood framework implemented in the program gsi_sim (Anderson et al., 2008; Anderson, 2010) to assign individuals to a stock. Each fish was assigned to the stock in which the probability of its genotype occurring was greatest by using the allocate-sum procedure (Wood et al., 1987). We did not attempt to identify out-of-basin strays. For this study, we assumed that the stock was determined without error (a future study will examine uncertainty in genetic assignments). In essence, we treated the genetic data in the same way as we did for the age data.

Ackerman et al.[2] defined 10 genetically determined stocks used for assignments at LGD. The locations of these stocks included 1) the upper Salmon River (UPS); 2) Middle Fork Salmon River (including Chamberlain and Bargamin creeks) (MFS); 3) South Fork Salmon River (SFS); 4) lower Salmon River (LOS); 5) upper Clearwater River (Lochsa and Selway rivers) (UPC) ; 6) South Fork Clearwater River (including Clear Creek) (SFC); 7) lower Clearwater River (LOC); 8) Imnaha River (IMN); 9) Grande Ronde River (GRR); and 10) Tucannon River, Asotin Creek, and other tributaries to the Snake River downstream of the Clearwater River confluence (LSN).

The sampling design produced 3 data sets: 1) a census of numbers of fish returning to and migrating past the dam (window counts), 2) a hatchery-versus-wild data set for all trapped fish (trap data), and 3) a data set containing sex, age, and stock for a subsample of wild fish that were trapped (for compositional data). These 3 data sets were used to produce estimates and CIs for the number of wild fish by sex or age or stock.

[2] Ackerman, M. W., N. V. Vu, J. McCane, C. A. Steele, M. R. Campbell, A. P. Matala, J. E. Hess, and S. R. Narum. 2014. Chinook and steelhead genotyping for genetic stock identification at Lower Granite Dam. Project progress report. 2013 annual report. Idaho Dep. Fish Game, IDFG Rep. 14-01, 60 p. [Available at website]

Estimator and confidence intervals

Abundance of wild steelhead The window-count data provided the abundance of adult steelhead migrating past LGD, but our focus was on wild fish; therefore, we first had to partition the overall abundance estimate into a wild-versus-hatchery abundance estimate. The proportions of wild and hatchery steelhead changed over the season, but within each weekly or monthly stratum, proportions were assumed to be relatively constant. Given the window counts by strata, $C_1, C_2, \ldots, C_S$, the number of wild steelhead ($\widehat{W}$) was estimated with the following equation:

$$\widehat{W} = \sum_{s=1}^{S} \hat{p}_s C_s, \quad (1)$$

where $\hat{p}_1, \hat{p}_2, \ldots, \hat{p}_s$ = estimates of the proportion of wild steelhead by stratum from the trap data; and

$\widehat{p}_s = N_s/t_s$ (or denoted $\hat{p}$ for a pooled estimate).

These and all subsequent notations are defined in Table 1. Given the fixed numbers of adults counted at the dam for each stratum, we found a CI for the number of wild fish by using either an asymptotically normal interval or by a parametric bootstrap. The asymptotically normal interval is given as

$$\widehat{W} - Z_{\alpha/2} S_{\widehat{W}} \leq W \leq \widehat{W} + Z_{\alpha/2} S_{\widehat{W}}, \quad (2)$$

where $S^2_{\widehat{W}} = \sum_{s=1}^{S} C_s^2 S^2_{\hat{p}_s} = \sum_{s=1}^{S} C_s^2 \left(1 - \frac{t_s}{C_s}\right) \frac{\hat{p}_s(1-\hat{p}_s)}{t_s - 1}$; (3)

and $Z_{\alpha/2}$ = the $(100\alpha/2)$th percentile of a standard normal distribution.

For the parametric bootstrap, we assumed the bootstrap number of wild fish has a binomial distribution, $N_s^* \sim$ binomial $(t_s, \hat{p}_s | t_s)$ and $p_s^* = N_s^*/t_s$. We produced 500 sets (B) of $(p_1^*, p_2^*, \ldots, p_S^*)$, yielding $W_1^*, W_2^*, \ldots, W_B^*$. The $100\alpha/2$ and $(1-\frac{\alpha}{2})$ percentiles of $W_1^*, W_2^*, \ldots, W_B^*$ gave us the $100(1-\alpha)\%$ CI for the true number of wild steelhead that passed LGD for the year. In this study, we used 90% CIs as an acceptable tradeoff of the type-I error rate with the power to discern important differences.

Composition of wild steelhead When we had estimates of the number of wild fish migrating past LGD, we partitioned them into groups of interest for population assessments. There were 2 competing approaches for estimating numbers of wild fish by sex, age, or genetic origin: pooled or stratified. The compositional data set was about a tenth of the size of the hatchery-versus-wild data set (most fish were hatchery-origin; wild fish were subsampled at approximately 50%). There was ample data in the trap data set to estimate proportion of wild steelhead by stratum but not enough data for

Table 1

Definitions for notation used to describe parameters in estimating abundance and confidence intervals for the constituent groups that compose the run of steelhead (*Oncorhynchus mykiss*) in Snake River of the Pacific Northwest during spawning year 2011.

Parameter	Definition
A	Number of age groups
B	Number of bootstrap samples
C_s	Window count in stratum s; s=1,2,...S
F	Abundance of female steelhead
G	Number of genetic stocks
k	Number of categories in the compositional variable of interest
L	Lower bound of a confidence interval
M	Abundance of male steelhead
N_s	Number of wild steelhead trapped in stratum s; s=1,2...S
$\widehat{p_s}$	Estimated proportion of wild steelhead in stratum s; s=1,2...S
π_{is}	Estimated proportion of group i of the variable of interest (A, G, F / M) in stratum s; s=1,2...S
r_s	Number of wild steelhead subsampled in stratum s; s=1,2,...S
S	Number of time strata
t_s	Number of steelhead trapped in stratum s; s=1,2...S
U	Upper bound of a confidence interval
$\widehat{W_s}$	Estimated abundance of wild steelhead in period s; s=1,2...S

the wild compositional data for some strata. We could have pooled the compositional data over the season if we had assumed that we had sampled a fixed proportion of the wild fish for each stratum or if we had assumed that the composition proportions were constant. However, if neither condition was true, we had to focus on obtaining sufficient samples in each stratum to obtain stable estimates of composition proportions by stratum $\hat{\pi}_{is}$.

We defined the proportion of wild females in a stratum (π_{F_S}) as $P(female \mid wild,\ stratum\ s)$. Then we had ($\pi_{F_1}$, π_{M_1}), ..., (π_{F_S}, π_{M_S}) as the conditional probabilities for wild females and males for strata 1, ..., s. These proportions were estimated from data obtained from the subsample of the trapped fish; for example, for females $\hat{\pi}_{F_S} = r_{F_S}/(r_{F_S} + r_{M_S})$. Given estimates of these probabilities from wild fish examined in the trap, we used the following equation to estimate female abundance:

$$\hat{F} = \sum_{s=1}^{S} \hat{\pi}_{F_S} \hat{W}_S = \sum_{s=1}^{S} \hat{\pi}_{F_S} \hat{p}_s C_s, \quad (4)$$

and to estimate wild male abundance

$$\hat{M} = \sum_{s=1}^{S} \hat{\pi}_{M_S} \hat{W}_S = \sum_{s=1}^{S} \hat{\pi}_{M_S} \hat{p}_s C_s. \quad (5)$$

For the pooled estimators, we dropped the summation and subscript. Similar estimates were made for A (ages, BY2004–BY2008 in this study), G (genetically identified stocks), and $A \times G$ age groups for each stock. That is, the number of wild steelhead in any group is a weighted sum of the stratified window counts, in which the weights are estimates of the probabilities of being wild and being a member of a particular group, including any combinations of the compositional variables.

To find CIs for these estimates, we had to account for the variability of both the trap data and the compositional data. For the asymptotically normal interval, we used Goodman's (1960) estimated variance of a product:

$$s^2_{\hat{F}} = \sum_{s=1}^{S} C_s^2 (\hat{p}_s^2 s^2_{\hat{\pi}_{F_s}} + \hat{\pi}^2_{F_s} s^2_{\hat{p}_s} - s^2_{\hat{p}_s} s^2_{\hat{\pi}_{F_s}}, \quad (6)$$

yielding

$$\hat{F} - Z_{\alpha/2} s_{\hat{F}} \le F \le \hat{F} + Z_{\alpha/2} s_{\hat{F}}, \quad (7)$$

where $s^2_{F_s} = (1 - \frac{r_s}{\widehat{W}_s})\hat{\pi}_{F_s}(1 - \hat{\pi}_{F_s})/(r_s - 1)$.

For the pooled case, we used the following equation:

$$s^2_{\hat{F}} = \widehat{W}_{\cdot}^2 s^2_{\hat{\pi}_F} + \hat{\pi}^2_F s^2_{\widehat{W}} - s^2_{\widehat{W}} s^2_{\hat{\pi}_F}, \quad (8)$$

where $s^2_{\hat{\pi}_F} = (1 - \frac{r_{\cdot}}{\widehat{W}_{\cdot}})\hat{\pi}_F(1 - \hat{\pi}_F)/(r_{\cdot} - 1)$; and (9)

$\hat{\pi}_F$ = the proportion of wild females from the pooled sample.

Similar formulae for $\hat{M}$ and estimates of age, stock, and ages by stock follow in the next paragraph.

The bootstrap process described previously for obtaining the CI for the number of wild fish was extended by adding a conditional bootstrap loop based on the sex, age, and stock of wild fish in the trap. We defined pseudoreplicates parametrically, using

$$(F_s^*, M_s^*) \sim \text{binomial}(r_s, (\hat{\pi}_{F_s}, \hat{\pi}_{M_s}) \mid r_s, \text{wild}) \text{ and} \quad (10)$$

$$(\pi^*_{F_s} = \tfrac{F_s^*}{m_s}, \pi^*_{M_s} = \tfrac{M_s^*}{m_s}).$$

Bootstrap values for the total number of wild females, $F_1^*, \ldots, F_B^*$, were determined with the following equation:

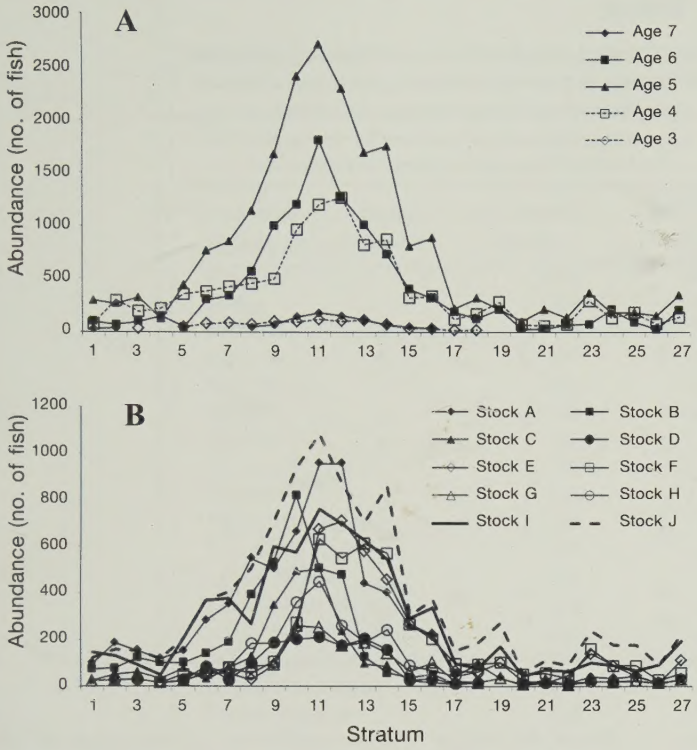

Figure 1

Simulated abundance of wild steelhead trout (*Oncorhynchus mykiss*) by weekly time strata for (**A**) 5 age groups and (**B**) 10 stocks, which are given generic designations, such as *Stock A*.

$$F^* = \sum_{s=1}^{S} \pi^*_{Fs} p^*_s C_s. \quad (11)$$

The percentile bootstrap CI for the true number of wild females, $[L_F, U_F]$, is determined by finding the $100\alpha/2$ and $100(1-\frac{\alpha}{2})$ percentiles. Similarly, we calculated a bootstrap CI for the number of wild males. Changing the binomial described previously to a multinomial, we generated B sets of $(\pi^*_{11},\ldots,\pi^*_{A1}),\ldots,(\pi^*_{1B},\ldots,\pi^*_{AB})$ to obtain bootstrap CIs for the true number of wild fish of ages 1, ..., A. We followed the same procedure for stocks 1, ..., G and $A \times G$ ages by stock (ages within stocks). To ensure accuracy across all groups being evaluated at a particular time, joint CIs for numbers of wild fish by sex or age or stock were calculated by using the methods of Mandel and Betensky (2008).

Simulations

Although our estimators and CIs are straightforward, we did not know their statistical properties. We designed a simulation of the sampling process to examine the properties of sex, age, and stock estimators and CIs, using the methods defined previously to analyze each simulated sample. We set the total passage of steelhead similar to the SY2011 observed count (200,000 fish). We set parameter values for all binomial and multinomial distributions similar to those of the stratified estimates obtained from the SY2011 data (Suppl. Tables 1 and 2). The percentage of wild steelhead ranged from 20% to 50%. The trapping rate varied from 3% to 14%, and the subsampling rate varied from 35% to 100%. Abundance and composition of the simulated population varied over 27 temporal strata loosely based on the character of the wild steelhead run in Snake River during SY2011 (Fig. 1). For simplicity, age and stock proportions in the population were generated by assuming age and stock are independent variables; therefore, we multiplied age and stock proportions to find age-by-stock proportions of the steelhead run.

We generated 500 samples from the population in the following manner. First, we simulated number of trapped fish (t_s) by generating binomial samples for each time stratum with the number of binomial trials equal to the number of fish returning during that stratum and with probability equal to the proportion of fish trapped within that stratum. Second, we simulated the number of trapped fish that were wild for each stratum by generating binomial samples with the number of trials equal to t_s and with probability equal to the true proportion of wild fish for that stratum. The remaining trapped fish were of hatchery origin. From these numbers, we generated a sample of trapped fish with 2 columns: time stratum and wild versus hatchery. The length of this data set was the sum of the numbers of wild fish trapped across the time strata ($\sum_{s=1}^{S} t_s$). Third, we calculated the number of wild fish whose sex, age, and stock had been determined in each stratum by multiplying the simulated number of wild fish trapped by the proportion subsampled. These numbers by stratum were the number of binomial or multinomial trials for sex or age or genetic stock (r_s). For example, we found the number of sampled fish that were wild females for a stratum by generating binomial trials of size r_s with probability equal to the true proportion of wild females during that stratum and with the remainder being males.

Knowing the random number of wild females and males trapped in each stratum, we put together a simulated subsample of fish by sex by forming a data set with two columns (for stratum and sex). The size of this sample was equal to the sum across the time strata of the numbers of handled fish, $\sum_{s=1}^{S} r_s$. Similar samples were simulated for age, stock, and stock by age (500 for each). The simulation generated 2 types of data from each sampling iteration: 1) a randomly generated trap sample with a random number of wild and hatchery fish, and 2) a randomly generated compositional sample with random numbers of females and males or numbers of fish of various ages or numbers of fish of various stocks.

Table 2

Number of simulations in which criteria for coverage levels for individual confidence intervals coverage were not met for combinations of estimator type (scenario). Simulations were conducted for 4 variables of interest with varying numbers of categories (k).

		Variable of interest (number of categories)			
Scenario	Criterion	Sex (k=2)	Brood year (k=5)	Stock (k=10)	Age×stock (k=50)
Pooled asymptotically normal					
	Coverage ≤0.85	0	1	5	18
	Coverage ≤0.80	0	0	3	6
Pooled parametric bootstrap					
	Coverage ≤0.85	0	0	5	13
	Coverage ≤0.80	0	0	3	2
Stratified asymptotically normal					
	Coverage ≤0.85	0	1	0	12
	Coverage ≤0.80	0	0	0	3
Stratified parametric bootstrap					
	Coverage ≤0.85	0	0	0	8
	Coverage ≤0.80	0	0	0	0

We obtained estimates of abundance and bootstrapped CIs for the groups of interest for every simulation iteration, using the window counts and the primary and secondary samples, as explained previously. After 500 simulation iterations, we had 500 estimates of the total number of wild steelhead, female and male wild, wild by age, and wild by stock. We also had 500 individual and joint CIs for each estimate. We saved the estimates and CIs for subsequent evaluation.

The evaluation of estimator performance was based on bias and CI coverage. We computed bias as the mean of the simulated estimates minus the true value. We computed the coverage of any individual CI by tallying the number of times the true population number fell inside the CI. For the pooled and stratified estimators, we tallied the number of cases for which the bias was ≥5%. Likewise, we tallied the number of cases for which the coverages for estimators were ≤0.85 (considered poor) and ≤0.80 (considered very poor).

Analysis of SY2011 data

We evaluated precision using the preferred estimator (determined from the simulations) that was applied to real data from SY2011; these data had more irregularities than the simulated data. For this application, we determined the age-by-stock proportions from the data, not as the product of age and stock proportions. We measured precision as the half-width of a (1-α)100% CI expressed as a percentage of the point estimate (P_{ind} for individual CIs or P_{joi} values for joint CIs). Researchers often set a stringent goal of a CI half-width ≤10% of the estimate. For management purposes, it is recommended that salmon stocks have unbiased abundance estimates with a coefficient of variation of 15% or less (Crawford and Rumsey[3]). For a 90% asymptotic CI (which indicates a critical value of the t distribution at 1.645), it follows that

$$\left|\widehat{W}-W\right| \leq 1.645se \leq 1.645(0.15)\widehat{W} \leq 0.25\widehat{W} \quad (12)$$

or

$$\left|\widehat{W}-W\right| / \widehat{W} \leq 0.25 \quad (13)$$

(i.e., half of the width of the CI interval should be ≤25% of the estimate). We compare the P_{ind} and P_{joi} values for all CIs with 0.10 and 0.25. To determine whether P_{ind} was related to the number of fish sampled or estimated size of the target group, we fitted power curves, using the results from all cases.

Results

Simulations

Performance of the pooled and stratified estimators was similar when the variable of interest had few categories, but the stratified estimators did better as complexity increased (Table 2). Detailed simulation results are provided in Suppl. Tables 3 and 4. All estimators produced acceptable accuracy and CI coverage when numbers of wild fish were estimated by sex. Similarly, all estimators provided acceptable accuracy

[3] Crawford, B. A., and S. M. Rumsey. 2011. Guidance for monitoring recovery of Pacific Northwest salmon and steelhead listed under the federal Endangered Species Act, 117 p. Northwest Region, National Marine Fisheries Service, NOAA. [Available at website.]

Table 3

Sample size (*n*, number of steelhead), abundance estimate, and individual and joint confidence interval half-width (%) for groups of wild steelhead trout (*Oncorhynchus mykiss*) that spawned in 2011. Values are given for groups defined by sex, brood year (BY), or stock (identified by the location where the stock spawns).

Group	*n*	Abundance	Individual	Joint
Total wild fish	4701	44,133	2.3	2.8
Females	1466	29,541	2.4	2.8
Males	732	14,592	2.8	3.2
BY2004	38	784	8.4	12.3
BY2005	520	11,239	3.6	4.8
BY2006	994	21,449	2.6	3.5
BY2007	473	10,103	3.7	5.0
BY2008	26	558	10.1	13.8
Grande Ronde	472	9442	7.1	11.9
Imnaha	168	3318	11.9	21.0
Lower Clearwater	173	3421	12.4	20.3
Lower Salmon	98	1941	16.3	26.5
Lower Snake	219	4374	10.3	17.5
Middle Fork Salmon	214	4312	10.8	15.9
South Fork Clearwater	233	4228	10.4	15.8
South Fork Salmon	135	2512	13.8	20.6
Upper Clearwater	215	3885	11.4	18.2
Upper Salmon	340	6699	8.1	12.8

when numbers by age were estimated, but the asymptotically normal CIs had poor coverage in one case for each estimator type. Average CI coverage among stocks was similar between the pooled estimators: 87.7% for the pooled asymptotically normal estimator and 88.2% for the pooled bootstrap estimator. Average CI coverage was slightly higher for the stratified estimators: 88.1% for the stratified asymptotically normal estimator and 89.0% for the stratified bootstrap estimator. The pooled estimators had unacceptable bias and very poor CI coverage for 3 of the 10 stocks, whereas the stratified estimators had acceptable accuracy for all stocks. Average CI coverage among stocks was similar for the pooled estimators: 81.5% for the pooled asymptotically normal estimator and 82.2% for the pooled bootstrap estimator. In contrast, average CI coverage was higher for the stratified estimators, although it was similar between them: 88.4% for the stratified asymptotically normal estimator and 89.0% for the stratified bootstrap estimator.

Problems with pooled estimators became even more prevalent when we addressed age by stock; however, the performance of the stratified estimators also began to suffer as the number of groups to be estimated increased to 50 (Table 2). The pooled estimators had unacceptable levels of bias in 21 cases, whereas the stratified estimators had unacceptable bias in 3 cases. Poor performance was most common in groups composed of steelhead from the least abundant BYs. Instances of poor CI coverage were usually, but not always, associated with unacceptably high bias. Overall, stratified estimators performed better than pooled estimators. Further, the bootstrap CIs had better coverage than the asymptotically normal CIs; in 3 instances, asymptotically normal CIs had very poor coverage (<80%), but there were no such instances for the bootstrap CIs. For this reason, we applied the stratified bootstrap estimator to the SY2011 data to develop guidelines for sampling and interpretation of such data.

Application of the stratified bootstrap estimator to data from SY2011

During SY2011, 208,296 steelhead were counted at LGD. Of these fish, 44,133 steelhead were estimated to be wild (21.2%, Table 3). The 90% CI was 43,152–45,140 wild steelhead. There were approximately twice as many females as males. Sex ratio varies annually, but the ratios seen in 2011 were typical. The middle age groups had more returning fish than the youngest and oldest age groups. Stocks were not evenly represented (e.g., the GRR stock had almost 4 times the number as the LOS stock) (Table 4). There were 46 stock-by-age groups in SY2011; estimated abundance ranged from 4912 individuals in the GRR stock in BY2006 to 21 individuals in the LSN stock in BY2004 (Table 4). The composition of a real steelhead run was not as balanced as that in the simplification used to generate the simulated data in this study, and this uneven distribution was most apparent in the age-by-stock groups.

Effects of using individual versus joint CIs depended on the complexity (i.e., number of groups) in the vari-

Table 4

Sample size (*n*, number of steelhead), abundance estimate, and individual and joint confidence interval half-width (%) for age groups (brood years) within stocks of wild steelhead trout (*Oncorhynchus mykiss*) that spawned in 2011. Groups are identified by brood year (BY) and the location where the stock spawns.

Group	*n*	Abundance	Individual	Joint
Grande Ronde BY2004	6	116	19.0	34.1
Grande Ronde BY2005	67	1501	8.6	16.2
Grande Ronde BY2006	222	4912	7.4	12.8
Grande Ronde BY2007	133	2875	7.7	14.2
Grande Ronde BY2008	2	38	31.9	54.5
Imnaha BY2004	2	43	35.1	63.3
Imnaha BY2005	22	537	17.2	32.0
Imnaha BY2006	82	1781	12.9	23.7
Imnaha BY2007	43	957	13.8	26.0
Lower Clearwater BY2004	1	32	46.8	84.2
Lower Clearwater BY2005	24	522	14.7	25.7
Lower Clearwater BY2006	78	1693	12.7	23.2
Lower Clearwater BY2007	49	1097	13.5	24.2
Lower Clearwater BY2008	4	78	30.2	55.3
Lower Salmon BY2004	1	23	57.5	106.1
Lower Salmon BY2005	18	409	19.5	35.4
Lower Salmon BY2006	40	909	17.9	30.6
Lower Salmon BY2007	26	557	17.9	31.1
Lower Salmon BY2008	2	44	48.3	87.6
Lower Snake BY2004	1	21	50.8	91.9
Lower Snake BY2005	13	324	16.2	29.5
Lower Snake BY2006	99	2268	11.4	20.2
Lower Snake BY2007	72	1614	11.4	29.4
Lower Snake BY2008	6	147	23.1	40.5
Middle Fork Salmon BY2004	10	222	16.2	31.4
Middle Fork Salmon BY2005	99	2245	11.7	21.7
Middle Fork Salmon BY2006	72	1543	11.8	23.2
Middle Fork Salmon BY2007	6	303	22.1	40.4
South Fork Clearwater BY2004	3	59	28.2	50.3
South Fork Clearwater BY2005	44	906	12.1	22.5
South Fork Clearwater BY2006	144	3010	10.5	19.6
South Fork Clearwater BY2007	12	254	22.6	40.9
South Fork Salmon BY2004	6	132	28	51.8
South Fork Salmon BY2005	75	1612	14.3	25.2
South Fork Salmon BY2006	31	695	18.3	33.5
South Fork Salmon BY2007	3	73	34.2	62.2
Upper Clearwater BY2004	5	99	25.1	47.8
Upper Clearwater BY2005	120	2425	11.0	20.1
Upper Clearwater BY2006	63	1283	12.2	22.7
Upper Clearwater BY2007	3	54	29.8	54.0
Upper Clearwater BY2008	1	24	53.0	97.6
Upper Salmon BY2004	2	39	29.7	54.2
Upper Salmon BY2005	35	758	10.6	21.0
Upper Salmon BY2006	156	3356	8.8	16.3
Upper Salmon BY2007	107	2319	9.1	17.9
Upper Salmon BY2008	10	227	15.4	28.1

able of interest (Table 3). Widths of the joint CIs for females and males were not markedly wider than those of the individual CIs. For age, the widths of the joint CIs were 1.2–3.4 times the widths of the individual CIs. For stock, the joint CIs were 1.2–2.5 times wider. For some age-by-stock groups, the joint CIs were considerably wider than those of the individual CIs (Table 4).

Attainment of precision goals depended on the group and whether individual or joint CIs were considered (Tables 3 and 4). All sex and age groups met the 10%

research goal for precision if P_{ind} was used, except for the BY2008 group (P_{ind}=10.1%). With the use of P_{joi}, the 10% goal was met for all sex and age groups, except the BY2004 and BY2008 groups. Stock groups did not meet the 10% goal, except the GRR and UPS stocks, if P_{ind} was used. All sex, age, and stock groups met the 25% management goal for individual and joint CIs, except the LOS stock if P_{joi} was used. Of the stock by age groups, 11% met the 10% precision goal if P_{ind} was used, but none met the goal if P_{joi} was used. There was wider disparity in attainment of the 25% goal; 70% of the age-by-stock groups met the goal if P_{ind} was used, but only 35% of the age-by-stock groups met the goal if P_{joi} was used.

In general, half-widths of the CIs declined and stabilized as the number of fish sampled and estimated abundance of the groups involved increased (Fig. 2). Precision scaled approximately with the cube root of sample size, indicating that reducing the CI width by half would require approximately 8 times as many samples. Values of P_{ind} within a percentage point of the 10% precision criterion were obtained when there were 26–233 fish from a given category in the subsample (mean=140) and when there were 558–4374 steelhead in the category (mean=2794). Values of P_{ind} closest to the 25% criterion were obtained when there were 5 and 6 fish in a subsample and when there were 99–147 steelhead in a category. The power functions parameterized from the group estimates yielded values of 96 samples and 1982 steelhead at the 10% criterion and 7 samples and 147 steelhead at the 25% precision criterion.

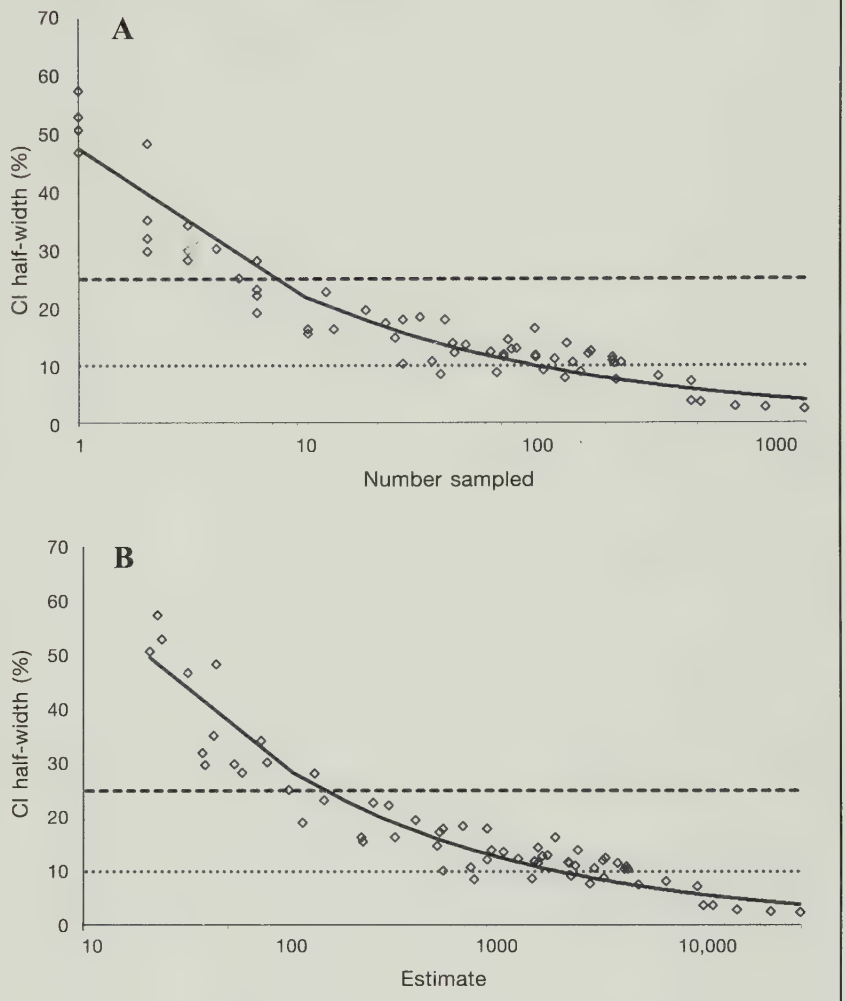

Figure 2

Relationship of confidence interval (CI) half-width for groups of wild steelhead (*Oncorhynchus mykiss*) spawning in 2011 in Snake River, Pacific Northwest, to (**A**) number of fish sampled (CI half-width=47.48[number sampled]$^{-0.341}$, coefficient of multiple determination [R^2]=0.872), and (**B**) abundance estimate (CI half-width=144.74[abundance]$^{-0.352}$, R^2=0.870). Precision criteria levels of 10% (dotted line) and 25% (dashed line) CI half-widths are shown for reference.

Discussion

The stratified estimators had biases <5%, except for a few cases in the most complex analysis (age by stock). Individual CIs for most constituent groups had coverages very near the nominal 90%. For conservation assessments, the greatest need is data on abundance of each stock. Coverage of CIs was good even for the smallest stock. Age structure is important for computation of productivity for each stock (i.e., for summarizing the adult progeny from a brood year returning across years and for computing progeny per parent). Accuracy of productivity estimates typically are largely controlled by the most abundant age groups, which had unbiased estimates in our study. When the stratified estimators were used, only a few of the smallest stock-by-age groups had bias ≥5.0% or CI coverage <85%.

Conversely, pooled estimators performed poorly except for the simplest variables of interest: sex and age. As variable complexity increased from age (5 cases) to stock (10 cases) to age-by-stock (50 cases), the proportion of estimates biased >5% increased from 0% to 30% to nearly half, respectively. Initially, we expected pooled estimators to be acceptable because of the highly con-

trolled sampling regime at LGD, which was very consistent for SY2011. The realized sampling rate in the simulation (the product of trap rate and subsample rate) averaged 4.7% (standard deviation 1.3%). However, stock and age composition changed through the run, as did the number of steelhead crossing the dam. As the variable of interest became more complex, accuracy and precision of pooled estimators decreased.

Steinhorst, et al. (2010) estimated the run composition of fall-run Chinook salmon (*O. tshawytscha*) at LGD on the basis of counts from observation windows from 18 August through 15 December (their method 1). They used a stochastic model based on a fast Fourier transform to model the distribution of daily window counts, which were summed to obtain total abundance. Steinhorst, et al. (2010) used 2 bootstrap steps—a nonparametric bootstrap associated with the Fourier model and a parametric bootstrap applied to an estimate of composition pooled over the season. They did not report composition by stratum because composition was calculated with a complex accounting algorithm that could not be applied to individual strata. In essence, they assumed that either the proportions of their sex-by-age-by-origin groups were fairly uniform over the season or that a constant proportion of the run was sampled for each stratum. However, if the groups of interest returned at different times, a pooled estimate of composition applied to total escapement would not be accurate, especially over longer temporal spans (e.g., the steelhead run). In our study, the simulation results from the pooled estimators indicated precisely that outcome.

Precision may be computed for each group of interest, one at a time (i.e., P_{ind}), or more conservatively across all groups within a variable of interest (P_{joi}), minimizing study-wide error. However, the conservative approach resulted in wider CIs; for example, joint CIs were 14–17% wider than the individual CIs for sex in the SY2011 run. For stocks, P_{joi} values were about 47–76% wider than P_{ind} CIs. Given the number of stocks, we were not paying a large penalty for computing joint CIs. For age-by-stock groups, the joint CIs were on average 85% wider than the individual CIs (range: 71–158%). This difference likely was due to the uneven distribution of numbers by age and the large number of age-by-stock groups. Because we were trying to achieve joint coverage across so many groups simultaneously, a much greater expansion of the CIs was necessary. The results of our study show the cost to statistical power caused by the inclusion of many groups in an analysis. Investigators must consider whether the more conservative approach affects the usefulness of the resulting estimates and which groups are truly of management interest. For the latter consideration, investigators may combine some groups or decide that loss of precision is acceptable for their application. In our case, we combined strata to achieve greater sample sizes and used total age rather than the combinations of years spent in freshwater and years spent in saltwater that salmon biologists often use (Quinn, 2005).

Precision is related to the amount of information available, and the quality of this information declines as group size becomes smaller or as the realized sample rate is reduced. The problem in our case was that the steelhead run in Snake River is protracted over time, compounded by the complexity of the life history and stock structure of steelhead. Therefore, multinomial proportions must be estimated for many groups over many time strata unless the groups of interest can be simplified. Even so, we generally met the research goal of half the 90% CI width within 10% of the estimate for sex and age groups present in SY2011. For stock groups, we met the management goal of half the 90% CI width within 25% of the estimate for sex and age groups but our 10% precision goal was not attained, except with the 2 largest stocks when the less stringent P_{ind} measure was used.

To develop guidance for interpretation of the estimates we obtained from the data, we relied on P_{ind} because it was not affected by the number of other groups in the analysis. Precision of the estimates for individual groups declined rapidly when group abundance was <2500 individuals or when <100 individuals from that group were collected in the subsample. However, if there were few fish in a group, analysts and managers probably would be content with a more lenient precision criterion. For example, if our estimate was 50 and the CI was 20–80, the percent halfwidth would be 60% of the estimate but the fact that the true number is between 20 and 80 should be sufficiently precise for management purposes, especially if the numbers of fish in other groups are decidedly larger. With P_{ind} as a measure of precision, the 10% research precision goal could be reached if group abundance were to exceed 2000 individuals or if >100 samples from that group were collected. The 25% management precision goal was much more attainable and was achieved at group abundances >150 individuals and when very few samples were collected (<10). These values can be used as thresholds for the lenient precision criterion in our application.

Our results have implications for monitoring fish populations. If the interest is on the largest groups in a mixed population, most sampling programs will yield sufficient results. However, weak stocks are frequently a problem for conservation and fisheries management, and precision of abundance estimates of smaller groups becomes important. Obviously, there is a tradeoff between sample size and number of subdivisions that can be maintained. Previous work by Gerritsen and McGrath (2007) has supported this notion, but their criteria for success focused on overall (average) precision. Thompson (1987) found that a sample size of 510 fish should suffice under a worst case scenario for $\alpha = 0.05$ (equal proportions among groups, but number of groups does not matter) as long as desired precision is expressed in absolute terms. If desired precision is expressed in relative terms (as was done in our study), no sample size will be sufficient if group size approaches zero. However, our results provide useful guidance for

determining the groups that will have reliable estimates in complex scenarios. Even at lower fish abundances, we can define a lenient precision criterion with practical value.

The estimation approach described in this article is very flexible and can be customized for many scenarios. In this study, we assumed that window counts were a census, and stock and age were determined without error. In most applications, abundance is determined from a sample rather than a census. Further, there is uncertainty in the determination of stock and age for each fish. Additional uncertainty (e.g., genetic variability or noncensus estimates of total abundance) can be incorporated into our framework by adding additional bootstrap steps to reflect the source of the additional variance (e.g., method 2 in Steinhorst et al., 2010). Another practical issue is that samples for genetic analysis can now be processed en masse, but ages must be read from scale samples individually; hence, more fish can be identified to stock than can be aged. The bootstrap routine can be altered such that all genetic information is used to estimate stock abundance, and age composition is applied within each stock estimate (i.e., age composition is conditional on stock).

The stratified estimator in our study produced unbiased estimates, and the parametric bootstrap CIs had good coverage and acceptable precision. In complex scenarios, estimates of abundance of small groups will have poor precision and some may be biased, but a stratified estimate with a conservative joint CI can be of practical use if the numbers of fish in other groups are much larger. The 2-step bootstrap approach is flexible and can be adapted to incorporate other sources of variability or sampling constraints.

Acknowledgments

Funding for this project was provided by Bonneville Power Administration under project numbers 1990-055-00, 1991-073-00, and 2010-026-00. M. Campbell reviewed earlier drafts of this article. We gratefully acknowledge the thorough critiques given by 3 anonymous reviewers.

Literature cited

Anderson, E. C.
2010. Assessing the power of informative subsets of loci for population assignment: standard methods are upwardly biased. Mol. Ecol. Resour. 10:701–710.

Anderson, E. C., R. S. Waples, and S. T. Kalinowski.
2008. An improved method for predicting the accuracy of genetic stock identification. Can. J. Fish. Aquat. Sci. 65:1475–1486.

Campbell, M. R., C. C. Kozfkay, T. Copeland, W. C. Schrader, M. W. Ackerman, and S. R. Narum.
2012. Estimating abundance and life history characteristics of threatened wild Snake River steelhead stocks by using genetic stock identification. Trans. Am. Fish. Soc. 141:1310–1327.

Ford, M. J. (ed.).
2011. Status review update for Pacific salmon and steelhead listed under the Endangered Species Act: Pacific Northwest. NOAA Tech. Memo. NMFS-NWFSC-113, 281 p.

Gerritsen, H. D., and D. McGrath.
2007. Precision estimates and suggested sample sizes for length-frequency data. Fish. Bull. 105:116–120.

Goodman, L. A.
1960. On the exact variance of products. J. Am. Stat. Assoc. 55:708–713.

Harmon, J. R.
2003. A trap for handling adult anadromous salmonids at Lower Granite Dam on the Snake River, Washington. North Am. J. Fish. Manage. 23:989–992.

Hughes, J. B., and J. E. Hightower.
2015. Combining split-beam and dual-frequency identification sonars to estimate abundance of anadromous fishes in the Roanoke River, North Carolina. North Am. J. Fish. Manage. 35:229–240.

Latremouille, D. N.
2003. Fin erosion in aquaculture and natural environments. Rev. Fish. Sci. 11:315–335.

Mandel, M., and R. A. Betensky.
2008. Simultaneous confidence intervals based on the percentile bootstrap approach. Comput. Stat. Data Analys. 52:2158–2165.

Pella, J. J., and G. B. Milner.
1987. Use of genetic marks in stock composition analysis. *In* Population genetics and fisheries management (N. Ryman and F. Utter, eds.), p. 274–276. Univ. Wash. Press, Seattle, WA.

Pritt, J. J., M. R. DuFour, C. M. Mayer, P. M. Kocovsky, J. T. Tyson, E. J. Weimer, and C. S. Vandergroot.
2013. Including independent estimates and uncertainty to quantify total abundance of fish migrating in a large river system: walleye (*Sander vitreus*) in the Maumee River, Ohio. Can. J. Fish. Aquat. Sci. 70:803–814.

Quinn, T. P.
2005. The behavior and ecology of Pacific salmon and trout, 388 p. Univ. Wash. Press. Seattle, WA.

Raymond, H. L.
1988. Effects of hydroelectric development and fisheries enhancement on spring and summer Chinook salmon and steelhead in the Columba River basin. North Am. J. Fish. Manage. 8:1–24.

Rudstam, L. G., J. M. Jech, S. L. Parker-Stetter, J. K. Horne, P. J. Sullivan, and D. M. Mason.
2013. Fisheries acoustics. *In* Fisheries techniques, 3rd ed. (A. V. Zale, D. L. Parrish, and T. M. Sutton, eds.), p. 597–636. Am. Fish. Soc., Bethesda, MD.

Shaklee, J. B., T. D. Beacham, L. Seeb, and B. A. White.
1999. Managing fisheries using genetic data: case studies from four species of Pacific salmon. Fish. Res. 43:45–78.

Steele, C. A., E. C. Anderson, M. W. Ackerman, M. A. Hess, N. R. Campbell, S. R. Narum, and M. R. Campbell.
2013. A validation of parentage-based tagging using hatchery steelhead in the Snake River basin. Can. J. Fish. Aquat. Sci. 70:1046–1054.

Steinhorst, K., D. Milks, G. P. Naughton, M. Schuck, and B. Arnsberg.
2010. Use of statistical bootstrapping to calculate confidence intervals for the fall Chinook salmon run reconstruction to Lower Granite Dam. Trans. Am. Fish. Soc. 139:1792–1801.

Tarbox, K. E., and R. E. Thorne.
1996. Assessment of adult salmon in near-surface waters of Cook Inlet, Alaska. ICES J. Mar. Sci. 53:397–401.

Thompson, S. K.
1987. Sample size for estimating multinomial proportions. Am. Stat. 41:42–46.

Wagner, P. G.
2007. Fish counting at large hydroelectric projects. *In* Salmonid field protocols handbook: techniques for assessing status and trends in salmon and trout populations (D. H. Johnson, B. M. Shrier, J. S. O'Neal, J. A. Knutzen, X. Augerot, T. A. O'Neil, T. N. Pearsons, eds.), p. 173–195. Am. Fish. Soc., Bethesda, MD.

Wood, C. C., S. McKinnell, T. J. Mulligan, and D. A. Fournier.
1987. Stock identification with the maximum-likelihood mixture model: sensitivity analysis and application to complex problems. Can. J. Fish. Aquat. Sci. 44: 866–881.

National Marine Fisheries Service
NOAA

Fishery Bulletin
established in 1881

Spencer F. Baird
First U.S. Commissioner of Fisheries and founder of *Fishery Bulletin*

Flexible Bayesian analysis of the von Bertalanffy growth function with the use of a log-skew-*t* distribution

Freddy Omar López Quintero[1]
Javier E. Contreras-Reyes (contact author)[1,2]
Rodrigo Wiff[3]
Reinaldo B. Arellano-Valle[4]

Email address for contact author: javier.contreras@ifop.cl

[1] Departamento de Matemática
Universidad Técnica Federico Santa María
Avenida España 1680
Valparaíso 2390123, Chile

[2] División de Investigación Pesquera
Instituto de Fomento Pesquero
Avenida Almirante Blanco Encalada 839
Valparaíso 2361827, Chile

[3] Center of Applied Ecology and Sustainability
Pontificia Universidad Católica de Chile
Avenida Libertador Bernardo O'Higgins 328
Santiago 8331150, Chile

[4] Departamento de Estadística
Pontificia Universidad Católica de Chile
Avenida Vicuña Mackenna 4860
Santiago 7820436, Chile

Abstract—The von Bertalanffy growth function is the model most widely applied to describe growth in fish populations. Parameters describing this function usually are estimated from observed lengths at different ages by using maximum likelihood and by assuming Gaussian distributed errors. In harvested populations, observed length at age usually involves a high level of skewness and extreme values because of the size-selective sampling process. Some approaches, based on the maximum-likelihood method for making inferences, have been developed to resolve such issues. We propose a Bayesian framework for estimating growth parameters for nonlinear regression models—a framework that is based on the family of log-skew-*t* distributions and which provides an approach that is flexible enough for modeling the presence of asymmetries and heavy tails. This framework based on a method in which 1) the error accounts for both skewness and heavy-tailed distributions of a log-skew-*t* model, and 2) the observed length at each age has a heteroscedastic error distribution. The proposed method was applied and compared with the methods of previous models by using observed length-at-age data for the southern blue whiting (*Micromesistius australis*), an important fish species harvested in the southeast Pacific. Comparisons indicated that the proposed model is the best for describing data on southern blue whiting.

Manuscript submitted 6 January 2016.
Manuscript accepted 30 September 2016.
Fish. Bull. 115:13–26 (2017).
Online publication date: 27 October 2016.
doi: 10.7755/FB.115.1.2

The views and opinions expressed or implied in this article are those of the author (or authors) and do not necessarily reflect the position of the National Marine Fisheries Service, NOAA.

Growth is one of the most important measurable life-history traits in individual organisms because it is fundamental in creating an understanding of both population and ecosystem functions. Several models have been proposed to describe animal growth. The most widely applied model, however, is the von Bertalanffy growth function (VBGF; von Bertalanffy, 1938). This model has been used to describe length at age for a wide range of species across several taxa, such as mammals (English et al., 2012), birds (Tjørve and Tjørve, 2010), and reptiles (Lehman and Woodward, 2008), although it is most extensively applied to fish species (Pardo et al., 2013). The VBGF is based on principles underpinning the physiology of growth (von Bertalanffy, 1938; Wiff and Roa-Ureta, 2008), gives an adequate description of growth with the use of only 3 parameters, and states that the rate of growth of an individual is determined by the difference between the buildup of body mass and loss due to energy expenditures for maintenance. In harvested fish populations, the usual data available to estimate these parameters are cross-sectional, and a single length and age measurement is taken from each sampled individual. The VBGF describes the expected growth rate for the population, on the basis of length-at-age data composed of individuals with variable growth rates.

Maximum-likelihood techniques derived from Gaussian and log-Gaussian errors normally are used to estimate VBGF parameters (Millar, 2002; Siegfried and Sansó, 2006). Yet, in fish populations, this assumption often fails because these distributions are typically skewed, present heavy tails or have extreme values. Skewed distributions usually result from the size-selective sampling process (Montenegro and Branco, 2016). In addition, in harvested fish populations, an accumulative effect of fishing exploitation exists for size at age. Growth rates vary among individuals (Sainsbury, 1980), and fishing selectivity removes faster growing individuals from each particular

age class. Hence, the bias in sampling for length at age that favors fast-growing individuals of each age class (Taylor et al., 2005). Therefore, the assumption of Gaussianity to estimate parameters of the VBGF is not adequate (Contreras-Reyes and Arellano-Valle, 2013; Montenegro and Branco, 2016). Moreover, the assumption of Gaussianity implies that length may take negative values and, therefore, is nonsensical (Xiao, 1994; Millar, 2002).

Different approaches have been proposed to overcome this drawback and fitting the VBGF. They can be separated roughly into 2 categories. In the first one, models, such as the one in Taylor et al. (2005), provide a mechanistic approach to dealing with skewed length-at-age data, with a combined process of growth, selectivity, and mortality when fitting the VBGF. The second category is a more empirical approach in which skewed and heavy-tailed length-at-age data are modeled by using the maximum-likelihood method and assuming a non-Gaussian distribution (Contreras-Reyes and Arellano-Valle, 2013) and by using Bayesian analysis (Millar, 2002; Siegfried and Sansó, 2006). Millar (2002) proposed a Bayesian framework to estimate parameters of the VBGF, using a multiplicative error model with log-normal distribution. Contreras-Reyes and Arellano-Valle (2013) calculated the maximum-likelihood estimates for the VBGF with the family of skew- distributions (Azzalini and Capitanio, 2003), a flexible class that extends the known Student distribution (e.g., Geweke, 1993). Such models can incorporate asymmetric and heavy-tailed errors, with presence of heteroscedasticity (Montenegro and Branco, 2016). Contreras-Reyes et al. (2014) reanalyzed the skew- approach to incorporate a log-skew-*t* distribution under multiplicative error distribution.

In this study, we examined our proposed Bayesian method for estimating the VBGF parameters on the basis of a log-skew-*t* distribution. This new framework merges the benefits provided by Bayesian analysis (Siegfried and Sansó, 2006) and the log-skew-*t* distribution (Contreras-Reyes et al., 2014) for estimating parameters of the VBGF for harvested fish populations. Additionally, our approach allows for heteroscedasticity in errors, modeled as power and exponential functions (Contreras-Reyes and Arellano-Valle, 2013). This Bayesian framework is applied to data of length-at-age composition of southern blue whiting (*Micromesistius australis*), an important species fished in the southeast Pacific.

Materials and methods

Log-skew-*t* von Bertalanffy growth model

We let $L(x_i)$ be the expected value of the length related to an th individual at age x_i, $L_\infty > 0$, $K > 0$, $t_0 < \min\{x_1, \ldots x_n\}$, and n is the sample size. The VBGF defines growth in length as

$$L(x_i) = L_\infty(1 - e^{-K(x_i - t_0)}). \quad (1)$$

Equation 1 represents the simplest formulation of the VBGF, described by 3 parameters:

where L_∞ = the asymptotic length (in length units,e.g., centimeters);
K = the growth rate coefficient expressed per unit of time; and
t_0 = the theoretical age (usually in years) when the length is zero.

Parameters of the VBGF usually are estimated from observed length-at-age pairs, such as (x_i, y_i), $i = 1, \ldots, n$, where y_i is the ith observed length at age x_i. Equation 1 was described in terms of multiplicative structure (Millar, 2002; Siegfried and Sansó, 2006; Contreras-Reyes et al., 2014) for random errors:

$$y_i = L(x_i)\varepsilon_i, \quad (2)$$

where ε_i = non-negative random errors, usually assumed to be independent, identically distributed errors with a mean of 1. Given this assumption, the VBGF in Equation 2 corresponds to the nonlinear regression with multiplicative random errors. We easily recovered the additive structure of the original model in Equation 2 by applying log scale in the following way:

$$y_i' = L'(x_i) + \varepsilon_i', \text{ with } \log y_i', L'(x_i) = \log L_i = L_i', \text{ and}$$

$$\varepsilon_i' = \log \varepsilon_i, i = 1, \ldots, n, \quad (3)$$

in which ε_i' were assumed to be independent, identically distributed, random errors with zero mean.

Contreras-Reyes et al. (2014) assumed a log-skew-*t* distribution (Azzalini et al., 2003) for the multiplicative and heteroscedastic random errors. Specifically, they assumed that the multiplicative errors ε_i, $i = 1, \ldots, n$, were independent random variables following a log-skew-*t* distribution with parameters $\mu_i \in \mathbb{R}$ (location), $\sigma_i^2 > 0$ (scale and dispersion), $\lambda_i \in \mathbb{R}$ (skewness and shape), and $\nu > 0$ (degrees of freedom), a distribution that is denoted by

$$\varepsilon_i' \sim LST(\mu_i, \sigma_i^2, \lambda, \nu), i = 1, \ldots, n. \quad (4)$$

This approach is equivalent to considering that the transformed errors ε_i, $i = 1, \ldots, n$, are independent and have a skew distribution (Branco and Dey, 2001; Azzalini and Capitanio, 2003) denoted by

$$\varepsilon_i' \sim ST(\mu_i, \sigma_i^2, \lambda, \nu), i = 1, \ldots, n. \quad (5)$$

In turn, this notation indicates that the transformed response variables (lengths) are derived from

$$y_i' \sim ST(\mu_i + L_i', \sigma_i^2, \lambda, \nu), i = 1, \ldots, n. \quad (6)$$

namely, that the density of y_i' is given by

$$f(y_i' \mid x_i, \mu_i, \sigma_i^2, \lambda, \nu) = \frac{2}{\sigma_i} t(z_i; \nu) T\left(\lambda z_i \sqrt{\frac{\nu+1}{\nu+z_i^2}}; \nu+1\right), \quad (7)$$

$y_i' \in \mathbb{R}$,

where

$z_i = (y_i' - \mu_i - L_i') / \sigma_i$ is a standardized version of y_i',

$$t(z;\nu)=\frac{\Gamma\left[\frac{\nu+1}{2}\right]}{\Gamma(\nu/2)(\pi\nu)^{\frac{1}{2}}}\left(1+\frac{z^2}{\nu}\right)^{-\frac{\nu+1}{2}}, \quad (8)$$

$z \in \mathbb{R}$ is the symmetric Student-t density with v degrees of freedom, and $T(z;\nu)$ represents the respective cumulative distribution function. In other words, we assumed that the original response y_i followed a log-skew-t distribution (Marchenko and Genton, 2010), which is denoted by

$$y_i \sim LST(\mu_i + L_i, \sigma_i^2, \lambda, \nu), i = 1, \ldots, n. \quad (9)$$

We assumed that $\nu > 1$ and considered the first moment of the skew-t distribution (Branco and Dey, 2001); therefore, the extra parameter μ_i had tobe chosen as

$$\mu_i = \sqrt{\frac{\nu}{\pi}}\frac{\Gamma[(\nu-1)/2]}{\Gamma(\nu/2)}\frac{\lambda\sigma_i}{\sqrt{1+\lambda^2}}, \quad (10)$$

so that the transformed errors ε_i' have a zero mean. This condition ensured that $E(y_i') = L_i'$ and allowed us to identify the constant in the additive version of the regression model.

Heteroscedasticity was introduced by means of the dispersion parameters σ_i^2 and modeled by using a nonnegative function $m(\rho; x_i)$ depending on age x_i and a heteroscedastic parameter $\rho \in \mathbb{R}$ as $\sigma_i^2 = \sigma^2 m(\rho; x_i)$, where $\sigma^2 > 0$. When $\rho = 0$, homoscedasticity is recovered as $\sigma_i^2 = \sigma^2 m(0; x_i) = \sigma^2$. In our study, we considered 2 specific functions for modeling heteroscedasticity: the exponential function $m(\rho; x_i) = e^{\rho x_i}$ and the power function $m(\rho; x_i) = x_i^{2\rho}$. In both functions, if $m(0; x_i) = 1$, it corresponds to the homoscedastic case.

Asymmetry and heavy tails produced by extreme values of length-at-age data were controlled by the parameters of shape (λ) and degrees of freedom (ν).

Extension to a Bayesian framework

We advanced a Bayesian analysis for the log-skew-t VBGF described in the previous section. Therefore, we first noted from the independence assumption and Equation 7 that the likelihood function of the unknown parameter vector $\theta = (\beta^\top, \sigma^2, \rho, \lambda, \nu)^\top$ is

$$f(\mathbf{y}' \mid \mathbf{x}, \theta) = \prod_{i=1}^{n}\left(\frac{2}{\sigma_i}\right)t(z_i;\nu)T\left(\lambda z_i\sqrt{\frac{\nu+1}{\nu+z_i^3}};\nu+1\right), \quad (11)$$

where $\beta = (L_\infty, K, T_0)^\top$ are VBGF parameters, $\mathbf{y}' = (y_1', \ldots, y_n')^\top$, $\mathbf{x} = (x_1, \ldots, x_n)^\top$, and z_i is as it was previously defined. To complete our Bayesian model specification, we needed to elicit a prior distribution for the unknown parameter vector, say $\pi(\theta)$. Therefore, the Bayesian inference on θ (or function of θ) was based on the posterior distribution $\pi(\theta \mid \mathbf{x}, \mathbf{y}') \propto f(\mathbf{y}' \mid \mathbf{x}, \theta)\pi(\theta)$. This posterior distribution does not have a closed form (Cancho et al., 2011), but an estimation could still be calculated by using a Markov chain Monte Carlo (MCMC) algorithm (Chib and Greenberg, 1995; Cowles and Carlin, 1996; Robert and Casella, 2004).

Given the available methods, we chose to implement a hand-tailored component-wise Metropolis–Hasting transition scheme; in other words, we selected an approach in which θ is divided into individual pieces that are easily updated sequentially with a random walk algorithm. Our selection was based on simplicity and the need to control all steps in the sampling. Other options included the use of variants of BUGS language (Lunn et al., 2012), the AD ModelBuilder (Fournier et al., 2012), or Stan software (Gelman et al., 2015). Note that our selected approach is different from that followed by Siegfried and Sansó (2006), who employed an algorithm that included both Gibbs, as well as Metropolis–Hasting steps. An advantage of using this MCMC scheme is that the procedure is subdivided into several univariate steps. All proposal distributions were tuned to achieve acceptance rates of 25–45% (Robert and Casella, 2004). Specifically, we considered the different components of as independent (Siegfried and Sansó, 2006); in other words, $\pi(\theta)$ becomes the product of the marginal prior distributions of $(\beta^\top, \sigma^2, \rho, \lambda, \nu)$. It follows that only these marginal prior distributions must be elicited to complete our Bayesian model.

Prior distributions for the VBGF parameters β were chosen as follows. Given that L_∞ is strictly positive, we assumed a left truncated normal distribution with large variance (e.g., 100) as the prior distribution for this parameter. Other possible and natural choices were log-normal, gamma, or even distributions with support in a reasonable and restricted interval. Because parameters K and $-t_0$ are both positive, we used gamma as prior distributions for them (Xiao, 1994; Siegfried and Sansó, 2006). Contreras-Reyes et al. (2014) reported estimates of around 0.16 for southern blue whiting, a value that incidentally conforms to the value obtained by Siegfried and Sansó (2006) for blue shark (*Prionace glauca*). We used this information to specify that the mean of the gamma prior distribution of was around 0.15. For $-t_0$, Contreras-Reyes et al. (2014) obtained $-\hat{t}_0 = 2.5$,, which indicates a prior distribution for this parameter.

For the scale parameter σ^2, we considered the classical inverse gamma prior distribution suitable for this type of parameter (Zhang et al., 2009). The heteroscedastic parameter ρ usually takes positive or negative values. To give the full power of estimation to the data, we chose a noninformative prior, $\pi(\rho) \propto 1$. For the shape parameter λ, we set a normal prior distribution with a zero mean and large variance. The parameter defining the degrees of freedom, v, should be strictly larger than 2 to ensure the existence of variance in the log-skew-t model; therefore, we considered an exponential prior distribution with mean equaling 2 (Geweke, 1993; Cancho et al., 2011) and truncated at the interval $(2, \infty)$.These prior specifications are summarized in Table 1.

Comparisons and selection of models

For sake of comparison, we considered 2 additional models with constant variance function derived from the log-normal distribution. The first one (hereafter, re-

Table 1

Elicited prior specifications for log-normal and log-skew-t models used to examine a Bayesian analysis of the von Bertalanffy growth function. $TN_{(0,\infty)}(0,100)$ represents the $N(0,100)$-density truncated at $(0,\infty)$, and $TE_{(2,\infty)}(0.5)$ denotes the exponential density truncated at the $(2,\infty)$ interval. The parameters are the asymptotic length (L_∞), growth rate coefficient (K), theoretical age in years when the length is zero ($-t_0$), heteroscedasticity (ρ), inverted dispersion (σ^{-2}), skewness (λ), and degrees of freedom (ν).

Parameter	Log-normal (type I)	Log-normal (type II)	Log-skew-t
L_∞(cm)	$\pi(L_\infty) \propto 1$	$TN_{(0,\infty)}(0,100)$	$TN_{(0,\infty)}(0,100)$
$K(y^{-1})$	$Gamma(15,100)$	$Gamma(15,100)$	$Gamma(15,100)$
$-t_0$(y)	$Gamma(10,4)$	$Gamma(10,4)$	$Gamma(10,4)$
ρ	–	–	$\pi(\rho) \propto 1$
σ^{-2}	$Gamma(0.1,0.1)$	$Gamma(0.1,0.1)$	$Gamma(0.1,0.1)$
λ	–	–	$N(15,100)$
ν	–	–	$TE_{(2,\infty)}(0.5)$

ferred to as *type-I model*) was similar to that developed by Siegfried and Sansó (2006), and the second one included a modification of the prior distribution of L_∞ so that it was the same as that proposed in the log-skew-t model. All these prior specifications are summarized in Table 1. The following models were considered:

- Log-normal (type I) with constant variance function;
- Log-normal (type II) with constant variance function;
- Log-skew-t with constant variance function;
- Log-skew-t with exponential variance function;
- Log-skew-t with power variance function.

Selecting the "best" model is an important aspect in statistical analysis. In the rest of this section, we describe how we implemented the deviance information criterion (DIC) and the widely applicable information criterion (WAIC) for model selection.

Deviance information criterion The DIC proposed by Spiegelhalter et al. (2002) is based on the posterior mean of the deviance, and it can be approximated by the MCMC algorithm as follows:

$$\widehat{DIC} = 2\sum_{i=1}^{n}\left(\log f(y_i' \mid x_i,\bar{\theta}) - \frac{4}{B}\sum_{s=1}^{B}\log f(y_i' \mid x_i,\theta_s)\right), \quad (12)$$

where $\bar{\theta} = \frac{1}{B}\sum_{s=1}^{B}\theta_s$ is the mean of a sample $\theta_1,\ldots,\theta_B$ obtained from the posterior distribution $\pi(\theta \mid \delta)$. The DIC is related to the effective number of parameters:

$$\hat{p}_{DIC} = 2\left(\log f(\mathbf{y}' \mid \mathbf{x},\bar{\theta}) - \frac{1}{B}\sum_{s=1}^{B}\log f(\mathbf{y}' \mid \mathbf{x},\theta_s)\right). \quad (13)$$

The widely applicable information criterion The WAIC (e.g., Gelman et al., 2014) is based on the computed log-pointwise-posterior-predictive density, complemented by a correction for the effective number of parameters to adjust for overfitting:

$$\widehat{WAIC} = \sum_{i=1}^{n}\log\left(\frac{1}{B}\sum_{s=1}^{B}\log f(y_i' \mid x_i,\theta_s)\right) - \hat{p}_{WAIC}. \quad (14)$$

Also, the WAIC is related to the effective number of parameters:

$$\hat{p}_{WAIC} = 2\sum_{i=1}^{n}\left(\log\left(\frac{1}{B}\sum_{s=1}^{B}\log f(y_i' \mid x_i,\theta_s)\right) - \frac{1}{B}\sum_{s=1}^{B}\log f(y_i' \mid x_i,\theta_s)\right). \quad (15)$$

Compared with DIC, WAIC has the property of averaging over the posterior density by using each iterated θ_s, instead of being replaced by the mean $\bar{\theta}$. In addition, $\hat{p}_{WAIC}$ is more numerically stable than $\hat{p}_{DIC}$ because it averages separately for each observation y_i' (Gelman et al., 2014).

Influential analysis

The statistical stability of the proposed models exposed to perturbations of the data were analyzed by using influential analysis. We considered the Kullback–Leibler (KL) divergence measure (Kullback and Leibler, 1951) to quantify the effect on the inferences produced by excluding one observation or a group of observations from the full data set. The KL-divergence had been considered previously in Bayesian influential analysis for elliptical and skew-elliptical models (Arellano-Valle et al., 2000; Vidal et al., 2006).

We let $P = \pi(\theta \mid S)$ and $P_{-i} = \pi(\theta \mid S_{-i})$ be the posterior distribution of θ obtained from the full data $S = (\mathbf{x}, \mathbf{y}')$ and the data without the ith observation $S_{-i} = (\mathbf{x}_{-i}, \mathbf{y}'_{-i})$, respectively. The KL-divergence between P and P_{-i} was given by

$$K(P,P_{-i}) = \int \pi(\theta \mid S)\log\left\{\frac{\pi(\theta|S)}{\pi(\theta|S_{-i})}\right\}d\theta. \quad (16)$$

To identify influential observations, Peng and Dey (1995) showed that if $p_i >> 1/2$, where

$$p_i = \tfrac{1}{2}\left(1+\sqrt{1-e^{-2K(P,P_{-i})}}\right), \ \tfrac{1}{2} \le p_i \le 1, \quad (17)$$

then the ith observation is considered influential. Additionally, because the integral in Equation 16 cannot be written in closed form, it still can be approximated by sampling from the posterior distribution of θ via the MCMC algorithm. In fact, if $\theta_1,\ldots,\theta_B$ is a sample of size B from $\pi(\theta \mid S)$, then the MCMC estimator of $K(P,P_{-i})$ is computed as

$$\hat{K}(P,P_{-i}) = \log\left\{\frac{1}{\frac{1}{B}\sum_{s=1}^{B}\frac{1}{f(y_i' \mid \mathbf{x},\theta_s)}}\right\} + \frac{1}{B}\sum_{s=1}^{B}\log f(y_i' \mid \mathbf{x},\theta_s), \quad (18)$$

with $f(y_i' \mid \mathbf{x},\theta_s)$ given by Equation7 and $\theta_s = (\beta_s,\sigma_s^2,\rho_s,\lambda_s,\upsilon_s)^{\top}$ (e.g., Cancho et al., 2011). It should be noted that we computed the KL-divergence between P and P_{-i} using the ith marginal sample density $f(y_i' \mid \mathbf{x},\theta_s)$, but we did so without considering the posteriors $\pi(\theta \mid S)$ and $\pi(\theta \mid S_{-i})$.

In addition, given the new sample with removed observations, we quantified the change produced for each new estimate with respect to the full sample. In several cases, the estimates were notably different for these samples (Contreras-Reyes and Arellano-Valle, 2013). We used restricted data S_{-J} in which a set of J observations was removed. Then, we computed the percentage of relative change (RC) of estimates by following Contreras-Reyes and Arellano-Valle (2013). The RC was defined by

$$RC(\hat{\theta}_k,\hat{\theta}_{k,J}) = 100\left|1-\frac{\hat{\theta}_{k,J}}{\hat{\theta}_k}\right|, \quad (19)$$

where $\hat{\theta}_{k,J}$ and $\hat{\theta}_k$ are the posterior median estimates of kth component of θ obtained from the posterior distributions $\pi(\hat{\theta} \mid S_{-J})$ and $\pi(\hat{\theta} \mid S)$, respectively. Therefore, we computed the change (in percentage) of each parameter of the VBGF.

Application

Data We evaluated the performance of the proposed model, using the available data for southern blue whiting. This dataset was based on 24,942 individuals collected from a region spanning latitudes from 46°S to 6°S over the period 1997–2010 by the Instituto de Fomento Pesquero (Contreras-Reyes, unpubl. data). Random samples of fish were collected by onboard scientific observers during each catch haul of southern blue whiting were caught. All these fish were measured to the nearest centimeter, and both otoliths of each fish were extracted onboard. Otoliths were then taken to the laboratory, where age was determined by reading annual growth increments in the sagittal otoliths. The southern blue whiting is assumed to recruit once a year; therefore, age is treated as a discrete variable with a 1-year interval. Otolith age assignment involved killing sampled fish; therefore, each data point represents 1 individual fish. Fish in the catch had observed ages between 1 and 25 years and a size range of 20–75 cm in total length (Céspedes et al., 2013). Contreras-Reyes et al. (2014) reported extreme values in young and old age classes and reported asymmetry caused by fishing selectivity. Both these issues justify the use of heavy-tailed and skewed distributions in VBGF errors.

MCMC sampling For inference, 4 chains were selected from each applied Bayesian model. The length of the chains necessary to reach convergence differed depending on the treated model: it was around 20,000 iterations for all log-skew-t models and around 100,000 iterations for the log-normal homoscedastic model. We considered a burn-in period to be 10,000 iterations for the first model and 20,000 for the log-normal homoscedastic model. In addition, all models conformed with the traditional diagnostic convergence tests, such as Geweke and Heidelberger–Welch, when tests were applied to individual chains (Cowles and Carlin, 1996; Carlin and Louis, 2000). However, results of the Raftery–Lewis test, also applied to individual chains, indicated that we should take the largest thinning of chains (Link and Eaton, 2011) because values were highly correlated. In addition, visual examination throughout trace and autocorrelation plots (not shown) indicated that convergence was reached for all parameters in all models. This situation was transferred to the effective sample size, which can be interpreted as the number of independent samples necessary to yield the same precision as the (serially dependent) MCMC samples. Effective sample size is especially important in resampling and should not be confused with the degree of over dispersionusually found in length-at-age compositions.

For all models, the parameters with higher and lower values of effective sample size were υ and K, respectively. Finally, $\hat{R}$ Gelman's indexes (Gelman and Rubin, 1992) were all near 1, indicating that the specific parameter had good convergence after the burn-in period was eliminated. This test was applied to 4 chains for each parameter and each model.

Software Statistical methods used in this article were implemented in the software R, vers. 3.1.0 or higher (R Core Team, 2014). The MCMC was developed in C++ embedded in the R package RcppArmadillo, vers. 0.4.300.0 or higher (Eddelbuettel and Sanderson, 2014). Diagnostic analysis was conducted with the coda package, vers. 0.16-1 or higher, in R (Plummer et al., 2006). Von Bertalanffy growth curves were estimated in each realization by simulating estimated parameters several times (e.g., 10,000) with the models proposed previously in the *Comparisons and selection of models* section. Such simulated observations are called *fake data*, according to Gelman and Hill (2007, Ch. 16). Afterward, the 95% highest posterior density (HPD) was computed across ages. The generation of the log-skew-t values was conducted by using fake data in the R package sn, vers. 0.4-11 (Azzalini, 2008).

Table 2

Values from models fitted to simulated length-at-age data after log-skew-t distribution with constant variance, with asymptotic length (L_∞) = 59.72, growth rate coefficient (K) = 0.16, theoretical age in years when the length is zero ($-t_0$) = 2.5, heteroscedasticity(ρ) = –0.5, and dispersion (σ^2) = 0.05 considered by ranging the parameters of skewness (λ) and degrees of freedom (ν) in the set {–3, –1,0}×{3,12,100}.

		(λ, ν)								
Model	Parameter	(–3,3)	(–3,12)	(–3,100)	(–1,3)	(–1,12)	(–1,100)	(0,3)	(0,12)	(0,100)
Log-normal (type I)										
Constant	L_∞	56.789	57.568	57.458	57.519	57.790	57.923	59.717	59.665	59.653
	K	0.158	0.157	0.160	0.155	0.161	0.163	0.161	0.164	0.164
	$-t_0$	2.603	2.541	2.530	2.652	2.491	2.427	2.430	2.381	2.354
	σ^2	0.004	0.002	0.001	0.006	0.002	0.002	0.011	0.003	0.003
Log-normal (type II)										
Constant	L_∞	56.797	57.578	57.456	57.595	57.810	57.938	59.739	59.635	59.640
	K	0.157	0.157	0.160	0.154	0.161	0.163	0.160	0.164	0.164
	$-t_0$	2.606	2.545	2.529	2.684	2.502	2.435	2.445	2.377	2.351
	σ^2	0.004	0.002	0.001	0.006	0.002	0.002	0.011	0.003	0.003
Log-skew-t										
Constant	L_∞	56.570	57.179	57.346	57.395	57.965	57.859	59.809	59.614	59.654
	K	0.160	0.161	0.161	0.160	0.159	0.163	0.153	0.163	0.163
	$-t_0$	2.521	2.453	2.501	2.515	2.518	2.460	2.644	2.403	2.373
	σ^2	0.003	0.003	0.003	0.003	0.004	0.003	0.003	0.004	0.004
	λ	–3.842	–3.627	–3.266	–1.375	–1.683	–1.718	–0.472	–0.885	–1.224
	ν	3.626	16.640	18.471	3.640	11.739	17.457	3.130	13.739	16.752
Log-skew-t										
Exponential	L_∞	56.886	57.651	57.520	57.645	57.801	58.059	59.993	59.624	59.700
	K	0.158	0.156	0.159	0.155	0.161	0.160	0.153	0.163	0.162
	$-t_0$	2.490	2.510	2.491	2.590	2.473	2.490	2.640	2.403	2.372
	ρ	–0.125	–0.121	–0.126	–0.107	–0.117	–0.144	–0.135	–0.069	–0.049
	σ^2	0.005	0.005	0.004	0.006	0.006	0.006	0.005	0.005	0.005
	λ	–3.517	–3.528	–2.917	–1.196	–1.713	–1.458	–0.249	–0.545	–1.126
	ν	3.217	11.846	15.961	3.296	10.977	15.346	2.804	12.430	15.929
Log-skew-t										
Power	L_∞	56.929	57.645	57.495	57.691	57.829	58.049	59.951	59.610	59.705
	K	0.155	0.155	0.159	0.153	0.160	0.160	0.153	0.163	0.162
	$-t_0$	2.570	2.553	2.512	2.635	2.503	2.487	2.647	2.403	2.382
	ρ	–0.023	–0.021	–0.020	–0.021	–0.023	–0.025	–0.022	–0.007	–0.003
	σ^2	0.004	0.004	0.003	0.005	0.005	0.004	0.004	0.004	0.004
	λ	–3.702	–3.670	–3.075	–1.291	–1.778	–1.585	–0.342	–0.863	–1.198
	ν	3.341	13.131	17.094	3.476	11.855	16.640	2.940	13.372	16.574

Results

Simulations

To assess the effect of error distribution in the VBGF parameters, length-at-age data were simulated from a log-skew-t distribution with a constant variance and the estimated growth parameters of Contreras-Reyes et al. (2014) (see the *Comparisons and selection of models* section). Different cases were evaluated by considering a range for λ and ν in the set of {–3,–1,0}×{3,12,100} (Table 2). This procedure permits assessment of the closeness of estimates in absence and presence of skewness and heavy-tailed simulated data. Each simulation considered 30,000 realizations. For λ = –3, estimates of L_∞ indicated the largest differences with real values, and the smaller differences were reported in K and $-t_0$. The largest differences of ν for estimated and simulated data were produced for ν = 100 (which approximates the log-skew-normal distribution) and for λ = 0 (which approximates the log-normal distribution). The log-skew-t model presented estimates similar to the initial parameters λ = –1 and ν = 12.

Modeling data from southern blue whiting

In the case of the parameters of error distribution, the σ^2 posterior estimates are small values because of the application of the log-transformation, and the υ posterior estimates are smaller than 15, indicating the presence of extreme values (Table 3). In these models, the shape parameters λ are close to –1, indicating a non-

Table 3

Estimates from fitted log-normal and log-skew-*t* models, with standard deviations (SDs) and 95% highest posterior density (HPD) intervals. The parameters are the asymptotic length (L_∞), growth rate coefficient (K), theoretical age in years when the length is zero ($-t_0$), dispersion (σ^2), heteroscedasticity (r), skewness (λ), and degrees of freedom (ν).

Model	Parameter	Estimate	SD	95% HPD
Log-normal (type I)				
Constant	L_∞	59.249	0.091	(59.064, 59.439)
	K	0.167	0.001	(0.165, 0.170)
	$-t_0$	2.323	0.035	(2.250, 2.396)
	σ^2	0.004	3×10−5	(0.0042, 0.0044)
Log-normal (type II)				
Constant	L_∞	59.249	0.090	(59.060, 59.425)
	K	0.167	0.001	(0.165, 0.170)
	$-t_0$	2.323	0.034	(2.248, 2.391)
	σ^2	0.004	0.000	(0.0042, 0.0044)
Log-skew-*t*				
Constant	L_∞	59.212	0.086	(59.055, 59.386)
	K	0.166	0.001	(0.164, 0.169)
	$-t_0$	2.382	0.034	(2.322, 2.454)
	σ^2	0.005	1×10−4	(0.0047, 0.0053)
	λ	−1.012	0.051	(−1.105, −0.916)
	ν	11.020	0.643	(9.853, 12.210)
Log-skew-*t*				
Exponential	L_∞	59.666	0.085	(59.527, 59.815)
	K	0.161	0.001	(0.159, 0.163)
	$-t_0$	2.488	0.036	(2.428, 2.549)
	ρ	−0.039	0.002	(−0.043, −0.035)
	σ^2	0.008	2×10−4	(0.007, 0.008)
	λ	−1.080	0.050	(−1.181, −0.977)
	ν	13.351	0.884	(11.757, 15.144)
Log-skew-*t*				
Power	L_∞	59.573	0.090	(59.386, 59.755)
	K	0.162	0.001	(0.159, 0.165)
	$-t_0$	2.454	0.042	(2.367, 2.541)
	ρ	−0.180	0.009	(−0.197, −0.161)
	σ^2	0.011	0.001	(0.010, 0.013)
	λ	−1.096	0.053	(−1.200, −0.997)
	ν	14.322	1.047	(12.457, 16.586)

symmetric length-at-age distribution. In addition, log-normal models yielded very similar posterior estimates for VBGF and σ^2. Interestingly, standard errors for all parameters were very precise, in a similar way to that of previous studies of frequentist inference (Contreras-Reyes and Arellano-Valle, 2013; Contreras-Reyes et al., 2014). This level of precision probably is a result of a strong underlying structure of the data.

Using the DIC and WAIC criteria of Equations 12 and 14, respectively, we found the log-skew-*t* model with power heteroscedastic function to be the best model (Table 4). As Table4 indicates, the log-normal model is the least useful among the selected models.

The fitted curve of the power-variance log-skew-*t* model to the observed length-at-age data is presented in Figure 1A. The model is adequate for younger ages (1–8 years), but for older ages (>15 years) the observed length tends to converge to $\hat{L}_\infty = 59.52$ (Table 3). The log-skew-*t* model provides more precise 95% HPD intervals for older ages (>13 years; Fig. 1B) and less precise for young ages (0–5 years) in comparison with the log-normal model. Intervals of 95% HPD of log-skew-*t* model fit indicate that the observations were affected by the negative heteroscedastic parameter $\hat{\rho}$ (Fig. 1C). In addition, constant variance was assumed for the log-normal model and, therefore, the model underestimated the real variance in the age at length containing extreme values. The posterior densities of VBGF and variance parameters corresponding with the homoscedastic log-normal and power-variance log-skew-*t* models are compared in Figure 2. The asymmetry and dispersion of the posterior densities of VBGF were similar for the different error distributions. However, for the variance parameter, the posterior density was leptokurtic when log-normal error distribution was used.

Considering the boxplots of residuals by age from

Table 4

Summary of chain diagnostics for the fitted models: effective sample size (ESS), credibility $\hat{R}$ of Gelman index, Geweketest (G), Heidelberger–Welch test (HW), and Raftery–Lewis test (RL). In addition, the deviance information criterion (DIC) and widely applicable information criterion (WAIC) values for each model are reported, with their estimated number of parameters, p_{DIC} and p_{WAIC}, respectively. The parameters are the asymptotic length (L_∞), growth rate coefficient (K), theoretical age in years when the length is zero ($-t_0$), dispersion (σ^2), heteroscedasticity (ρ), skewness (λ), and degrees of freedom (ν).

Model	Parameter	ESS	$\hat{R}$	G	HW	RL	DIC	p_{DIC}	WAIC	p_{WAIC}
Log-normal (type I)										
Constant	L_∞	1134.673	1.002	1.543	0.817	39.4	−65275.66	4.338	−65275.66	7.079
	K	760.156	1.003	−1.241	0.850	82.6				
	$-t_0$	934.834	1.003	1.518	0.799	63.0				
	σ^2	52477.971	1.000	1.111	0.572	4.6				
Log-normal (type II)										
Constant	L_∞	749.129	1.005	−1.891	0.226	32.4	−65275.659	4.338	−66623.850	8.181
	K	463.168	1.008	1.499	0.050	50.3				
	$-t_0$	569.197	1.008	−1.817	0.456	35.3				
	σ^2	29883.554	1.000	1.510	0.093	3.4				
Log-skew-t										
Constant	L_∞	211.801	1.022	1.665	0.143	14.9	−66231.757	2.918	−66227.642	6.133
	K	81.302	1.037	−1.118	0.500	30.0				
	$-t_0$	91.705	1.041	1.230	0.393	60.5				
	σ^2	656.456	1.002	1.662	0.654	6.7				
	λ	596.318	1.004	−1.598	0.638	13.3				
	ν	1927.670	1.005	−1.232	0.408	5.1				
Log-skew-t										
Exponential	L_∞	204.714	1.054	−1.174	0.436	8.2	−66559.569	6.420	−66556.535	9.048
	K	112.927	1.077	1.232	0.471	43.7				
	$-t_0$	162.885	1.078	−1.696	0.264	16.9				
	ρ	561.808	1.013	−1.335	0.504	8.5				
	σ^2	179.131	1.029	1.015	0.673	116.0				
	λ	1404.850	1.010	1.490	0.247	8.7				
	ν	856.653	1.007	−0.771	0.159	10.9				
Log-skew-t										
Power	L_∞	200.944	1.008	−1.293	0.087	7.7	−66625.510	6.482	−66623.850	8.181
	K	99.489	1.052	0.979	0.086	16.0				
	$-t_0$	128.952	1.053	−1.223	0.052	16.9				
	ρ	706.436	1.008	−0.580	0.096	8.7				
	σ^2	189.195	1.029	0.631	0.615	23.6				
	λ	1656.937	1.004	1.700	0.355	5.6				
	ν	289.711	1.016	−0.481	0.495	24.5				

the fitted log-skew-t model (Fig. 3), we can observe that residuals indicate a flat pattern and that their mean is concentrated around zero. We noted also a decreasing variance in older fish, produced in part by the negative value of the estimated heteroscedasticity ($\hat{\rho}$ = −0.18). Furthermore, extreme values for younger and older fish (<6 and >15 years) were detected by the estimated degree of freedom ($\hat{\upsilon}$ =14.32; Table 3).

Influential analysis

Peng–Dey's criterion (Eq. 17, p_i = 0.5) is suitable for certain nonlinear regression models with normal errors and many observations are considered influential (Fig. 4). As expected, we found that the log-normal model has more influential observations than the power log-skew-t model for each probability. Therefore, we selected, in Table 5, only the probabilities 0.70, 0.60, 0.55, and 0.51 for those influential observations in log-normal and power log-skew-t models. For the selected model, when p_i = 0.51, the largest number of restricted observations was recorded and the RC of the error distribution parameters was raised. When the number of influential observations increased (in terms of the p_i) and were removed, the degree of freedom parameter also increased. Because several of these observations are extreme values (Contreras-Reyes et al., 2014), the error distribution shifts from log-skew-t to log-skew-t

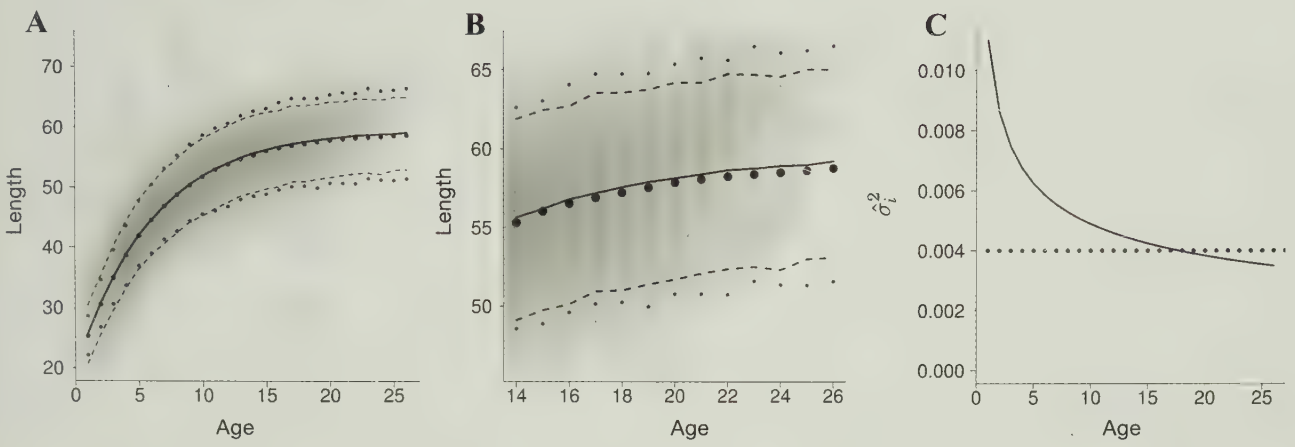

Figure 1

(**A**) Observations of length-at-age composition for southern blue whiting (*Micromesistius australis*) collected from a region spanning latitudes 46°S to 56°S over the period 1997–2010 (gray shaded areas), with von Bertalanffy growth function (VBGF) fits: the solid black line corresponds to the fit of the log-skew-model with a heteroscedastic power variance function (Table 3). Black points correspond to the log-normal model fit with constant (homoscedastic) variance function (Table 3). Gray dotted lines and points correspond to the 95% highest posterior density intervals for log-skew-*t* and log-normal model fits, respectively. (**B**) The log-skew-*t* model fit includes the respective zoom subplot for fish at ages 14–26. (**C**) Heteroscedastic variance function ($\hat{\sigma}_i^2$) for log-skew-*t* (solid line) and log-normal (points) model fits.

normal. Among the VBGF parameters, $-t_0$ showed the largest RC variation, although RC values of the VBGF parameters were small given the absence of influential observations.

The relationship between the paucity of observations for young (1–5 years) and old (16–24 years) age classes and heteroscedastic variance can be interpreted from Table 5 for the cases when p_i = 0.55 and 0.51 as follows. For p_i = 0.55, 67.5% and 17.5% of young and old individuals, respectively, were obtained for the sample from 40 influential observations. For p_i = 0.51, 35.4% and 23.0% of young and old individuals were obtained for the sample, respectively, from 3106 influential observations. When the estimates for $\tilde{\sigma}^2$, $\hat{\nu}$, and $\hat{\rho}$, from the *Log-skew-t von Bertalanffy growth model* section, were considered, the heteroscedastic variance σ_i^2 decreased mainly when young and old individuals (extreme values) were excluded from the sample.

Correlation analysis

An important aspect in fisheries research related to VBGF analysis is the correlation between parameters (Pilling et al., 2002; Siegfried and Sansó, 2006; Shelton and Mangel, 2012). High correlation among the 3VBGF parameters is common in fish populations (Ratkowsky, 1986; Pardo et al., 2013). Correlation between parameters was analyzed by using the scatter plots in Figure 5. The highest correlation was found between K and $-t_0$ (–0.94), followed by the correlation between L_∞ and K (–0.89) (Xiao, 1994; Pilling et al., 2002; Siegfried and Sansó, 2006) and by the correlation between L_∞ and $-t_0$ (0.71) (Ratkowsky, 1986; Pilling et al., 2002). Ratkowsky (1986) found that correlations between VBGF parameters may depend on the parameters that are used. Other choices of parameters should produce a low correlation between the VBGF parameters. However, in our model, the solution for K is affected by values of L_∞ and $-t_0$ under the classical VBGF parametrization.

The relationship between estimates of L_∞ and K are similar to the ones found by Siegfried and Sansó (2006), but, in contrast to their results, we found a large correlation between (K, $-t_0$) and (L_∞,$-t_0$). This finding could have occurred for different reasons, such as the species studied and the specific Bayesian method employed. However, the use of maximum-likelihood estimation (not shown) also verified high correlations between those parameters. The scatter plots did not show a clear correlation for error distribution parameters, except for the relationship between σ^2 and ρ given by the heteroscedastic power function, where the correlation was –0.82.

Discussion

In this study, we embedded previous log-skew-*t* distribution analyses in a Bayesian framework. This approach, namely using log-skew-*t* distribution, has several advantages over previous frequentist inference. First, in a Bayesian framework, prior knowledge of the model parameters can be included in the modeling process in terms of a prior distribution, and our inferences were based on the posterior distribution, therefore, allowing

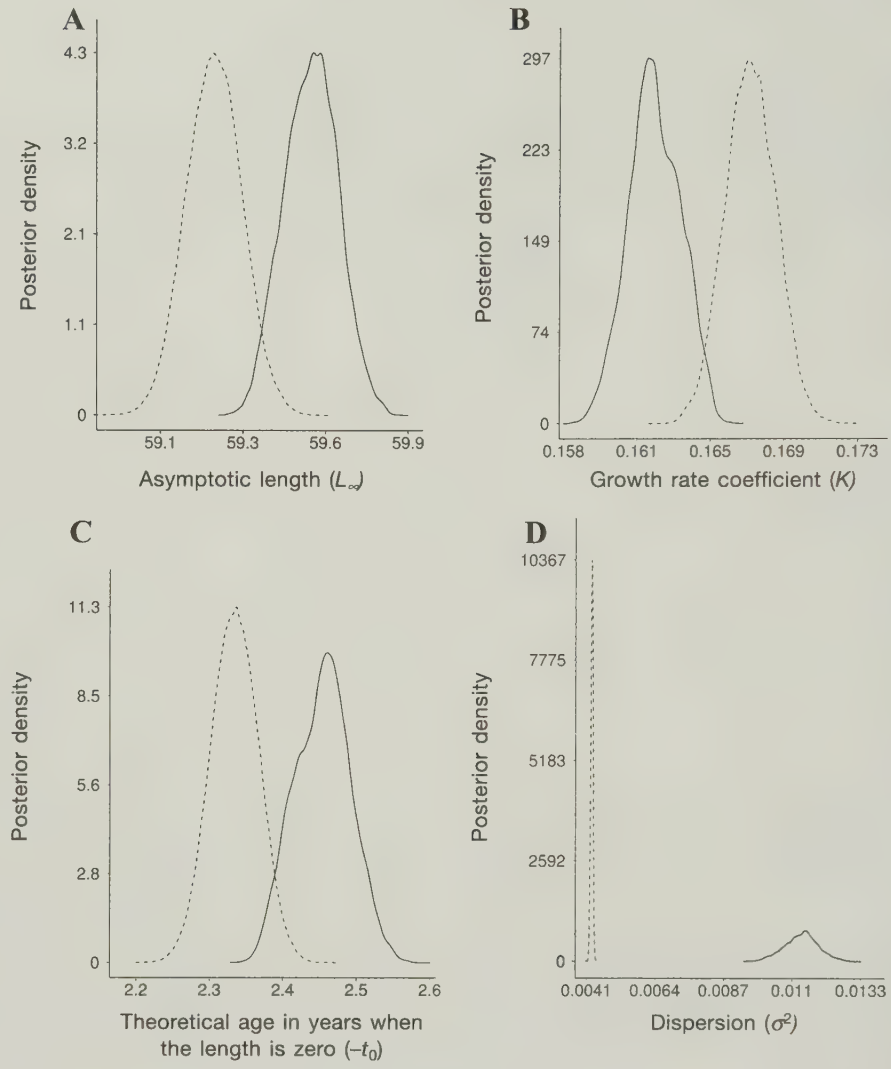

Figure 2

Posterior densities for estimates of 3 von Bertalanffy growth function (VBGF) parameters, (**A**) asymptotic length (L_∞), (**B**) growth rate coefficient (K), (**C**) theoretical age in years when the length is zero ($-t_0$), and (**D**) dispersion (σ^2) estimates of from the log-skew-t model with power heteroscedastic variance (solid line) and the homoscedastic log-normal model (dotted line).

for probability statements for our statistical conclusions. Second, the degrees of freedom parameter v is directly estimated from the posterior density, whereas, in the frequentist approach used by Contreras-Reyes and Arellano-Valle (2013) and Contreras-Reyes et al. (2014), they are obtained manually by using profiles of the log-likelihood function. Thirdly, an additional parameter λ is also considered by the log-skew-t approach, allowing us to model different degrees of skewness in data—something that the traditional log-normal model does not make possible. Finally, boundary restrictions on each prior density can be incorporated in Bayesian analysis, and avoids deriving nonsensical parameters of the VBGF (Gasbarra et al., 2007).

Contreras-Reyes et al. (2014) computed the VBGF for both sexes in southern blue whiting using the maximum-likelihood method and a heteroscedastic log-skew-t model. Estimates reported in Contreras-Reyes et al. (2014) are similar to those reported here for southern blue whiting, except for the heteroscedastic parameter ρ. In this study, $\hat{\rho}$ was significantly higher than the one reported in Contreras-Reyes et al. (2014) because a prior distribution was specified for the heteroscedastic parameter. This specification allows us to model the decreasing variance of lengths better across ages, given the paucity of observations in young (1–5 years) and older (16–24 years) fish (Fig. 1C). An adequate modeling of variance, especially in young ages,

Table 5

Summary of the log-skew-*t* model fitted with power heteroscedastic variance function for the full and restricted data and its respective percentage of relative change (RC) for the probabilities (p_i), of 0.70, 0.60, 0.55 and 0.51. The parameters are the asymptotic length (L_∞), growth rate coefficient (K), theoretical age in years when the length is zero ($-t_0$), heteroscedasticity (ρ), dispersion (σ^2), skewness (λ), degrees of freedom (ν), sample size (n), and number of influential observations (Influ. observ.).

	Restricted data (S_{-1})							
Parameters	$p_i = 0.70$	RC (%)	$p_i = 0.60$	RC (%)	$p_i = 0.55$	RC (%)	$p_i = 0.51$	RC (%)
L_∞ (*cm*)	59.559	0.024	59.550	0.039	59.445	0.215	59.588	0.025
K (y^{-1})	0.163	0.617	0.163	0.617	0.164	1.235	0.161	0.617
$-t_0$ (y)	2.446	0.326	2.455	0.041	2.391	2.567	2.501	1.915
ρ	−0.179	0.556	−0.180	0.000	−0.168	6.667	−0.141	21.667
σ^2	0.012	9.091	0.013	18.182	0.012	9.091	0.008	27.273
λ	−1.181	7.755	−1.231	12.318	−1.305	19.069	−1.801	64.325
ν	19.198	34.046	22.304	55.732	30.223	111.025	80.796	464.139
n	24936		24932		24902		21836	
Influ. observ.		6		10		40		3106

will improve the estimation of t_0. In addition, considering the influential analysis, the estimated parameters from the restricted data indicate significant differences with those obtained with the full data set, particularly for the degree of freedom parameter of the error distribution. However, numerous subjects were not evaluated in this article—topics such as other sources of uncertainly or data-related problems that can lead to bias in an estimation (Ortiz and Palmer[1]). Particularly, we did not address the direct influence of the prior specification on the final estimates (Fig. 5C), a topic that will be of interest for future research.

Siegfried and Sansó (2006) and Hamel (2015) considered log-normal distributions to be appropriate for the asymmetry observed in the length-at-age data in harvested fish populations. However, in such data, we can usually find different degrees of skewness and heavy-tailed and extreme values in which log-normal distribution does not give a good description of observations. The log-normal model may underestimate the real variance contained in the data (Slatkin, 2013). In such cases, log-skew-*t* models (such as the one proposed here), could yield a fair description of the observed length-at-age data, as was the case for the southern blue whiting, in which the log-skew-*t* model turned out to be the best among all competing models. In addition, the proposed model gives great flexibility in modelling heteroscedasticity by adding a function dependent on the scale of σ^2 and a heteroscedastic parameter ρ. The assumption of asymmetry and heavy tails and the log-transformed nature of the log-skew-*t* model reduces the standard errors of the estimated parameters of the VBGF (Contreras-Reyes et al., 2014).

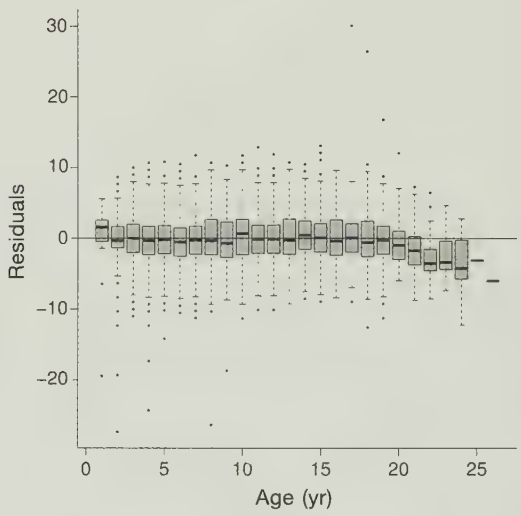

Figure 3

Boxplots of residuals versus ages of southern blue whiting (*Micromesistius australis*) from the log-skew-*t* model with power heteroscedastic function. The dark black lines correspond to the observed median, the gray shaded boxes represent the observed interval from the 25% residual quartile to the 75% residual quartile, the error bars are the observed interval from minimum to maximum residual value, and the dots are atypical residual values.

The Bayesian analysis that we developed and describe in this article provides a flexible framework that allows biologically meaningful estimates of the VBGF. This method also takes into account the uncertainty and kurtosis produced by extreme values common in

[1] Ortiz, M., and C. Palmer. 2008. Review and estimates of von Bertalanffy growth curves for king mackerel Atlantic and Gulf of Mexico stock units. SEDAR16-DW-12, 20 p. [Available at website.]

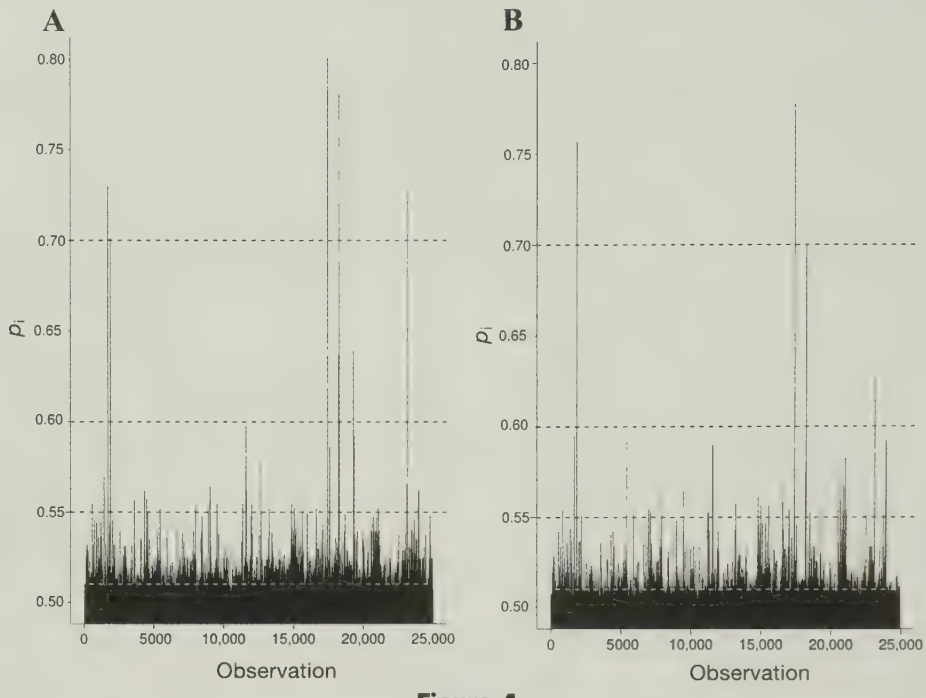

Figure 4

Probabilities (p_i) derived according to Kullback-Leibler divergence criteria for the (**A**) log-normal and (**B**) power log-skew-*t* models. The dotted lines are the probabilities of 0.51, 0.55, 0.60, and 0.70.

length-at-age data (Quiroz et al., 2010; Montenegro and Branco, 2016). This framework is particularly relevant when dealing with harvested fish populations for which length-at-age data collected from fishing operations usually contain missing observations and indicate bias toward fast-growing individuals of each age class. A correct specification of the VBGF is critical because growth is an important aspect of contemporary stock assessment models (Zhu et al., 2016) upon which biomass estimates and conservation measures are based.

Acknowledgments

The authors are grateful to the Instituto de Fomento Pesquero (Valparaíso, Chile) for providing access to the data used in this work. The research of F. López Quintero was supported partially by a doctoral grant from Pontificia Universidad Católica de Valparaíso (Valparaíso, Chile). The research of J. Contreras-Reyes was supported partially by Comisión Nacional de Investigación Científico y Tecnológico (CONICYT) doctoral scholarship 2016 number 21160618 (Res. Ex. 4128/2016). R. Wiff was funded by Fondo Nacional de Desarrollo Científico y Tecnológico (FONDECYT) postdoctoral project number 3130425 and by the Center of Applied Ecology and Sustainability (CAPES) project CONICYT FB 0002. R. Arellano-Valle was funded by FONDECYT (Chile) grants 1120121 and 1150325. We are sincerely grateful to 3 anonymous reviewers for their comments and suggestions that greatly improved an early version of this manuscript.

Literature

Arellano-Valle, R. B., M. Galea-Rojas, and P. Iglesias Zuazola.
2000. Bayesian sensitivity analysis in elliptical linear regression models. J. Stat. Plann. Inference 86:175–199.

Azzalini, A.
2008. The R package sn: the skew-normal and skew-t distributions (version 0.4-6). [Available at website.]

Azzalini, A., and A. Capitanio.
2003. Distributions generated by perturbation of symmetry with emphasis on a multivariate skew t-distribution. J. R. Stat. Soc., B 65:367–389.

Azzalini, A., T. del Cappello, and S. Kotz.
2003. Log-skew-normal and log-skew-*t* distributions as models for family income data. J. Income Distrib. 11:12–20.

Branco, M., and D. K. Dey.
2001. A general class of multivariate skew-elliptical distributions. J. Multivariate Anal. 79:93–113.

Cancho, V. G., D. K. Dey, V. H. Lachos, and M. G. Andrade.
2011. Bayesian nonlinear regression models with scale mixtures of skew-normal distributions: estimation and case influence diagnostics. Comput. Stat. Data Anal. 55:588–602.

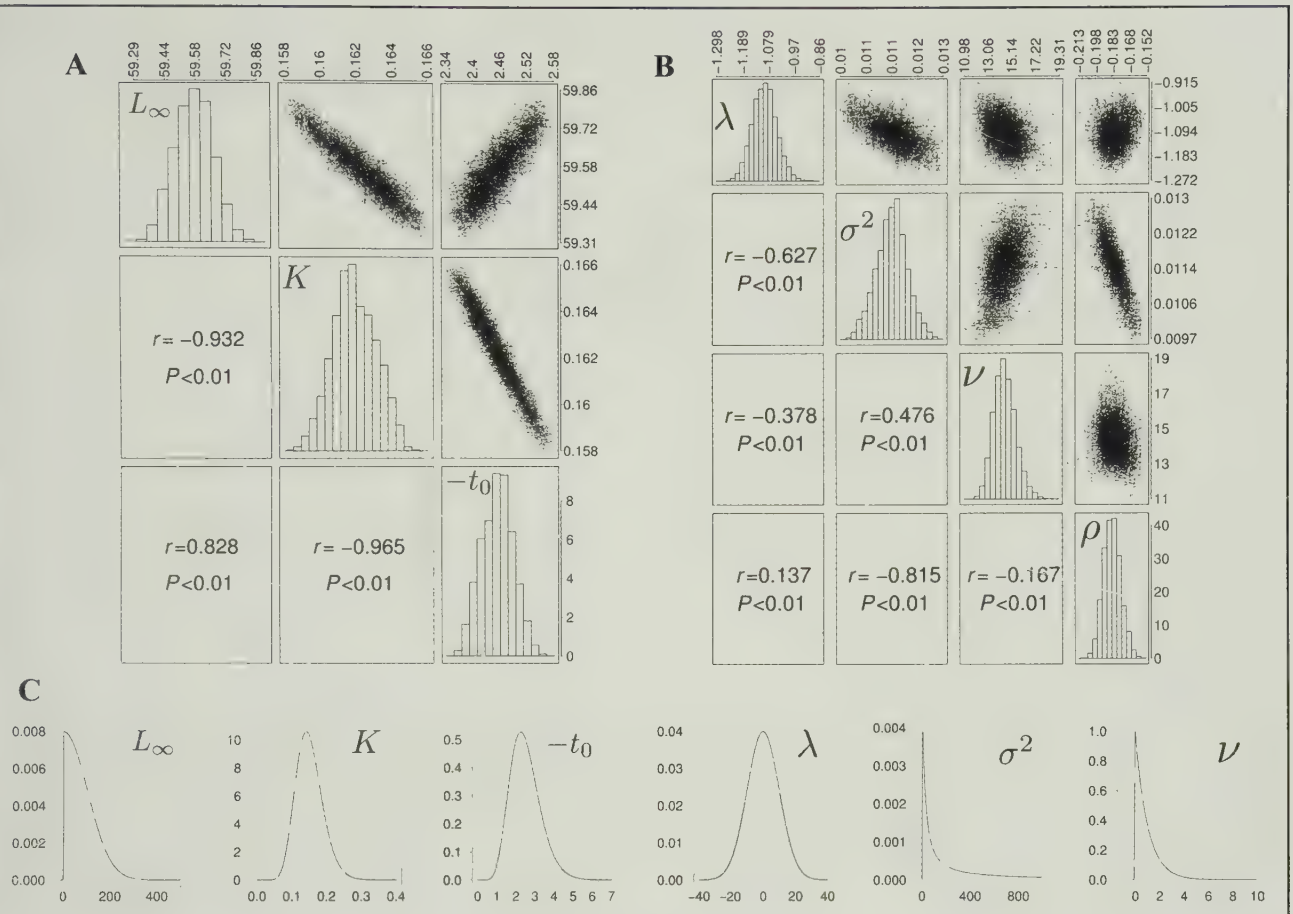

Figure 5

Histograms and scatter plots for (**A**) asymptotic length ($\hat{L}_\infty$), growth rate coefficient ($\hat{K}$), and theoretical age in years when the length is zero ($\hat{t}_0$) and for (**B**) skewness ($\hat{\lambda}$), dispersion ($\hat{\sigma}^2$), degrees of freedom ($\hat{\nu}$), and heteroscedasticity ($\hat{\rho}$), related to the log-skew-*t* model with power heteroscedastic function. (**C**) Prior densities of all parameters, except for ρ ($\rho \propto 1$). For all plots, *r* is the Pearson correlation coefficient and is presented with its corresponding *P*-value.

Carlin, B. P., and T. A. Louis.
2000. Bayes and empirical Bayes methods for data analysis, 2nd ed., 440 p. Chapman & Hall/CRC, Boca Raton, FL.

Céspedes, R., V. Ojeda, L. Adasme, L. Muñoz, K. Hunt, L. Cid, M. Miranda, and A. Villalón.
2013. Programa de seguimiento de las pesquerías demersales y aguas profundas, 2013: demersales sur austral, 175 p. Instituto de Fomento Pesquero, Valparaíso, Chile.

Chib, S., and E. Greenberg.
1995. Understanding the Metropolis-Hastings algorithm. Am. Stat. 49:327–335.

Contreras-Reyes, J. E., and R. B. Arellano-Valle.
2013. Growth estimates of cardinalfish (*Epigonus crassicaudus*) based on scale mixtures of skew-normal distributions. Fish. Res. 147:137–144.

Contreras-Reyes, J. E., R. B. Arellano-Valle, and T. Mariella Canales.
2014. Comparing growth curves with asymmetric heavy-tailed errors: application to southern blue whiting (*Micromesistius australis*). Fish. Res. 159:88–94.

Cowles, M. K., and B. P. Carlin.
1996. Markov chain Monte Carlo convergence diagnostics: a comparative review. J. Am. Stat. Assoc. 91:883–904.

Eddelbuettel, D., and C. Sanderson.
2014. RcppArmadillo: accelerating R with high-performance C++ linear algebra. Comput. Stat. Data Anal. 71:1054–1063.

English, S., A. W. Bateman, and T. H. Clutton-Brock.
2012. Lifetime growth in wild meerkats: incorporating life history and environmental factors into a standard growth model. Oecologia 169:143–153.

Fournier, D.A., H. J. Skaug, J. Ancheta, J. Ianelli, A. Magnusson, M. N. Maunder, A. Nielsen, and J. Sibert.
2012. AD Model Builder: using automatic differentiation for statistical inference of highly parameterized complex nonlinear models. Optim. Methods Softw. 27:233–249.

Gasbarra, D., M. Pirinen, M. J. Sillanpää, E. Salmela, and E. Arjas.
2007. Estimating genealogies from unlinked marker data: a Bayesian approach. Theor. Popul. Biol. 72:305–322.

Gelman, A., and D. B. Rubin.
1992. Inference from iterative simulation using multiple sequences. Stat. Sci. 7:457–511.
Gelman, A., and J. Hill.
2007. Data analysis using regression and multilevel/hierarchical models, 625 p. Cambridge Univ. Press, Cambridge, UK.
Gelman, A., J. Hwang, and A. Vehtari.
2014. Understanding predictive information criteria for Bayesian models. Stat. Comput. 24:997–1016.
Gelman, A., D. Lee, and J. Guo.
2015. Stan: a probabilistic programming language for Bayesian inference and optimization. J. Educ. Behav. Stat. 40:530–543.
Geweke, J.
1993. Bayesian treatment of the independent Student-*t* linear model. J. Appl. Econom. 8:S19–S40.
Hamel, O.S.
2015. A method for calculating a meta-analytical prior for the natural mortality rate using multiple life history correlates. ICES J. Mar. Sci. 72:62–69.
Kullback, S., and R. A. Leibler.
1951. On information and sufficiency. Ann. Math. Stat. 22:79–86.
Lehman, T. M., and H. M. Woodward.
2008. Modeling growth rates for sauropod dinosaurs. Paleobiology 34:264–281.
Link, W. A., and M. J. Eaton.
2012. On thinning of chains in MCMC. Methods Ecol. Evol.3:112–115.
Lunn, D., C. Jackson, N. Best, A. Thomas., and D. Spiegelhalter.
2012. The BUGS book: a practical introduction to Bayesian analysis, 399 p. Chapman & Hall/CRC, Boca Raton, FL.
Marchenko, Y. V., and M. G. Genton.
2010. Multivariate log-skew-*t* elliptical distributions with applications to precipitation data. Environmetrics 21:318–340.
Millar, R.B.
2002. Reference priors for Bayesian fisheries models. Can. J. Fish. Aquat. Sci. 59:1492–1502.
Montenegro, C., and M. Branco.
2016. Bayesian state-space approach to biomass dynamic models with skewed and heavy-tailed error distributions. Fish. Res. 181:48–62.
Pardo, S.A., A. B. Cooper, and N. K. Dulvy.
2013. Avoiding fishy growth curves. Methods Ecol. Evol. 4:353–360.
Peng, F., and D. K. Dey.
1995. Bayesian analysis of outlier problems using divergence measures. Can. J. Stat. 23:199–213.
Pilling, G. M., G. P. Kirkwood, and S. G. Walker.
2002. An improved method for estimating individual growth variability in fish, and the correlation between von Bertalanffy growth parameters. Can. J. Fish. Aquat. Sci. 59:424–432.
Plummer, M., N. Best, K. Cowles, and K. Vines.
2006. CODA: convergence diagnosis and output analysis for MCMC. R News 6(1):7–11. [Available at website.]
Quiroz, J.C., R. Wiff, and B. Caneco.
2010. Incorporating uncertainty into estimation of natural mortality for two species of Rajidae fished in Chile. Fish. Res. 102:297–304.
R Core Team.
2014. R: alanguage and environment for statistical computing. R Foundation for Statistical Computing, Vienna, Austria. [Available at website, accessed May 2014.]
Ratkowsky, D. A.
1986. Statistical properties of alternative parameterizations of the von Bertalanffy growth curve. Can. J. Fish. Aquat. Sci. 43:742–747.
Robert, C. P., and G. Casella.
2004. Monte Carlo statistical methods, 2nd ed., 644 p. Springer, New York.
Sainsbury, K.J.
1980. Effect of individual variability on the von Bertalanffy growth equation. Can. J. Fish. Aquat. Sci. 37:241–247.
Shelton, A.O., and M. Mangel.
2012. Estimating von Bertalanffy parameters with individual and environmental variations in growth. J. Biol. Dyn. 6:3–30.
Siegfried, K.I., and B. Sansó.
2006. Two Bayesian methods for estimating parameters of the von Bertalanffy growth equation. Environ. Biol. Fish. 77:301–308.
Slatkin, M.
2013. A method for estimating the effective number of loci affecting a quantitative character. Theor. Popul. Biol. 89:44–54.
Spiegelhalter, D. J., N. G. Best, B. P. Carlin, and A. vander Linde.
2002. Bayesian measures of model complexity and fit. J. R. Stat. Soc., B 64:583–639.
Taylor, N. G., C. J. Walters, and S. J. D. Martell.
2005. A new likelihood for simultaneously estimating von Bertalanffy growth parameters, gear selectivity, and natural and fishing mortality. Can. J. Fish. Aquat. Sci. 62:215–223.
Tjørve, K. M. C., and E. Tjørve.
2010. Shapes and functions of bird-growth models: how to characterise chick postnatal growth. Zoology 113:326–333.
Vidal, I., P. Iglesias, M. D. Branco, and R. B. Arellano-Valle.
2006. Bayesian sensitivity analysis and model comparison for skew elliptical models. J. Stat. Plann. Inference 136:3435–3457.
von Bertalanffy, L.
1938. A quantitative theory of organic growth (Inquiries on growth laws. II). Hum. Biol. 10:181–213.
Wiff, R., and R. Roa-Ureta.
2008. Predicting the slope of the allometric scaling of consumption rates in fish using the physiology of growth. Mar. Freshw. Res. 59:912–921.
Xiao, Y.
1994. von Bertalanffy growth models with variability in, and correlation between, K and L_{∞}. Can. J. Fish. Aquat. Sci. 51:1585–1590.
Zhang, Z., J. Lessard, and A. Campbell.
2009. Use of Bayesian hierarchical models to estimate northern abalone, *Haliotiskamtschatkana*, growth parameters from tag-recapture data. Fish. Res. 95:289–295.
Zhu, J., M. N. Maunder, A. M. Aires-da-Silva, C., and Y. Chen.
2016. Estimation of growth within Stock Synthesis models: management implications when using length-composition data. Fish. Res. 180:87–91.

National Marine Fisheries Service
NOAA

Fishery Bulletin
established in 1881

Spencer F. Baird
First U.S. Commissioner of Fisheries and founder of *Fishery Bulletin*

Using logbook data to determine the immediate mortality of blue sharks (*Prionace glauca*) and tiger sharks (*Galeocerdo cuvier*) caught in the commercial U.S. pelagic longline fishery

Derek R. Dapp (contact author)[1]
Charlie Huveneers[2]
Terence I. Walker[1]
John Mandelman[3]
David W. Kerstetter[4]
Richard D. Reina[1]

Email address for contact author: derek.r.dapp@gmail.com

[1] School of Biological Sciences
Monash University
Wellington Road
Clayton, Victoria 3800, Australia
Present address for contact author: Washington Department of Fish and Wildlife
600 Capitol Way North
Olympia, Washington 98501–1091

[2] School of Biological Sciences
Flinders University
G.P.O. Box 2100
Adelaide, South Australia 5001, Australia

[3] Anderson Cabot Center for Ocean Life
New England Aquarium
Central Wharf
Boston, Massachusetts 02110-3399

[4] Department of Marine and Environmental Sciences
Halmos College of Natural Sciences and Oceanography
Nova Southeastern University
8000 North Ocean Drive
Dania Beach, Florida 33004

Abstract—Commercial fisheries are recognized as one of the greatest threats to shark populations worldwide, but factors affecting the likelihood of shark mortality during fishery capture are poorly understood. We used the U.S. pelagic fishery logbook data from 1992 through 2008 to quantify the effects of several variables (fisheries regulatory periods, geographic zone, target catch, and sea surface temperature) on mortality of blue sharks (*Prionace glauca*) and tiger sharks (*Galeocerdo cuvier*). Mortality rates and trends in both species closely matched those recorded from other sources, and therefore indicated that the data on sharks discarded dead and discarded alive in the U.S. pelagic fishery logbook are accurate. The introduction of fisheries management regulations (fin weight to carcass weight ratios in 1993 [to prevent finning] and the prohibition of J-hooks in 2004) presumably decreased the immediate mortality rate of captured blue and tiger sharks (by 8.0% in blue sharks after 2004 and 4.4% in tiger sharks after 1993). Other factors that we examined had a statistically significant effect on mortality, but additional variables should be recorded or made available in logbook data to enable the determination of other causes of mortality. Our results show that the U.S. pelagic fishery logbook data can be used as a powerful tool in future studies of the immediate mortality of longline-caught animals.

Manuscript submitted 18 March 2016.
Manuscript accepted 17 October 2016.
Fish. Bull. 115:27–41 (2017).
Online publication date: 16 November 2016.
doi: 10.7755/FB.115.1.3

The views and opinions expressed or implied in this article are those of the author (or authors) and do not necessarily reflect the position of the National Marine Fisheries Service, NOAA.

An estimated one-quarter of all chondrichthyan (sharks, rays, and chimaeras) species are classed as threatened according to the International Union for Conservation of Nature (IUCN) Red List Categories and Criteria, a system for the classification of species by extinction risk, with fishing pressure being the primary threatening process (Dulvy et al., 2014). Targeted shark species often possess protracted life history strategies that make them inherently vulnerable to overfishing (Hoenig and Gruber, 1990; Smith et al., 1998). These shark species are considered a lucrative target for commercial fisheries and are fished primarily for their flesh and fins (Dent and Clarke, 2015). However, some species are captured incidentally, considered *bycatch*, and discarded either because of low commercial value or in response to fisheries management requirements (also called *regulatory discards*) (Bonfil, 1994). Sharks can experience mortality before processing, retention, or release by fishermen; we refer to such mortality as *immediate mortality* in this study

(synonymous with *at-vessel*, *hooking*, and *initial* mortality; Dapp et al., 2016a). The immediate mortality of incidentally caught sharks can be substantial (Dapp et al., 2016a), and incidental capture has been identified as a major driver of declines in shark populations (Dulvy et al., 2014).

Immediate mortality rates of sharks during longline capture can be influenced by a multitude of factors, such as, but not limited to, capture duration, hook type, hook size, species-specific biology, and crew-specific handling practices (Campana et al., 2009; Morgan and Carlson, 2010; Dapp et al., 2016a, 2016b; Gilman et al., 2016). Factors contributing to the immediate mortality of sharks caught by the U.S. Atlantic pelagic longline fishery have previously been examined by using the data set of the National Marine Fisheries Service (NMFS) Pelagic Observer Program (POP) (Serafy et al., 2012; Gallagher et al., 2014). A recent assessment by Gallagher et al. (2014), who used the POP data set, revealed that hook depth, soak time, sea-surface temperature (SST), target catch (assumed to be either swordfish or species of tunas), and fork length had varying effects on the likelihood of immediate mortality for 12 species of sharks.

We expanded upon earlier research by investigating how additional factors (geographic zone and management regulations) contribute to the likelihood of immediate mortality of longline-caught sharks, using the U.S. pelagic fishery logbook (USPL) data set[1]. Temporal analysis of immediate mortality rates with this data set can provide valuable information on the efficacy of regulatory measures designed to decrease immediate mortality of sharks. For example, Serafy et al. (2012) attributed temporal differences in immediate mortality of several species to management regulations requiring the use of circle hooks during longline fishing. Similarly, zone-specific rates of immediate mortality can provide information on how operational differences between geographic zones and fleets cause variations in immediate mortality.

The USPL data set is the largest U.S. fishery data source available in terms of number of animals caught. The large sample size of this data set makes it more suitable than experimentally derived data sets for analyzing spatiotemporal influences on the mortality rates of sharks. The USPL data set comprises mandatory data recorded by commercial fishermen and has been a valuable resource in previous studies of changes in shark relative abundance or catch rates (Baum et al., 2003; Baum and Myers, 2004; Mandelman et al., 2008; Baum and Blanchard, 2010). However, issues with species identification and misreporting can limit the value of logbook data (Burgess et al., 2005). Accordingly, the accuracy of commercial logbook data should be scrutinized and carefully compared with data collected by trained observers.

[1] NMFS (National Marine Fisheries Service). Southeast Fisheries Science Center, Miami Laboratory, 75 Virginia Beach Drive, Miami, FL 33149.

Despite these concerns, Mandelman et al. (2008) and Baum and Blanchard (2010) concluded that catch rates for several easily identifiable, commercially valuable, or commonly captured species of sharks in the USPL data set were not significantly different from catch rates recorded in the POP data set. However, several congeneric species that have similar names or are morphologically similar (e.g., silky shark [*Carcharhinus falciformis*], dusky shark [*C. obscurus*], and night shark [*C. signatus*]; longfin mako [*Isurus paucus*] and shortfin mako [*I. oxyrinchus*]; and common thresher shark [*Alopias vulpinus*] and pelagic thresher [*A. pelagicus*]) were consistently misidentified in the USPL data set, even by trained observers (Reardon et al., 2006; Baum and Blanchard, 2010).

We sought to expand upon earlier studies of logbook accuracy by comparing the immediate mortality rates of sharks with accurately recorded catch rates of sharks recorded in the USPL data set to the immediate mortality rates of these species recorded in the POP data set. This comparison allowed us to determine whether records of dead and live discards were accurately recorded in the USPL data set. It is important to appreciate that the USPL was not designed for this purpose; it was implemented as a marine resource management tool to monitor fishery changes in catch per unit of effort (additional information is available from the website). However, if shark mortality is accurately recorded within the USPL data set, the large number of records in the data set will make it a powerful and statistically robust tool for identifying factors that contribute to immediate mortality during longline capture.

For our analysis, we summarized the number of sharks retained, discarded dead, and discarded alive by the U.S. pelagic longline fleet from 1992 through 2008 by using the USPL data set. In addition, we evaluated the accuracy of mortality recordings by commercial fishermen in the USPL data set by comparing our results with the findings from previous immediate mortality studies in which similar species, fishing techniques, and locations were used. If accuracy was validated, we went on to assess factors contributing to the likelihood of shark bycatch being discarded dead to propose new variables that can be included when recording logbook data to enhance data collection.

Materials and methods

Overview of the data set and study methods

To achieve our goals, we first screened the USPL data set for the period of 1982–2008 to remove inaccurate records. Quantitative species-specific comparisons of immediate mortality between this data set and other published sources were made to assess the accuracy of the USPL data set. If accuracy was verified, a statistical analysis of shark mortality was then conducted to determine factors correlated with immediate mortality within the USPL data set.

Data screening

Data screening was conducted on the USPL data set to remove longline sets or individual captures that were deemed likely to be inaccurate. A summary of longline sets and individual captures removed from the data set is available in Supplementary Table 1. Longline sets and recorded captures were removed from the analysis in the following cases:

- Longline sets that were made before 1992 because records from 1982 through 1992 did not specify whether discards were alive or dead
- Multiple gear types (e.g., pelagic longline and gillnet or pelagic longline and bottom longline) were used or sets did not use longline gear
- Improbable SST (e.g., <1°C), or no SST was reported
- Location data were likely to be inaccurate because all latitude and longitude values were reported as 0°, latitude and longitude values were unreported, or longline set location was recorded outside of the designated geographic zones
- Target catch was not reported as swordfish (*Xiphias gladius*), species of shark, dolphinfish (*Coryphaena hippurus*), or any species of tunas (*Thunnus* spp.). If target catch was not reported as one of these categories, the target catch was specified as *other* and was considered unknown
- Specific groupings (e.g., geographic zones, targeted species, regulatory periods) with less than 100 individuals of a given species
- Longline sets where fishermen retained any individuals of the species being examined. This approach was necessary because the condition of whether sharks were alive or dead was not recorded at the time of processing. Mortality of individuals that were retained was unrelated to the environmental and operational factors examined in our analysis
- Longline sets that targeted sharks, because retention was likely in these longline sets. Longline sets that targeted sharks were included for the analysis of blue shark (*Prionace glauca*) because this species was not typically retained by shark-targeting longline fishermen (i.e., in less than 5% of longline sets that reported targeting sharks before data screening)
- Geographic zone groupings that had less than 100 recorded captures during each regulatory period when interaction effects (blue shark only) were examined. A table that shows excluded groupings and their associated sample sizes can be found in the supplementary materials section (Suppl. Table 2)

Some variables recorded in the USPL were excluded from our analyses. Use of live or dead bait was not included as a factor because the majority of longline sets had either dead or unrecorded bait types (e.g., 99.8% of the examined longline sets that captured blue shark). Gangion length was not included as a factor in the analysis because the units of measurement (e.g., centimeters and inches) that were used were unspecified and varied among longline sets. Immediate mortality rates during demersal longline sets were not compared with those during pelagic longline sets because the few individuals remaining in the data set after data screening was completed were recorded on demersal longline sets (e.g., less than 0.1% of blue sharks were caught during demersal longline sets). Although the number of hooks between floats has been used in previous studies as a proxy for target catch (Serafy et al., 2012; Gallagher et al., 2014), this variable was not included in our analysis because target catch was explicitly recorded in the USPL, and, therefore, available.

Species-specific immediate mortality rates (expressed as percentages) were calculated by dividing the number of dead discards by the number of total discards. This approach was used because immediate mortality was not directly recorded by fishermen in the USPL, unwanted shark bycatch is typically released by commercial fishermen without bringing it onboard vessels (Moyes et al., 2006), and regulations require that live shark bycatch is released unharmed (NMFS[2]). In addition, we removed from our analysis longline sets that retained (rather than released) individuals of the species being examined.

Species that were likely to be identified accurately by fishermen and considered in our analysis included blue sharks, porbeagle (*Lamna nasus*), oceanic whitetip sharks (*Carcharhinus longimanus*), and tiger sharks (*Galeocerdo cuvier*) (Mandelman et al., 2008; Baum and Blanchard, 2010). Although we report the likelihood of retention, being discarded dead, and being discarded alive for 2 occasionally retained species (oceanic whitetip sharks and porbeagles; NMFS[3]), we were unable to analyze the immediate mortality rates of these species using the USPL data set because it could not be determined whether individual animals were alive or dead when landed and retained. Instead, we examined immediate mortality in bycatch of blue and tiger sharks because these species have meat of low value (Vannuccini, 1999; Mandelman et al., 2008; Simpfendorfer, 2009) and are rarely retained by U.S. fisheries (NMFS[4]) and because a metric of dead discards in relation to live discards would accurately reflect immediate mortality rates following capture.

The effect of capture location on immediate mortality was investigated by using the 11 zones of the U.S. pelagic longline fishery that are based on geography

[2] NMFS (National Marine Fisheries Service). 1993. Fishery management plan for sharks of the Atlantic Ocean, 287 p. [Available from website, accessed December 2015.]

[3] NMFS (National Marine Fisheries Service). 2006. Final consolidated Atlantic highly migratory species fishery management plan, 1600 p. [Available from website, accessed March 2016.]

[4] NMFS (National Marine Fisheries Service). 2015. Stock assessment and fishery evaluation (SAFE) report for Atlantic highly migratory species. 170 p. [Available from website, accessed March 2016.]

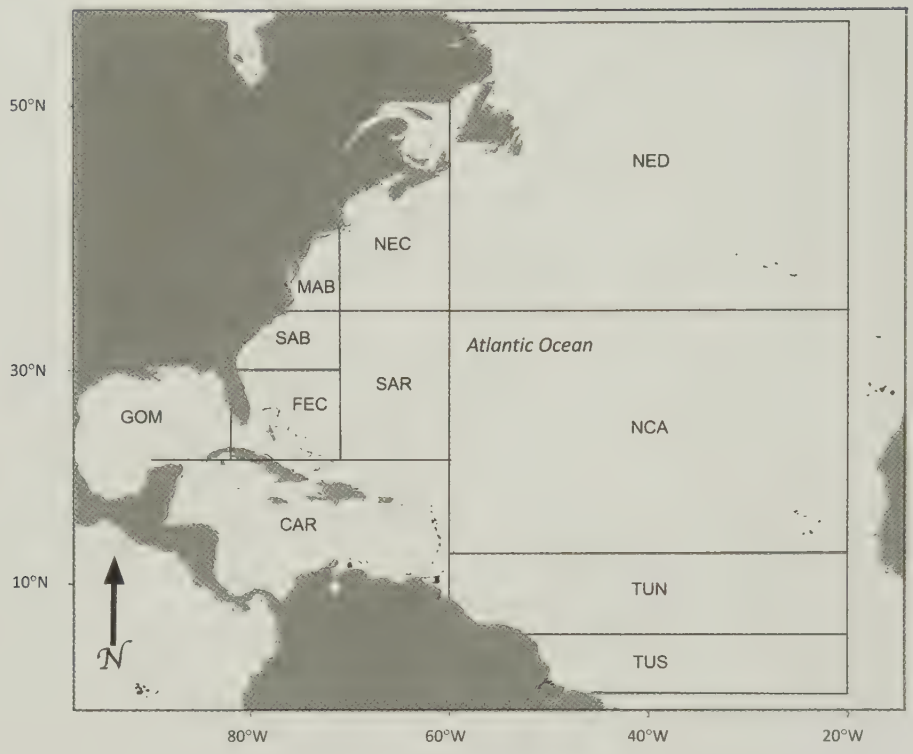

Figure 1

The 11 geographic zones of the U.S. pelagic longline fishery that were analyzed for this study to determine the immediate mortality of blue sharks (*Prionace glauca*) and tiger sharks (*Galeocerdo cuvier*) for the period 1992–2008. The geographic zones are Caribbean (CAR), Florida east coast (FEC), Gulf of Mexico (GOM), Mid-Atlantic Bight (MAB), north central Atlantic (NCA), northeast coastal (NEC), northeast distant (NED), South Atlantic Bight(SAB), Sargasso Sea (SAR), tuna north (TUN), and tuna south (TUS).

(Cramer and Adams, 2000; Mandelman et al., 2008; Fig. 1). These geographic zones were Caribbean (CAR), Gulf of Mexico (GOM), Florida east coast (FEC), Mid-Atlantic Bight (MAB), north central Atlantic (NCA), northeast coastal (NEC), northeast distant (NED), South Atlantic Bight (SAB), Sargasso Sea (SAR), tuna north (TUN), and tuna south (TUS). Target catch and operating procedures for the pelagic longline fleet vary among geographic zones, with each described in detail in Hoey and Moore[5] and in the NMFS consolidated fishery management plan for highly migratory species (NMFS[2]).

Within the USPL, target catch was reported as swordfish, yellowfin tuna (*Thunnus albacares*), bigeye tuna (*Thunnus obesus*), mixed species of tunas, species of sharks, dolphinfish, or other. In accordance with previous studies, yellowfin tuna, bigeye tuna, and mixed species of tunas were grouped into a single category designated as targeting tunas during the mortality analysis (Serafy et al., 2012; Gallagher et al., 2014). However, a large portion of the data reported targeting of multiple species (e.g., swordfish and species of tunas in longline sets). Accordingly, for a separate analysis of the immediate mortality of target catch, we used a reduced data set that excluded longline sets in which multiple species were targeted.

Statistical analysis

We used generalized linear models with a logit link function for each species. This statistical family was chosen because the dependent variable was binary, the data fitted model assumptions, and Pearson's χ^2 residual tests confirmed that logistic models fitted the data appropriately. The response variable (*immediate mortality*) was coded with a value of 0 or 1 according to whether an individual shark was discarded alive or dead, respectively. The final model used for blue sharks was

$$\textit{Immediate mortality} = \textit{SST} + \textit{Regulatory period} + \textit{Geographic zone} + \textit{Regulatory period} \times \textit{Geographic zone}. \quad (1)$$

An interaction effect was not examined during the

[5] Hoey, J. J., and N. Moore. 1999. Captain's report: multispecies catch characteristics for the U.S. Atlantic pelagic longline fishery. 78 p. National Fisheries Institute Inc., Arlington, VA. [Available from website, accessed September 2015.]

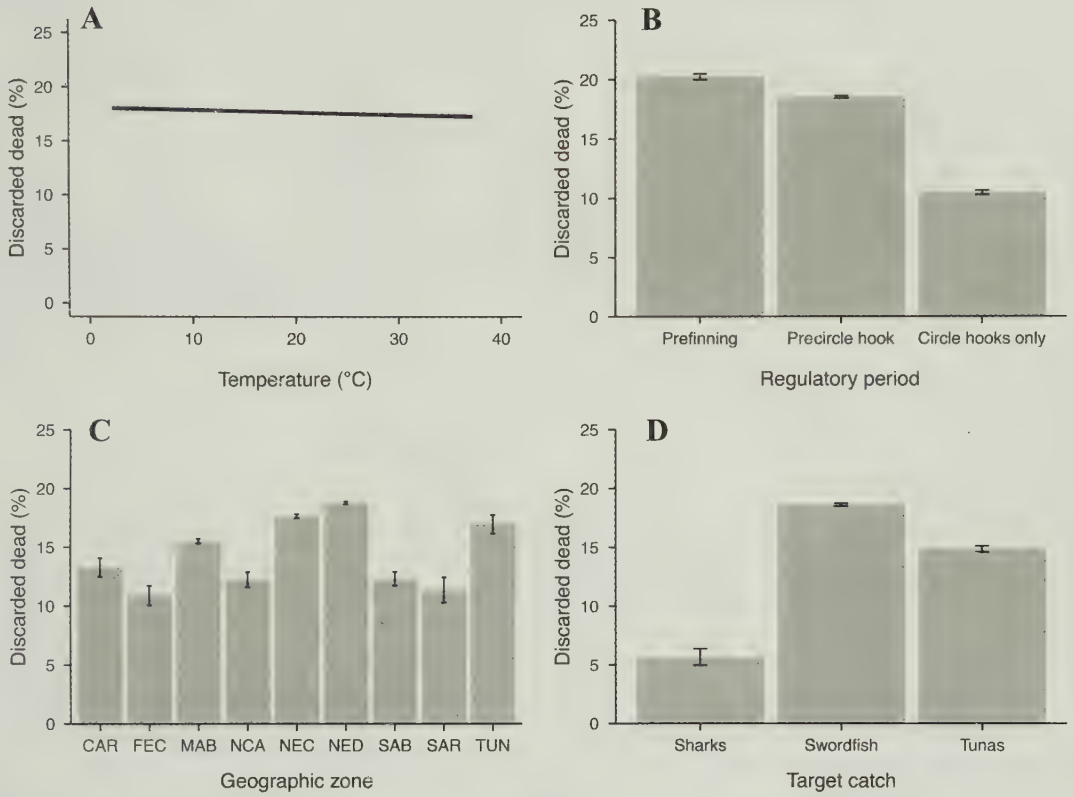

Figure 2

The effect of analyzed factors: (**A**) sea-surface temperature, (**B**) regulatory period, (**C**) geographic zone, and (**D**) target catch (swordfish or tunas), on the immediate mortality of discarded blue sharks (*Prionace glauca*) in the U.S. Atlantic pelagic longline fishery. Regulatory period refers to the period before the establishment of fin-to-carcass ratios (January1992–February 1993), prior to the prohibition of the use of J-hooks (March 1993–August 2004), and during which the use of circle hooks was mandatory (August 2004–December 2008), denoted as *prefinning*, *precircle hook*, and *circle hooks only* in the figure. Bars represent the mean immediate mortality, and error bars indicate 95% confidence intervals. The geographic zones are Caribbean (CAR), Florida east coast (FEC), Mid-Atlantic Bight (MAB), north central Atlantic (NCA), northeast coastal (NEC), northeast distant (NED), South Atlantic Bight (SAB), Sargasso Sea (SAR), and tuna north (TUN).

analysis of tiger shark because its examination required the use of a reduced data set. The model created by using the reduced data set that included the interaction explained less deviance (expressed as a percentage) in the model than did a model that used the full data set (Suppl. Table 3). The final model used for tiger sharks was

$$\textit{Immediate mortality} = \textit{SST} + \textit{Regulatory period} + \textit{Geographic zone}. \quad (2)$$

Predictor variables were *SST* (measured in degrees Celcius), *regulatory period* (January 1992–February 1993, March 1993–July 2004, August 2004–December 2008), and *geographic zone* (CAR, GOM, FEC, MAB, NCA, NEC, NED, SAR, SAB, TUN, TUS). Wald tests were used to determine whether the overall effect of each predictor variable on immediate mortality was statistically significant ($P<0.05$). To portray biologically meaningful results, statistically significant predictor variables were examined in isolation in Figures 2, 3, and 4.

The variable *regulatory period* was defined according to changes in the management of the fisheries. During the first period (January 1992–February 1993), shark finning was legal and few regulations existed to protect shark populations. The implementation of the first fishery management plan for sharks of the Atlantic marked the beginning of the second regulatory period (March 1993–July 2004; NMFS[2]). This plan provided management for 39 species of sharks, establishing bag limits and a fin-to-carcass weight ratio of 5% or less and requiring the release of sharks not retained under commercial quotas or bag limits. J-hooks were the predominant hook type used during this regulatory period (Hoey and Moore[1]; Watson et al., 2005). The final period examined (August 2004–

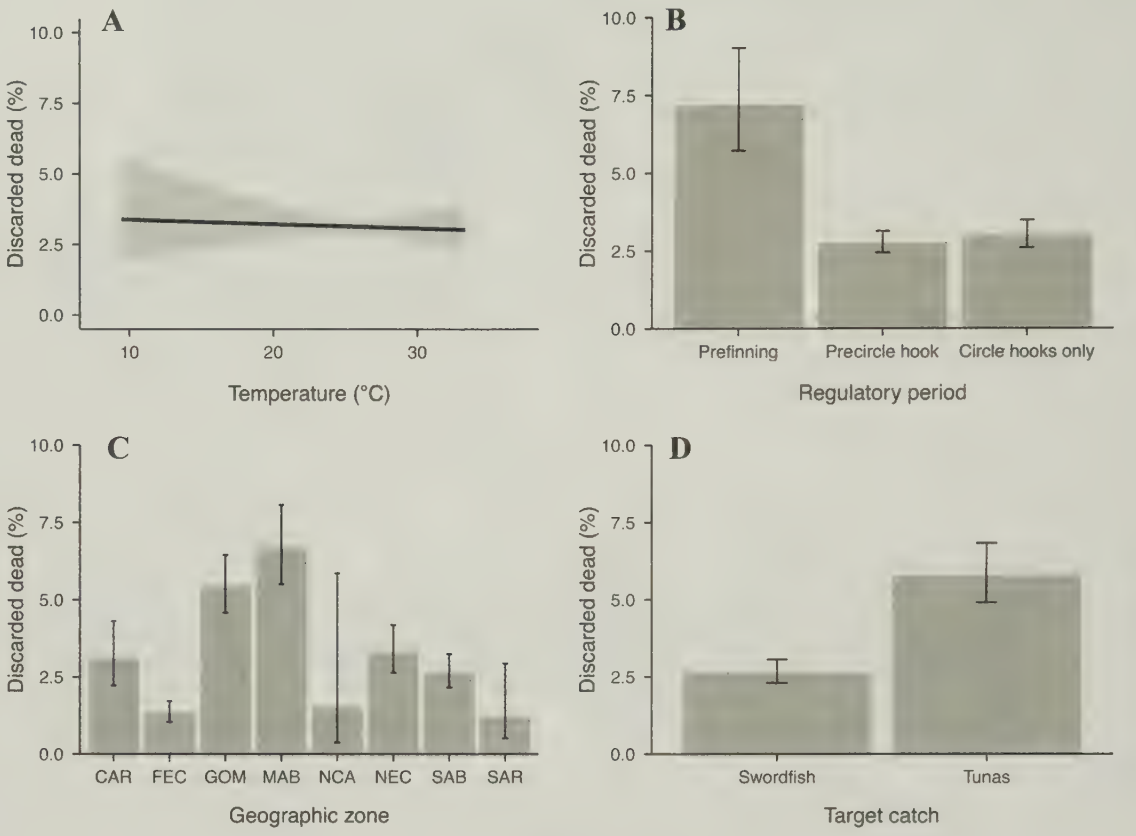

Figure 3

The effect of analyzed factors: **A**) sea surface temperature, (**B**) regulatory period, (**C**) geographic zone, and (**D**) target catch (swordfish or tunas), on the immediate mortality of discarded tiger shark (*Galeocerdo cuvier*) in the U.S. Atlantic pelagic longline fishery. Regulatory period refers to the period before the establishment of fin-to-carcass ratios (January 1992–February 1993), before the prohibition of the use of J-hooks (March 1993–August 2004), and during which the use of circle hooks was mandatory (August 2004–December 2008), denoted as *prefinning*, *precircle hooks*, and *circle hooks only* in the figure. Bars represent the mean immediate mortality, and error bars indicate 95% confidence intervals. The geographic zones are Caribbean (CAR), Florida east coast (FEC), Gulf of Mexico (GOM), Mid-Atlantic Bight (MAB), north central Atlantic (NCA), northeast coastal (NEC), South Atlantic Bight (SAB), and Sargasso Sea (SAR).

December 2008) was characterized by a new mandatory use of circle hooks for U.S. pelagic longline vessels (NMFS[2]). Although this rule was implemented to reduce bycatch mortality of species of turtles (NMFS[2]), circle hooks are less likely than traditionally used J-hooks to be swallowed by some species of shark. The use of these hooks, therefore, reduces occurrences of internal injuries and immediate mortality rates in some species (Kerstetter and Graves, 2006; Campana et al., 2009; Serafy et al., 2012; Gilman et al., 2016; but see Yokota et al., 2006).

In accordance with the methods of Serafy et al. (2012), we considered only specific regulatory periods in our analysis. There were other measures enacted that were required for the use of longlines in commercial fisheries during the period examined, but they were not incorporated into models because they were unlikely to have had a substantial effect on the immediate mortality of sharks. A few examples of regulatory measures enacted include the fishery management plan for Atlantic tunas, swordfish, and sharks (which was enacted in 1999 to prohibit the retention of several species of sharks and reduce commercial coastal quotas for sharks; these regulations did not affect our analysis because we examined discarded animals and species only) and time or area closures (e.g., the closing of the NED zone in 2002; NMFS[2]).

To determine how target catch influenced immediate mortality, the following generalized linear models with a logit link function were used:

$$Immediate\ mortality = Target. \quad (3)$$

Target = target catch and was defined as catch of tunas, swordfish, or sharks.

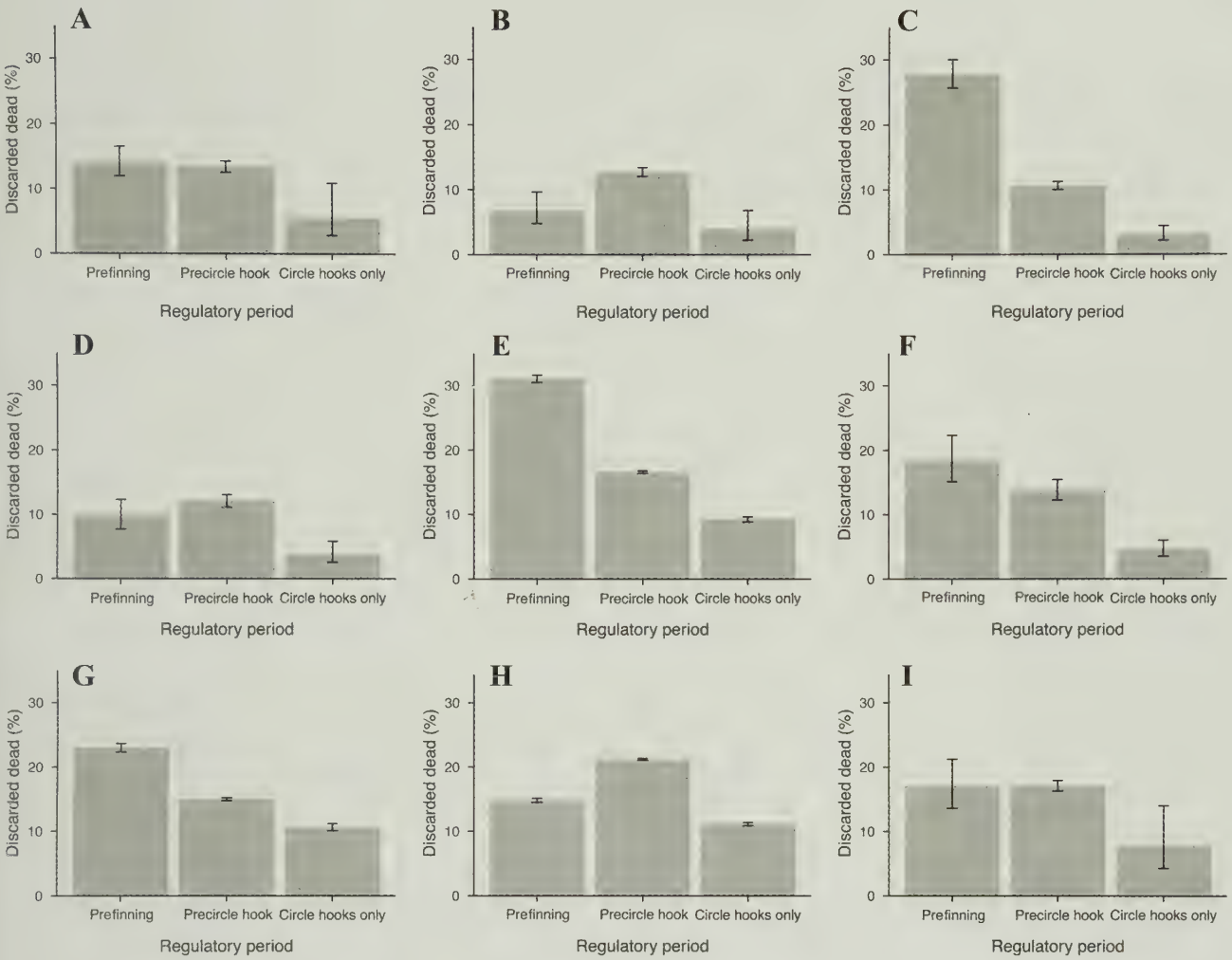

Figure 4

The immediate mortality rates of blue sharks (*Prionace glauca*) caught in the U.S. Atlantic pelagic longline fishery by regulatory period and geographic zone. Regulatory period refers to the period prior to the establishment of fin-to-carcass ratios (January 1992–February 1993),before the prohibition of the use of J-hooks (March 1993–August 2004), and during which the use of circle hooks was mandatory (August 2004–December 2008), denoted as *prefinning*, *precircle hooks*, and *circle hooks only* in the figure. The geographic zones are (**A**) Caribbean, (**B**) north central Atlantic, (**C**) South Atlantic Bight, (**D**) Florida east coast, (**E**) northeast coastal, (**F**) Sargasso Sea, (**G**) Mid-Atlantic Bight, (**H**) northeast distant (H), and (**I**) tuna north. Bars represent the mean immediate mortality, and error bars indicate 95% confidence intervals.

This variable was examined in isolation because records with multiple species had to be removed from the data set for the target catch analysis, resulting in a reduced data set. The reduced data sets, however, did not have the sample sizes necessary to examine all the geographic zones and regulatory periods.

All statistical analyses were conducted with R[6] statistical software, vers. 2.14.2 (R Core Team, 2012).

Results

Shark retention and total numbers reported before data screening

There were 1,436,061 reported captures of sharks between 1992 and 2008 in the USPL data set (Table 1). Blue sharks accounted for approximately 60% of the total catch (Table 1). Numbers reported for other species caught are available in Table 1.

The percentage of animals retained varied considerably among species, with the blue shark having the lowest (1%; Table 1) and the porbeagle having the

[6] Mention of trade names or commercial companies is for identification purposes only and does not imply endorsement by the National Marine Fisheries Service, NOAA.

Table 1

The numbers (and percentages) of sharks retained, discarded alive, and discarded dead on longline sets reported in the U.S. pelagic longline logbook data set from 1992 through 2008. Numbers reported are total numbers before data screening. An asterisk (*) indicates species for which numbers reported are likely to be accurate. Numbers recorded for species other than blue sharks (*Prionace glauca*), tiger sharks (*Galeocerdo cuvier*), oceanic whitetip sharks (*Carcharhinus longimanus*), and porbeagle (*Lamna nasus*) should be interpreted with caution because it was likely that these species were consistently misidentified.

Species	Number	Retained	Discarded alive	Discarded dead
Blue shark*	863,153	9362 (1%)	702,955 (81%)	150,836 (17%)
Sandbar shark	167,887	157,261 (94%)	7973 (5%)	2653 (2%)
Blacktip shark	91,723	77,033 (84%)	9669 (11%)	5021 (5%)
Shortfin mako	66,750	51,710 (77%)	10,696 (16%)	4344 (7%)
Dusky shark	53,561	30,934 (58%)	16,376 (31%)	6251(12%)
Silky shark	42,647	18,236 (43%)	14,472 (34%)	9939 (23%)
Tiger shark*	33,063	4975 (15%)	26,737 (81%)	1351 (4%)
Hammerhead (unidentified)	23,238	10,024 (43%)	8050 (35%)	5164 (22%)
Bigeye thresher	13,227	3675 (28%)	7255 (55%)	2297 (17%)
Scalloped hammerhead	13,062	5629 (43%)	4097 (31%)	3336 (25%)
Spinner shark	11,439	9340 (82%)	1560 (14%)	539 (5%)
Night shark	11,082	3084 (28%)	4432 (40%)	3566 (32%)
Oceanic whitetip shark*	10,847	2422 (22%)	7254 (67%)	1171 (11%)
Smooth hammerhead	9922	4433 (45%)	3646 (37%)	1843 (19%)
Porbeagle*	8113	3980 (49%)	3312 (41%)	821 (11%)
Longfin mako	7367	2523 (34%)	3887 (53%)	957 (13%)
Thresher (unidentified)	5248	2313 (44%)	2197 (42%)	738 (14%)
Bignose shark	2288	992 (43%)	940 (41%)	356 (16%)
White shark	1435	488 (34%)	879 (61%)	68 (5%)
All recorded sharks	1,436,061	398,415 (28%)	836,395 (58%)	201,251 (14%)

highest (49%; Table 1) rates of retention of the 4 species deemed to be accurately reported. When animals retained were included in our analyses, the porbeagle was the species least likely (41%) to be released alive by fishermen among the 4 species deemed to be accurately reported (Table 1). In contrast, tiger and blue sharks were the most likely species examined (both 81%; Table 1) to survive initial capture by the U.S. pelagic longline fleet.

Quantitative comparisons of mortality rates with rates from other published sources

The rates of immediate mortality reported for commonly discarded species, specifically the blue shark (1% retained after data screening completed) and the tiger shark (3% retained after data screening completed), in the USPL data set were similar to rates of immediate mortality reported for these species in other data sources. Rates of immediate mortality for the tiger shark were 3%, 3%, and 3% in the POP data set, in the USPL data set, and for the mean of 5 studies of immediate mortality, respectively (Table 2). For the blue shark, rates of immediate mortality were 15%, 18%, and 19% in the POP data set, in the USPL data set, and for the mean of 11 studies of immediate mortality, respectively (Table 2). In contrast, rates of immediate mortality for occasionally retained species (i.e., oceanic whitetip sharks and porbeagles) deviated considerably from the rates in the POP data set (Table 2).

Immediate mortality analysis

Because rates of immediate mortality for blue and tiger sharks were comparable with estimates from other sources (Table 2), factors affecting mortality of these species were assessed. All factors tested had a statistically significant effect on immediate mortality of blue sharks (Table 3; Fig. 2). Similar factors affected immediate mortality of tiger sharks, including regulatory period, geographic zone, and target catch (Table 3, Fig. 3). Both models explained only a small percentage of the deviance within the data set: 1.6% for blue sharks and 4.5% for tiger sharks (Table 3).

In both species, rates of immediate mortality during examined regulatory periods were significantly different. Before March 1993, 7.2% (95% confidence interval [CI]: 5.7% to 9.0%) of tiger sharks were discarded dead; however, from March 1993 through August 2004, only 2.8% (95% CI: 2.4% to 3.1%) were discarded dead (Fig. 3). The percentage of discards of tiger sharks that were dead did not differ significantly between periods from March 1993 through August 2004 and periods after Au-

Table 2

The observed immediate mortality, calculated as the percentage of total discards that were dead discards, in the U.S. pelagic fishery logbook (USPL) data set for the period 1992–2008, after data screening was completed. Expected immediate mortality rate is given as a mean and range from existing sources that reported the immediate mortality rates of a species examined during longline capture. The expected immediate mortality rate column also provides the mean rate of immediate mortality recorded by the Pelagic Observer Program (POP), National Marine Fisheries Service, in Gallagher et al. (2014). Superscript [1] denotes that the observed immediate mortality rate is likely to be inaccurate because of the discrepancy between observed (USPL) and expected (POP) percentages.

Species	Number examined	Observed immediate mortality	Expected immediate mortality	Sources
Blue shark	806,598	17.7%	Range: 5–34% Mean: 19% POP: 15%	(Francis et al., 2001; Moyes et al., 2006; Hight et al., 2007; Petersen, 2008; Campana et al., 2009; Coelho et al.[1]; Musyl et al., 2011; Bromhead et al., 2012; Coelho et al., 2012; Griggs and Baird, 2013; Gallagher et al., 2014)
Tiger shark	15,474	3.1%	Range: 0–7% Mean: 3% POP: 3%	(Morgan et al., 2009; Scott-Denton et al., 2011; Coelho et al., 2012; Afonso and Hazin, 2014; Gallagher et al., 2014)
Oceanic whitetip shark[1]	6348	15.8%[1]	Range: 5–34% Mean: 24% POP: 26%	(Musyl et al., 2011; Bromhead et al., 2012; Coelho et al., 2012; Gallagher et al., 2014)
Porbeagle[1]	2619	27.2%[1]	Range: 21–39% Mean: 32% POP: 21%	(Francis et al., 2001; Griggs and Baird, 2013; Gallagher et al., 2014)

[1]Coelho, R., P. G. Lino, and M. N. Santos. 2011. At-haulback mortality of elasmobranchs caught on the Portuguese longline swordfish fishery in the Indian Ocean. Indian Ocean Tuna Comm. IOTC-2011-WPEB07-31, 9 p. IOTC, Victoria Mahé, Seychelles. [Available from website, accessed March 2015.]

gust 2004, with a mean difference in percentages of 3.0% (95% CI: 2.6% to 3.5%; (Fig. 3).

The immediate mortality model for blue sharks had a statistically significant interaction effect between regulatory period and geographic zone. Rates of immediate mortality for blue sharks caught before March 1993 were lower in 2 zones (NCA and NED), higher in 3 zones (MAB, NEC, and SAB), and not significantly different in 4 zones (CAR, FEC, SAR, and TUN) than rates of immediate mortality for blue sharks caught between March 1993 and August 2004 (Figs. 1 and 4). However, after the implementation in August 2004 of regulations for the mandatory use of circle hooks, the immediate mortality of blue sharks had a statistically significant decrease in every geographic zone analyzed when compared with the regulatory period between March 1993 and August 2004 (Figs. 1 and 4). Between the period March 1993–August 2004 and the period August 2004–December 2008, the rate of immediate mortality in geographic zones decreased by a mean of 8.0% (standard error [SE] 0.5) and by a range of 4.4–10.1% for 9 geographic zones examined.

Discussion

Accuracy of logbook data

Despite being limited to blue and tiger sharks, our analysis with the USPL data set provided useful information about immediate mortality over a temporal and spatial scale not possible with other data sets. In previous studies, where USPL and POP data sets were compared, catch rates were determined to have been reported accurately for easily identifiable, commonly captured, and marketable species of sharks (blue, tiger, porbeagle, and oceanic whitetip sharks) (Mandelman et al., 2008; Baum and Blanchard, 2010). Our results show that the numbers of dead and live discards of bycatch species (i.e., blue and tiger sharks) recorded by commercial fishermen in the USPL data set are also similar to those recorded in the POP data set, indicating accuracy, and that the USPL is a useful, massive source of long-term data with value for management of sharks and fisheries, particularly in relation to shark bycatch over time. Given the large sample size of the

Table 3

The effect of sea surface temperature (SST), regulatory period, and geographic zone on the immediate mortality of blue and tiger sharks in the U.S. Atlantic pelagic longline fishery during the period 1992–2008. NS denotes a nonsignificant effect of the factor on mortality. An asterisk (*) denotes significant results with *P*-values less than 0.05. An interaction effect was not examined in the model for immediate mortality of tiger shark (represented by N/A below).

Species	SST	Regulatory period	Geographic zone	Regulatory period × geographic zone	Deviance explained
Blue shark	*	*	*	*	1.6%
	χ^2=15	χ^2=7	χ^2=2761	χ^2=4648	
	P<0.05	P<0.05	P<0.05	P<0.05	
	1.6%				
Tiger shark	NS	*	*	N/A	4.5%
		χ^2=49	χ^2=137		
		P<0.05	P<0.05		

data set and the mandatory collection of such data, the USPL data set will be a powerful and economical tool in future studies for analyzing shark mortality trends, but the current problem of reliable species identification needs to be addressed.

The rates of immediate mortality for 2 occasionally retained species deviated from the rates reported in the POP data set: 6% higher for porbeagles and 10% lower for oceanic whitetip sharks. Despite differences with the POP data set, the rates of immediate mortality for these species reported in the USPL data set were determined to be within the range of immediate mortality rates reported in other sources (Table 2). Although this comparability indicates that the reporting of immediate mortality in the USPL for these species may be accurate, we recommend interpreting these values with caution. During the screening of data, all longline sets that retained individuals of the species being examined were removed. This approach left only longline sets that had discarded sharks in the data set but it was assumed that the likelihood of retention was the same for dead and live sharks. This supposition is false because fishermen may be more likely to retain sharks that are dead or moribund than they are to keep live sharks (Gilman et al., 2008). Because of this limitation, for occasionally retained species, the factors that influence immediate mortality during capture cannot be accurately assessed by using the designated categories in the USPL data set. Therefore, it would be necessary for the USPL to include the number of live and dead or moribund animals retained in order for data to be reliable when some animals are kept as part of a catch.

Factors contributing to mortality in blue and tiger sharks

The establishment of fin-to-carcass weight ratios has afforded greater protection for tiger sharks than the implementation of the mandatory use of circle hooks. The large number of sharks discarded dead before March 1993 may be attributable to the high value of the fins of tiger shark compared with that of the fins of other shark species because "finned sharks" (sharks whose fins were removed in the catch) were likely to be recorded as *discarded dead* rather than retained during this period (Clarke et al., 2006). The effect of circle hooks on immediate mortality is likely to be species-specific (Serafy et al., 2012), and immediate mortality of tiger sharks did not decrease after the start of regulations for the mandatory use of circle hooks.

In contrast with the effect on survival of tiger sharks, the prohibition of the use of J-style hooks had a more positive effect on the survival of blue sharks than the establishment of fin-to-carcass ratios (for zone-specific effects, see Fig. 4). We are unsure why differences in mortality rates varied according to geographic zones between the period before March 1993 and the period March 1993–August 2004. However, statistically significant decreases in rates of immediate mortality for blue sharks in every geographic zone analyzed after August 2004 have indicated that the mandated change in hook type has had a positive effect on the survival of blue shark caught as bycatch.

Several studies have reported that the use of circle hooks instead of J-style hooks can reduce immediate mortality of blue sharks (Campana et al., 2009; Carruthers et al., 2009; Afonso et al., 2011; Afonso et al., 2012; Epperly et al., 2012; Godin et al., 2012; Gilman et al., 2016; but see Kerstetter and Graves, 2006; Yokota et al., 2006; Curran and Bigelow, 2011; Serafy et al., 2012) because such hooks decrease the likelihood of hooking in the gut (gut-hooking) in this species (Watson et al., 2005; Afonso et al., 2011). We cannot determine the specific postrelease survival rate for released animals, but delayed death due to gut-hooking may have been a further significant cause of mortality that

has since been reduced or removed by the shift to circle hooks (Campana et al., 2009). Despite the decreases in rates of immediate mortality noted in this study, catch rates for species of sharks may increase when circle hooks are used and this increase may have contributed to a greater number of animals being captured (see meta-analysis by Gilman et al., 2016).

The reported effect of SST on immediate mortality of blue shark varies among studies. Clarke et al. (2013) and Gallagher et al. (2014) found a positive relation between the immediate mortality rate of blue sharks and SST. In contrast, Campana et al. (2009), Epperly et al. (2012), Serafy et al. (2012), and Coelho et al. (2013) reported that temperature had no effect on the rate of immediate mortality rate for blue sharks. Although we identified that the influence of SST on immediate mortality as statistically significant in blue sharks, immediate mortality rates were lower by only 0.5% at an SST of 30°C than at an SST of 10°C, indicating that other factors exert more influence on mortality of blue sharks. Statistical significance is more likely to be detected in studies with a very large sample size, as in our study, even when the effect that sample size has on mortality is minor (for more information on how sample sizes can influence *P*-values, see Sullivan and Feinn, 2012). Sea-surface temperature had no effect on immediate mortality of tiger shark (Fig. 3)—a finding that is consistent with the results of Gallagher et al. (2014). Although SST has been reported to have little influence on the immediate mortality rates of species we examined, higher SSTs are thought to increase physiological stress during fishery capture (Cicia et al., 2012; Hoffmayer et al., 2012; Guida et al., 2016) and the effect of SST on mortality is likely to be species specific.

Blue sharks caught on longline sets that targeted swordfish were more likely to be discarded dead than those caught on longline sets that targeted tunas or sharks (Fig. 2). However, the majority (83%) of blue shark caught on longline sets that targeted swordfish were caught in the NED zone, and blue sharks caught in the NED zone had higher mean rates of immediate mortality than those caught in other geographic zones (Fig. 2). It is unknown why blue shark caught in the NED zone had higher immediate mortality rates than those caught in other geographic zones. Tiger sharks exhibited the opposite trend; individuals caught on longline sets that targeted tunas were more likely to be discarded dead than those caught on longline sets that targeted swordfish. Several gear and operational strategies differ between longline sets that target tunas and those that target swordfish. For example, longline sets that target swordfish are typically left fishing nearer the water's surface and overnight, but longline sets that target tunas are typically set deeper and left from sunrise to sunset (NMFS[2]). Despite the identification of some operational differences, the exact causes of increased immediate mortality rates of tiger sharks during capture on longline sets that target tunas compared with mortality rates during sets that target swordfish remain unclear and will require additional investigation.

Deviance in the data explained by our models was low (1.6% for blue sharks and 4.5% for tiger sharks), indicating that important factors that contributed to immediate mortality may not have been recorded in the USPL data set or included in our analysis. Factors that potentially contributed to immediate mortality during capture and that were not investigated include capture duration, body size, sex, differences between SST and air temperature, capture depth, degree of movement restriction, behavior during capture, hook size, individual crew handling practices, and bait used (Campana et al., 2009; Cicia et al., 2012; Serafy et al., 2012; Dapp et al., 2016a). These factors were not considered in our analysis because they were not recorded in the USPL. Despite the potential effect of unknown factors, models for immediate mortality of sharks typically explain a low percentage of the deviance in the data (e.g., 7% in Campana et al., 2009; 2–5% in Coelho et al., 2012; 3–6% in Clarke et al., 2013), and more research is necessary to evaluate the variety and extent of factors affecting immediate mortality of sharks.

One caveat concerning our analysis is that temporal differences in immediate mortality were attributed to regulatory measures, but explicit recordings of hook type and number of animals finned were not available. We assumed that before August 2004 longline fisheries had used J-hooks because J-hooks were the predominant hook type used by the U.S. Atlantic pelagic longline fishery during this time period (Hoey and Moore[1]; Watson et al., 2005). Before the requirement to use circle hooks was established in August 2004, circle hooks were not used with some vessels, but because hook type was not recorded within the USPL, we could not identify the vessels with which they were used. Despite this limitation, time period has been previously used as a proxy for hook type in the U.S. Atlantic pelagic longline fishery (Serafy et al., 2012). Additionally, we postulated that the number of dead discards of tiger sharks decreased after March 1993 because of the establishment of fin-to-carcass ratios that reduced the economic viability of retaining shark fins. Because the number of sharks that had been finned was not explicitly recorded, it is possible that other unknown variables could have decreased immediate mortality of tiger sharks after this time period. Despite this caveat, there were clear trends of decreasing immediate mortality after regulatory measures, and these management initiatives are likely to have positively affected the survival of blue sharks and tiger sharks.

One statistical limitation in our study was that target catch was examined by using a univariate model because of the need to use a reduced data set to examine this factor. A univariate approach ignores the effect of other potentially important factors and such effects should be considered when interpreting our results.

Another caveat concerning our study is that the USPL data set used is reported by fishermen. Inaccuracies may arise in the USPL data set as a result

of misidentification, over-reporting, or underreporting (Burgess et al., 2005). Screening data removed many records that were likely inaccurate; however, some inaccuracies are not possible to readily identify and may have passed through the data screening process. Regardless of these concerns, immediate mortality and catch rates for the 2 species examined, blue and tiger sharks, closely match the rates reported in observer records and by other sources. Accordingly, the inaccurate records that could not be identified were unlikely to have had a substantial effect on our results.

Recommendations

Although the USPL originally was designed to examine catch per unit of effort, if several additional variables were recorded in it, improved estimates of immediate mortality could be derived from this data set. Two additional categories, *at-vessel alive* and *at-vessel dead*, could be used to determine the number of animals that survive initial capture, and these categories would be required to determine factors that contribute to immediate mortality. An understanding of factors contributing to immediate mortality (Frick et al., 2010a; Frick et al., 2010b; Dapp et al., 2016b) could help fisheries managers to make well-informed management decisions. This information can also be used by commercial fishermen to improve the quality of their catch by avoiding environmental or operational conditions that result in increased likelihood of death of sharks in catches before the sharks are landed.

Other changes to recording variables or to presenting data in the USPL data set can be made to contribute to our understanding of fisheries-induced mortality and catch rates in future studies. Some variables (e.g., soak time and other targeted species) that were recorded in the USPL during the period examined were not made publicly available; a greater availability of these data would allow examination of additional, potentially important factors. Average gangion length was reported in the USPL, but we did not incorporate this factor into our analysis because lengths consistently were reported inaccurately (e.g., average gangion lengths >46 m were reported in 50% of longline sets). We are unsure why gangion length was often recorded inaccurately by fishermen, but a greater awareness of proper recording techniques for this variable could result in its use in future studies of immediate mortality. We recommend that 2 additional variables that can influence mortality or catch rates, namely air temperature during hauling and estimated set depth, should be added to future USPL reporting forms. In addition, several other variables that were not examined in our study but could influence catch and mortality rates have been included in recent iterations of the reporting form for the USPL (2015 form available from website; 2003 form available from website). These variables—bait used, hook type, hook size, and hook offset—should be incorporated into future analyses in which the USPL data set is used.

There were 19 categories (species or groupings) of sharks that were recorded by fishermen in the UPSL data set (Table 1). Only 4 of these categories were considered for analysis because of problems with identification and uncertainty about the accuracy of the recordings. The International Plan of Action for the Conservation and Management of Sharks outlined improved shark identification as one of its primary objectives and as a critical step to acquiring data to assess shark stocks (FAO[7]). We recommend that fishermen use shark identification guides or undertake shark identification training (or both) to improve the accuracy of entries in the USPL data set for cryptic species and species that are similar in appearance to other species.

We are the first to use the USPL data set to assess immediate mortality rates of longline-caught tiger and blue sharks. Rates of immediate mortality for these species closely match results from previous studies, and this similarity indicates accurate recording by commercial fishermen (Table 2). Because the USPL data set covers the entirety of the U.S. Atlantic commercial longline fishery, it can be used to determine long-term changes in mortality over a wide geographic scale that may not be achievable with other data sets. If additional variables are recorded by commercial fishermen, the USPL data set can be used to accurately discern causes of mortality during fishery capture in a wide range of species. Although our analysis was restricted to examining bycatch of sharks, the inclusion of additional variables could allow for mortality examinations of targeted teleosts and targeted sharks over a vast temporal and spatial scale.

The results of our study indicate the value of logbook data for scientific studies. In addition to providing immediate mortality rates, logbook data can be used to analyze catch rates, spatiotemporal catch trends, and species distributions (Cheng et al., 2001; Mandelman et al., 2008). The accessibility of the USPL data set to the general public promotes its use and advances our knowledge of fisheries science. Many other long-term government data sets have been collected, but they are not publicly available for analysis. Although we recognize the legal requirements for the protection of a fisherman's personal information, greater availability of governmental logbook and observer data would allow for the examination of fishery trends on a worldwide scale and will be necessary to implement effective global strategies for species management.

Our results indicate that fisheries management regulations have had a positive effect on the survival of the 2 shark species examined. The establishment of fin-to-carcass ratios has reduced the number of tiger shark discarded dead in the U.S. commercial long-

[7] FAO (Food and Agriculture Organization of the United Nations). 1999. International plan of action for reducing incidental catch of seabirds in longline fisheries. International plan of action for conservation and management of sharks. International plan of action for the management of fishing capacity, 26 p. FAO, Rome. [Available from website.]

line fishery. Additionally, fin-to-carcass ratios have not increased retention rates for tiger sharks (the mean percentages retained were 16% in 1992–1993 and 14% in 1993–2008) because these sharks are large-bodied animals, boats often have limited deck space, and their meat has a low commercial value (Mandelman et al., 2008; Simpfendorfer, 2009). Similarly, regulations that require the use of circle hooks during commercial longline operations have decreased the rate of immediate mortality for blue shark by 8.0%. Our study adds support to the assumption that fisheries regulations have been beneficial to some species, and results from recent studies indicate that species of sharks caught in the U.S. longline fishery are stable or increasing in abundance (Carlson et al., 2012).

Acknowledgments

Financial support to conduct this work was provided by the Australian Research Council Linkage Project LP110200572, the Holsworth Wildlife Research Endowment, Fisheries Victoria, the Australian Fisheries Management Authority, Melbourne Aquarium, and Monash University. We thank 3 anonymous reviewers for providing feedback on previous iterations of our manuscript.

Literature cited

Afonso, A. S., and F. H. V. Hazin.
2014. Post-release survival and behavior and exposure to fisheries in juvenile tiger sharks, *Galeocerdo cuvier*, from the South Atlantic. J. Exp. Mar. Biol. Ecol. 454:55–62.

Afonso, A. S., F. H. V. Hazin, F. Carvalho, J. C. Pacheco, H. Hazin, D. W. Kerstetter, D. Murie, and G. H. Burgess.
2011. Fishing gear modifications to reduce elasmobranch mortality in pelagic and bottom longline fisheries off Northeast Brazil. Fish. Res. 108:336–343.

Afonso, A. S., R. Santiago, H. Hazin, and F. H. V. Hazin.
2012. Shark bycatch and mortality and hook bite-offs in pelagic longlines: interactions between hook types and leader materials. Fish. Res. 131:9–14.

Baum, J. K., and R. A. Myers.
2004. Shifting baselines and the decline of pelagic sharks in the Gulf of Mexico. Ecol. Lett. 7:135–145.

Baum, J. K., and W. Blanchard.
2010. Inferring shark population trends from generalized linear mixed models of pelagic longline catch and effort data. Fish. Res. 102:229–239.

Baum, J. K., R. A. Myers, D. G. Kehler, B. Worm, S. J. Harley, and P. A. Doherty.
2003. Collapse and conservation of shark populations in the Northwest Atlantic. Science 299:389–392.

Bonfil, R.
1994. Overview of world elasmobranch fisheries. FAO Fish. Tech. Pap. 341, 119 p. FAO, Rome.

Bromhead, D., S. Clarke, S. Hoyle, B. Muller, P. Sharples, and S. Harley.
2012. Identification of factors influencing shark catch and mortality in the Marshall Islands tuna longline fishery and management implications. J. Fish Biol. 80:1870–1894

Burgess, G. H., L. R. Beerkircher, G. M. Cailliet, J. K. Carlson, E. Cortes, K. J. Goldman, R. D. Grubbs, J. A. Musick, M. K. Musyl, and C. A. Simpfendorfer.
2005. Is the collapse of shark populations in the northwest Atlantic Ocean and Gulf of Mexico real? Fisheries 30:19–26.

Campana, S. E., W. Joyce, and M. J. Manning.
2009. Bycatch and discard mortality in commercially caught blue sharks *Prionace glauca* assessed using archival satellite pop-up tags. Mar. Ecol. Prog. Ser. 387:241–253.

Carlson, J. K., L. F. Hale, A. Morgan, and G. Burgess.
2012. Relative abundance and size of coastal sharks derived from commercial shark longline catch and effort data. J. Fish Biol. 80:1749–1764.

Carruthers, E. H., D. C. Schneider, and J. D. Neilson.
2009. Estimating the odds of survival and identifying mitigation opportunities for common bycatch in pelagic longline fisheries. Biol. Conserv. 142:2620–2630.

Cheng, C. H., T. Kawasaki, K. P. Chiang, and C. H. Ho.
2001. Estimated distribution and movement of hairtail *Trichiurus lepturus* in the Aru Sea, based on the logbook records of trawlers. Fish. Sci. 67:3–13.

Cicia, A. M., L. S. Schlenker, J. A. Sulikowski, and J. W. Mandelman.
2012. Seasonal variations in the physiological stress response to discrete bouts of aerial exposure in the little skate, *Leucoraja erinacea*. Comp. Biochem. Physiol. A. 162:130–138.

Clarke, S. C., J. E. Magnussen, D. L. Abercrombie, M. K. McAllister, and M. S. Shivji.
2006. Identification of shark species composition and proportion in the Hong Kong shark fin market based on molecular genetics and trade records. Conserv. Biol. 20:201–211.

Clarke, S. C., M. P. Francis, and L. H. Griggs.
2013. Review of shark meat markets, discard mortality and pelagic shark data availability, and a proposal for a shark indicator analysis. NZ Fish. Assess. Rep. 2013/65, 78 p. Minist. Prim. Ind., Wellington, New Zealand. [Available at website, accessed January 2015.]

Coelho, R., J. Fernandez-Carvalho, P. G. Lino, and M. N. Santos.
2012. An overview of the hooking mortality of elasmobranchs caught in a swordfish pelagic longline fishery in the Atlantic Ocean. Aquat. Living Resour. 25:311–319.

Coelho, R., P. Infante, and M. N. Santos.
2013. Application of generalized linear models and generalized estimation equations to model at-haulback mortality of blue sharks captured in a pelagic longline fishery in the Atlantic Ocean. Fish. Res. 145:66–75.

Cramer, J., and H. Adams.
2000. Large pelagic logbook newsletter—1998. NOAA Tech. Memo. NMFS-SEFSC-433, 25 p.

Curran, D., and K. Bigelow.
2011. Effects of circle hooks on pelagic catches in the Hawaii-based tuna longline fishery. Fish. Res. 109:265–275.

Dapp, D. R., T. I. Walker,C. Huveneers, and R. D. Reina.
2016a. Respiratory mode and gear type are important determinants of elasmobranch immediate and post-release mortality. Fish Fish. 17:507–524.

Dapp, D. R., C. Huveneers, T. I. Walker, M. Drew, and R. D. Reina.
2016b. Moving from measuring to predicting bycatch mortality: predicting the capture condition of a longline-caught pelagic shark. Front. Mar. Sci. 2:126.

Dent, F., and S. Clarke.
2015. State of the global market for shark products. FAO Fish. Aquac. Tech. Pap. 590, 187 p. FAO, Rome.

Dulvy, N. K., S. L. Fowler, J. A. Musick, R. D. Cavanagh, P. M. Kyne, L. R. Harrison, J. K. Carlson, L. N. K. Davidson, S. V. Fordham, M. P. Francis, et al.
2014. Extinction risk and conservation of the world's sharks and rays. eLife 2014;3:e00590

Epperly, S. P., J. W. Watson, D. G. Foster, and A. K. Shah.
2012. Anatomical hooking location and condition of animals captured with pelagic longlines: the Grand Banks experiments 2002–2003. Bull. Mar. Sci. 88:513–527.

Francis, M. P., L. H. Griggs, and S. J. Baird.
2001. Pelagic shark bycatch in the New Zealand tuna longline fishery. Mar. Freshw. Res. 52:165–178.

Frick, L. H., R. D. Reina, and T. I. Walker.
2010a. Stress related physiological changes and post-release survival of Port Jackson sharks (*Heterodontus portusjacksoni*) and gummy sharks (*Mustelus antarcticus*) following gill-net and longline capture in captivity. J. Exp. Mar. Biol. Ecol. 385:29–37.

Frick, L. H., T. I. Walker, and R. D. Reina.
2010b. Trawl capture of Port Jackson sharks, *Heterodontus portusjacksoni*, and gummy sharks, *Mustelus antarcticus*, in a controlled setting: effects of tow duration, air exposure and crowding. Fish. Res. 106:344–350.

Gallagher, A. J., E. S. Orbesen, N. Hammerschlag, and J. E. Serafy.
2014. Vulnerability of oceanic sharks as pelagic longline bycatch. Global Ecol. Conserv. 1:50–59.

Gilman, E., S. Clarke, N. Brothers, J. Alfaro-Shigueto, J. Mandelman, J. Mangel, S. Petersen, S. Piovano, N. Thomson, P. Dalzell, et al.
2008. Shark interactions in pelagic longline fisheries. Mar. Policy 32:1–18.

Gilman, E., M. Chaloupka, Y. Swimmer, and S. Piovano.
2016. A cross-taxa assessment of pelagic longline by-catch mitigation measures: conflicts and mutual benefits to elasmobranchs. Fish Fish. 17:748–784.

Godin, A. C., J. K. Carlson, and V. Burgener.
2012. The effect of circle hooks on shark catchability and at-vessel mortality rates in longlines fisheries. Bull. Mar. Sci. 88:469–483.

Griggs, L. H., and S. J. Baird.
2013. Fish bycatch in New Zealand tuna longline fisheries 2006–07 to 2009–10. NZ Fish. Assess. Rep. 2013/13, 73 p. Minist. Prim. Ind., Wellington, New Zealand. [Available from website, accessed May 2015.]

Guida, L., T. I. Walker, and R. D. Reina.
2016. Temperature insensitivity and behavioural reduction of the physiological stress response to longline capture by the gummy shark, *Mustelus antarcticus*. PLoS One 11(2):e0148829.

Hight, B. V., D. Holts, J. B. Graham, B. P. Kennedy, V. Taylor, C. A. Sepulveda, D. Bernal, D. Ramon, R. Rasmussen, and N. C. Lai.
2007. Plasma catecholamine levels as indicators of the post-release survivorship of juvenile pelagic sharks caught on experimental drift longlines in the Southern California Bight. Mar. Freshw. Res. 58:145–151.

Hoenig, J. M., and S. H. Gruber.
1990. Life-history patterns in the elasmobranchs: implications for fisheries management. *In* Elasmobranchs as living resources: advances in biology, ecology, systematics, and the status of fisheries. NOAA Tech. Rep. NMFS 90 (H. L. Pratt Jr., S. H. Gruber, and T. Taniuchi, eds.), 1–16 p.

Hoffmayer, E. R., J. M. Hendon, and G. R. Parsons.
2012. Seasonal modulation in the secondary stress response of a carcharhinid shark, *Rhizoprionodon terraenovae*. Comp. Biochem. Physiol. A. 162:81–87.

Kerstetter, D. W., and J. E. Graves.
2006. Effects of circle versus J-style hooks on target and non-target species in a pelagic longline fishery. Fish. Res. 80:239–250.

Mandelman, J. W., P. W. Cooper, T. B. Werner, and K. M. Lagueux.
2008. Shark bycatch and depredation in the U.S. Atlantic pelagic longline fishery. Rev. Fish Biol. Fish. 18:427–442.

Morgan, A., and J. K. Carlson.
2010. Capture time, size and hooking mortality of bottom longline-caught sharks. Fish. Res. 101:32–37.

Morgan, A., P. W. Cooper, T. Curtis, and G. H. Burgess.
2009. Overview of the U.S. East Coast bottom longline shark fishery, 1994–2003. Mar. Fish. Rev.71(1):23–38.

Moyes, C. D., N. Fragoso, M. K. Musyl, and R. W. Brill.
2006. Predicting postrelease survival in large pelagic fish. Trans. Am. Fish. Soc.
135:1389–1397.

Musyl, M. K., R. W. Brill, D. S. Curran, N. M. Fragoso, L. M. McNaughton, A. Nielsen, B. S. Kikkawa, and C. D. Moyes.
2011. Postrelease survival, vertical and horizontal movements, and thermal habitats of five species of pelagic sharks in the central Pacific Ocean. Fish. Bull. 109:341–368.

Petersen, S. L.
2008. Understanding and mitigating vulnerable bycatch in southern African trawl and longline fisheries. Ph.D. thesis, 285 p. Univ. Cape Town, Cape Town, South Africa.

R Core Team.
2012. R: a language and environment for statistical computing. R Foundation for Statistical Computing, Vienna, Austria. [Available from website, accessed July 2013.]

Reardon, M. B., L. Gerber, and R. D. Cavanagh.
2006. *Isurus paucus*. The IUCN Red List of Threatened Species 2006: e.T60225A12328101..

Scott-Denton, E., P. F. Cryer, J. P. Gocke, M. R. Harrelson, D. L. Kinsella, J. R. Pulver, R. C. Smith, and J. A. Williams.
2011. Descriptions of the U.S. Gulf of Mexico reef fish bottom longline and vertical line fisheries based on observer data. Mar. Fish. Rev. 73(2):1–26.

Serafy, J. E., E. S. Orbesen, D. J. G. Snodgrass, L. R. Beerkircher, and J. F. Walter.
2012. Hooking survival of fishes captured by the UnitedStates Atlantic pelagic longline fishery: impact of the 2004 circle hooks rule. Bull. Mar. Sci. 88:605–621.

Simpfendorfer, C.
2009. *Galeocerdo cuvier*. The IUCN Red List of Threatened Species 2009:

Smith, S. E., D. W. Au, and C. Show.
1998. Intrinsic rebound potentials of 26 species of Pacific sharks. Mar. Freshw. Res. 49:663–678.

Sullivan, G. M., and R. Feinn.
2012. Using effect size—or why the *P* value is not enough. J. Grad. Med. Educ. 4:279–282.

Vannuccini, S.
1999. Shark utilization, marketing and trade. FAO Fish. Tech. Pap. 389, 470 p. FAO, Rome.

Watson, J. W., S. P. Epperly, A. K. Shah, and D. G. Foster.
2005. Fishing methods to reduce sea turtle mortality associated with pelagic longlines. Can. J. Fish. Aquat. Sci. 62:965–981.

Yokota, K., M. Kiyota, and H. Minami.
2006. Shark catch in a pelagic longline fishery: comparison of circle and tuna hooks. Fish. Res. 81:337–341.

National Marine
Fisheries Service
NOAA

Fishery Bulletin
established in 1881

Spencer F. Baird
First U.S. Commissioner
of Fisheries and founder
of *Fishery Bulletin*

Preliminary assessment of a direct age-determination method for 3 commercially important crustaceans from Alaska

Raouf Kilada (contact author)[1,2]
Joel B. Webb[3]
Kevin W. McNeel[4]
Laura M. Slater[5]
Quinn Smith[6]
Jayde Ferguson[7]

Email address for contact author: rwkilada@gmail.com

[1] Department of Biology
University of New Brunswick (Saint John)
100 Tucker Park Road
Saint John, New Brunswick E2L 4L5, Canada

[2] Department of Marine Science
Suez Canal University
Ismailia 41522, Egypt

[3] Division of Commercial Fisheries
Alaska Department of Fish and Game
P.O. Box 115526
Juneau, Alaska 99811-5526

[4] Age Development Unit, Mark, Tag, and Age Laboratory
Alaska Department of Fish and Game
P.O. Box 115526
Juneau, Alaska 99811-5526

[5] Division of Commercial Fisheries
Alaska Department of Fish and Game
351 Research Court
Kodiak, Alaska 99615

[6] Division of Commercial Fisheries
Alaska Department of Fish and Game
P.O. Box 110024
Juneau, Alaska 99811-0024

[7] Pathology Laboratory
Alaska Department of Fish and Game
333 Raspberry Road
Anchorage, Alaska 99518-1599

Abstract—Management of commercially important crab and shrimp species in Alaska has been hindered by the inability to directly determine the age of individual animals. We investigated the applicability of a recently developed method of age determination to red king crab (*Paralithodes camtschaticus*), southern Tanner crab (*Chionoecetes bairdi*), and spot shrimp (*Pandalus platyceros*) from Alaska. The cuticle structures of the mesocardiac ossicles of crabs and the eyestalks of spot shrimp were visualized with histological staining to identify the endocuticle, where growth bands have been observed in other crustaceans. For all species, paired light and dark bands were observed in longitudinal, thin sections of these structures in the majority of specimens examined. The proximal portion of the mesocardiac ossicle, where growth bands were observed, was absent in the foregut exuviae of red king and southern Tanner crabs that molted in captivity. If validated, counts of growth bands hold promise as a reliable measure for determining age of these species.

Manuscript submitted 10 August 2015.
Manuscript accepted 25 October 2016.
Fish. Bull. 115:42–49 (2017).
Online publication date: 15 November 2016.
doi: 10.7755/FB.115.1.4

The views and opinions expressed or implied in this article are those of the author (or authors) and do not necessarily reflect the position of the National Marine Fisheries Service, NOAA.

For many fish and invertebrate species, age can be determined directly from growth bands recorded in calcified hard structures. These structures include bones, scales, and otoliths in fish species (Campana, 2001) and statoliths and shell sections in a variety of invertebrates (Jensen, 1969; Kilada et al., 2007; Abele et al., 2009). Similar methods have not been applied to decapod crustaceans because of the presumed loss and replacement of calcified structures during ecdysis (Vogt, 2012). Instead, indirect methods, including captive observations, tag-recapture experiments, accumulation of lipofuscin in neural tissue, and analysis of size-frequency distributions, have been applied to infer age (Hartnoll, 2001; Vogt, 2012; Pinchuk et al., 2016).

A lack of reliable age information impedes assessment and management of crustacean fisheries (Caddy, 1986). In Alaska, some major crab stocks are assessed and managed by using length-based population models (e.g., Zheng et al., 1995), in which data on abundance, harvest, growth, and mortality are integrated. However, the accuracy of these models may be compromised if the growth or mortality rates are not truly representative of processes in situ. In contrast, age-structured models implicitly account for variability in growth and mortality by incorporating compre-

Table 1

Collection location, date, sex, and number of individual red king crab (*Paralithodes camtschaticus*), southern Tanner crab (*Chionoecetes bairdi*), and spot shrimp (*Pandalus platyceros*) collected in Alaska during 2013–2014 for investigation of presence of growth bands in thin sections of the mesocardiac ossicle of the gastric mill of red king and southern Tanner crabs and in eyestalks of spot shrimp.

Species	Collection location	Collection date	Sex	*n*
Red king crab	Bristol Bay, Alaska	June 2013	Female	30
Southern Tanner crab	Marmot Bay, Kodiak, Alaska	June 2014	Male	34
Spot shrimp	Seymour Canal, southeast Alaska	February and June 2014	Male and female	30

hensive size- and abundance-at-age data (Quinn and Deriso, 1999).

A direct method for determining age based on counting bands in the endocuticle layer has been presented for decapod crustaceans (Leland et al., 2011; Kilada et al., 2012). Bands were initially described in the ossicles of the gastric mill for 6 species (Leland et al., 2011; Kilada et al., 2012) and in the eyestalks of 2 additional species (Kilada et al., 2012). These observations have since been extended to additional crab, lobster, and shrimp species and to euphausids (Kilada and Acuna, 2015; Kilada et al., 2015; Sheridan et al., 2015; Kilada and Ibrahim, 2016; Krafft et al., 2016) and have been further supported by technical development, corroboration, and validation (Sheridan et al., 2015; Leland et al., 2015).

Our objective was to evaluate the potential of this method for 3 commercially important species in Alaska: the red king crab (*Paralithodes camtschaticus*), southern Tanner crab (*Chionoecetes bairdi*), and spot shrimp (*Pandalus platyceros*). Feasibility was evaluated 1) by identifying the endocuticle layer by histological examination, 2) by observing the presence or absence of growth bands in the endocuticle of the mesocardiac ossicles of crabs and eyestalks of shrimp, and 3) by determining whether the region of the mesocardiac ossicle, where growth bands have been observed, may be retained during ecdysis for these crab species. The mesocardiac ossicle was selected as the primary structure for investigation in the 2 crab species because of the presence of clear bands and evidence of possible retention through ecdysis (Leland et al. 2011; Kilada et al., 2012). The eyestalks of shrimp were selected because of the dissimilarity between crab and shrimp gastric mill ossicles and because of the evidence of the presence of bands in the eyestalk of shrimp (Kilada et al., 2012).

Materials and methods

Histological examination

Red king crab and spot shrimp were collected in southeast Alaska in 2014, by using pot gear, and southern Tanner crab were collected near Kodiak, Alaska, in 2014 by using trawl gear (n=3 for each species). Gastric mills of red king and southern Tanner crabs and paired eyestalks of spot shrimp were dissected and preserved in Bouin's fixative for approximately 1 month and then transported to the Fish Pathology Laboratory of the Alaska Department of Fish and Game in Anchorage, Alaska. Before processing, mesocardiac ossicles of some red king crabs were trimmed to fit within histological cassettes (1 cm^2), but most ossicles and eyestalks did not require trimming. Structures were transferred to 70% ethanol and decalcified with Evans and Krajian fluid (Evans and Krajian, 1930). Tissues were dehydrated, infiltrated, and embedded in paraffin with an automatic tissue processor. Histological cassettes were cut longitudinally into 6-µm sections with a rotary microtome, and sections were mounted onto glass slides. Sections of mesocardiac ossicles of crabs and eyestalks of spot shrimp were prepared and stained with Masson's trichrome (Thermo Fisher Scientific[1], Waltham, MA) and permanently mounted with Permount mounting medium (Thermo Fisher Scientific). Masson's trichrome was expected to stain the endocuticle and exocuticle layers blue and the membranous layer (hypodermis) and epicuticle red. The cuticle layers (for detailed description, see Vatcher et al., 2015) were then examined with a Zeiss microscope (Carl Zeiss Microscopy, Jena, Germany) and photographed with a Jenoptik digital camera and ProgRes CapturePro software (JENOPTIK Optical Systems Inc., Jupiter, FL).

Presence of growth bands

Red king crab, southern Tanner crab, and spot shrimp (n=30, 34, and 30, respectively) of a range of body sizes were collected across Alaska in 2013 and 2014 (Table 1). Carapace length (CL) and shell condition of red king crabs, carapace width (CW) and shell condition of southern Tanner crabs, CL of spot shrimp, and sex (identified from pleopod morphological features for shrimp) of all specimens were record-

[1] Mention of trade names or commercial companies is for identification purposes only and does not imply endorsement by the National Marine Fisheries Service, NOAA.

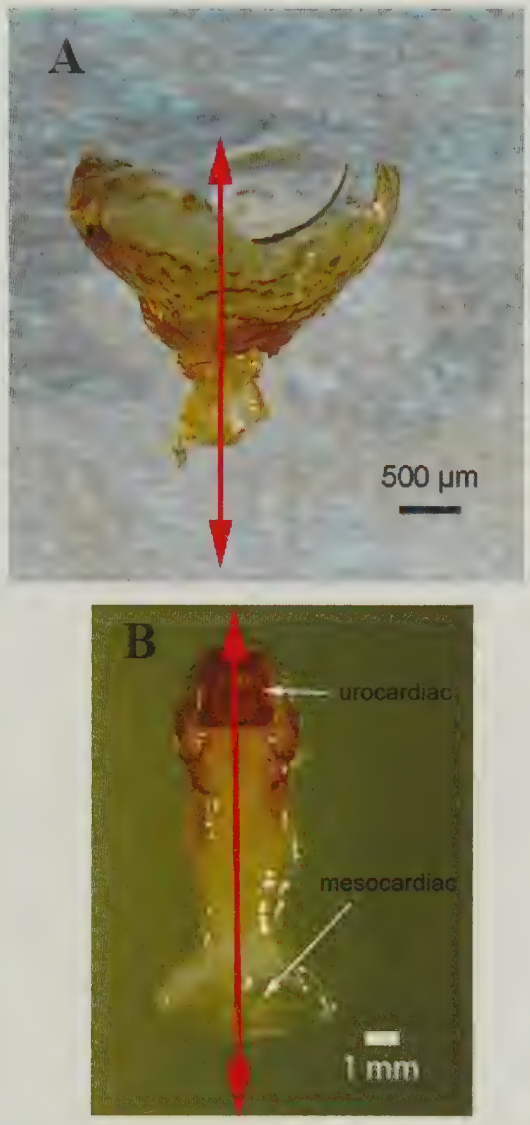

Figure 1

Locations of the longitudinal axes used for preparation of thin sections indicated by red arrows for (**A**) the eyestalk of spot shrimp (*Pandalus platyceros*) and (**B**) the dorsal ossicle (urocardiac and mesocardiac) of red king (*Paralithodes camtschaticus*) and southern Tanner (*Chionoecetes bairdi*) crabs, as illustrated with the ossicle of a southern Tanner crab. Red king and southern Tanner crabs and spot shrimp were collected in Alaska during 2013–2014 for this study of a direct age-determination method.

ed at the time of collection. Shell condition, a subjective index of epibionts and wear on the exoskeleton, was noted because it has proven useful for evaluating differences in the recency of molting in crab species (Jadamec et al., 1999; Donaldson and Byersdorfer, 2002). Crab gastric mills and shrimp eyestalks were dissected, cleaned, and preserved in a mixture of ethanol, glycerol, and distilled water (with a volume ratio of 70:4:26).

Structures were embedded in cold cure epoxy resin and sectioned longitudinally (Fig. 1) with a diamond-bladed IsoMet Low Speed Saw (Buehler, Lake Bluff, IL) at the University of New Brunswick in Saint John, New Brunswick, Canada. Several serial sections (with thickness of 160–180 µm) were prepared per structure and mounted with epoxy individually on slides, polished by hand with dry, 0.3-µm-grit lapping film, covered with 90% ethyl alcohol, and viewed under transmitted light with a CX41 Olympus compound microscope (Olympus Corp., Tokyo) at 100–400× magnification. All cuticular layers were examined throughout the thin sections, and bands were recognized as alternating (bipartite) translucent and opaque zones in the endocuticle of crab mesocardiac ossicles and shrimp eyestalks. Photographs were taken with a DP72 Olympus digital camera (Olympus Corp.) attached to the microscope.

Examination of exuvial gastric structures

Two female red king crab were captured by divers in southeast Alaska and 3 male southern Tanner crab were captured by pot and trawl gear near Kodiak, Alaska, in 2014. Female red king crabs were immature and grasped by males in situ (precopulatory guarding of mate), indicating that the pubertal molt to maturity was imminent. All crabs were held in aquaria with flow-through seawater at ambient seawater temperature and monitored daily until they molted. After ecdysis, the exuvial gastric mill structures were removed and photographed. At 1 week after the molt, the whole stomach was dissected from the crab, and the gastric mill structures were photographed for comparison with the same structures from the exuviae.

Results

Histological examination of the cuticle

The endocuticular layer was visually differentiated from other cuticular layers in the mesocardiac ossicles of red king and southern Tanner crabs (Fig. 2) and in the eyestalks of spot shrimp (Fig. 3) after ossicles were stained with Masson's trichrome. The epicuticle, exocuticle, and membranous layers were clearly visible in thin sections of crab mesocardiac, where red indicated the membranous layer and epicuticle (Fig. 2). Lamellar structure, of alternating light and dark stained bands, were more discernible in the mesocardiac of a southern Tanner crab (Fig. 2B) and the exo- and endocuticle of the eyestalk of a spot shrimp (Fig. 3B) than in the mesocardiac of a red king crab (Fig. 2C) at similar magnification. The cuticle layers of the eyestalks of spot shrimp tended to separate during histological sectioning (Fig. 3A).

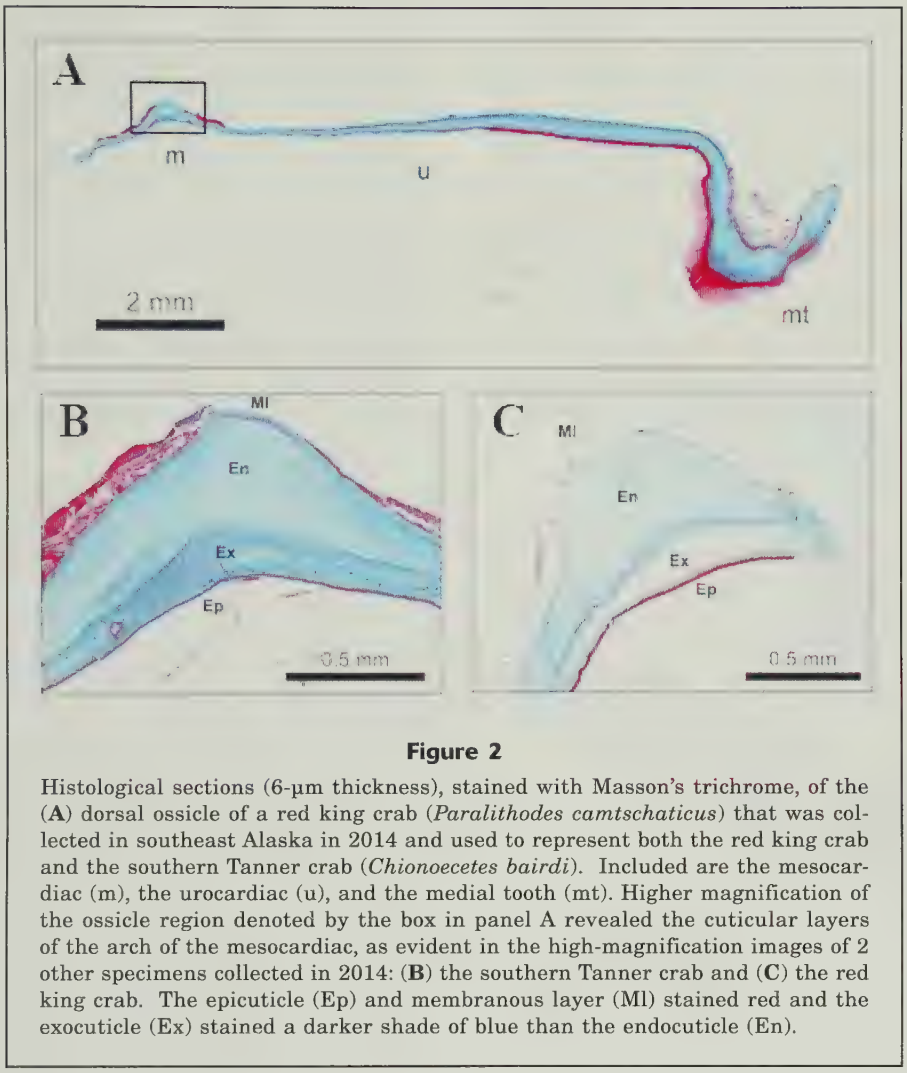

Figure 2

Histological sections (6-µm thickness), stained with Masson's trichrome, of the (**A**) dorsal ossicle of a red king crab (*Paralithodes camtschaticus*) that was collected in southeast Alaska in 2014 and used to represent both the red king crab and the southern Tanner crab (*Chionoecetes bairdi*). Included are the mesocardiac (m), the urocardiac (u), and the medial tooth (mt). Higher magnification of the ossicle region denoted by the box in panel A revealed the cuticular layers of the arch of the mesocardiac, as evident in the high-magnification images of 2 other specimens collected in 2014: (**B**) the southern Tanner crab and (**C**) the red king crab. The epicuticle (Ep) and membranous layer (Ml) stained red and the exocuticle (Ex) stained a darker shade of blue than the endocuticle (En).

Presence of growth bands

Thin sections were successfully obtained from the mesocardiac ossicles from 19 red king crabs and 32 southern Tanner crabs and single eyestalks from 18 spot shrimp. For mesocardiac sections of both crab species, bipartite band patterns (exclusive of the lamellae) were clearest in the location of maximum endocuticle thickness in relation to the exo- and epicuticle that was at the proximal end of the structure (Figs. 2A, 4, A–B). For spot shrimp, bands were clearest at the proximal end of the eyestalk with respect to the anterior tip of the cephalothorax (Figs. 3A, 4C).

Ossicular retention throughout ecdysis

Comparison of gastric mill structures in exuviae with those of postmolt stomachs of crabs indicated differences in presence of regions of the gastric mill. The cusp of the medial tooth of the urocardiac and zygocardiac ossicles of the gastric mill, along with the portion of the ossicle adjacent to each tooth, were the primary structures present in the exuviae of both southern Tanner and red king crabs (Fig. 5A). For both crab species, the anterior portion of mesocardiac, the pterocardiac, and the anterior portions of the zygocardiac ossicles were not visible in the exuviae, but they were present and robust in a postmolt crab, indicating that these portions were potentially retained or resorbed and subsequently replaced (Fig. 5, B and D).

Discussion

The presence of bands in the endocuticle layer of the mesocardiacs of southern Tanner and red king crabs and in the eyestalks of spot shrimp indicated that determining age on the basis of band counts may be feasible, as it is for other crustacean species (e.g., Leland et al., 2011; Kilada et al., 2012; Leland et al., 2015; Kilada et al., 2015; Sheridan et al., 2015; Kilada and Ibrahim, 2016; Krafft et al., 2016). Histological charac-

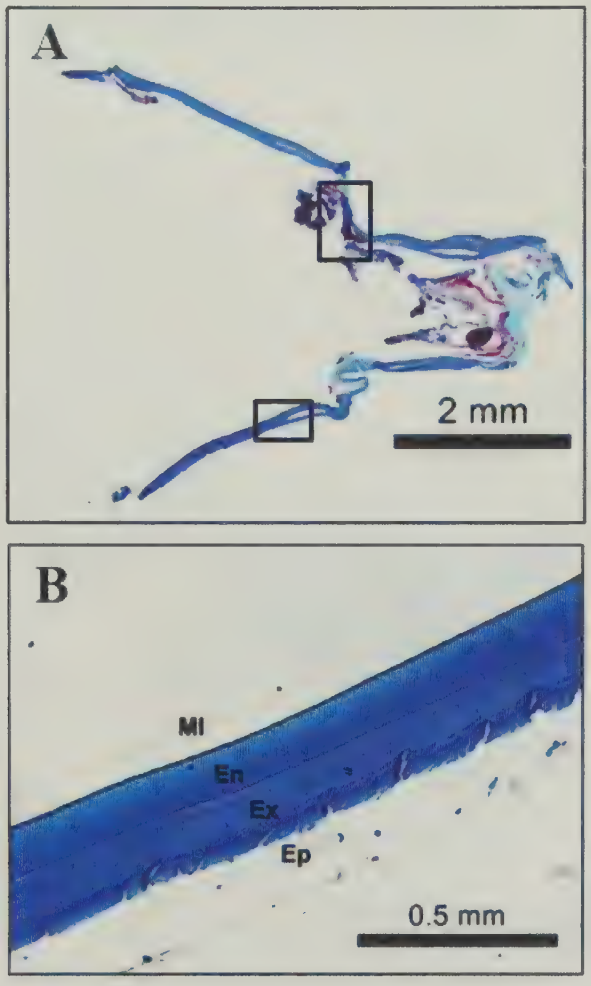

Figure 3

Histological sections (6-µm thickness), stained with Masson's trichrome, of the eyestalk of a spot shrimp (*Pandalus platyceros*) collected in Alaska in 2014, showing (**A**) the entire eyestalk and (**B**) the cuticular layering, as seen in the inset in the smaller, lower small box in panel A, including the epicuticle (Ep), exocuticle (Ex), endocuticle (En), and membranous layer (Ml). The larger box indicates the location within the structure where growth bands were observed in Figure 4C.

terization of the mesocardiac ossicles of the crab species and of the eyestalk of the spot shrimp defined the boundaries between cuticular layers—boundaries that are critical for developing band counting criteria. As with results from studies of other species (e.g., Kilada et al., 2012; Leland et al., 2015), there was preliminary evidence that a portion of the mesocardiac ossicle, where band patterns are observed in the endocuticle, is either retained or replaced during molting. A structure that is retained through ecdysis would be useful for evaluating band information.

The cuticle layers of the mesocardiac ossicles of red king and southern Tanner crabs and the eyestalks of spot shrimp were similar to those observed in other studies of decapod crustaceans (see Roer and Dillaman, 1984, and references therein; Vatcher et al., 2015). Differences in staining results may be due to differences in the specific calcium compound involved in the biomineralization within each region (Vatcher et al., 2015). As in results for blue crab (*Callinectes sapidus*) with the use of acridine orange (a different histological stain) (Vatcher et al., 2015), the medial tooth of the urocardiac stained similarly and was continuously connected to the epicuticle in both crab species examined in this study (Fig. 2A). This result further supports the hypothesis that the hardened cusp of the tooth is of epicuticular rather than exocuticular origin (Vatcher et al., 2015).

Bipartite patterns were readily visible in the mesocardiac ossicles of red king and southern Tanner crabs and in the eyestalks of spot shrimp. Recurrence of this pattern in multiple individuals indicates that band counts may be promising as indicators of growth variability through the lifetime of these species. Before this experiment, bands were observed in eyestalks of snow crab (*C. opilio*), which is a congener of the southern Tanner crab (Kilada et al., 2012). We evaluated the mesocardiac of the southern Tanner crab because of the possibility that this structure may be retained through ecdysis (Kilada et al., 2012; Leland et al., 2015; but also see Vatcher et al., 2015). To our knowledge, description of growth bands in red king crabs is a first for the family Lithodidae. The appearance of bands in spot shrimp was very similar to that observed in the eyestalks of a congener, the northern shrimp (*P. borealis*) (Kilada et al., 2012). Finally, most notably for the red king crab, a high proportion of the structures evaluated for growth bands were damaged during embedding or preparing thin sections. Structures were, by necessity, shipped dry before they were embedded in resin, and this condition likely contributed to their fragility and high fracture rate during the embedding and sectioning processes. Embedding structures before shipping could effectively mitigate this problem.

The absence of the basal region of the mesocardiac (where band patterns are observed in thin sections) in exuviae of southern Tanner and red king crabs indicated that this portion of the ossicle was either retained or replaced within 1 week after molting (Fig. 5, A and C). Recently it has been hypothesized that the endocuticle region of the pterocardiac and mesocardiac ossicles is retained through molting (Kilada et al., 2012; Leland et al., 2015). Calcein marks in the endocuticle were visible after several molts and portions of the ossicles were absent in the exuviae of lobster and crayfish species. However, for the blue crab, histological characterization of the cuticular layers of the dorsal ossicle (dorsomedial tooth) indicated that the dorsal cuticle (Roer and Dillaman, 1984), like the endocuticle, is resorbed during the premolt stage and resynthesized during the postmolt stage (Vatcher et al., 2015). As with brachyuran crabs (Brösing, 2014), the gastric teeth differed

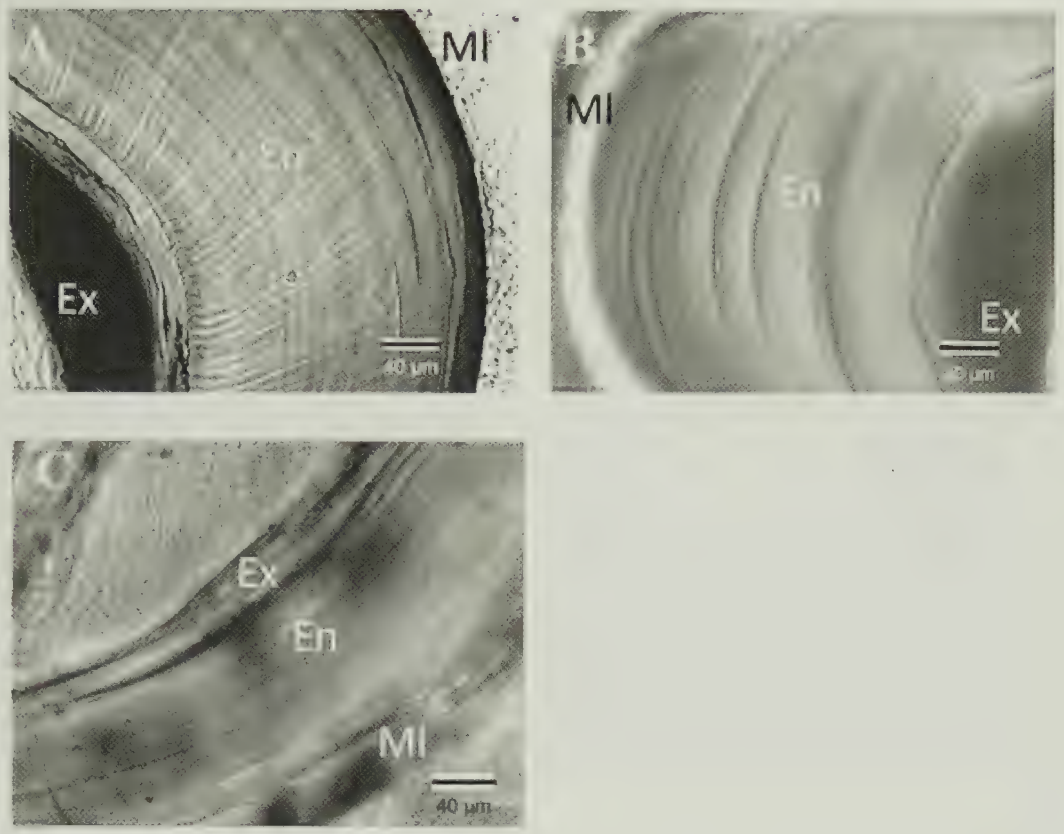

Figure 4

Bipartite growth band patterns in the endocuticle of the arch of the mesocardiac ossicle of the gastric mill (for reference, see Fig. 2) of (**A**) a red king crab (*Paralithodes camtschaticus*) collected in Bristol Bay, Alaska, in June 2013; (**B**) a southern Tanner crab (*Chionoecetes bairdi*) collected in Marmot Bay, Alaska, in June 2014; and (**C**) in the proximal portion of the eyestalk of a spot shrimp (*Pandalus platyceros*) collected in Seymour Canal, Alaska, in May 2014, all under transmitted light. The endocuticle (En), exocuticle, (Ex), and membranous layer (Ml) are labeled for orientation.

in biomineralization from other portions of the gastric mill (Vatcher et al., 2015) and remained in the exuviae of both crab species examined in this study.

Our results are an initial step toward developing and further evaluating growth bands as a possible indicator of age for commercially valuable crustaceans in Alaska. Key areas for further research include evaluations of variability (precision) in band count and clarity among the primary ossicles (pterocardiac, zygocardiac, and mesocardiac) of the gastric mill (Leland et al., 2011; Leland et al., 2015; Sheridan et al., 2015), innovation in preparation techniques for thin sections (Sheridan et al., 2015), definitions of criteria for identifying bands (e.g., Leland et al. 2015), determination of the fate (retention or replacement) of the endocuticle during molting (Vatcher et al., 2015), and corroboration of band counts with current understanding of species-specific growth, life history, and longevity based on indirect methods. Ultimately, hypotheses should also be developed regarding the mechanism by which growth bands are formed and retained in structures that are molted (shrimp eyestalk) or possibly retained (e.g., gastric mill ossicles) (Kilada et al., 2012; Leland et al., 2015; Vatcher et al., 2015).

Rigorous validation of bands as indices of age will also be necessary before their application in stock assessment and fisheries management (Beamish and McFarlane, 1983; Campana, 2001; Leland et al., 2011). Validation techniques potentially applicable to the species investigated in this study include the use of autofluorescent stains and the use of specimens with known ages. Autofluorescent stains, such as calcein, can create discrete marks in calcified hard parts that can be used to examine band deposition with

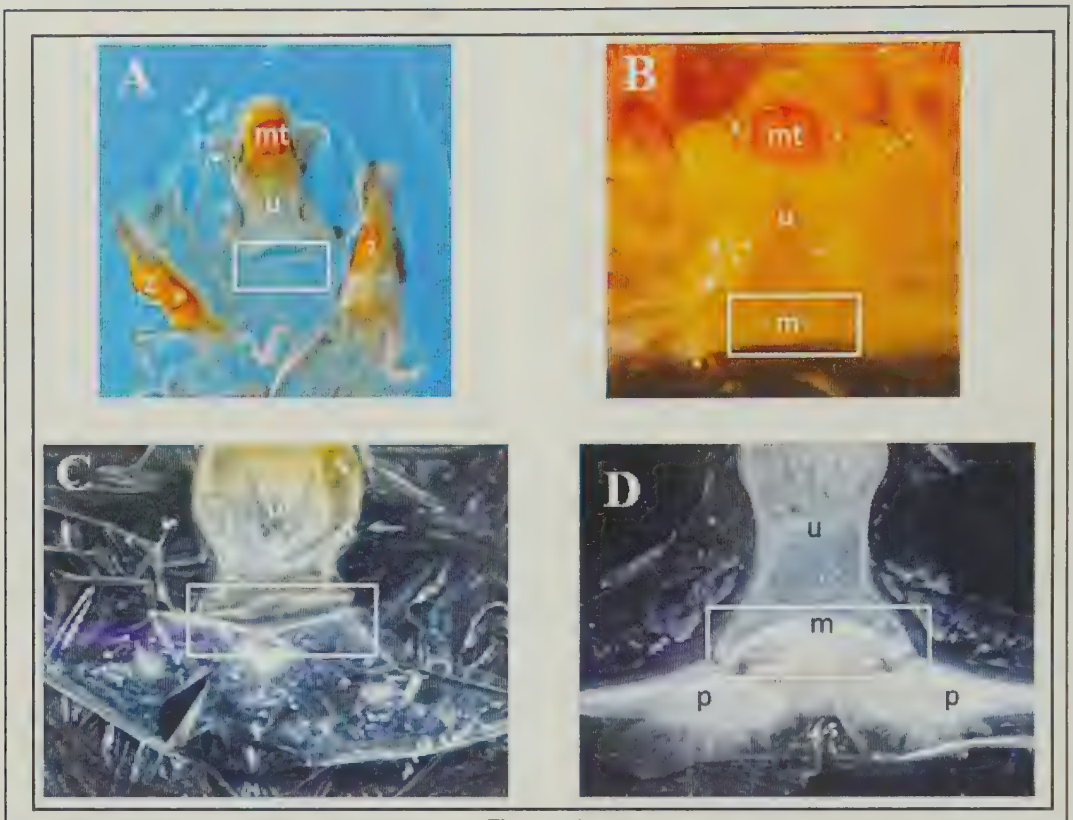

Figure 5

(**A**) Image of the primary ossicles of the gastric mill seen in the exuvia of a red king crab (*Paralithodes camtschaticus*) collected in Bristol Bay, Alaska, in June 2013. Included are the lateral teeth of the zygocardiac ossicle (z) and the medial tooth (mt) and urocardiac (u) of the dorsal (uro- and mesocardiac) ossicle, showing that the portion of the ossicle containing the arch of the mesocardiac (m, indicated by the box and illustrated in Fig. 2) was absent. (**B**) Image of the dorsal ossicle of the same red king crab 1 week after ecdysis, showing that the entire mesocardiac was present (boxed). (**C**) The base of the dorsal ossicle for the exuvia of a southern Tanner crab (*Chionoecetes bairdi*) collected in Marmot Bay, Alaska, in June 2014, showing that the urocardiac was present but the mesocardiac (boxed) and pterocardiac ossicles were absent. (**D**) Image of the gastric mill ossicles, showing that the mesocardiac (boxed) and pterocardiac ossicles (p) were present in the ossicle of the southern Tanner crab 1 week after ecdysis.

elapsed time after marking (Kilada et al., 2012; Leland et al., 2015). Further, determining band counts for crustaceans for which ages are known (e.g., animals reared in captivity) will be necessary to further understand dynamics of band formation (Leland et al., 2015).

Acknowledgments

This project was funded by the Alaska Department of Fish and Game. Thanks are extended to C. Siddon and D. Pengilly of the Alaska Department of Fish and Game for their support and to D. Oxman for an earlier review of this manuscript. Three anonymous reviewers contributed to significant improvement of the manuscript through review of a previous draft. This short contribution is professional publication number PP-280 of the Alaska Department of Fish and Game.

Literature cited

Abele, D., T. Brey, and E. Philipp.
2009. Bivalve models of aging and the determination of molluscan lifespans. Exp. Gerontol. 44:307–315.

Beamish, R. J., and G. A. McFarlane.
1983. The forgotten requirement for age validation in fisheries biology. Trans. Am. Fish. Soc. 112:735–743.

Brösing, A.
2014. Foregut structures of freshly moutled exuviae from *Maja crispate*, *Cancer pagurus* and *Pseudosesarma moeschi* (Decapoda: Brachyura). J. Nat. Hist. 48:543–555.

Caddy, J. F.
1986. Modelling stock-recruitment processes in Crustacea: some practical and theoretical perspectives. Can. J. Fish. Aquat. Sci. 43:2330–2344.
Campana, S. E.
2001. Accuracy, precision, and quality control in age determination, including a review of the use and abuse of age validation methods. J. Fish Biol. 59:197–242.
Donaldson, W. E., and S. C. Byersdorfer.
2005. Biological field techniques for lithodid crabs. Alaska Sea Grant College Program, AK-SG-05-03, 82 p. Univ. Alaska, Fairbanks. AK.
Evans, N. and A. Krajian.
1930. New method of decalcification. Arch. Path. 10:447.
Hartnoll, R. G.
2001. Growth in Crustacea—twenty years on. *In* Advances in decapod crustacean research: proceedings in the 7th colloquium Crustacea Decapoda Mediterranea; Lisbon, Portugal, 6–9 September 1999 (J. P. M. Paula, A. A. V. Flores, and C. H. J. M. Fransen, eds.), p. 111–122. Springer Science+Business Media, Dordrecht, Netherlands.
Jadamec, L. S., W. E. Donaldson, and P. Cullenberg.
1999. Biological field techniques for *Chionoecetes* crabs. Alaska Sea Grant College Program AK-SG-99-02, 80 p. Univ. Alaska, Fairbanks, AK.
Jensen, M.
1969. Age determination of echinoids. Sarsia 37:41–44. Article
Kilada, R., and E. Acuña.
2015. Direct age determination by growth band counts of three commercially important crustacean species in Chile. Fish. Res. 170:134–143.
Kilada, R., and N. K. Ibrahim.
2016. Preliminary investigation of direct age determination using band counts in the gastric mill of the blue swimmer crab (*Portunus pelagicus* Linneus, 1758) in two salt-water lakes in the eastern Mediterranean. J. Crust. Biol. 36:119–128.
Kilada, R. W., D. Roddick, and K. Mombourquette.
2007. Age determination, validation, growth and minimum size of sexual maturity of the greenland smoothcockle (*Serripes groenlandicus*, Bruguiere, 1789) in eastern Canada. J. Shellfish Res. 26:443–450.
Kilada, R., B. Sainte-Marie, R. Rochette, N. Davis, C. Vanier, and S. Campana.
2012. Direct determination of age in shrimps, crabs, and lobsters. Can. J. Fish. Aquat. Sci. 69:1728-–1733.
Kilada, R., A.-L. Agnalt,, N. H. Arboe, S. Bjarnason, A. Burmeister, E. Farestveit, Ó. S. Gíslason, A. Guðlaugsdóttir, D. Guðmundsdóttir, J. P. Jónasson, et al.
2015. Feasibility of using growth band counts in age determination of four crustacean species in the Northern Atlantic. J. Crust. Biol. 35:499–503.
Krafft, B. A., M. Kvalsund, G. Søvik, E. Farestveit, and A.-L. Agnalt.
2016. Detection of growth zones in the eyestalk of the Antarctic krill *Euphausia superba* (Dana, 1852) (Euphausiacea). J. Crust. Biol. 36:267–273.
Leland, J. C., J. Coughran, and D. J. Bucher.
2011. A preliminary investigation into the potential value of gastric mills for ageing crustaceans. *In* New frontiers in crustacean biology: proceedings of the TCS summer meeting, Tokyo, 20–24 September 2009. Crustacean Monographs 15 (A. Asakura, ed.), p. 57–68.
Leland, J. C., D. J. Bucher, and J. Coughran
2015. Direct age determination of a subtropical freshwater crayfish (redclaw, *cherax quadricarinatus*) using ossicular growth marks. PLoS ONE 10(8):e0134966.
Pinchuk, A. I., H. R. Harvey, and G. L. Eckert.
2016. Development of biochemical measures of age in the Alaskan red king crab *Paralithodes camtschaticus* (Anomura): validation, refinement and initial assessment. Fish. Res. 183:92–98.
Quinn, T. J., II, and R. B. Deriso.
1999. Quantitative fish dynamics, 560 p. Oxford Univ. Press Inc., New York.
Roer, R., and R. Dillaman.
1984. The structure and calcification of the crustacean cuticle. Am. Zool. 24:893–909.
Sheridan, M., R. Officer, I. O'Connor, and C. Lordan.
2015. Investigating the feasibility of using growth increments for age determination of Norway lobster (*Nephrops norvegicus*) and brown crab (*Cancer pagurus*). J. Crust. Biol. 35:495–498.
Vatcher, H. E., R. D. Roer, and R. M. Dillaman.
2015. Structure, molting, and mineralization of the dorsal ossicle complex in the gastric mill of the blue crab, *Callinectes sapidus*. J. Morphol. 276:1358–1367.
Vogt, G.
2012. Ageing and longevity in the Decapoda (Crustacea): a review. Zool. Anz. 251: 1–25.
Zheng, J., M. C. Murphy, and G. H. Kruse.
1995. A length-based population model and stock–recruitment relationships for red king crab, *Paralithodes camtschaticus*, in Bristol Bay, Alaska. Can. J. Fish. Aquat. Sci. 52:1129–1246.

National Marine
Fisheries Service
NOAA

Fishery Bulletin
established in 1881

Spencer F. Baird
First U.S. Commissioner
of Fisheries and founder
of *Fishery Bulletin*

Influence of bait type on catch rates of predatory fish species on bottom longline gear in the northern Gulf of Mexico

William B. Driggers III (contact author)[1]
Matthew D. Campbell[1]
Kristin M. Hannan[2]
Eric R. Hoffmayer[1]
Christian M. Jones[1]
Lisa M. Jones[1]
Adam G. Pollack[2]

Email address for contact author: william.driggers@noaa.gov

[1] Mississippi Laboratories
Southeast Fisheries Science Center
National Marine Fisheries Service, NOAA
P.O. Drawer 1207
Pascagoula, Mississippi 39567

[2] Riverside Technology Inc.
Mississippi Laboratories
Southeast Fisheries Science Center
National Marine Fisheries Service, NOAA
P.O. Drawer 1207
Pascagoula, Mississippi 39567

Abstract—Identifying effective methods of reducing shark bycatch in hook-based fisheries has received little attention despite reports of declines in some shark populations. Previously proposed shark bycatch mitigation measures include gear modifications, time and area closures, avoidance of areas with high shark abundance, use of repellents, and use of specific bait types. Regardless of the method of shark bycatch reduction, knowledge of the effects of the chosen method on the catch rates of targeted fish species should be understood. To examine the effects of bait type on catch rates of sharks and teleosts on bottom longline gear, standardized gear was deployed with bait alternating between Atlantic mackerel (*Scomber scombrus*) and northern shortfin squid (*Illex illecebrosus*). For all shark species examined, except the scalloped hammerhead (*Sphyrna lewini*), a preference for hooks baited with Atlantic mackerel was observed. Commercially and recreationally important teleosts had no significant preference for a specific bait, with the exception of the red drum (*Sciaenops ocellatus*), which had a significant preference for hooks baited with northern shortfin squid. Bait preference decreased as total catch rate increased on individual longline sets. Our results point to the use of specific baits as a viable method to reduce shark catch rates without decreasing catches of targeted teleosts.

Manuscript submitted 10 November 2015.
Manuscript accepted 27 October 2016.
Fish. Bull. 115:50–59 (2017).
Online publication date: 10 November 2016.
doi: 10.7755/FB.115.1.5

The views and opinions expressed or implied in this article are those of the author (or authors) and do not necessarily reflect the position of the National Marine Fisheries Service, NOAA.

Because of reported declines in some shark populations, there has been increasing interest in mitigating bycatch rates of shark species in longline fisheries that target teleosts (Francis et al., 2001; Beerkircher et al., 2002; Gilman et al., 2008; Ward et al., 2008). Within the northern Gulf of Mexico, commercial fishing for sharks has occurred since the 1920s (Rogers, 1920) and continues to present day. Although directed commercial fishing effort for sharks in the region has waxed and waned over the years, shark bycatch continues to be an important source of mortality, particularly in hook-based fisheries, such as the snapper and grouper bottom longline fishery (e.g., Scott-Denton et al., 2011).

Proposed or enacted efforts to curtail shark bycatch in longline fisheries have included gear modifications (Ward et al., 2008), reductions in gear soak time (Carruthers et al., 2011), adjustments in fishing depth (Rey and Muñoz-Chápuli, 1991), time and area closures (Watson et al., 2009), avoidance of areas of known high shark abundance (Walsh et al., 2009), use of repellents (Robbins et al., 2011) and use of specific bait types (Gilman et al., 2007). Ultimately, for any bycatch reduction method to be fully embraced within a fishery, it will be necessary that catch rates of targeted species not be negatively affected when a specific approach is applied. Ideally, a bycatch reduction approach would minimize bycatch rates and not affect catch rates of target species and cause the least amount of economic hardship and changes to proven fishing practices. Among measures proposed to mitigate shark bycatch, use of bait that

does not decrease catch rates of target species yet reduces rates of shark capture could be the most easily implemented and likely to be readily accepted within a fishery.

Past studies have shown that catch rates of certain shark species are affected by the use of specific bait types. For example, Gilman et al. (2007) analyzed data collected in the pelagic longline fishery in Hawaii and determined that the catch rate of blue sharks (*Prionace glauca*) was reduced by 36% when fish, rather than squid, were used as bait. Similarly, Watson et al. (2005) conducted experimental longline sets in the western North Atlantic Ocean and found catch rates of blue sharks were 31–40% (depending on hook type) lower on hooks baited with fish than on hooks baited with squid. Although results of these studies are potentially biased by use of multiple hook types and sizes, their results strongly indicate that use of a specific bait type could be a means to reduce bycatch of sharks.

Hook-based fisheries in the northern Gulf of Mexico that target grouper (Serranidae), snapper (Lutjanidae), and tilefish (Malacanthidae) species frequently capture sharks (Gulak et al., 2013). For example, the Atlantic sharpnose shark (*Rhizoprionodon terraenovae*) was the sixth-most captured fish species among the approximately 180 fish species reported in observer data collected from the bottom longline fishery for reef fish in the Gulf of Mexico (Scott-Denton et al., 2011). Furthermore, smoothhound (*Mustelus* spp.) and blacknose (*Carcharhinus acronotus*) sharks were among the 20 most frequently captured fish taxa within the same fishery (Scott-Denton et al., 2011). The size and type of hooks vary in the bottom longline fishery for reef fish in the Gulf of Mexico (Gulak et al., 2013), and bait type is inconsistent, depending on personal preference, availability, and price, among other factors (Prytherch, 1983; Scott-Denton et al., 2011). Because there is high variability in the gear and bait used within this fishery, use of observer data to examine potential effects of bait type on the catch rates of specific species is problematic. Our goal was to conduct a controlled experiment to test the effects of 2 readily available bait types commonly used in the bottom longline fishery for reef fish on catch rates of sharks and economically important teleosts in this region. Additionally, we examined density-dependent effects on preferences for the 2 bait types for both groups of fish species.

Materials and methods

Bottom longline gear was deployed from the NOAA Ship *Oregon II* at sampling sites in the northern Gulf of Mexico from 11 March through 13 April 2015. Sampling sites were selected on the basis of 18.5-km grids within predefined geographic areas (from Pascagoula, Mississippi, to Cape San Blas, Florida) and depth (9–1000 m) constraints. However, obstructions (e.g., other vessels, reefs, petroleum platforms, and safety fairways) caused the locations of some sampling sites to be different from the positions that were originally planned. The bounds of the sampling universe were selected to maximize sampling opportunities within temporal limitations.

Bottom longline gear consisted of 1842 m of 4.0-mm monofilament mainline and 100 gangions. Each gangion was 3.7 m in length and constructed of an AK snap (size 150), 3.2 m of 3.0-mm-diameter monofilament, 0.5 m of 2.4-mm-diameter fishing wire, and a 15/0 circle hook (Mustad #39960D[1], O. Mustad & Son A.S, Gjörvik, Norway). Each gangion was baited with Atlantic mackerel (*Scomber scombrus*) or northern shortfin squid (*Illex illecebrosus*). Both bait types were cut so that they were of the same approximate dimensions and appropriately sized for the hook. Gangions were deployed so that each bait type alternated along the length of the mainline (i.e., northern shortfin squid, Atlantic mackerel, northern shortfin squid, Atlantic mackerel), and the starting bait type was selected randomly for each longline set.

Gear soak time, defined as time elapsed between deployment of the terminal high flyer during gear deployment and retrieval of the first high flyer during haulback, was approximately 1 h at sampling sites with depths less than 400 m and 2 h at sampling sites with depths greater than 400 m. However, the actual time each hook spends in the water can vary due to a number of factors, such as hook position along the mainline, differences in gear setting and retrieving speeds, and delays related to handling times that were associated with the number of organisms captured. Therefore, the time each hook entered the water at deployment and exited the water during retrieval was electronically monitored. The elapsed time between deployment and retrieval of each hook was considered hook soak time.

The status of each retrieved hook was monitored and recorded as *whole bait present*, *partial bait present*, *no bait present*, *missing hook*, or *organism captured*. To determine whether baits of Atlantic mackerel and northern shortfin squid were retained equally on hooks, data from gangions classified with a status of *whole bait present* were compared by using chi-square tests with Yates correction for continuity. Using the same test, we investigated potential differences in bait retention between Atlantic mackerel and northern shortfin squid when there were hook interactions with feeding organisms other than those retained on a hook. For this investigation, the categories *partial bait present* and *no bait present* were combined. We combined them because of the subjective nature of the *partial bait present* category (i.e., the status of a hook was classified the same whether, for example, a small piece of bait tissue had been removed or most of the bait had been removed). The category *missing hook* was not included in analyses because, in the limited number of cases for which this status was recorded, the hook

1 Mention of trade names or commercial companies is for identification purposes only and does not imply endorsement by the National Marine Fisheries Service, NOAA.

Table 1

Catch composition and length ranges, by bait type, of fish species caught on bottom longline gear in the northern Gulf of Mexico in March and April 2015. The bait types are Atlantic mackerel (*Scomber scombrus*) and northern shortfin squid (*Illex illecebrosus*). All measurements are reported in fork length, with the exceptions of values for tilefish (*Lopholatilus chamaeleonticeps*) and red drum (*Sciaenops ocellatus*) that are reported in total length, as well as values for clearnose skates (*Raja eglanteria*) that are reported in disc width. Results of Kolmogorov–Smirnov (K-S), Mann–Whitney (M-W), and chi-square (with Yates correction) tests, used to test for differences in species-specific length distributions, median lengths, and catch rates between bait types, respectively, are provided with associated *P*-values.

Species	Atlantic mackerel		Northern shortfin squid		K-S (*P*)	M-W (*P*)	Chi-square (*P*)
	n	size range (mm)	*n*	size range (mm)			
Carcharhinus acronotus	61	563–1053	12	587–1061	1.19 (0.12)	238.0 (0.06)	31.56 (<0.01)
Carcharhinus plumbeus	45	1025–1800	7	1183–1546	0.95 (0.33)	98.0 (0.13)	26.33 (<0.01)
Centrophorous uyato	43	610–951	21	478–948	0.77 (0.59)	419.5 (0.65)	6.89 (<0.01)
Galeocerdo cuvier	20	910–2620	10	785–1812	1.12 (0.16)	52.5 (0.05)	2.70 (0.10)
Hyporthodus flavolimbatus	14	593–865	6	560–795	0.62 (0.83)	31.5 (0.83)	2.45 (0.12)
Lopholatilus chamaeleonticeps	12	497–895	14	465–905	0.70 (0.72)	97.0 (0.52)	0.04 (0.85)
Lutjanus campechanus	56	370–876	45	536–860	0.55 (0.92)	1208.0 (0.89)	0.99 (0.32)
Mustelus canis	18	754–1187	6	810–1081	0.86 (0.45)	39.0 (0.42)	5.04 (0.02)
Mustelus sinusmexicanus	40	686–1167	24	713–1120	0.76 (0.62)	379.0 (0.34)	3.52 (0.06)
Raja eglanteria	7	384–410	16	349–446	0.78 (0.57)	47.0 (0.97)	2.78 (0.09)
Rhizoprionodon terraenovae	344	574–895	139	486–860	0.69 (0.73)	21,969.0 (0.80)	86.16 (<0.01)
Sciaenops ocellatus	5	825–910	21	838–1005	1.32 (0.06)	82.0 (0.06)	8.65 (<0.01)
Sphyrna lewini	12	860–1890	9	750–1860	1.13 (0.14)	78.0 (0.09)	0.19 (0.66)
Squalus complex	21	410–680	10	445–655	0.64 (0.80)	89.5 (0.66)	3.22 (0.07)

could have been hung on the bottom and, as a result, gear failure could have occurred during retrieval. Additionally, to determine whether retention of the 2 bait types differed with increasing soak time, the distribution of hook soak times for hooks retrieved with *whole bait present* of Atlantic mackerel was compared to the distribution of soak times for hooks retrieved with *whole bait present* of northern shortfin squid by using a Kolmogorov–Smirnov test.

All captured individuals were identified to the lowest possible taxonomic level and measured to the nearest millimeter. Fork length (FL) and total length (TL) were measured from the tip of the rostrum to the caudal notch and to the tip of the upper lobe of the caudal fin while the fin was fully extended, respectively. For batoids, disc width was measured between apices of the pectoral fins. Species-specific identifications were not possible in a limited number of instances as a result of a fish escaping a hook before being landed (i.e., catch was confirmed but identification was not possible). In those cases, all individuals could be identified to at least the family level. A Kolmogorov–Smirnov test was used to test for differences in the species-specific length distributions of individuals caught on each bait type. When length distribution data of a species were normally distributed (as indicated by values of kurtosis and skewness being between −2 and 2) and homoscedastic (as assessed with an *F*-test), a *t*-test was used to determine whether differences existed in species-specific mean length at capture for each bait type. When length distribution data failed to meet the assumptions of parametric statistics, a Mann–Whitney *W* test was used to compare median length of each species caught by bait type.

Chi-square tests with Yates correction for continuity were used to determine whether there was a bait-related effect on species-specific catch rates. Species included in analyses were limited to those that had a minimum of 20 individuals captured regardless of bait type (Table 1). Additionally, because of low species-specific capture rates and the close morphological similarities of the Cuban dogfish (*Squalus cubensis*) and the shortspine spurdog (*S. mitsukurii*) (both species with fewer than 20 individuals captured), these squalid shark species were treated as a complex. For those species that showed a significant bait preference and were captured on a minimum of 10 longline sets, we examined if there was a change in the degree of bait preference with increasing total catch. For this examination, an index of bait preference (IBP) was calculated with the following equation:

$$IBP = (\textit{number of individuals captured on mackerel} - \textit{number of individuals captured on squid}) / \textit{total number of individuals captured}.$$

The IBP values ranged from 1 (all individuals captured with Atlantic mackerel bait) to −1 (all individuals captured with northern shortfin squid bait). The value of 0 indicated that an equal number of individuals were caught on both bait types. To obtain a nonparametric estimation of the relationship between species-specific IBP and total catch, a locally weighted scatterplot

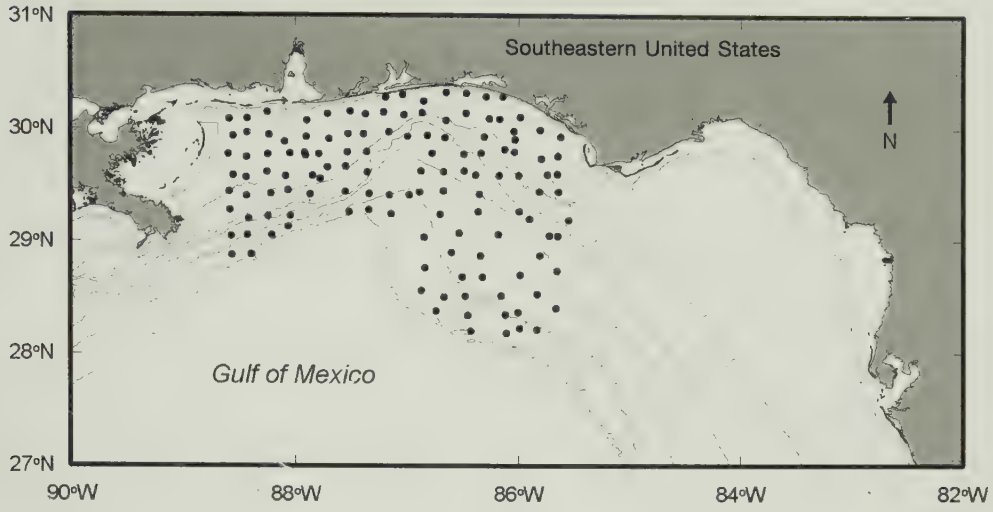

Figure 1

Map of sites where sampling was conducted with bottom longline gear in the northern Gulf of Mexico in March and April 2015. Black circles represent each sampling site. The grey lines indicate the isobaths at 10, 50, 100, 200, 500, and 1000 m.

smoothing (LOWESS) with a 75% smoothing factor was applied to scatterplots to determine whether a trend was present in the relationship. All statistical tests were considered significant at an α level of 0.05.

Results

During March and April 2015, 131 longline sets were completed (Fig. 1) for this study, resulting in deployments of 13,100 hooks and the capture of 1196 individual fish. Hook soak times ranged from 77 to 257 min (mean of 118.6 min, standard deviation [SD] 39.4), and hook-specific bait status was recorded for 12,888 gangions. Bait status of 212 hooks was not recorded due to technical difficulties; however, these hooks represented less than 2% of the gangions deployed. Of the monitored hooks, 8 were retrieved with the hook missing as a result of crimp failure (e.g. splitting or slipping). Of the 1944 gangions that were retrieved with whole bait present, there was no significant difference in the number of Atlantic mackerel (n=956) and northern shortfin squid (n=988) retained on hooks (χ^2=0.49, P=0.48). This result indicates that both bait types were equally retained on hooks during deployment, soak, and retrieval in the absence of interactions with feeding organisms. Interactions between bait and feeding organisms were evident on 9742 gangions that were retrieved with partial or no bait remaining on hooks. In these cases, bait damage or loss was more common with northern shortfin squid (n=5033) than with Atlantic mackerel (n=4709) (χ^2=10.71, P<0.01). There was no significant difference in the distributions of hook soak times when hooks were retrieved with whole bait present (Kolmogorov–Smirnov statistic=0.97, P=0.31) (Fig. 2).

All captured organisms were fish species with the exception of 1 loggerhead sea turtle (*Caretta caretta*), captured with bait of northern shortfin squid, and 1 giant isopod, *Bathynomus giganteus*, captured with Atlantic mackerel. The total catch and size range of each species analyzed are presented in Table 1. There were no significant differences in species-specific length distributions for individuals caught by bait type (P-values for all species were >0.05) (Table 1), and length distribution data were non-normal or heteroscedastic, with the exception of data for the red drum. The mean size of red drum captured on hooks baited with Atlantic mackerel (mean: 859.0 mm TL [SD 32.1]) was significantly smaller than the mean size of individuals captured with northern shortfin squid (mean: 903.7 mm TL [SD 40.0]) (t= −2.31, P=0.03).

There was a significant difference in the median length of tiger sharks (*Galeocerdo cuvier*) captured on each bait type, with the median length of tiger sharks being smaller on hooks baited with northern shortfin squid (1337 mm FL) than on hooks baited with Atlantic mackerel (1922 mm FL) (W=52.5, P=0.05). There were no statistically significant species-specific differences in the median length of any other species between the 2 bait types at α=0.05 (Table 1). However, at an α level of 0.10, there were significant differences in the median length of blacknose sharks (W=238.0, P=0.06) and scalloped hammerheads (*Sphyrna lewini*) (W=78.0, P=0.09) captured on the 2 bait types. For blacknose sharks, median length at capture was smaller when these sharks were caught with northern shortfin squid (1073 mm FL versus 1120 mm FL), whereas for scalloped hammerheads the median length at capture was smaller when these sharks were caught with Atlantic mackerel (1443 mm FL versus 1812 mm FL).

The results of chi-square tests indicate significant differences in the expected and observed catches for 5 shark and 1 teleost species (Table 1). All of the shark species for which a statistically significant preference

for a single bait type was observed were captured more frequently with Atlantic mackerel than with northern shortfin squid. For example, sandbar sharks (*Carcharhinus plumbeus*) were caught 6.4 times more frequently with Atlantic mackerel than with northern shortfin squid. Furthermore, for those shark species that showed no statistically significant preference for a specific bait type, all were captured more frequently on hooks baited with Atlantic mackerel, and chi-square test *P*-values were ≤0.10, with the exception of the value for the scalloped hammerhead (*P*=0.66).

Unlike other elasmobranchs, clearnose skates (*Raja eglanteria*) were caught more frequently on hooks baited with northern shortfin squid; however, there was no statistically significant difference in the observed and expected catch of this species between the 2 bait types (χ^2=2.78, *P*=0.09). Among teleosts, red drum was the only species for which a significant bait preference (χ^2=8.65, *P*<0.01) was observed, and this species was caught 4.2 times more frequently with northern shortfin squid than with Atlantic mackerel. Other commercially and recreationally important teleosts that were captured include red snapper (*Lutjanus campechanus*) (χ^2=0.99, *P*=0.32) and tilefish (*Lopholatilus chamaeleonticeps*) (χ^2 =0.04, *P*=0.85), neither of which had an observed significant bait preference. Although a significant bait preference was not found for yellowedge grouper (*Hyporthodus flavolimbatus*) (χ^2=2.45, *P*=0.12), 70% of all individuals of this species were captured on hooks baited with Atlantic mackerel.

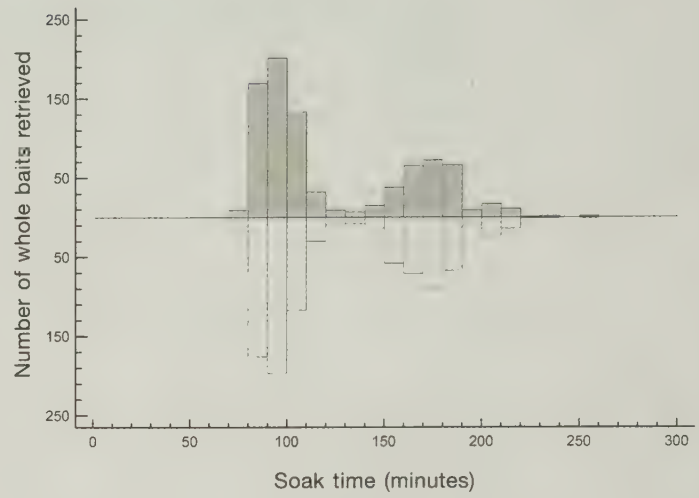

Figure 2

Comparison by bait type of the number of hooks retrieved with whole bait present over the range of hook soak times used in this study for which predatory fish species were caught on bottom longline gear in the northern Gulf of Mexico during March and April 2015. Gray bars represent the bait that was Atlantic mackerel (*Scomber scombrus*) and white bars represent the bait that was northern shortfin squid (*Illex illecebrosus*).

The relationship between IBP and total catch was examined for Atlantic sharpnose shark, blacknose shark, sandbar shark, and red snapper. For all 3 shark species, a preference for hooks baited with Atlantic mackerel was observed at low rates of total catch; however, as catch rates increased, IBP values trended toward 0 (Fig. 3). This trend was most evident for sandbar sharks, which were captured exclusively on hooks baited with Atlantic mackerel when the total catch consisted of 12 of fewer fish (Fig. 3). A preference for hooks baited with Atlantic mackerel also was observed for red snapper at low rates of total catch; however, unlike what was observed for sharks, red snapper were captured regularly on hooks baited with northern shortfin squid regardless of total catch size (Fig. 3). Furthermore, when more than 20 individuals were captured on a longline set, red snapper were captured exclusively on hooks baited with northern shortfin squid (Fig. 3).

Discussion

The results of our study indicate that when given the choice between hooks baited with northern shortfin squid or with Atlantic mackerel, the degree of bait preference varies among fish species and that, when present, bait preference generally declines with increasing rates of total catch on longline gear. Specifically, shark species commonly captured as bycatch on longline gear in the northern Gulf of Mexico preferentially selected Atlantic mackerel over northern shortfin squid, particularly when total catch rates were low. Although a statistically significant preference for hooks baited with Atlantic mackerel was documented only for the Atlantic sharpnose shark, blacknose shark, sandbar shark, smooth dogfish (*Mustelus canis*), and little gulper shark (*Centrophorous uyato*), the same trend was evident for all elasmobranch species captured, with the exceptions of the scalloped hammerhead and clearnose skate. There was no difference between the 2 bait types in catch rates, and therefore no difference in bait preference, for economically important teleosts, with the exception of the red drum. Together, these results provide support for an easily applied measure to reduce rates of shark bycatch and cause no effect on catch rates of target species or need for gear modifications.

Several previous studies reported declines in catch rates of blue sharks that were associated with specific bait types (Watson et al., 2005; Gilman et al., 2007; Foster et al., 2012) and found that bycatch of blue sharks was reduced when fish rather than squid were used as bait. Although our findings superficially seem in opposition to those of Watson et al. (2005) and Gilman et al. (2007), differences among the studies can be explained by the diets of the species examined and, therefore, support the use of specific bait types to re-

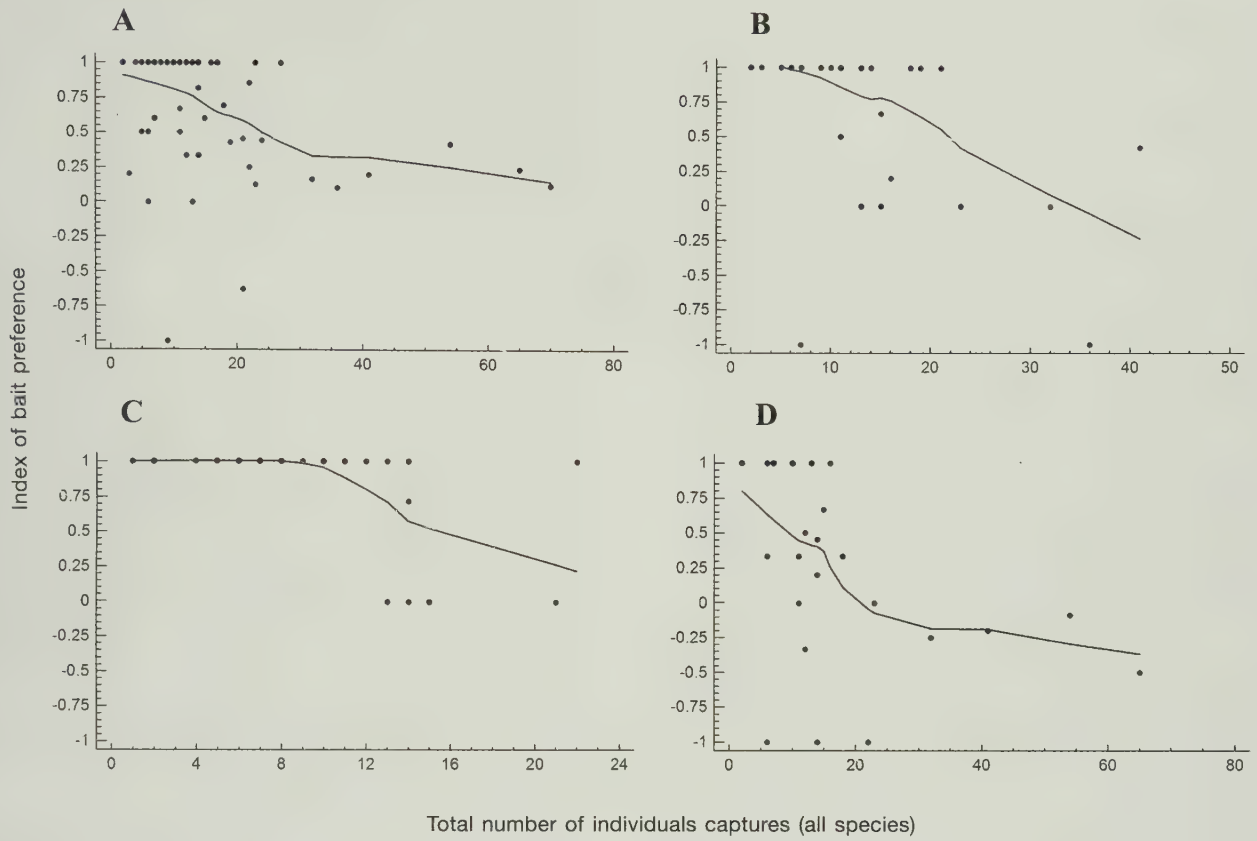

Figure 3

Comparison of relationships between index of bait preference and total capture number of all species on individual longline sets deployed in the northern Gulf of Mexico during March and April 2015 for (**A**) Atlantic sharpnose sharks (*Rhizoprionodon terraenovae*), (**B**) blacknose sharks (*Carcharhinus acronotus*), (**C**) sandbar sharks (*C. plumbeus*), and (**D**) red snapper (*Lutjanus campechanus*). The black lines represent locally weighted regression lines (determined through application of locally weighted scatterplot smoothing).

duce bycatch rates of sharks. Watson et al. (2005) and Gilman et al. (2007) examined bycatch of blue sharks in pelagic longline fisheries and found that catch rates of this species declined when mackerel were used as bait. Similarly, Foster et al. (2012) found the use of Atlantic mackerel as bait to decrease bycatch of blue sharks; however, they also indicated that hooks baited with Atlantic mackerel were more efficient at capturing porbeagles (*Lamna nasus*) and shortfin makos (*Isurus oxyrinchus*).

Cortés (1999) presented an exhaustive literature review of the diets of 149 shark species and found that the diet of blue sharks was dominated by cephalopods (49.4%). By comparison, teleost fish species composed 55–98.2% of the diets of Atlantic sharpnose sharks, blacknose sharks, porbeagles, sandbar sharks, scalloped hammerheads, and shortfin makos (Cortés, 1999). The 2 shark species that we examined and that do not have a primarily piscivorous diet, according to Cortés (1999), were the tiger shark and the smooth dogfish. The diet of tiger sharks was primarily composed of teleost fish species (35.4%), and sea turtles (23.8%), whereas crustaceans (64.3%) and teleost fish species (16.6%) dominated the diet of smooth dogfish. Cephalopods were reported by Cortés (1999) to constitute 0.0–15.5% of the diets of the shark species we captured. The results of our study, combined with those of Watson et al. (2005), Gilman et al. (2007), and Foster et al. (2012), indicate that, despite being frequently characterized as opportunistic (e.g., Strasburg, 1958; Lowe et al., 1996), sharks, when presented with a choice between a bait that is a common prey item and one that is not a significant dietary component, will actively select the former.

Although not statistically significant, the catch rate of clearnose skates was 2.7 times higher on hooks with northern shortfin squid than on hooks with Atlantic mackerel, indicating a strong preference for the former. This result was similar to the findings of Ariz et al. (2006) and Coelho et al. (2012), who found that batoids, more specifically ray species, captured on long-

line gear are caught at a higher rate on hooks baited with northern shortfin squid than on hooks baited with Atlantic mackerel. Ebert and Bizzarro (2007) showed that the clearnose skate has a diverse diet, with approximately 21% fish and less than 1% squid species as prey items reported in stomach contents. However, Schwartz (1996) found that the fish component of the diet of clearnose skates was composed of small-bodied fish species, such as the striped anchovy (*Anchoa hepsetus*), Atlantic croaker (*Micropogonias undulatus*), spot (*Leiostomus xanthurus*), and blackcheek tonguefish (*Symphurus plagiusa*). This finding indicates that a limited gape size resulted in more clearnose skates being captured on hooks with northern shortfin squid because that bait type is more malleable and, therefore, more easily manipulated than Atlantic mackerel.

Among teleosts, no consistent trend in preference for one bait type over another was found. For example, red snapper and tilefish showed no significant preference for either bait type; however, red drum had a significant preference for northern shortfin squid. Conversely, although not statistically significant, there was an obvious trend with yellowedge grouper toward a preference for Atlantic mackerel. The lack of bait preference shown by red snapper and tilefish was expected because both species are widely reported to be omnivorous and opportunistic (e.g., Steimle et al., 1999; Gallaway et al., 2009; Moser et al.[2]). Yellowedge grouper have been reported to feed primarily on brachyuran crab and teleost fish species (Heemstra and Randall, 1993); therefore, the trend toward a preference for hooks baited with Atlantic mackerel was not unexpected.

In contrast, the preference for bait of northern shortfin squid exhibited by red drum was not clearly related to the known diet of this species. The results of a number of studies indicate that red drum forage on a diverse group of prey, including invertebrate and fish species and that their prey varies depending on life stage, habitat, and season (e.g., Overstreet and Heard, 1978; Scharf and Schlicht, 2000). For example, Boothbly and Avualt (1971) examined the stomach contents of red drum sampled within a coastal marsh system along the coast of Louisiana and determined that crustaceans dominated the diet from late spring through fall but fish species became more important during colder months. As pointed out by Overstreet and Heard (1971) and Scharf and Schlicht (2000), dietary shifts likely were related to seasonally mediated changes in abundance of prey species. However, Matlock (1987) reported that, in general, adult red drum consume more individuals that are fish species than individuals that are invertebrate species. Therefore, the preference that red drum showed for the northern shortfin squid in our study cannot be explained on the basis of dietary composition reported in the literature because Atlantic mackerel would have been the expected preferred bait type. Although the most likely explanation is gape limitation, another possible explanation is that red drum were outcompeted for hooks baited with Atlantic mackerel and opportunistically fed on northern shortfin squid. However, it does not appear that red drum were outcompeted because all sets where red drum were captured had relatively low catch rates of other fish species.

There was a clear decrease in bait preference with increasing total catch rates for Atlantic sharpnose, blacknose, and sandbar sharks. This trend was most obvious for sandbar sharks: on sets with less than 13 other captured individuals, regardless of species, 100% of sandbar sharks were caught on hooks baited with Atlantic mackerel. At catch rates of 13 or more individuals, regardless of species, on a set, the likelihood that sandbar sharks would be captured on hooks baited with northern shortfin squid increased. This decrease in bait preference indicates that Atlantic sharpnose, blacknose, and sandbar sharks become more opportunistic when in the presence of competitors or that fewer hooks baited with Atlantic mackerel were available later in the set (as a result of depredation of preferred bait types or a captured fish occupying a hook) and late arriving individuals did not have an equal number of both bait types from which to choose.

As total catch rates increased, the trend of Atlantic sharpnose, blacknose, and sandbar sharks moved toward no preference for a particular bait type (i.e., IBP approached 0) and the trend of red snapper moved toward a preference for northern shortfin squid (i.e., IBP<0). This result indicates that sharks were still actively selecting hooks baited with Atlantic mackerel despite more hooks baited with northern shortfin squid being available. Conversely, the trend in bait preference of red snapper at increasing total catch rates indicates that they were feeding opportunistically on the most abundant bait type available. This latter point can be more clearly demonstrated by comparing the IBP values of the Atlantic sharpnose shark with those of the red snapper. On longline sets with greater than 25 individuals captured, IBP values were exclusively greater than 0 for the Atlantic sharpnose shark and less than 0 for red snapper. Another possible explanation for the shift toward a reduced preference for Atlantic mackerel at high catch rates could be differences in retention rates of the 2 bait types as hook soak time increased. However, there was no significant difference in the distribution of soak times for hooks retrieved with whole bait present for each bait type.

Beyond species-specific dietary preferences, it is possible that differences in foraging strategies among the species we examined, at least in part, led to differences in catch rates of fish species on the 2 bait types. All shark species that we examined are active, roaming predators. Speed et al. (2010) estimated that the home range (excluding seasonal migrations) of small-bodied

[2] Moser, J. G., Jr., A. G. Pollack, G. W. Ingram Jr., C. T. Gledhill, T. A. Henwood, and W. B. Driggers III. 2012. Developing a survey methodology for sampling red snapper, *Lutjanus campechanus*, at oil and gas platforms in the northern Gulf of Mexico. Southeast Data, Assessment, and Review, SEDAR31-DW26, 23 p. [Available from website.]

coastal shark species that are not reef obligate or constrained within a bounded area (e.g., bay or estuary) can be up to 100 km^2. For example, through acoustic monitoring, Heupel et al. (2006) determined the mean home range of the bonnethead (*Sphyrna tiburo*) was 8.31 km^2; however, some individuals used areas of up to approximately 74 km^2. Larger-bodied species, such as the tiger shark, have been documented to have vast home ranges, on the order of 1000s of square kilometers (Heithaus et al., 2007).

Conversely, most of the teleosts that we captured, with the exception of the red drum, are relatively sedentary and have a high degree of site fidelity in offshore waters to discrete structures, such as lumps and depressions (e.g., Able et al., 1993; Gallaway et al., 2009). For example, Jones et al. (1989) documented tilefish and yellowedge grouper in the western Gulf of Mexico occupying discrete burrows with openings ranging from 0.25 to 8 m wide. Able et al. (1982) hypothesized that these structures serve as refuge from predators, and Jones et al. (1989) suggested that individuals have long-term fidelity to specific burrows. Although it is unknown how far these individuals move from their burrows to forage, the aforementioned studies all indicate that, in contrast with coastal shark species, most teleost species that we examined remain in relatively close proximity to a specific location. Therefore, it is possible that the teleosts that exhibited this behavior in our study were attracted to bait on the basis of proximity rather than preference.

In contrast, because shark species rely, in part, on chemotaxis to locate prey from a distance (e.g., Sheldon, 1911; Løkkeborg et al., 2014), it is possible that the area of bait influence was greater for Atlantic mackerel than for northern shortfin squid and led to sharks homing in more frequently on hooks baited with Atlantic mackerel. Chemotaxis, however, is unlikely to have affected bait preference given the relatively close gangion spacing (~ 18 m apart), diffusion and mixing of scent plumes from individual baits with increasing distance from the gear, and the setting of gear parallel to the axis of a current that resulted in a single plume of odorants from both Atlantic mackerel and northern shortfin squid. Therefore, given that these 2 species have significantly different relative concentrations of low-molecular-weight metabolites that are known attractants or stimulants of feeding behavior in fish species (Carr et al., 1996), it is more likely that higher catch rates of most shark species on hooks baited with Atlantic mackerel was a result of preference and not the area of bait influence.

A potential criticism of our study is that we used alternating bait types on each longline set rather than making comparisons on the basis of single-bait sets. Although numerous bait preference studies have used an alternating bait design similar to the one in our study (e.g., Broadhurst and Hazin, 2001; Woll et al., 2001; Yokota et al., 2009), it was suggested by Watson et al. (2005) and Foster et al. (2012) that the use of alternating bait types can bias results because of a potential interaction effect of bait types. Both Watson et al. (2005) and Foster et al. (2012) examined effects of bait and hook type on catch rates of epipelagic organisms caught on pelagic longline gear and therefore they focused on highly mobile species, such as sea turtles, sharks, swordfish, and tunas, that occupy a single habitat (epipelagic zone).

Conversely, we used bottom longline gear in a highly dynamic area in terms of prey density, foraging behaviors of target species, currents, depth, dissolved oxygen, salinity, temperature, turbidity, substrate types, and patchy habitats. Therefore, because many of these variables affect feeding behavior and the ability of fish species to locate baited hooks (Løkkeborg et al., 2014), we believe the use of alternating bait types is justified and best suited to answer the questions we were addressing. Had we used a single-bait approach, we would have needed to account for each of the biotic and abiotic variables for individual longline sets. However, although we acknowledge that the use of alternating bait types could have introduced a potential bait interaction effect, we did expose an equal number of both bait types to all conditions encountered, thereby limiting the number of potentially biasing factors to one.

Additionally, several of the species we encountered are infrequently captured and occur in large aggregations. For example, of the 79 little gulper sharks collected, 62% were caught on 2 sets. Further, although little gulper sharks are infrequently captured in shelf waters of the northern Gulf of Mexico, when present, they are found in large schools (senior author, personal observ.). Had single-bait sets been used and had a set occurred in proximity to a school of little gulper sharks, the resulting data would be indicative of the high density of little gulper sharks in the area and not of a preference for a specific bait type.

Ward et al. (2004) examined the theoretical effect of hook soak time on pelagic longline catches in the Pacific Ocean and determined that catch rates can be affected by, among other issues, baits falling off during deployment of longline sets, by deterioration that results in baits falling off hooks, or by a time-related reduction in the degree of attraction. Godin et al. (2012), in a metadata analysis, stated that the catch of sharks, in general, was reduced when Atlantic mackerel were used as bait. They went on to reason that squid, when compared to mackerel, was a more effective bait because it remains on hooks longer, does not deteriorate as rapidly, and does not lose its attraction properties over time.

Although we were not able to quantify the attractant properties of the 2 bait types, our results are in direct opposition to those of Godin et al. (2012) in that we found both bait types were retained on hooks equally and that bait damage or loss was greater for hooks baited with northern shortfin squid. The disparity in the 2 studies is likely attributable to the data sources of Godin et al. (2012) primarily reporting catch of blue sharks and to differences in hook soak times among studies. For example, Godin et al. (2012) included fish-

eries-dependent data sources, and commercial longline gear is generally set for much longer periods (e.g., >8 h) than the 1–4 h we allowed gear to soak. Future work should examine the "endurance" of the 2 bait types beyond the maximum hook soak time of 4 h in our study as well as the effect of hook soak time on catch rates and bait performance.

Our results, as well as those of the aforementioned studies, indicate that species-specific catch rates can be impacted significantly by the type of bait used. Therefore, an understanding of species-specific bait preferences of target and bycatch species is imperative, a point also highlighted by Coelho et al. (2012). Furthermore, because ontogenetic (e.g., Wells et al., 2008) and seasonal shifts (e.g., Boothby and Avault, 1971) in dietary preferences are well established among fish species, it will be necessary to identify preferences across all life stages and seasons so that no one stage is adversely affected or seasonally vulnerable. Future research will be needed to determine whether the use of a single bait type (i.e., northern shortfin squid) effectively will reduce the catch rates of shark species in the Gulf of Mexico snapper and grouper bottom longline fishery or whether sharks will opportunistically feed on a single bait type at the same rate as a preferred bait type in the absence of choice.

Acknowledgments

We thank the crew of the NOAA Ship *Oregon II*, S. Garner, M. Hendon, N. Hopkins, J. Lewis, J. McKinney, J. Moser, B. Noble, B. Prohaska, K. Rademacher, and T. Wallace for assistance in the collection of samples.

Literature cited

Able, K. W., C. B. Grimes, R. A. Cooper, and J. R. Uzmann.
1982. Burrow construction and behavior of the tilefish, *Lopholatilus chamaeleonticeps*, in Hudson Submarine Canyon. Environ. Biol. Fish. 7:199–205.

Able, K. W., C. B. Grimes, R. S. Jones, and D. C. Twichell.
1993. Temporal and spatial variation in habitat characteristics of tilefish (*Lopholatilus chamaeleonticeps*) off the east coast of Florida. Bull. Mar. Sci. 53:1013–1026.

Ariz, J., A. Delgado de Molina, M. L. Ramos, and J. C. Santana.
2006. Check list and catch rate data by hook type and bait for bycatch species caught by Spanish experimental longline cruises in the south-western Indian Ocean during 2005. Indian Ocean Tuna Commission, IOTC-2006-WPBy-04, 10 p.

Beerkircher, L. R., E. Cortés, and M. Shivji.
2002. Characteristics of shark bycatch observed on pelagic longline off the southeastern United States, 1992–2000. Mar. Fish. Rev. 64(4):40–49.

Boothby, R. N, and J. W. Avault Jr.
1971. Food habits, length-weight relationship, and condition factor of the red drum (*Sciaenops ocellata*) in southeastern Louisiana. Trans. Am. Fish. Soc. 100:290–295.

Broadhurst, M. K., and F. H. V. Hazin.
2001. Influence of type and orientation of bait on catches of swordfish (*Xiphias gladius*) and other species in an artisanal sub-surface longline fishery off northeastern Brazil. Fish. Res. 53:169–179.

Carr, W. E. S., J. C. Netherton III, R. A. Gleeson, and C. D. Derby.
1996. Stimulants of feeding behavior in fish: analyses of tissues of diverse marine organsims. Biol. Bull. 190:149–160.

Carruthers, E. H., J. D. Neilson, and S. C. Smith.
2011. Overlooked bycatch mitigation opportunities in pelagic longline fisheries: soak time and temperature effects on swordfish (*Xiphias gladius*) and blue shark (*Prionace glauca*) catch. Fish. Res. 108:112–120.

Coelho, R., M. N. Santos, and S. Amorim.
2012. Effects of hook and bait on targeted and bycatch fishes in an equatorial Atlantic pelagic longline fishery. Bull. Mar. Sci. 88:449–467.

Cortés, E.
1999. Standardized diet compositions and trophic levels of sharks. ICES J. Mar. Sci. 56:707–717.

Ebert, D. A., and J. J. Bizzarro.
2007. Standardized diet compositions and trophic levels of skates (Chondrichthyes: Rajiformes: Rajoidei). Environ. Biol. Fish. 80:221–237.

Foster, D. G., S. P. Epperly, A. K. Shah, and J. W. Watson.
2012. Evaluation of hook and bait type on the catch rates in the western North Atlantic Ocean pelagic longline fishery. Bull. Mar. Sci. 88:529–545.

Francis, M. P., L. H. Griggs, and S. J. Baird.
2001. Pelagic shark bycatch in the New Zealand tuna longline fishery. Mar. Freshw. Res. 52:165–178.

Gallaway, B. J., S. T. Szedlmayer, and W. J. Gazey.
2009. A life history review for red snapper in the Gulf of Mexico with an evaluation of the importance of offshore petroleum platforms and other artificial reefs. Rev. Fish. Sci. 17:48–67.

Gilman, E., D. Kobayashi, T. Swenarton, N. Brothers, P. Dalzell, and I. Kinan-Kelly.
2007. Reducing sea turtle interactions in the Hawaii-based longline swordfish fishery. Biol. Conserv. 139:19–28.

Gilman, E., S. Clarke, N. Brothers, J. Alfaro-Shigueto, J. Mandelman, J. Mangel, S. Petersen, S. Piovano, N. Thomson, P. Dalzell, et al.
2008. Shark interactions in pelagic longline fisheries. Mar. Policy 32:1–18.

Godin, A. C., J. K. Carlson, and V. Burgener.
2012. The effect of circle hooks on shark catchability and at-vessel mortality rates in longline fisheries. Bull. Mar. Sci. 88:469–483.

Gulak, S. J. B., M. P Enzenauer, and J. K. Carlson.
2013. Characterization of shark and reef fish bottom longline fisheries: 2012. NOAA Tech. Memo. NMFS-SEFSC-652, 42 p.

Heemstra, P. C., and J. E. Randall.
1993. FAO species catalogue, vol. 16. Grouper of the world (family Serranidae, subfamily Epinephelinae): an annotated and illustrated catalogue of the grouper, rockcod, hind, coral grouper and lyretail species known to date. FAO Fisheries Synopsis 125, 382 p. FAO, Rome.

Heithaus, M. R., A. J. Wirsing, L. M. Dill, and L. I. Heithaus.
2007. Long-term movements of tiger sharks satellite-

tagged in Shark Bay, Western Australia. Mar. Biol. 151:1455–1461.

Heupel, M. R., C. A. Simpfendorfer, A. B. Collins, and J. P Tyminski.
2006. Residency and movement patterns of bonnethead sharks, *Sphyrna tiburo*, in a large Florida estuary. Environ. Biol. Fish. 76:47–67.

Jones, R. S., E. J. Gutherz, W. R. Nelson, and G. C. Matlock.
1989. Burrow utilization by yellowedge grouper, *Epinephelus flavolimbatus*, in the northwestern Gulf of Mexico. Environ. Biol. Fish. 26:277–284.

Løkkeborg, S., S. I. Siikavuopio, O. B. Humborstad, A. C. Utne-Palm, and K. Ferter.
2014. Towards more efficient longline fisheries: fish feeding behaviour, bait characteristics and development of alternative baits. Rev. Fish Biol. Fish. 24:985–1003.

Lowe, C. G., B. M. Wetherbee, G. L. Crow, and A. L. Tester.
1996. Ontogenetic dietary shifts and feeding behavior of the tiger shark, *Galeocerdo cuvier*, in Hawaiian waters. Environ. Biol. Fish. 47:203–211.

Matlock, G. C.
1987. The life history of the red drum. *In* Manual of red drum aquaculture (G. W. Chamberlain, R. J. Miget, and M. G. Haby, eds.). p. 1–47. Texas Agricultural Extension Service and Sea Grant College Program, Texas A&M University, College Station, TX.

Overstreet, R. M., and R. W. Heard.
1978. Food of the red drum, *Sciaenops ocellatus*, from the Mississippi Sound. Gulf Res. Rep. 6:131–135.

Prytherch, H. F.
1983. A descriptive survey of the bottom longline fishery in the Gulf of Mexico. NOAA Tech. Memo. NMFS-SE-FC-122, 33 p.

Rey, J. C., and R. Muñoz-Chápuli.
1991. Relation between hook depth and fishing efficiency in surface longline gear. Fish. Bull. 89:729–732.

Robbins, W. D., V. M. Peddemors, and S. J. Kennelly.
2011. Assessment of permanent magnets and electropositive metals to reduce the line-based capture of Galapagos sharks, *Carcharhinus galapagensis*. Fish. Res. 109:100–106.

Rogers, A.
1920. Industrial uses for the shark and porpoise. J. Am. Leather Chem. Assoc. 15:241–244.

Scharf, F. S., and K. K. Schlicht.
2000. Feeding habits of the red drum (*Sciaenops ocellatus*) in Galveston Bay, Texas: seasonal diet variation and predator-prey size relationships. Estuaries 23:128–139.

Schwartz, F. J.
1996. Biology of the clearnose skate, *Raja eglanteria*, from North Carolina. Fla. Sci. 59:82–95.

Scott-Denton, E., P. F. Cryer, J. P. Gocke, M. R. Harrelson, D. L. Kinsella, J. R. Pulver, R. C. Smith, and J. Williams.
2011. Descriptions of the U.S. Gulf of Mexico reef fish bottom longline and vertical line fisheries based on observer data. Mar. Fish. Rev. 73(2):1–26.

Sheldon, R. E.
1911. The sense of smell in selachians. J. Exp. Zool. 10:51–62.

Speed, C. W., I. C. Field, M. G. Meekan, and C. J. A. Bradshaw.
2010. Complexities of coastal shark movements and their implications for management. Mar. Ecol. Prog. Ser. 408:275–293.

Strasburg, D. W.
1958. Distribution, abundance, and habits of pelagic sharks in the central Pacific Ocean. Fish. Bull. 58:335–361.

Steimle, F. W., C. A. Zetlin, P. L. Berrien, D. L. Johnson, and S. Chang.
1999. Tilefish, *Lopholatilus chamaeleonticeps*, life history and habitat characteristics. NOAA Tech. Memo. NMFS-NE-152, 30 p.

Walsh, W. A., K. A. Bigelow, and K. L. Sender.
2009. Decreases in shark catches and mortality in the Hawaii-based longline fishery as documented by fishery observers. Mar. Coast. Fish. 1:270–282.

Ward, P., R. A. Myers, and W. Blanchard.
2004. Fish lost at sea: the effect of soak time on pelagic longline catches. Fish. Bull. 102:179–195.

Ward, P, E. Lawrence, R. Darbyshire, and S. Hindmarsh.
2008. Large-scale experiment shows that nylon leaders reduce shark bycatch and benefit pelagic longline fishers. Fish. Res. 90:100–108.

Watson, J. W., S. P. Epperly, A. K. Shah, and D. G. Foster.
2005. Fishing methods to reduce sea turtle mortality associated with pelagic longlines. Can. J. Fish. Aquat. Sci. 62:965–981.

Watson, J. T., T. E. Essington, C. E. Lennert-Cody, and M. A. Hall.
2009. Trade-offs in the design of fishery closures: management of silky shark bycatch in the eastern Pacific Ocean tuna fishery. Conserv. Biol. 23:626–635.

Woll, A. K., J. Boje, R. Holst, and A. C. Gundersen.
2001. Catch rates and bait selectivity in longline fishery for Greenland halibut (*Reinhardtius hippoglossoides*, Walbaum) at East Greenland. Fish. Res. 51:237–246.

Wells, R. J. D., J. H. Cowan Jr., and B. Fry.
2008. Feeding ecology of red snapper *Lutjanus campechanus* in the northern Gulf of Mexico. Mar. Ecol. Prog. Ser. 361:213–225.

Yokota, K., M. Kiyota, and H. Okamura.
2009. Effect of bait species and color on sea turtle bycatch and fish catch in a pelagic longline fishery. Fish. Res. 97:53–58.

National Marine
Fisheries Service
NOAA

Fishery Bulletin
established in 1881

Spencer F. Baird
First U.S. Commissioner
of Fisheries and founder
of *Fishery Bulletin*

Reproductive strategy of white anglerfish (*Lophius piscatorius*) in Mediterranean waters: implications for management

Ana I. Colmenero (contact author)
Víctor M. Tuset
Pilar Sánchez

Email address for contact author: colmenero@icm.csic.es

Institut de Ciències del Mar (ICM)
Consejo Superior de Investigaciones Científicas (CSIC)
Passeig Marítim de la Barceloneta 37-49
08003 Barcelona, Spain

Abstract—Reproductive parameters of the white anglerfish (*Lophius piscatorius*) in the northwestern Mediterranean Sea were studied in 556 specimens collected monthly aboard commercial fishing vessels that were trawling at depths of 12–836 m. The main spawning season occurred from February through June. The size at maturity was estimated to be 48.8 cm in total length (TL) for males, 59.9 cm TL for females, and 51.3 cm TL for both sexes combined. The white anglerfish has group-synchronous oocyte development and determinate fecundity. It is a total spawner (spawns all its eggs once during a spawning season) and has a batch fecundity ranging from 661,647 to 885,214 oocytes, a relative batch fecundity of 66–128 oocytes per gram of female gutted weight, and a potential fecundity with values from 54,717 to 104,506 oocytes per kilogram of female total weight. This study is the first to provide the reproductive biology of white anglerfish in the northwestern Mediterranean Sea and provide valuable information that can be used to improve the stock assessment and ensure proper management of this species.

Manuscript submitted 2 November 2015.
Manuscript accepted 21 October 2016.
Fish. Bull. 115:60–73 (2017).
Online publication date: 15 November 2016.
doi: 10.7755/FB.115.1.6.

The views and opinions expressed or implied in this article are those of the author (or authors) and do not necessarily reflect the position of the National Marine Fisheries Service, NOAA.

The genus *Lophius*, commonly known as anglerfish, monkfish, or goosefish, belong to a family of bathydemersal fishes, which live and feed on the bottom of the seafloor generally below 200 m (Caruso, 1986). It includes 7 species distributed around the world. The white anglerfish (*Lophius piscatorius*) is found in the northeast Atlantic Ocean and the Mediterranean Sea, and the black anglerfish (*Lophius budegassa*) coexists with white anglerfish over most of its range, although the black anglerfish has a more southerly distribution in the Atlantic (Caruso, 1986). The shortspine African angler (*Lophius vaillanti*) is found in the eastern Atlantic (Maartens and Booth, 2005). The devil anglerfish (*Lophius vomerinus*) occupies the southeast Atlantic and the northern and western Indian Ocean (Walmsley et al., 2005). The blackfin goosefish (*Lophius gastrophysus*) inhabits the western Atlantic, and the goosefish (*Lophius americanus*) occurs in the northwest Atlantic (Caruso, 1983). Finally, the yellow goosefish (*Lophius litulon*) is distributed in the northwest Pacific, in the Gulf of Po-Hai, in the Yellow Sea, and in the East China Sea (Yoneda et al., 1997).

We focused on white anglerfish, which can be found on the continental shelf and slope, inhabiting depths from the shoreline to >1000 m (Afonso-Dias and Hislop, 1996). In the Mediterranean Sea, this species cohabits with black anglerfish, and even though the distributions of both species overlap, no ecological competition exists between them because of a temporal segregation in their daily biorhythms (Colmenero et al., 2010). Both of these species of *Lophius* play an important role in the trophic structure of benthodemersal ecosystems because they represent major predators, along with the European hake (*Merluccius merluccius*) (Díaz et al., 2008). In the community structure of the northwestern Mediterranean Sea, species of anglerfish are considered top predators (Coll et al., 2006; Valls et al., 2014). They are also reported to be important in the deep-sea community (depths from 200 m to the bottom of the ocean) because they are the most abundant species (Labropoulou and Papaconstantinou, 2000; Maiorano et al., 2010).

Despite the fact that the deep sea is the largest ecosystem on the planet, is highly diverse, and has a wealth of resources, it is still mostly unknown and poorly understood in comparison with shallow-water ar-

eas: therefore environmental management in deep waters is difficult (Ramirez-Llodra et al., 2010). In the last few decades, the decline of traditional fisheries on the continental shelf, the increasing demand for food sources, and rapid technological developments have resulted in an increasing exploitation of deep-sea resources (Koslow et al., 2000; Ramirez-Llodra et al., 2011) and in an incremental increase in the global mean depth of fishing (Watson and Morato, 2013).

This rise in deep-sea fishing has affected catches of *Lophius* species, given the growing demand for human consumption of this group of fish that is leading to an increase in worldwide commercial exploitation and targeting of anglerfishes (Fariña et al., 2008). Total catch reported globally for white anglerfish reached more than 26,500 metric tons (t) in 2014 (FAO Global Capture Production database, website) and total catch of anglerfishes in the northwestern Mediterranean Sea for the same year added up to 660 t (Tudó Vila[1]). Landings in our study area were composed primarily of black anglerfish (86%) and generally only a small percentage of white anglerfish (14%) (Tudó Vila[1]), but, for landings in Atlantic waters, the opposite is true; white anglerfish (94%) dominate the catch (Dobby et al., 2008). Although the European Commission previously has conducted stock assessments of black anglerfish in the western Mediterranean Sea, there is no corresponding assessment for white anglerfish. The lack of information about the structure of the population of white anglerfish in this region and the lack of knowledge of the basic biology of this species are the main reasons for the absence of any assessment. The actual management regulations applied for black anglerfish generally are those applied to bottom trawling (European Union Council Regulation 1967/2006), with recommendations aimed at reducing the fishing effort of the fleet in order to avoid loss in stock productivity and decreases in landings (Cardinale et al.[2]).

The small quantity of white anglerfish available from landings in Mediterranean waters makes studies of this species challenging. Studies conducted in the Mediterranean Sea have been scarce, and they have been focused on temporal and spatial distribution of this species (Ungaro et al., 2002; Colmenero et al., 2010), age and growth (Tsimenidis and Ondrias, 1980; Tsimenidis, 1984), feeding ecology (López et al., 2016), morphometrics (Negzaoui-Garali and Ben Salem, 2008), parasites (Colmenero et al., 2015a), and ova characteristics (Colmenero et al., 2015b). Among these studies, only Ungaro et al. (2002) analyzed some of the biological features of this species by using data available from trawl surveys, including data on distribution, abundance, stock demography, and size at maturity. The latter work is valuable but is limited because sampling occurred only in the spring and summer; a whole year of sampling is recommended to obtain more accurate biological information.

A study of reproductive ecology is important for an understanding of population dynamics, and it is critical for assessing the effects of harvesting on fish populations when attempting to develop appropriate management strategies. Recruitment is recognized as a key process for maintaining sustainable populations, and the relationship between the reproductive output of the population and the resulting recruitment is central to understanding how a fish population will respond to constant stressors such as fishing (Chambers and Trippel, 1997). Although knowing more about the relationships between life history strategies and productivity with depth could help managers understand the potential response of a deep-sea species to fishing (Drazen and Haedrich, 2012), it is first necessary to conduct biological studies of fish to gain knowledge of the reproductive system of a species (Koslow et al., 1995). Such studies include gonad morphology (external and cellular description of the ovary and testis), reproductive pattern (hermaphroditism or gonochorism), reproductive behavior, reproductive cycle, spawning season duration, size at maturity, sex ratio, size at sexual transition, and fecundity.

All of this information can be applied at the population level to evaluate reproductive potential and to serve as a basis for limits on fishing that aim in order to keep recruitment at sustainable levels (García-Díaz et al., 2006). Because reproductive strategy varies within species, depending on the area of distribution of each species and the depth distribution of each species in each area (Rotllant et al., 2002), there is a need for knowledge about reproduction of deep-sea fish species. Such information is needed particularly in the Mediterranean Sea because the data available for this region are limited (Morales-Nin et al., 1996; D'Onghia et al., 2008; Muñoz et al., 2010; Bustos-Salvador et al., 2015), and, furthermore, target species of fisheries have been the focus of only a few studies (Rotllant et al., 2002; Recasens et al., 2008).

The goal of this study was to describe the reproductive parameters—gonadal morphology, spawning season, size at sexual maturity, oocyte development, and fecundity—of white anglerfish in the northwestern Mediterranean Sea in order to provide valuable information and scientific background to improve stock assessments and effective management for *Lophius* species in Mediterranean waters.

Materials and methods

Sampling and data collection

Between June 2007 and December 2010, 556 white anglerfish, with total lengths (TLs) of 9–120 cm, were

[1] Tudó Vila, P. 2015. Unpubl. data. Directorate of Fishing and Maritime Affairs, Government of Catalonia, Avinguda Diagonal 523-525, 08029 Barcelona, Spain.

[2] Cardinale, M., D. Damalas, and C. G. Osio (eds.). 2015. Scientific, Technical and Economic Committee for Fisheries (STECF)—Mediterranean Assessments, part 2 (STECF-15-06), 396 p. Publications Office of the European Union, Luxembourg. [Available from website.]

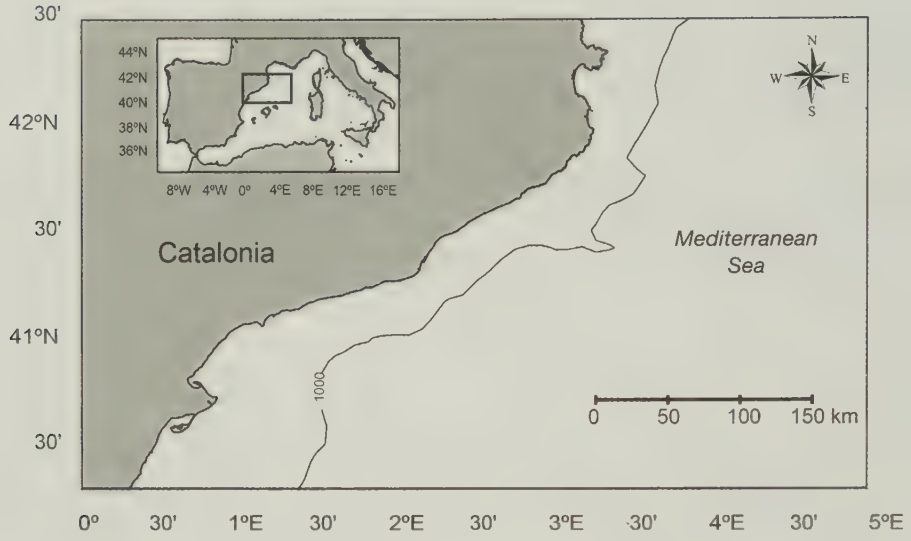

Figure 1

Map of the northwestern Mediterranean Sea showing the study area where white anglerfish (*Lophius piscatorius*) were collected from fishing grounds off the Catalan coast between June 2007 and December 2010.

collected monthly aboard commercial fishing vessels that were trawling at depths of 12–836 m. Fish were sampled from 467 stations located in the fishing grounds off the Catalan coast in the northwestern Mediterranean Sea from 40°5.980′N to 43°39.310′N and from 0°32.922′E to 3°35.718′E (Fig. 1). For each individual, TL was measured to the nearest centimeter, total weight (TW) and gutted weight (GW) were measured to the nearest gram, and gonad weight (GNW) and liver weight (LW) were measured to the nearest 0.01 g. The sex of all fish was determined and assigned macroscopically to a gonadal stage on the basis of a scale of 5 maturity phases proposed by Colmenero et al. (2013): immature (phase I), developing or regenerating (phase II), spawning capable (phase III), actively spawning (phase IV), and regressing (phase V).

Fish that were too small (<20 cm TL) for their sex to be determined or for assignment to a gonadal phase were classified as indeterminate. Macroscopic gonadal stage was validated histologically, according to the most advanced cell within the gonad (West, 1990). Gonads were fixed in 10% buffered formalin solution, dehydrated in ascending solutions of alcohols and embedded in a methacrylate polymer resin, sectioned at a thickness of 4 µm with a manual microtome Leica Reichert-Jung 2040[3] (Leica Microsystems, Wetzlar, Germany), stained with Lee's stain (methylene blue and basic fuchsin), and mounted in a synthetic resin of dibutyl phthalate xylene on microscope slides. Gonads were classified according to their size and color and the presence or absence of specific inclusions (oil droplets, yolk, postovulatory follicles, or sperm), as well as the type of oocytes (Wallace and Selman, 1981).

[3] Mention of trade names or commercial companies is for identification purposes only and does not imply endorsement by the National Marine Fisheries Service, NOAA.

Reproductive biology

The spawning season was estimated by analyzing the monthly variation in the percentage of maturity phases and the changes in gonadosomatic index (GSI) and hepatosomatic index (HSI) for mature fish of each sex (Afonso-Dias and Hislop, 1996; Colmenero et al., 2013). Because indeterminate individuals (n=27) were not considered, 251 males and 278 females were used to determine both indices, which were calculated according to Yoneda et al. (2001) as

$$GSI = (GNW / GW) \times 100 \quad (1)$$

and

$$HSI = (LW / GW) \times 100. \quad (2)$$

The lengths at which 25%, 50%, and 75% of sampled fish reached sexual maturity were estimated by fitting the proportion of sexually mature males and females (phase III, phase IV, or phase V) and for both sexes combined to the logistic equation (Colmenero et al., 2013):

$$P = 100 / (1 + \exp [a + bTL]), \quad (3)$$

where P = the percentage of mature individuals as a function of size class (measured in TL); and
a and b are specific parameters that can change during the life cycle.

A logarithmic transformation was applied to this equation to calculate the parameters a and b by means of linear regression.

Oocyte development and fecundity

Oocyte diameters obtained from 21 randomly selected specimens at all phases of maturity were measured to the nearest 0.01 µm with an image analysis program (Image-Pro Plus, vers. 5.0, Media Cybernetics, Inc., Rockville, MD) in combination with an Axioskop 2 Plus microscope (Carl Zeiss Microscopy, LLC, Thornwood, NY), and a ProgRes C14 digital microscope camera (Jenoptik AG, Jena, Germany). Only oocytes sectioned through the nucleus were taken into account. The developmental stages of the oocytes were categorized according to the descriptions in Colmenero et al. (2013) that were adapted from Wallace and Selman (1981). The mean oocyte diameter by developmental stage was determined by calculating the diameter of all oocytes encountered in each subsample, and the range was set with the smallest and largest oocytes found at each developmental oocyte stage.

Fecundity was determined by using the gravimetric method described by Hunter and Goldberg (1980). Because homogeneity in oocyte distribution within ovaries of white anglerfish has already been established (Afonso-Dias and Hislop, 1996), ovarian tissue subsamples of approximately 500 mg were taken randomly from 2 specimens with ovaries in phase III that had neither postovulatory follicles nor atretic oocytes present. Whole tissue subsamples were placed on several slides and covered with cover slips, then photographed with a Canon Powershot SD870 IS digital camera (Canon USA, Melville, NY). Oocytes were counted manually with Image-Pro Plus.

Batch fecundity (BF), the total number of hydrated oocytes produced in a single spawning event by an individual female, of each female was determined by means of this equation:

$$BF = (\textit{oocyte number} / \textit{sampled GNW}) \times \textit{total GNW}, \quad (4)$$

where *BF* is the product of the number of secondary vitellogenic oocytes per unit of weight multiplied by the total ovarian weight (Yoneda et al., 2001). Relative batch fecundity (RBF), the total number of mature eggs released by a female during the spawning batch per gram of female GW, was calculated with the following equation (Pavlov et al., 2009):

$$RBF = BF / GW. \quad (5)$$

Potential fecundity was calculated as the number of vitellogenic oocytes divided by TW in kilograms for each mature female and then averaged (Murua et al., 2003).

Results

Gonad morphology

The gonad of female white anglerfish has 2 ribbon-like ovarian lobes connected to each other at their posterior end. One side of the "ribbon" consists of an ovigerous membrane from which a single layer of oocyte clusters, which contain oocytes at different developmental stages, projects into the lumen. The other side is nonovigerous and secretes a gelatinous material during maturation that fills the ovarian lumen, where mature oocytes develop (Fig. 2). During maturation, the gonad increases in size until it fills the abdominal cavity (Fig. 3). Testes are a pair of elongated organs with a bean shape in transverse section. Spermatogenesis takes place in a capsule-like sac called a *cyst*, but it is completed in the lumina of the lobules. The cysts appear to be arranged with a gradient of germ cells of increasing maturation from the cortex to the sperm duct (Fig. 4).

Spawning season

The monthly distribution of maturity phases (Fig. 5) revealed a peak in reproduction during spring, when a major portion of the spawning females and the highest value of GSI (0.77) were found. Spawning capable females (phase III) were caught primarily between April and June, and females in the actively spawning phase (IV) were observed in November, December, and March—the latter month having the maximum occurrence (11%). Females in immature, regressing, and developing or regenerating phases (I, V, and II, respectively) were found year-round, although the highest percentage of immature individuals (49%) was observed in January. The GSI values followed the same pattern shown in these maturity phases: highest during spring, decreasing during summer and autumn, and increasing again during winter. Males in all maturity phases were observed throughout the year, but with a maximum percentage of mature males (66%) in February and March. Immature males were found primarily in July (69%). The mean GSI for females increased as their ovaries developed and peaked in phase IV. For males, the mean GSI increased with testicular development and reached a maximum in phase IV (Table 1). The mean HSI for females and males increased during the summer and autumn months and decreased during winter and spring. On the basis of these observations, a main spawning season was found from February through June and a secondary one occurred in November and December.

Size at sexual maturity

The maturity ogive for males indicates that the length at which 50% of them reached sexual maturity (L_{50}) was 48.4 cm TL (Fig. 6A). Maturity in males occurred at about 37% of their maximum observed TL. The smallest mature male found was 32.5 cm TL, and the largest immature male was 50 cm TL. The maturity ogive for females indicates that L_{50} was 59.9 cm TL (Fig. 6B). Female maturity occurs at about 30% of their maximum observed TL. Like the smallest male, the smallest mature female was 32.5 cm TL. The largest immature female measured 56 cm TL. The maturity ogive for the sexes combined indicates an L_{50} of 51.3

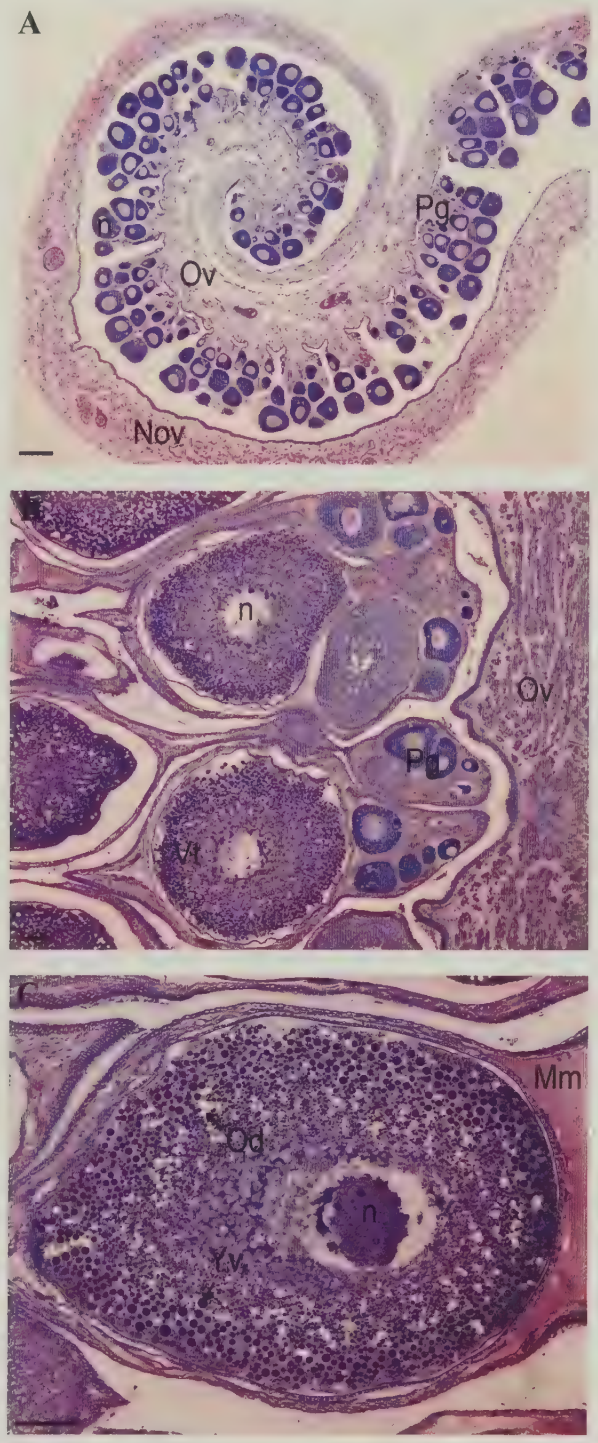

Figure 2

Histological sections from ovaries of female white anglerfish (*Lophius piscatorius*) in 3 phases of maturity: (**A**) immature, (**B**) spawning capable, and (**C**) actively spawning. Ov=ovigerous membrane, Nov=nonovigerous membrane, n=nucleus, Pg=primary growth stage, Vt=vitellogenesis stage, Od=oil droplet, Yv=yolk vesicle, Mm=mucus matrix. Scale bars=100 µm.

cm TL. The lengths at which 25% and 75% of fish attained maturity were 43.5 and 53.4 cm TL for males, 48.6 and 71.1 cm TL for females, and 44.7 and 58 cm TL for the sexes combined.

Oocyte development and fecundity

Oocytes in different developmental stages were found in each maturity phase. They were organized in clusters where a gradient in the size of the oocyte was observed. A group of oocytes differentiated from others as the ovaries developed, indicating that white anglerfish has group-synchronous oocyte development and can be considered to have determinate fecundity (Fig. 7). Ovaries at each maturity phase contained primary oogonia- and perinucleolar-stage oocytes. Chromatin nucleolar were difficult to find and were present only in immature phase. Females at the cortical alveolar stage were not found in our samples. Vitellogenic and hydrated oocytes were located in females capable of spawning. Oocyte diameters at each stage of oocyte development are shown in Table 2.

Batch fecundity ranged from 661,647 to 885,214 oocytes from 2 females that measured 76 and 105 cm TL, 6331 and 16,178 g TW, and 5182 and 13,330 g GW, respectively. Relative batch fecundity ranged from 66 to 128 oocytes/g GW (average of 97 oocytes/g GW [standard deviation, SD 43]). Potential fecundity values moved from 54,717 to 104,506 oocytes/kg TW with a mean of 79,612 oocytes/kg TW (SD 35,206).

Discussion

Relevance of reproductive traits for sustainable management

Fishing activity during spawning seasons may affect population parameters, specifically composition of the size distribution, mortality rate, sexual structure of the population, size at maturity, and changes in the spawning season. These parameters, in turn, can increase the risk of over-exploitation of a stock.

Fishing during spawning periods may result in targeting a specific size class of the population and thus increasing the chance of catching the older (and larger) age classes and making the stock vulnerable to reproductive collapse (van Overzee and Rijnsdorp, 2015). Because spawning is generally limited to specific areas and times (Cushing, 1990), the conservation of resources can be enhanced by limiting fishing activity in a spatiotemporal frame. Furthermore, fishing pressure has been documented to have reduced initial size at maturity—an issue that is a concern particularly for late-maturing species (Stewart et al., 2010). If size of capture is below the size at first maturity, there is a genuine risk of recruitment overfishing. Therefore, knowledge of the spawning season and the size at maturity can help managers establish closed seasons and prevent fishing at this vulnerable time in the life cycle

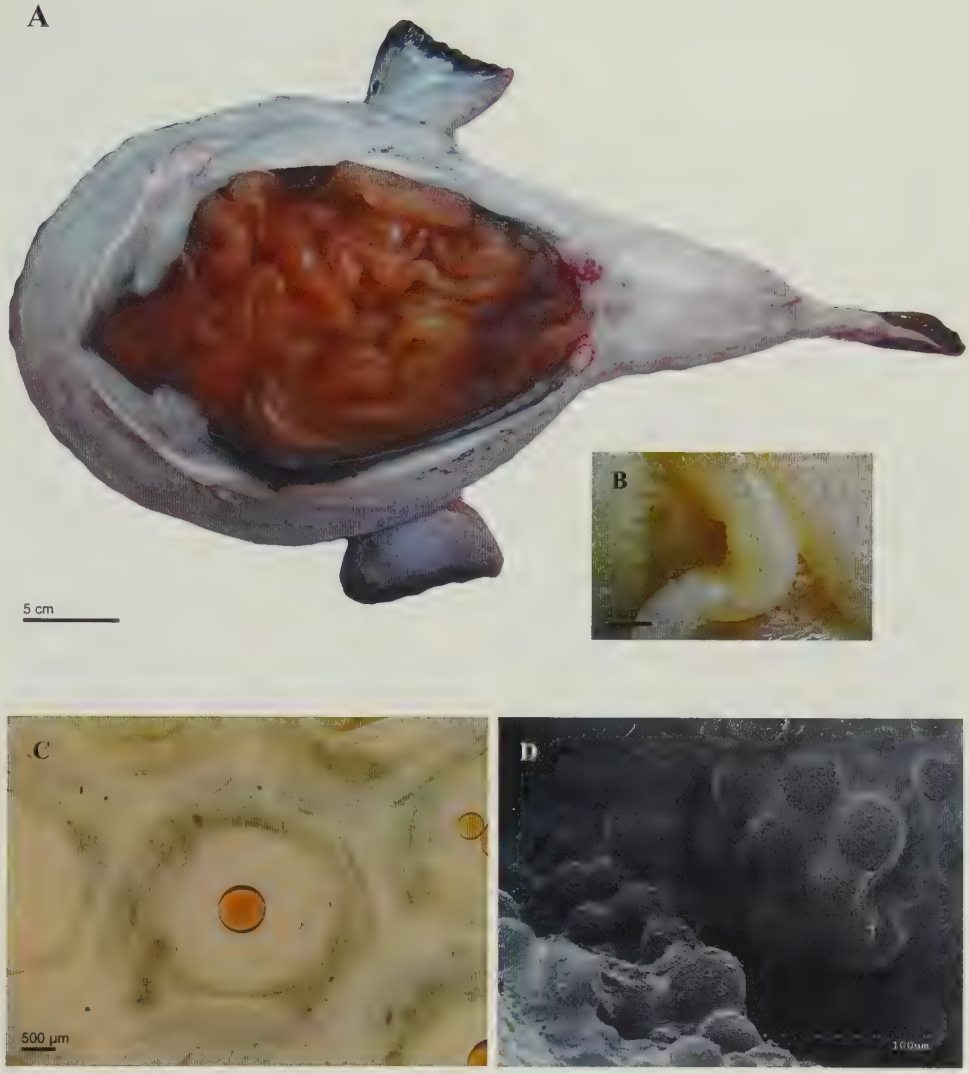

Figure 3

Images of a female of the species *Lophius* showing (**A**) an ovary that occupies the entire abdominal cavity; (**B**) a close-up of the female gonad; and (**C**) a hexagonal chamber of the mucoid veil, which contains an unfertilized egg of white anglerfish (*Lophius piscatorius*) and (**D**) a scanning electron micrograph of yolk vesicles from the inside of the ovum of a white anglerfish.

of fish species by preserving breeding individuals and establishing a legal minimum size.

The results of our study of white anglerfish in the northwestern Mediterranean Sea indicate that a long spawning period occurs during mid-winter and late spring, from February through June, although a secondary breeding period has been observed in November and December. These results agree with those obtained in studies that were focused on the northeastern Atlantic Ocean, where this species spawns from November through June (Fulton, 1898; Afonso-Dias and Hislop, 1996; Hislop et al., 2001). However, a previous study in the northwestern Mediterranean Sea identified a spawning season during spring–summer (Ungaro et al., 2002). Discrepancies between the latter study and our work may be explained by the differences in sampling periods.

Nevertheless, spawning seasonality, which is associated with environmental conditions and local oceanographic features, varies between species as well as by geographical area. An example of this variability in spawning seasonality can be observed in 2 locations along the Atlantic–Iberian coast: on the Portuguese and western Spanish coasts, spawning of the white anglerfish takes place during winter–spring (Duarte et al., 2001), whereas on the northern Spanish coast (Bay

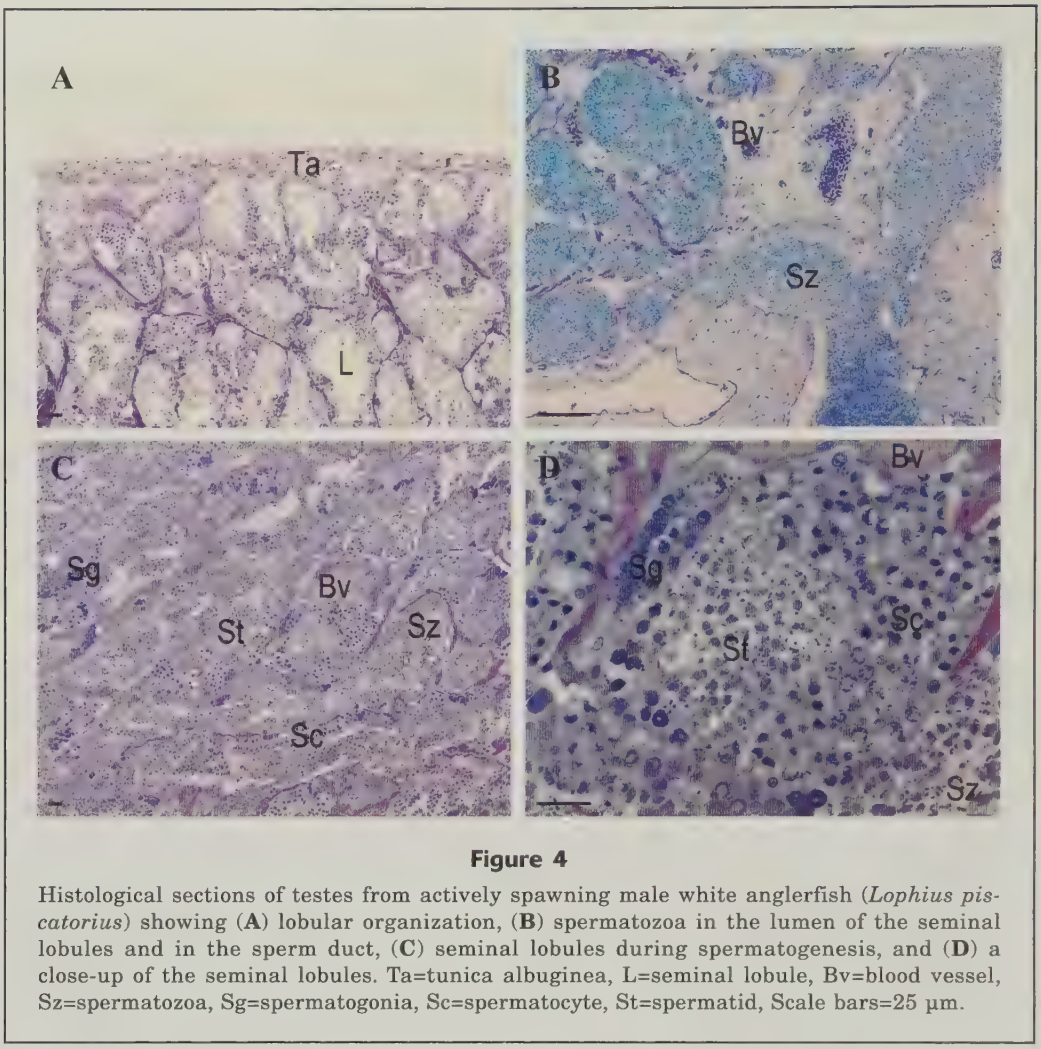

Figure 4

Histological sections of testes from actively spawning male white anglerfish (*Lophius piscatorius*) showing (**A**) lobular organization, (**B**) spermatozoa in the lumen of the seminal lobules and in the sperm duct, (**C**) seminal lobules during spermatogenesis, and (**D**) a close-up of the seminal lobules. Ta=tunica albuginea, L=seminal lobule, Bv=blood vessel, Sz=spermatozoa, Sg=spermatogonia, Sc=spermatocyte, St=spermatid, Scale bars=25 µm.

of Biscay), spawning occurs during summer (Quincoces et al.[4]). In fact, spawning activity for one of its congenerics, the black anglerfish, in the northwestern Mediterranean seems to occur from November through March and a secondary spawning occurs in August and September (Colmenero et al., 2013). Although a little overlap exists between spawning seasons of both of these *Lophius* species in Mediterranean waters, the main period is markedly different, and that difference lessens competition among these species.

Usually, species of *Lophius* have long spawning periods ranging between 4 and 6 months. Black anglerfish off the Spanish-Atlantic coasts spawn from November through February (Duarte et al., 2001), and in the Bay of Biscay the peak spawning period is from May through July (Quincoces et al.[5]). The goosefish off the East Coast of the United States has its reproductive period from May through June (Armstrong et al., 1992), spawning for the blackfin goosefish off the Brazilian coasts takes place during spring and summer (Valentim et al., 2007), and the yellow goosefish spawns between February and May in the East China Sea and the Yellow Sea (Yoneda et al., 2001). The devil anglerfish off the coast of South Africa has a well-defined summer breeding season (Griffiths and Hecht, 1986), and individuals of this species off the coast of Namibia spawn throughout the year with a slight increase between autumn and spring (Maartens and Booth, 2005).

Most deep-sea fish species reach sexual maturity at sizes larger than those of species that inhabit the continental shelf reach maturity, and, in some cases, males mature at smaller sizes than females (Rotllant et al., 2002; Pajuelo et al., 2008). A similar pattern was observed for white anglerfish—one in which females mature sexually at larger sizes (59.9 cm TL) than those recorded for males (48.4 cm TL). This pattern has also

[4] Quincoces, I., M. Santurtún, and P. Lucio. 1998. Biological aspects of white anglerfish (*Lophius piscatorius*) in the Bay of Biscay (ICES Division VIIIa, b, d), in 1996–1997. ICES Council Meeting (C.M.) Documents 1998/O:48, 29 p.

[5] Quincoces, I., P. Lucio, and M. Santurtún. 1998. Biology of black anglerfish *Lophius budegassa* in the Bay of Biscay waters, during 1996–1997. ICES Council Meeting (C.M.) Documents 1998/O:47, 28 p.

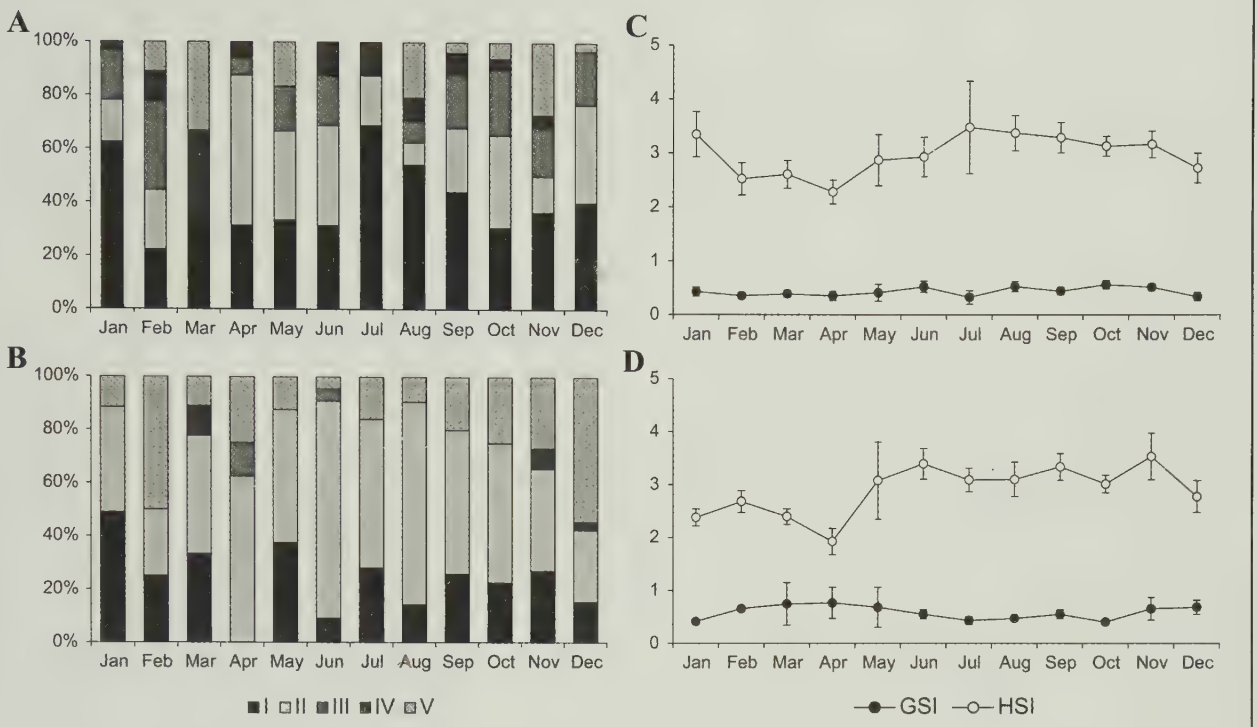

Figure 5

Monthly distribution of maturity phases of gonads for (**A**) males (n=251) and (**B**) females (n=278) and monthly changes in the mean gonadosomatic (GSI) and hepatosomatic (HSI) indices for (**C**) males (n=135) and (**D**) females (n=202) of white anglerfish (*Lophius piscatorius*) collected from the northwestern Mediterranean Sea between June 2007 and December 2010. On the basis of macroscopic examination, specimens were assigned to the following 5 phases: immature (phase I), developing or regenerating (phase II), spawning capable (phase III), actively spawning (phase IV), and regressing (phase V). Error bars indicate standard error of the mean.

been found for white anglerfish in other areas (Ofstad and Laurenson[6]) and for other species of anglerfish. Female black anglerfish, for example, mature at 48.2 cm TL, whereas males attain first maturity at 33.4 cm TL (Colmenero et al., 2013), and female devil anglerfish reach sexual maturity at 58.2 cm TL, whereas males of this species mature at 39.9 cm TL (Maartens and Booth, 2005). For the goosefish, L_{50} for females and males was estimated at 48.5 and 36.9 cm TL, respectively (Armstrong et al., 1992), and female yellow goosefish mature at 56.7 cm TL and males of this species mature at 36.2 cm (Yoneda et al., 2001). This dissimilarity in size at maturity is usually associated with a trade-off between life history traits, where early maturity involves a larger size but a slower growth (Stearns and Koella, 1986; Charnov, 2008).

Reproductive strategy

The reproductive strategy of white anglerfish is one of discontinuous oogenesis with synchronous development of vitellogenic oocytes and is, therefore, this species is considered a total spawner (Afonso-Dias and Hislop, 1996). The oocytes ovulate at once, and the eggs are released in either a unique event or over a short period of time, as part of a single episode during the spawning season (Murua and Saborido-Rey, 2003; Pavlov et al., 2009). This pattern of oocyte development and spawning patterns is also found in other species of *Lophius* (Leslie and Grant, 1990; Armstrong et al., 1992; Colmenero et al., 2013). Yoneda et al. (2001) suggested that yellow goosefish may have the potential to spawn more than once a year, on the basis of the observation of a captive specimen that released several infertile egg masses. However, this spawning behavior cannot be considered normal.

Female anglerfish spawn their eggs in a mucoid veil that floats near the surface. The veil consists of individual chambers that contain 1–3 eggs and has an opening that provides water circulation. In our study, we recognized in some chambers the presence of 2 eggs sharing the same chamber. Although this way of releasing eggs is not common among fish species, some Scorpaeniformes, such as the shortfin turkeyfish (*Dendrochirus brachypterus*) (Fishelson, 1978) or the short-

[6] Ofstad, L. H., and C. Laurenson. 2007. Biology of anglerfish *Lophius piscatorius* in Faroese waters. ICES Council Meeting (C.M.) Documents 2007/K:07, 16 p.

Table 1

Gonadosomatic (GSI) and hepatosomatic (HSI) indices at each maturity phase for male and female white anglerfish (*Lophius piscatorius*) collected from the northwestern Mediterranean Sea between June 2007 and December 2010. SE=standard error.

Sex	Maturity phase	GSI range	Mean GSI (SE)	HSI range	Mean HSI (SE)	*n*
Male	I	0.01–0.41	0.10 (0.01)	1.04–4.65	2.37 (0.07)	106
	II	0.06–1.07	0.25 (0.03)	0.27–5.11	2.67 (0.14)	54
	III	0.21–1.30	0.61 (0.05)	1.92–6.72	3.20 (0.18)	35
	IV	0.30–1.70	0.70 (0.09)	0.40–5.39	3.34 (0.28)	17
	V	0.19–1.11	0.50 (0.06)	2.04–5.10	3.35 (0.22)	17
Female	I	0.01–0.86	0.23 (0.02)	0.92–5.33	2.37 (0.11)	66
	II	0.04–1.22	0.40 (0.02)	0.42–7.79	2.87 (0.10)	133
	III	0.61–1.65	1.13 (0.52)	2.15–5.83	3.99 (1.85)	2
	IV	1.59–3.86	2.81 (0.52)	2.68–8.50	5.80 (1.20)	4
	V	0.18–2.44	0.66 (0.06)	0.36–8.59	3.03 (0.17)	60

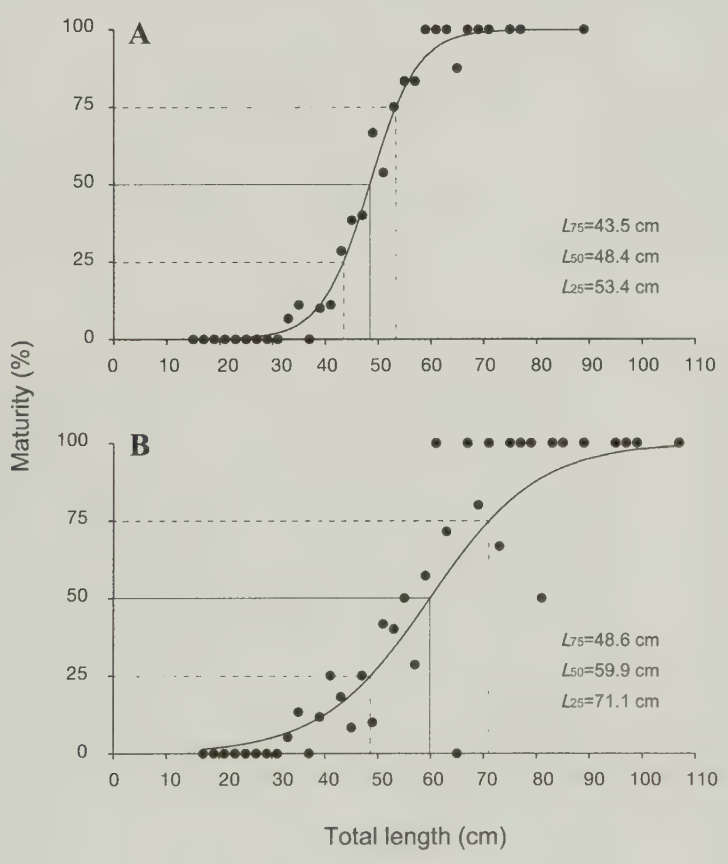

Figure 6

Maturity ogives for (**A**) male and (**B**) female white anglerfish (*Lophius piscatorius*) collected from the northwestern Mediterranean Sea between June 2007 and December 2010.

spine thornyhead (*Sebastolobus alascanus*) (Erickson and Pikitch, 1993), also spawn buoyant gelatinous egg masses. It has been proposed that the advantages of releasing eggs in these veils facilitate their dispersal; the egg veil floats near the surface and is subject to the actions of wind, currents, and waves. The veil also serves as protection for eggs against predation because of the presence of obnoxious or toxic substances in the veils (Armstrong et al., 1992). Moreover, the veil may help with the fertilization of eggs. When males are present and the egg ribbon is laid, the ribbon keeps the eggs together and prevents their dispersion through the water. The males then eject milt near the veil to guarantee fertilization of all the eggs (Dahlgren, 1928). Armstrong et al. (1992) suggested that sperm reach oocyte chambers through the pores that connect the chambers when the ribbon is extruded from the female and starts to absorb water.

Another feature of the reproduction of the white anglerfish to highlight is its type of spermatogenesis, which is known to be semicystic. Spermatogenesis starts inside the cysts that contain germinal cells in different stages of development from spermatogonia to spermatids, but it is not completed within the cyst. During spermatogenesis, the cyst breaks and spermatids are released from the cyst into the lumen of the lobule, where they become spermatozoa. This kind of spermatogenesis has been described previously in the family Lophiidae only in the blackmouth angler (*Lophiomus setigerus*) (Yoneda et al., 1998) and in black anglerfish

Table 2

Oocyte diameters, ranges and means with standard errors (SEs), and histological characteristics of ovarian follicles in white anglerfish (*Lophius piscatorius*), collected from the northwestern Mediterranean Sea between June 2007 and December 2010. SE=standard error, at each stage of oocyte development.

Stages of oocyte development	Mean oocyte diameter (μm) (SE)	Oocyte diameter (μm) range	Histological characteristics
Primary growth stage	82.79 (2.34)	12–203	Nucleus contains a large nucleolus and some peripheral nucleoli. Yolk granules are not present in the cytoplasm.
Cortical alveolar stage	256.10 (3.08)	207–316	Cortical alveolar vesicles and oil droplets appear in the cytoplasm. Yolk granules are not yet present in the cytoplasm. Nucleus is central within the yolk
Vitellogenesis	729.31 (17.58)	324–876	Yolk granules appear between cortical alveolar vesicles. As vitellogenesis advances, yolk granules fill the cytoplasm until they are in contact with the nucleus, which remains in a central position.
Migratory nucleus	939.31 (7.77)	902–1008	Yolk granules and oil droplets start to fuse. Nucleus migrates to one pole of the oocyte.
Hydration	1672.50 (4.77)	1523–1750	Yolk granules form a single mass. Nucleus is not present in the cytoplasm.

(Colmenero et al., 2013). This specialized spermatogenesis also has been found in other deep-sea species of Neoceratiidae (Jespersen, 1984) and of Macruridae (Fernandez-Arcaya et al., 2013), in the shore clingfish (*Lepadogaster lepadogaster*) (Mattei and Mattei, 1978), in species of Blennidae (Lahnsteiner and Patzner, 1990), in a species of *Ophidion* (Mattei et al., 1993), in the dusky jawfish (*Opistognathus whitehursti*) (Manni and Rasotto, 1997), and in species of *Scorpaena* (Muñoz et al., 2002; Sàbat et al., 2009), which also release their eggs in gelatinous substances.

Fecundity

Because of their particular reproduction behavior, which includes a high parental investment in the offspring, white anglerfish are likely to spawn once a year, and the population dynamics of this species are expected to be highly sensitive to external biological and ecosystem factors (ICES[7]). Spawning occurs in deep waters because mature white anglerfish have been described by Hislop et al. (2001) as migrating to deeper water before spawning. The same behavior is seen in yellow goosefish: adult fish migrate to deeper waters in response to seasonal changes in water temperature and gonadal maturation (Yoneda et al., 2002). These vertical migrations into deeper waters where commercial fishing and scientific surveys cannot reach could be the reason that very few mature females were captured during our study—a trend that is common in other studies of *Lophius* species (Ofstad and Laurenson[6]). Clearly, this low number of mature females will affect the estimation of such reproductive parameters as fecundity.

Generally, deep-sea species have low fecundity and large egg sizes (Gage and Tyler, 1991; Herring, 2002). The white anglerfish has determinate fecundity with values between 661,647 to 885,214 oocytes—levels that are high in comparison with other deep-sea species that inhabit the same depth strata but that are similar to the mean potential fecundity of its Mediterranean congeneric, the black anglerfish (Colmenero et al., 2013). Fecundity values vary among populations as a result of adaptations to local environmental conditions, and they are related to abiotic factors, such as temperature and salinity (Nissling and Dahlman, 2010; Thorsen et al., 2010), and to biotic factors, such as food supply, population density, allocation of energy to reproduction, and fish size (Treasurer, 1981; Merrett, 1994; Nash et al., 2000).

In this study, we were not able to determine correlations between fecundity and these factors because only 2 actively spawning females were collected. Eggs of white anglerfish have been reported to have a mean diameter of 2.72 mm (SD 0.08) (Colmenero et al., 2015b), a size that is considered large for pelagic eggs, which typically range from 0.5 to 5.5 mm in diameter (Ahlstrom and Moser, 1980). Larger eggs have more

[7] ICES (International Council for the Exploration of the Sea). 2012. Report of the working group on the assessment of southern shelf stocks of hake, monk and megrim (WGHMM), 10–16 May 2012, ICES Headquaters, Copenhagen, Denmark. ICES CM 2012/ACOM:11, 617 p.

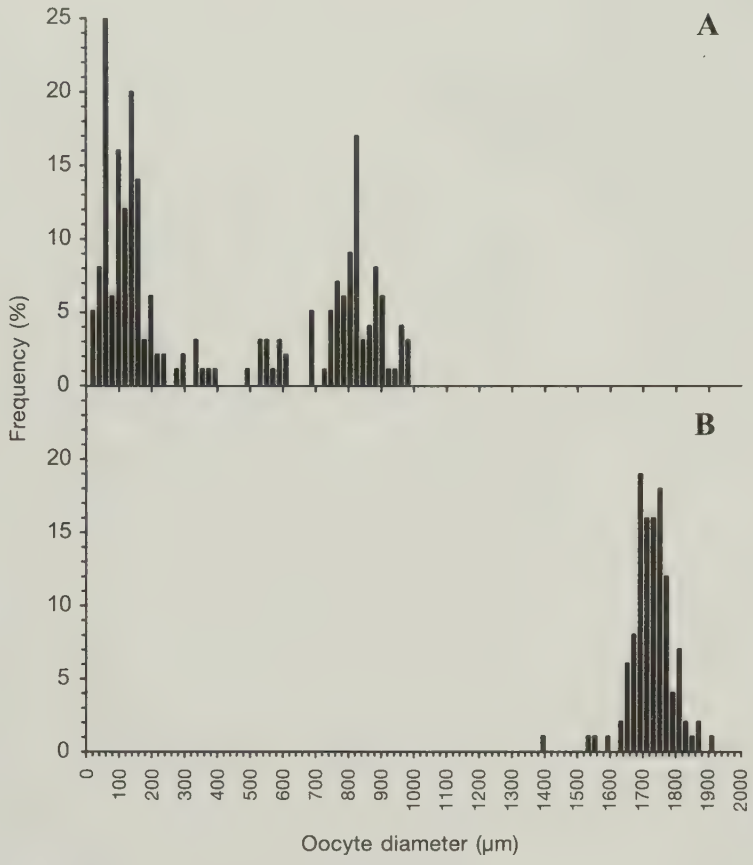

Figure 7

Distribution of oocyte diameters in (**A**) spawning capable and (**B**) actively spawning female white anglerfish (*Lophius piscatorius*) collected from the northwestern Mediterranean Sea between June 2007 and December 2010.

yolk, which increases the potential for larval survival (Duarte and Alcaraz, 1989). The only information available about egg diameters for other species of *Lophius* is for yellow goosefish, which occupy a bathymetric range that is similar to that occupied by white anglerfish and have a similar egg size (Yoneda et al., 2001). In contrast, the black anglerfish has an egg diameter of 1.88 mm (SD 0.12), a size that is nearly 1.5 times smaller than the diameters reported for the white anglerfish and yellow goosefish, and inhabits shallower waters than those inhabited by the other 2 species (Colmenero et al., 2015b). A comparative study of egg sizes in deep-sea species found that egg size increased significantly with depth (Fernandez-Arcaya[8]). Egg size is important to offspring survival in many organisms, and large eggs survive better than small ones in environments where dissolved oxygen is low (Hendry and Day, 2003).

General remarks

In this study, we estimated the spawning season, size at sexual maturity, and fecundity of white anglerfish. Considering the parameter values that we obtained, we can conclude that this species is one that employs a *K* reproductive strategy. In general, this strategy is defined by a large body size, longevity, late maturation, and low fecundity (Pianka, 1970, 1974). A wide range of deep-sea demersal fish species generally display life history characteristics consistent with *K*-selection (Adams, 1980; Gage and Tyler, 1991). These traits make deep-sea fish stocks highly vulnerable to fishing and capable of little resilience to over-exploitation, increasing the urgency for the conservation and management of this group of animals (Koslow et al., 2000; Morato et al., 2006; Norse et al., 2012).

Theoretically, the *K*-strategy for deep-sea fish species should imply a low fecundity; however, some species, such as the North Pacific armorhead (*Pseudopentaceros wheeleri*), wreckfish (*Polyprion americanus*), and splendid alfonsino (*Beryx splendens*), have high fecundities (Sedberry et al., 1996; Lehodey et al., 1997; Humphreys, 2000). White angelfish and species of *Lophius* in general also should be included in this group because of their high fecundity (Afonso-Dias and Hislop, 1996; Colmenero et al., 2013). This variability in reproductive strategy is the result of adaptation to environmental changes, such as temperature, bathymetric pressure, light, and food availability (Herring, 2002; Brown-Peterson et al., 2011). Likely, the high fecundity and the low economic value of the white anglerfish, at least until the last decades of the 20th century, has allowed the stock to be sustainable within acceptable limits. With the recent expansion of anglerfish fisheries, sustainability is in question, and our study is the first step toward an informed assessment of this deep-sea resource and its management with an ecosystem perspective.

Acknowledgments

The authors would like to thank the crew of the fishing vessels *Avi Pau*, *Estel·lada*, *Germans Félix*, *San Benito*, and *Port de Roses* for allowing us to conduct sampling aboard their vessels. We also thank M. Baeta and L.

[8] Fernandez-Arcaya, U. 2015. Personal commun. Departamento de Recursos Marinos Renovables, Institut de Ciències del Mar, Passeig Marítim de la Barceloneta, 37-49, 08003 Barcelona, Spain.

Martínez for helping with data collection, A. Ospina for assisting with the map of the study area, and C. Barría, N. Amat, and R. Alarcon for their valuable comments. We offer special thanks to K. Denning for revising the English of the early draft. This study was part of the project Monitoratge del recursos pesquers i marisquers al litoral català of the Directorate of Fishing and Maritime Affairs, Government of Catalonia.

Literature cited

Adams, P. B.
1980. Life history patterns in marine fishes and their consequences for fisheries management. Fish. Bull. 78:1–12.

Afonso-Dias, I. P., and J. R. G. Hislop.
1996. The reproduction of anglerfish *Lophius piscatorius* Linnaeus from the north-west coast of Scotland. J. Fish Biol. 49:18–39.

Ahlstrom, E. H., and H. G. Moser.
1980. Characters useful in identification of pelagic marine fish eggs. CalCOFI Rep. 21:121–131.

Armstrong, M. P., J. A. Musick, and J. A. Colvocoresses.
1992. Age, growth, and reproduction of the goosefish *Lophius americanus* (Pisces: Lophiiformes). Fish. Bull. 90:217–230.

Brown-Peterson, N. J., D. M. Wyanski, F. Saborido-Rey, B. J. Macewicz, and S. K. Lowerre-Barbieri.
2011. A standardized terminology for describing reproductive development in fishes. Mar. Coast. Fish. 3:52–70.

Bustos-Salvador, F., U. Fernandez-Arcaya, E. Ramirez-Llodra, J. Aguzzi, L. Recasens, and G. Rotllant.
2015. Reproductive biology of NW Mediterranean tonguefish *Symphurus nigrescens* and *Symphurus ligulatus*. J. Mar. Biol. Assoc. U.K. 95:1041–1049.

Caruso, J. H.
1983. The systematics and distribution of the lophiid anglerfishes: II. Revisions of the genera *Lophiomus* and *Lophius*. Copeia 1983:11–30.
1986. Lophiidae. *In* Fishes of the North-eastern Atlantic and the Mediterranean (P. J. P. Whitehead, M.-L. Bauchot, J.-C. Hureau, J. Nielsen, and E. Tortonese, eds.), p. 1362–1363. UNESCO, Paris.

Chambers, R. C., and E. A. Trippel (eds.).
1997. Early life history and recruitment in fish populations, 596 p. Chapman and Hall, London.

Charnov, E. L.
2008. Fish growth: Bertalanffy k is proportional to reproductive effort. Environ. Biol. Fish. 83:185–187.

Colmenero, A. I., J. Aguzzi, A. Lombarte, and A. Bozzano.
2010. Sensory constraints in temporal segregation in two species of anglerfish, *Lophius budegassa* and *L. piscatorius*. Mar. Ecol. Prog. Ser. 416:255–265.

Colmenero, A. I., V. M. Tuset, L. Recasens, and P. Sánchez.
2013. Reproductive biology of Black Anglerfish (*Lophius budegassa*) in the northwestern Mediterranean Sea. Fish. Bull. 111:390–401.

Colmenero, A. I., C. Barría, S. W. Feist, and V. M. Tuset.
2015a. Observations on the occurrence of *Spraguea lophii* in Mediterranean lophiids. Parasitol. Res. 114: 1977–1983.

Colmenero, A. I., V. M. Tuset, J.-M. Fortuño, and P. Sánchez.
2015b. The chorion ultrastructure of ova of *Lophius* spp. J. Fish Biol. 86:1881–1886.

Coll, M., I. Palomera, S. Tudela, and F. Sardà.
2006. Trophic flows, ecosystem structure and fishing impacts in the South Catalan Sea, Northwestern Mediterranean. J. Mar. Syst. 59:63–96.

Cushing, D. H.
1990. Plankton production and year-class strength in fish populations: an update of the match/mismatch hypothesis. Adv. Mar. Biol. 26:249–293.

D'Onghia, G., P. Maiorano, and L. Sion.
2008. A review on the reproduction of grenadiers in the Mediterranean with new data on the gonad maturity and fecundity. Am. Fish. Soc. Symp. 63:169–184.

Dahlgren, U.
1928. The habits and life history of *Lophius*, the anglerfish. Nat. Hist. 28:18–32.

Díaz, P., J. Santos, F. Velasco, A. Serrano, and N. Pérez.
2008. Anglerfish discard estimates and patterns in Spanish Northeast Atlantic trawl fisheries. ICES J. Mar. Sci. 65:1350–1361.

Dobby, H., L. Allan, M. Harding, C. H. Laurenson, and H. A. McLay.
2008. Improving the quality of information on Scottish anglerfish fisheries: making use of fishers' data. ICES J. Mar. Sci. 65:1334–1345.

Drazen, J. C., and R. L. Haedrich.
2012. A continuum of life histories in deep-sea demersal fishes. Deep-Sea Res. Oceanogr., I 61:34–42.

Duarte, C. M., and M. Alcaraz.
1989. To produce many small or few large eggs: a size-independent reproductive tactic of fish. Oecologia 80:401–404.

Duarte, R., M. Azevedo, J. Landa, and P. Pereda.
2001. Reproduction of anglerfish (*Lophius budegassa* Spinola and *Lophius piscatorius* Linnaeus) from the Atlantic Iberian coast. Fish. Res. 51:349–361.

Erickson, D. L., and E. K. Pikitch.
1993. A histological description of shortspine thornyhead, *Sebastolobus alascanus*, ovaries: structures associated with the production of gelatinous egg masses. Environ. Biol. Fish. 36:273–282.

Fariña, A. C., M. Azevedo, J. Landa, R. Duarte, P. Sampedro, G. Costas, M. A. Torres, and L. Cañás.
2008. *Lophius* in the world: a synthesis on the common features and life strategies. ICES J. Mar. Sci. 65:1272–1280.

Fernandez-Arcaya, U., E. Ramirez-Llodra, G. Rotllant, L. Recasens, H. Murua, I. Quaggio-Grassiotto, and J. B. Company.
2013. Reproductive biology of two macrourid fish, *Nezumia aequalis* and *Coelorinchus mediterraneus*, inhabiting the NW Mediterranean continental margin (400–2000 m). Deep-Sea Res. Oceanogr., II 92:63–72.

Fishelson, L.
1978. Oogenesis and spawn-formation in the pigmy lion fish *Dendrochirus brachypterus* (Pteroidae). Mar. Biol. 46:341–348.

Fulton, T. W.
1898. The ovaries and ovarian eggs of the angler or frog-fish (*Lophius piscatorius*), and of the John Dory (*Zeus faber*). Annu. Rep. Fish. Board Scotl. 16:125–134.

Gage, J. D., and P. A. Tyler.
1991. Deep-sea biology: a natural history of organisms at the deep-sea floor, 524 p. Cambridge Univ. Press, Cambridge, UK.

García-Díaz, M., J. A. González, M. J. Lorente, and V. M. Tuset.
2006. Spawning season, maturity sizes, and fecundity in blacktail comber (*Serranus atricauda*) (Serranidae) from the eastern-central Atlantic. Fish. Bull. 104:159–166.

Griffiths, M. H., and J. Hecht.
1986. A preliminary study of age and growth of the monkfish *Lophius upsicephalus* (Pisces: Lophiidae) on the Agulhas Bank, South Africa. S. Afr. J. Mar. Sci. 4:51–60.

Hendry, A. P., and T. Day.
2003. Revisiting the positive correlation between female size and egg size. Evol. Ecol. Res. 5:421–429.

Herring, P.
2002. The biology of the deep ocean, 314 p. Oxford Univ. Press, Oxford.

Hislop, J. R. G., A. Gallego, M. R. Heath, F. M. Kennedy, S. A. Reeves, and P. J. Wright.
2001. A synthesis of the early life history of the anglerfish, *Lophius piscatorius* (Linnaeus, 1758) in northern British waters. ICES J. Mar. Sci. 58:70–86.

Humphreys, R. L, Jr.
2000. Otolith-based assessment of recruitment variation in a North Pacific seamount population of armorhead *Pseudopentaceros wheeleri*. Mar. Ecol. Prog. Ser. 204:213–223.

Hunter, J. R., and S. R. Goldberg.
1980. Spawning incidence and batch fecundity in northern anchovy, *Engraulis mordax*. Fish. Bull. 77:641–652.

Jespersen, .
1984. Spermatozoans from a parasitic dwarf male of *Neoceratias spinifer* Pappenheim, 1914. Vidensk. Medd. Dan. Nathist. Foren. 145:37–42.

Koslow, J. A., J. Bell, P. Virtue, and D. C. Smith.
1995. Fecundity and its variability in orange roughy: effects of population density, condition, egg size, and senescence. J. Fish Biol. 47:1063–1080.

Koslow, J. A., G. W. Boehlert, J. D. M. Gordon, R. L. Haedrich, P. Lorance, and N. Parin.
(northeastern Mediterranean). Hydrobiologia 440:281–296.
2000. Continental slope and deep-sea fisheries: implications for a fragile ecosystem. ICES J. Mar. Sci. 57:548–557.

Labropoulou, M., and C. Papaconstantinou.
2000. Community structure of deep-sea demersal fish in the North Aegean Sea. Hydrobiologia 440:281–296.

Lahnsteiner, F., and R. A. Patzner.
1990. Spermiogenesis and structure of mature spermatozoa in blenniid fishes (Pisces, Blenniidae). J. Submicros. Cytol. Pathol. 22:565–576.

Lehodey, P., R. Grandperrin, and P. Marchal.
1997. Reproductive biology and ecology of a deep-demersal fish, alfonsino *Beryx splendens*, over the seamounts off New Caledonia. Mar. Biol. 128:17–27.

Leslie, R. W., and W. S. Grant.
1990. Lack of congruence between genetic and morphological stock structure of the southern African anglerfish *Lophius vomerinus*. S. Afr. J. Mar. Sci. 9:379–389.

López, N., J. Navarro, C. Barría, M. Albo-Puigserver, M. Coll, and I. Palomera.
2016. Feeding ecology of two demersal opportunistic predators coexisting in the northwestern Mediterranean Sea. Est. Coast. Shelf Sci. 175:15–23.

Maartens, L., and A. J. Booth.
2005. Aspects of the reproductive biology of monkfish *Lophius vomerinus* off Namibia. Afr. J. Mar. Sci. 27:325–330.

Maiorano, P., L. Sion, R. Carlucci, F. Capezzuto, A. Giove, G. Costantino, M. Panza, G. D'Onghia, and A. Tursi.
2010. The demersal faunal assemblage of the north-western Ionian Sea (central Mediterranean): current knowledge and perspectives. Chem. Ecol. 26:219–240.

Manni, L., and M. B. Rasotto.
1997. Ultrastructure and histochemistry of the testicular efferent duct system and spermiogenesis in *Opistognathus whitehurstii* (Teleostei, Trachinoidei). Zoomorphology 117:93–102.

Mattei, C., and X. Mattei.
1978. La spermiogenèse d'un poisson téléostéen (*Lepadogaster lepadogaster*). II. Le spermatozoïde. Biol. Cell. 32:267–274.

Mattei, X., Y. Siau, O. T. Thiaw, and D. Thiam.
1993. Peculiarities in the organization of testis of *Ophidion sp.* (Pisces Teleostei). Evidence for two types of spermatogenesis in teleost fish. J. Fish Biol. 43:931–937.

Merrett, N. R.
1994. Reproduction in the North Atlantic oceanic ichthyofauna and the relationship between fecundity and species' sizes. Environ. Biol. Fish. 41:207–245.

Morales-Nin, B., E. Massutí, and C. Stefanescu.
1996. Distribution and biology of *Alepocephalus rostratus* from the Mediterranean Sea. J. Fish Biol. 48:1097–1112.

Morato, T., R. Watson, T. J. Pitcher, and D. Pauly.
2006. Fishing down the deep. Fish Fish. 7:24–34.

Muñoz, M., M. Casadevall, and S. Bonet.
2002. Testicular structure and semicystic spermatogenesis in a specialized ovuliparous species: *Scorpaena notata* (Pisces, Scorpaenidae). Acta Zool. 83:213–219.

Muñoz, M., C. Dimitriadis, M. Casadevall, S. Vila, E. Delgado, J. Lloret, and F. Saborido-Rey.
2010. Female reproductive biology of the bluemouth *Helicolenus dactylopterus dactylopterus*: spawning and fecundity. J. Fish Biol. 77:2423–2442.

Murua, H., and F. Saborido-Rey.
2003. Female reproductive strategies of marine fish species of the North Atlantic. J. Northwest Atl. Fish. Sci. 33:23–31.

Murua, H., G. Kraus, F. Saborido-Rey, P. R. Witthames, A. Thorsen, and S. Junquera.
2003. Procedures to estimate fecundity of marine fish species in relation to their reproductive strategy. J. Northwest Atl. Fish. Sci. 33:33–54.

Nash, R. D. M., P. R. Witthames, M. Pawson, and E. Alesworth.
2000. Regional variability in the dynamics of reproduction and growth of Irish Sea plaice, *Pleuronectes platessa* L. J. Sea Res. 44:55–64.

Negzaoui-Garali, N., and M. Ben Salem.
2008. Morphological characters and meristic counts in two anglerfishes, *Lophius budegassa* and *L. piscatorius* (Osteichthyes: Lophiidae) from Tunisian coastal waters (central Mediterranean). Ann. Ser. Hist. Nat. 18:17–26.

Nissling, A., and G. Dahlman.
2010. Fecundity of flounder, *Pleuronectes flesus*, in the Baltic Sea—reproductive strategies in two sympatric populations. J. Sea Res. 64:190–198.

Norse, E. A., S. Brooke, W. W. L. Cheung, M. R. Clark, I. Ekeland, R. Froese, K. M. Gjerde, R. L. Haedrich, S. S. Heppell, T. Morato, et al.
2012. Sustainability of deep-sea fisheries. Mar. Policy 36:307–320.

Pajuelo, J. G., J. M. Lorenzo, and R. Dominguez-Seoane.
2008. Gonadal development and spawning cycle in the digynic hermaphrodite sharpsnout seabream *Diplodus*

puntazzo (Sparidae) off the Canary Islands, northwest of Africa. J. Appl. Ichthyol. 24:68–76.

Pavlov, D. A., N. G. Emel'yanova, and G. G. Novikov.
2009. Reproductive dynamics. *In* Fish reproductive biology: implications for assessment and management (T. Jakobsen, M. J. Fogarty, B. A. Megrey, and E. Moksness, eds.), p. 48–90. Wiley-Blackwell, Oxford, UK.

Pianka, E. R.
1970. On r- and K-selection. Am. Nat. 104:592–597.
1974. Niche overlap and diffuse competition. Proc. Natl. Acad. Sci. U.S.A. 71:2141–2145.

Ramirez-Llodra, E., A. Brandt, R. Danovaro, B. De Mol, E. Escobar, C. R. German, L. A. Levin, P. M. Arbizu, L. Menot, P. Buhl-Mortensen, B. E. Narayanaswamy, C. R. Smith, D. P. Tittensor, P. A. Tyler, A. Vanreusel, and M. Vecchione.
2010. Deep, diverse and definitely different: unique attributes of the world's largest ecosystem. Biogeosciences 7:2851–2899.

Ramirez-Llodra, E., P. A. Tyler, M. C. Baker, O. A. Bergstad, M. R. Clark, E. Escobar, L. A. Levin, L. Menot, A. A. Rowden, C. R. Smith, et al.
2011. Man and the last great wilderness: human impact on the deep sea. PLoS ONE 6(8):e22588.

Recasens, L., V. Chiericoni, and P. Belcari.
2008. Spawning pattern and batch fecundity of the European hake (*Merluccius merluccius* (Linnaeus, 1758)) in the western Mediterranean. Sci. Mar. 72:721–732.

Rotllant, G., J. Moranta, E. Massutí, F. Sarda, and B. Morales-Nin.
2002. Reproductive biology of three gadiform fish species through the Mediterranean deep-sea range (147–1850 m). Sci. Mar. 66:157–166.

Sàbat, M., F. Lo Nostro, M. Casadevall, and M. Muñoz.
2009. A light and electron microscopic study on the organization of the testis and the semicystic spermatogenesis of the genus *Scorpaena* (Teleostei, Scorpaenidae). J. Morphol. 270:662–672.

Sedberry, G. R., J. L. Carlin, R. W. Chapman, and B. Eleby.
1996. Population structure in the pan-oceanic wreckfish, *Polyprion americanus* (Teleostei: Polyprionidae), as indicated by mtDNA variation. J. Fish Biol. 49:318–329.

Stearns, S. C., and J. C. Koella.
1986. The evolution of phenotypic plasticity in life-history traits: predictions of reaction norms for age and size at maturity. Evolution 40:893–913.

Stewart, J., K. Rowling, A.-M. Hegarty, and A. Nuttall.
2010. Size and age at sexual maturity of snapper *Pagrus auratus* in New South Wales 2008/09, 38 p. Industry & Investment NSW, Cronulla, North South Wales, Australia.

Thorsen, A., P. R. Witthames, G. Marteinsdóttir, R. D. M. Nash, and O. S. Kjesbu.
2010. Fecundity and growth of Atlantic cod (*Gadus morhua* L.) along a latitudinal gradient. Fish. Res. 104:45–55.

Treasurer, J. W.
1981. Some aspects of the reproductive biology of perch *Perca fluviatilis* L. Fecundity, maturation and spawning behaviour. J. Fish Biol. 18:729–740.

Tsimenidis, N.
1984. The growth pattern of otoliths of *Lophius piscatorius* L., 1758 and *Lophius budegassa* Spinola, 1807 in the Aegean Sea. Cybium 8:35–42.

Tsimenidis, N. C., and J. C. Ondrias.
1980. Growth studies on the angler-fishes *Lophius piscatorius* L., 1758 and *Lophius budegassa* Spinola, 1807 in Greek waters. Thalassografika 3:63–94.

Ungaro, N., G. Marano, R. Auteri, A. Voliani, E. Massutí, M. García-Rodríguez, and K. Osmani.
2002. Distribution, abundance and biological features of anglerfish (*Lophius piscatorius* and *Lophius budegassa*) (Osteichthyes: Lophiiformes) in the Mediterranean Sea. Sci. Mar. 66:55–63.

Valentim, M. F. M., E. P. Caramaschi, and M. Vianna.
2007. Biology and ecology of anglerfishes of the genus *Lophius* (Lophiidae, Lophiiformes) with emphasis in *Lophius gastrophysus* Miranda-Ribeiro, 1915: current status. Oecol. Bras. 11:503–520.

Valls, M., C. J. Sweeting, M. P. Olivar, M. L. Fernández de Puelles, C. Pasqual, N. V. C. Polunin, and A. Quetglas.
2014. Structure and dynamics of food webs in the water column on shelf and slope grounds of the western Mediterranean. J. Marine Syst. 138:171–181.

van Overzee, H. M. J., and A. D. Rijnsdorp.
2015. Effects of fishing during the spawning period: implications for sustainable management. Rev. Fish Biol. Fish. 25:65–83.

Walmsley, S. A., R. W. Leslie, and W. H. H. Sauer.
2005. The biology and distribution of the monkfish *Lophius vomerinus* off South Africa. Afr. J. Mar. Sci. 27:157–168.

Wallace, R. A., and K. Selman.
1981. Cellular and dynamic aspects of oocyte growth in teleosts. Am. Zool. 21:325–343.

Watson, R. A., and T. Morato.
2013. Fishing down the deep: accounting for within-species changes in depth of fishing. Fish. Res. 140:63–65.

West, G.
1990. Methods of assessing ovarian development in fishes: a review. Aust. J. Mar. Freshw. Res. 41:199–222.

Yoneda, M., M. Tokimura, H. Fujita, N. Takeshita, K. Takeshita, M. Matsuyama, and S. Matsuura.
1997. Age and growth of anglerfish *Lophius litulon* in the East China Sea and the Yellow Sea. Fish. Sci. 63:887–892.
1998. Reproductive cycle and sexual maturity of the anglerfish *Lophiomus setigerus* in the East China Sea with a note on specialized spermatogenesis. J. Fish Biol. 53:164–178.
2001. Reproductive cycle, fecundity, and seasonal distribution of the anglerfish *Lophius litulon* in the East China and Yellow seas. Fish. Bull. 99:356–370.

Yoneda, M., M. Tokimura, H. Horikawa, K. Yamamoto, M. Matsuyama, and S. Matsuura.
2002. Spawning migration of the anglerfish *Lophius litulon* in the East China and Yellow Seas. Fish. Sci. 68:310–313.

National Marine
Fisheries Service
NOAA

Fishery Bulletin
established in 1881

Spencer F. Baird
First U.S. Commissioner
of Fisheries and founder
of *Fishery Bulletin*

Population dynamics and secondary production of juvenile white shrimp (*Litopenaeus setiferus*) along an estuarine salinity gradient

Marvin M. Mace III[1]
Lawrence P. Rozas[2]

Email address for contact author: marvin.mace.iii@gmail.com

[1] Department of Biology
University of Louisiana at Lafayette
P.O. Box 42451
Lafayette, Louisiana 70504

[2] Estuarine Habitats and Coastal Fisheries Center
Southeast Fisheries Science Center
National Marine Fisheries Service, NOAA
646 Cajundome Boulevard
Lafayette, Louisiana 70506

Abstract—We used estimates of shrimp density, growth, mortality, and secondary production during an 84-d sampling period to compare the value of nursery habitat for juvenile white shrimp (*Litopenaeus setiferus*) among 3 salinity zones (intermediate, brackish, and saline zones) within Sabine Lake, an estuary of the northern Gulf of Mexico. Density, growth, mortality, and secondary production were generally higher in the saline or brackish zones and lowest in the intermediate zone. The saline and brackish zones appeared to provide the most important nursery habitat on a per-area basis, but the intermediate zone also may contribute substantially to total shrimp production; although production in the intermediate zone was modest, this zone encompasses a relatively large portion (26%) of coastal wetlands in Louisiana. The relative value of nursery areas can be dynamic; variation occurs both spatially (e.g., within an estuary and among estuaries) and temporally (e.g., from year to year). We documented within-estuary differences (i.e., differences among salinity zones within the estuary) in the value of nursery habitat for white shrimp in Sabine Lake and expect this value, especially in the intermediate zone, to vary interannually. The dynamic nature of habitats should be considered when assessing the value of estuarine nursery areas.

Manuscript submitted 16 October 2015.
Manuscript accepted 26 September 2016.
Fish. Bull. 115:74–88 (2017).
Online publication date: 22 November 2016.
doi: 10.7755/FB.115.1.7

The views and opinions expressed or implied in this article are those of the author (or authors) and do not necessarily reflect the position of the National Marine Fisheries Service, NOAA.

Penaeid shrimps support several valuable commercial fisheries in the United States. Three species, brown shrimp (*Farfantepenaeus aztecus*), pink shrimp (*F. duorarum*), and white shrimp (*Litopenaeus setiferus*), within the family make up most of the landings in terms of weight and economic value (NMFS[1]). Most white shrimp are landed in the western Gulf of Mexico, specifically in Louisiana and Texas (NMFS[1]).

The white shrimp is an estuarine-dependent species that occurs inshore during the early phase of its life history. Spawning takes place offshore from late spring to early fall, postlarvae migrate into estuarine habitat, and juvenile shrimp use this nursery habitat for ~7–16 weeks before returning offshore to complete their life cycle (Muncy, 1984; Baker et al., 2014). The importance of estuarine nursery areas in supporting populations of juvenile penaeid shrimps, such as white shrimp, is widely accepted, but the suitability of this habitat for penaeid shrimps often varies among and within estuaries (Vance et al., 1998; Rozas and Minello, 2010, 2011; Palmer and Montagna, 2015).

Vegetated aquatic habitats (e.g., tidal marshes, mangroves, and seagrasses) within estuaries are thought to provide essential habitat for many species of fish and crustaceans (Kneib, 1997; Kathiresan and Bingham, 2001; Heck et al., 2003; Minello et al., 2003). Tidal marshes, in particular, are believed to be important, especially for the young of commercially important species, including white shrimp (Boesch and Turner, 1984; Kneib, 1997). In coastal Louisiana, tidal marshes are disappearing at a rapid rate because of a variety of natural and anthropogenic causes (Turner, 1990), and identifying areas that are important nurseries for fishery species should be a priority for conserving coastal habitats.

The density (abundance) and vital rates (growth and mortality) of juvenile white shrimp in estuaries may be useful indicators of habitat value and their contribution to adult

[1] NMFS (National Marine Fisheries Service). 2015. Commercial fishery landings. [Available at website, accessed October 2015.]

stocks (Diop et al., 2007; NMFS, 2010; Baker et al., 2014). Abundance of early juvenile white shrimp is, for example, a good predictor of late juvenile shrimp abundance, which is itself a good predictor of the number of shrimp landed by the fishery (Diop et al., 2007). The white shrimp is harvested as an annual fishery crop (Nance et al., 2010), and survival during the juvenile life stage may have a larger effect on the adult population than adult mortality or fecundity (Baker et al., 2014). Mortality may decrease as the size of juvenile white shrimp increases (Baker and Minello, 2010); therefore, growth also could be an important factor that influences the recruitment success of white shrimp to the fishery.

Salinity is a major environmental factor thought to influence the use of estuarine nursery areas by white shrimp and other nekton at the landscape scale (Weinstein et al., 1980; Rakocinski et al., 1992; Wagner and Austin, 1999; Rozas and Minello, 2010). For example, juvenile white shrimp are reported to be most abundant in mesohaline and polyhaline environments of estuaries (Gunter et al., 1964; Howe et al., 1999; Minello, 1999; Rozas and Minello, 2010), although they range much more widely in salinities <1 and ≥35 (Gunter et al., 1964). These observations are based mainly on comparisons of shrimp density, abundance, or catch per unit of effort from samples collected within estuarine habitats of differing salinity. Density alone, however, may be an insufficient indicator of habitat quality (Van Horne, 1983); additional measures, such as growth, mortality, or secondary production, can provide a more comprehensive picture of habitat quality (Van Horne, 1983; Beck et al., 2001; NMFS, 2010; Dolbeth et al., 2012).

We are unaware of any other study in which this full suite of metrics (density, growth, mortality, and secondary production) has been incorporated to compare nursery areas of white shrimp along an estuarine salinity gradient. Few studies have examined the effect of salinity on growth and mortality of young white shrimp (Zein-Eldin and Griffith, 1969; Rozas and Minello, 2011), and available estimates indicate that secondary production of white shrimp is higher in estuaries of the northern Gulf of Mexico than in those of the U.S. Atlantic coast (Zimmerman et al., 2000; Kneib, 2003; Minello et al., 2008). Habitat-specific vital rates (growth and mortality) and estimates of secondary production are needed to fully assess and compare nursery areas among different salinity regimes. This information can be used 1) to identify important nursery areas and essential habitats (Beck et al., 2001), 2) to develop detailed population models and improve stock assessment models for white shrimp (Baker et al., 2014), and 3) to calibrate ecosystem models used to predict effects of human activities on this and other estuarine species (Rose et al., 2014).

The purpose of our study was to measure and compare the value of nursery habitat for white shrimp in 3 salinity zones in the Sabine Lake estuary along an estuarine salinity gradient. We collected quantitative density data from each salinity zone in summer and fall, when white shrimp were most abundant in the estuary. Length-frequency data from these samples were used to examine size distributions and to estimate growth and mortality rates among the 3 salinity zones. We used these data and the size-frequency method (Garman and Waters, 1983) to estimate and compare secondary production of white shrimp among salinity zones.

Materials and methods

Study site

Our study was conducted in the Sabine Lake estuary (hereafter referred to as Sabine Lake) which is located in southwest Louisiana within the area of the coast known as the Chenier Plain (Fig. 1). Sabine Lake encompasses an area of 375,979 ha; approximately half (49%) of that area is composed of marshes (Gosselink et al[2]). Marshes in coastal Louisiana are classified into salinity zones based on dominant vegetation (Chabreck, 1970; Visser et al., 1998, 2000). We selected 3 salinity zones (intermediate, brackish, and saline) using this vegetation classification rather than water salinity measured at sampling sites because conditions in estuaries are in constant flux. Vegetation (e.g., marsh type) represents average environmental conditions (e.g. salinity regime) integrated over time better than a single salinity measurement. The salinity ranges for these vegetation-based zones tend to be 0.5–5.0 for intermediate, 5.0–18.0 for brackish, and 18.0–36.0 for saline. Salinity in any zone, however, occasionally may extend outside the typical range. These 3 salinity zones are comparable to the oligohaline, mesohaline, and polyhaline zones, respectively, of the Venice system (Anonymous, 1958; Visser et al., 1998).

Sampling procedure

White shrimp were sampled during 6 sampling trips in 2011 (Table 1) that commenced on July 12 (trip 1) and 26 (trip 2), August 9 (trip 3), September 7 (trip 4) and 20 (trip 5), and October 4 (trip 6). A 1-m^2 drop sampler (Zimmerman et al., 1984) was used to collect 45–60 samples during each of these sampling trips, which each required 3 days to complete (with one salinity zone completed each day). Details of our sampling design are given in Mace and Rozas (2015). Briefly, we selected an area of 1 km×1 km within each salinity zone, divided it into 16 squares of equal size (0.25 km×0.25 km), and, before each sampling trip, we randomly selected 5 of these squares for sampling. To obtain a rep-

[2] Gosselink, J. G., C. L. Cordes, and J. W. Parsons. 1979. An ecological characterization study of the Chenier Plain coastal ecosystem of Louisiana and Texas. 3 vols., FWS/OBS-78/9, 78/10, and 78/11. Natl. Coast. Ecosyst. Team, Off. Biol. Serv., U.S. Fish Wildl. Serv., Slidell, LA.

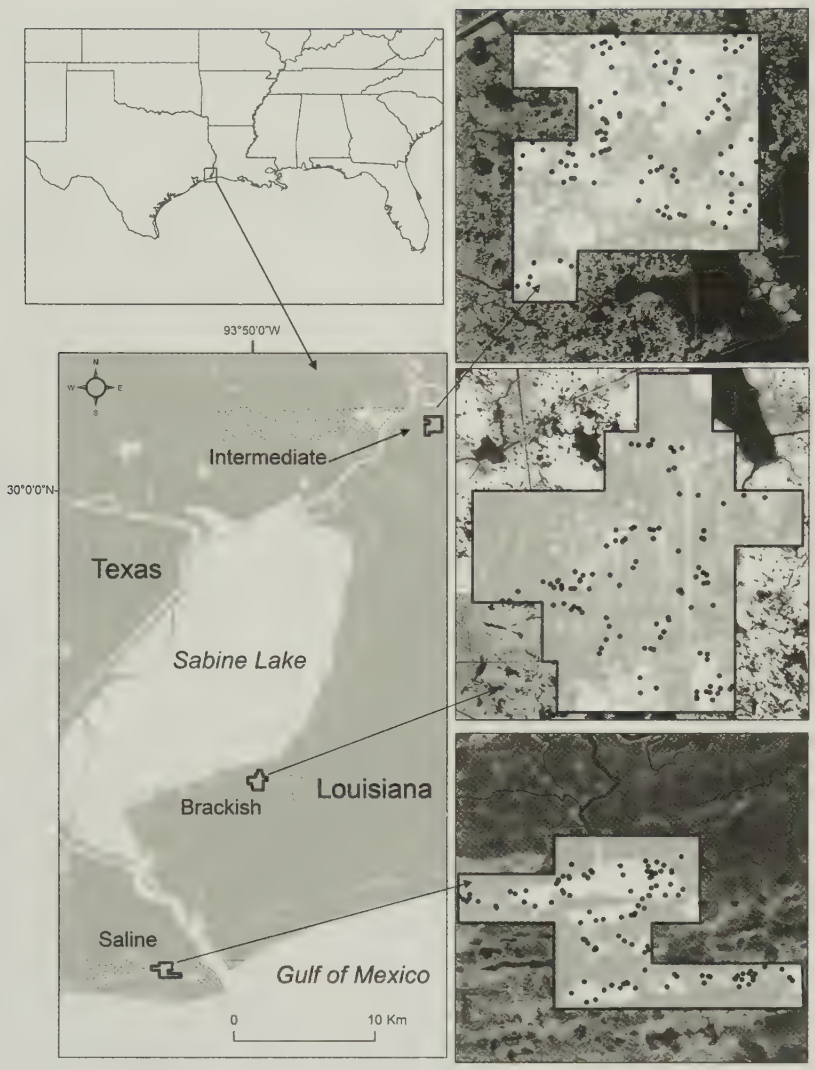

Figure 1

Map of the study area in Sabine Lake (at the border of Texas and Louisiana). Samples of juvenile white shrimp (*Litopenaeus setiferus*) were collected in 2011 to estimate density, natural mortality, growth, and secondary production at 3 locations along the estuarine salinity gradient (zones=intermediate, brackish, and saline) that were each 100 ha in size. Black dots represent locations where individual drop samples were collected.

resentative sample of the shrimp population from each selected square, a drop sample was taken from each of 4 habitat types where shrimp are known to occur: 1) marsh vegetation ≤1 m from the interface of marsh and open water (marsh edge), 2) shallow water ≤1 m from the marsh edge (SW1), 3) shallow water 1–5 m from the marsh edge (SW1–5), and 4) shallow water >5 m from the marsh edge (SW>5).

Locations of SW>5 sampling sites were determined by randomly selecting distances between 6 m from the nearest shore and the middle of the water body. Only 3 of the 4 habitat types were sampled on the first 3 sample dates in most of the salinity zones when low water levels precluded sampling at the marsh edge (Table 1). Before collecting each drop sample, salinity, temperature, depth, and turbidity were measured according to the protocol described in Rozas et al. (2012). Each nekton sample was placed on ice, preserved in 10% formalin at the end of the day, and transported to the laboratory for processing. In the laboratory, all organisms were separated from detritus, and juvenile penaeid shrimps were identified to species by using the characters from Pérez Farfante[3], Ditty (2011), and references therein. Carapace length was measured for all juvenile white shrimp as described in Mace and Rozas (2015).

The duration of flooding for each habitat was estimated by using water levels measured in the field and equations fitted for each salinity zone (Minello et al., 2012). We collected data on water levels at 20 randomly located transects within each salinity zone. Along each transect, water levels were measured at the marsh edge and at 0.5, 1, 2, 3, 4, and 5 m on each side of the marsh edge. To derive equations for estimating long-term water levels in each salinity zone, we regressed water-level data from temporary tide gauges placed in each salinity zone against data from nearby tide gauges of the NOAA Center for Operational Oceanographic Products and Services (CO-OPS: website) and the U.S. Geological Survey's Coastwide Reference Monitoring System (CRMS; website): NOAA station 8770570 for the saline zone, NOAA station 8770475 for the brackish zone, and CRMS site 0662 for the intermediate zone. We estimated the flooding durations (percentage of time water depth was ≥5 cm) at habitats in each salinity zone from July through October 2011 by relating the water depth measured at each transect sampling site to concurrent tide data calculated from these fitted equations.

Size

We examined size, measured as total length in millimeters, of white shrimp collected in our samples by comparing box plots of size for each salinity zone and sample date. Descriptive statistics, such as minimum,

[3] Pérez Farfante, I. 1970. Diagnostic characters of juveniles of the shrimps *Penaeus aztecus aztecus*, *P. duorarum duorarum*, and *P. brasiliensis* (Crustacea, Decapoda, Penaeidae). U.S. Fish Wildl. Serv., Specl. Sci. Rep. Fish. 599, 26 p.

Table 1

Distribution of samples used to estimate density, natural mortality, growth, and secondary production of juvenile white shrimp (*Litopenaeus setiferus*) in Sabine Lake. Samples were collected on 6 sampling trips in 2011 in 3 salinity zones (intermediate, brackish, and saline) and 4 habitat types (1—marsh edge, or marsh vegetation ≤1 m from the interface of marsh and open water [ME]; 2—shallow water ≤1 m from the marsh edge [SW1]; 3—shallow water 1–5 m from the marsh edge [SW1–5]; and 4—shallow water >5 m from the marsh edge [SW>5]).

			Habitat				
Zone	Trip	Date	ME	SW1	SW1–5	SW>5	Total
Intermediate	1	07/12/11	0	5	5	5	15
	2	07/26/11	0	5	5	5	15
	3	08/9/11	0	10	5	5	20
	4	09/9/11	5	5	5	5	20
	5	09/20/11	5	5	5	5	20
	6	10/4/11	5	5	5	5	20
Brackish	1	07/13/11	0	5	5	5	15
	2	07/27/11	0	5	5	5	15
	3	08/10/11	0	10	5	5	20
	4	09/7/11	5	5	5	5	20
	5	09/21/11	5	5	5	5	20
	6	10/5/11	5	5	5	5	20
Saline	1	07/14/11	0	5	5	5	15
	2	07/28/11	5	5	5	5	20
	3	08/11/11	0	10	5	5	20
	4	09/8/11	5	5	5	5	20
	5	09/22/11	5	5	5	5	20
	6	10/6/11	5	5	5	5	20

maximum, and mean size, were also computed for salinity zones and sample dates.

Density

We restricted our analysis of shrimp density to the last 3 sampling trips when sample sizes were equal both among habitats types and salinity zones (Table 1). Before analysis, these density data were $\ln(x+1)$ transformed to remove the relationship between the mean and variance present in untransformed data (Milliken and Johnson, 1992). We used an analysis of variance (ANOVA) with 3 factors: 1) salinity zone (intermediate, brackish, saline), 2) habitat type (marsh edge, SW1, SW1–5, SW>5), and 3) sampling trip (4 to 6). The ANOVA model included a 3-way interaction, all 2-way interactions, and all main effects. After a significant main effect of habitat type, 3 a priori contrasts were made: 1) marsh edge versus SW1, 2) SW1 versus SW1–5+SW>5, and 3) marsh edge versus SW1+SW1–5+SW>5. The first and third contrasts allowed us to compare marsh edge with adjacent shallow water and all shallow-water sites combined, respectively. We compared shallow-water sites near (<1 m) and those sites farther away from the marsh edge with the second contrast. Results were considered significant at $P<0.05$. We also estimated omega squared (ω^2) for each factor in the ANOVA, using the formulas for measured factors given in Olejnik and Algina (2003). Omega squared is an estimate of effect size that can be interpreted as the proportion of variance explained by a given factor in an ANOVA. All density data presented in the text, tables, and figures are untransformed means.

Mortality

We converted length-frequency distributions to age-frequency distributions to estimate mortality. Before converting to age-frequency distributions, length-frequency distributions were weighted to account for differences in the relative amount of habitat types within each salinity zone (Suppl. Table 1, avail. online). Weighting was accomplished by first constructing length-frequency distributions for each habitat type within a salinity zone and then multiplying the number of individuals in each size class by the total area of a given habitat type in that zone, resulting in 4 different length-frequency distributions for each zone on each sample date. Length-frequency data from samples collected in marsh edge habitat were applied to the entire marsh within 5 m of the shoreline, although densities of juvenile white shrimp may decline as distance from the shoreline increases from 1 to 5 m into marsh vegetation (Minello et al., 2008). Because we were interested in the entire

shrimp population in each salinity zone on each sample date, we combined length-frequency distributions from all 4 habitat types in each zone from each sample date. Finally, we converted the combined length-frequency distribution in each salinity zone on each sample date into a relative frequency distribution and apportioned the total number of shrimp collected in each zone on each sample date to fit this distribution. These weighted length-frequency distributions were used in subsequent analyses of mortality and growth.

Daily instantaneous mortality rates (Z) were estimated in each salinity zone by using a horizontal catch-curve analysis (Vetter, 1988). We assumed Z was equal to the daily instantaneous natural mortality rate (M) because there was no fishery for juvenile white shrimp in our study area, and we removed only a very small fraction of the total population during our sampling. We combined and converted length-frequency data from multiple sampling trips within each salinity zone to age-frequency data by assuming a growth rate of 1 mm TL/d, a reasonable assumption for juvenile penaeid shrimps in general (Dall et al., 1990) and white shrimp specifically (Rozas and Minello, 2011).

Using the age-frequency data, we calculated mortality with the following 2 methods: 1) a linear regression of the ln(density+0.1) against age, where the slope is an estimate of mortality (Ricker, 1975) and 2) the Chapman-Robson estimator (Chapman and Robson, 1960) with the standard error corrected for overdispersion (Smith et al., 2012). We started the catch curve with the regression method at the age of highest abundance and included all ages up to but not including the first age at which time there were ≤1 individual (Smith et al., 2012). For the Chapman-Robson estimator, we included all ages greater than the age of peak abundance. We compared mortality rates between catch-curve methods and among salinity zones by first taking the difference between 2 estimates and then constructing a 95% confidence interval (CI) for the difference. We considered results significantly different when the 95% CI of the difference between 2 estimates did not include zero (Schenker and Gentleman, 2001).

Growth

We calculated growth rates by following individual cohorts and using the mean size of a cohort on 2 consecutive sample dates to estimate a mean growth rate between sample dates. Individual cohorts of shrimp were identified from each of the length-frequency distributions on different sample dates in each salinity zone by using the mixdist package, vers. 0.5-4 (Macdonald and Du, 2012) in R, vers. 3.1.0 (R Core Team, 2014), and the mean growth rate for a cohort between sample dates was calculated as

$$G_{\text{absolute}} = \frac{\mu_{t+1} - \mu_t}{t_{t+1} - t_1},$$

where μ_t = the mean carapace length at time t; and
μ_{t+1} = the mean carapace length at time $t + 1$.

Before calculating growth, carapace length was converted to total length by using the formula TL = CL × 4.944 (Baker and Minello, 2010). This conversion makes it easier to compare our growth rates with published values. Mean growth rates among salinity zones were compared as described above for mortality rates.

For each sample date in each salinity zone, we attempted to model cohorts by using normal, lognormal, or gamma distributions based on previous observations of length-frequency distributions of penaeid shrimp as they immigrated into estuaries (Baxter and Renfro, 1967). We used Akaike's information criterion adjusted for small sample size (AICc), ΔAICc values (the difference in AICc values between a given model and the model with the lowest AICc value), and w_i values (AIC weights, which can be interpreted as an estimate of the probability that a given model is the best among all models considered, given the data) to compare and select the best model or models that described the shape and the mean size and standard deviation of the mean of shrimp cohorts (Burnham and Anderson, 2002).

Secondary production

Secondary production that occurred in each salinity zone over the 84-d sampling period was estimated in kilograms per hectare with the size-frequency method (Garman and Waters, 1983) because we were not able to track cohorts over all sample dates. The size-frequency method uses the mean number and weight of individuals in each size class over time to estimate the biomass lost as individuals move through the size-frequency distribution. We used shrimp up to 60 mm TL to estimate secondary production because shrimp larger than this size begin to emigrate from estuaries into the Gulf of Mexico (Pullen and Trent, 1969). We used the length-to-weight conversion given in Minello et al. (2008) to estimate mean shrimp weights and assumed this relationship was similar for all 3 salinity zones. We also estimated total biomass, measured in kilograms per hectare, within each salinity zone for the 84-d sampling period as the sum of the mean biomass of all size classes over all sample dates.

One of the most influential parameters affecting production estimates with the use of the size-frequency method is the cohort production interval (CPI) (Benke, 1979; Garman and Waters, 1983). The size-frequency method was originally developed to estimate production for insects whose larvae develop in aquatic habitats and produce only one generation per year. This original method was modified by including the CPI into the calculation to account for species that have multiple generations per year. Benke (1979) originally defined the CPI in terms of the amount of time taken to complete larval development (i.e., the aquatic stages when growth and production occur). Garman and Waters (1983) defined the CPI for fish as the average maximum age obtained by individuals in the population.

In our study, the age of a shrimp depended on its length because we estimated age from length; there-

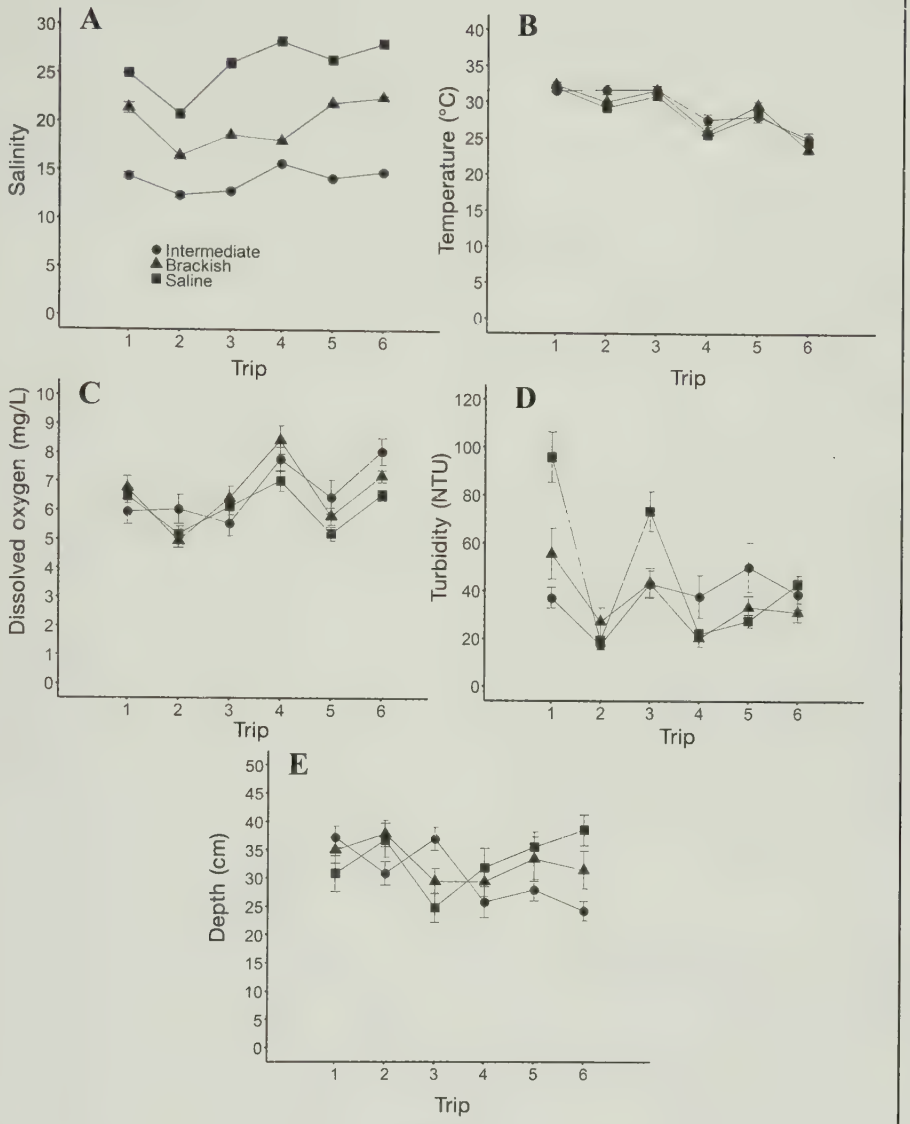

Figure 2

Mean water (**A**) salinity, (**B**) temperature, (**C**) dissolved oxygen, (**D**) turbidity (in nephelometric turbidity units, NTUs), and (**E**) depth within intermediate, brackish, and saline zones measured on 6 trips during which samples of juvenile white shrimp (*Litopenaeus setiferus*) were collected in 2011. Means and standard errors (1 SE) were computed from 15 to 20 replicate measurements.

fore, growth rates could have affected our age estimates and the resultant CPI. We used a conservative approach for initial estimates of secondary production by assuming that shrimp in each salinity zone had the same CPI of 53 d (i.e., the maximum age of a shrimp since recruitment to the population as a 7 mm TL postlarva until migration out of the population at 60 mm TL, assuming a growth rate of 1 mm TL/d). We also calculated secondary production using CPIs for shrimp in each salinity zone based on the growth rates we estimated as described above. For example, if the mean growth rate that we estimated for a salinity zone was 2 mm TL/d, a 60-mm-TL shrimp that arrived in the population at 7 mm TL would have aged 27 d since it arrived in the population. Therefore, the CPI based on this 2 mm TL/d growth rate would be 27.

Results

Environmental variables

Environmental variables, other than salinity, differed little among salinity zones (Fig. 2). Southwest Loui-

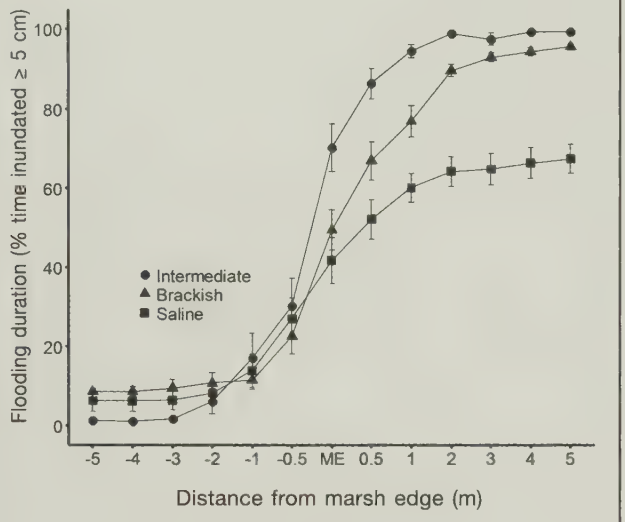

Figure 3

Comparison of mean flooding duration (number of hours water depth was ≥ 5 cm/total number of hours×100) for marsh edge and shallow-water sites among 3 different salinity zones (intermediate, brackish, and saline) in Sabine Lake from July 2011 through October 2011. Negative values indicate distances (from the marsh edge) within marsh vegetation, and positive values are distances from the marsh edge over shallow water. Means and standard errors (1 SE) were calculated from 20 replicate measurements.

siana experienced drought conditions starting in late 2010 until the end of 2011 (NOAA National Centers for Environmental Information, Climate Data Online, website, accessed October 2015). As a result, mean salinities during our study in Sabine Lake were slightly outside the range typical for the brackish zone and well above the normal range for the intermediate zone (Fig. 2). Mean water temperature varied little among salinity zones during each sampling trip and was slightly lower during the last 3 trips than during the first 3 trips. Mean dissolved oxygen was less variable during the first 3 sampling trips than during the last 3 trips, but no clear trend was detected in dissolved oxygen among salinity zones. We observed no consistent trend in either mean water depth or turbidity among salinity zones.

Flooding duration varied among salinity zones and distances from the marsh edge (Fig. 3). The marsh edge habitat was flooded for the highest percentage of the time in the intermediate zone (70%), followed by the brackish (50%) and saline (42%) zones. The mean duration of flooding of the vegetated marsh surface >0.5 m from the marsh edge (i.e., the negative numbers on the x-axis in Fig. 3) was relatively short (<20% of the time) in all 3 salinity zones. In the saline zone, shallow-water sites within 5 m of the marsh edge were flooded for relatively short durations as well (Fig. 3).

Size

White shrimp ranged in size from 4 to 126 mm TL, on the basis of data from all 6 sampling trips to the 3 salinity zones. Most shrimp (98%), however, were juveniles <60 mm TL, and, in general, size distributions and mean sizes were similar among salinity zones and sampling dates (Fig. 4). Mean size on most sampling dates ranged from 12 to 35 mm TL, except in the intermediate zone on trip 5 when mean size was 41 mm TL.

Density

Mean densities varied among habitat types, salinity zones, and sample dates (Table 2). The overall ANOVA model was significant (P<0.001) and accounted for 60% of the variation in the shrimp density data. All 3 main effects were significant, as were the interactions between habitat type and salinity zone and between salinity zone and sampling trip; the 3-way interaction was not significant (Table 3).

Habitat type was the most important factor in the model, and it accounted for an order of magnitude more variation (45%) in the density data than that of any other factor (≤6%, Table 3). The interaction of habitat type with salinity zone was weak, accounting for only 4% of the variation in the density data. Results from a priori contrasts indicated that shrimp densities were higher in the marsh edge habitat than in adjacent shallow water (P=0.0379), higher in shallow water near the marsh edge than in other shallow-water sites (P<0.0001), and higher at the marsh edge sites than at all shallow-water sites combined (P<0.0001).

Mean shrimp density in each habitat type was generally highest in the saline zone. For example, mean shrimp densities at the marsh edge sites were estimated as 41.5 individuals/m^2 (standard error [SE] 10.2), 56.7 individuals/m^2 (SE 11.2), and 85.1 individuals/m^2 (SE 22.6) for the intermediate, brackish, and saline zones, respectively (Table 2). The SW1 habitat type was an exception; mean density at this type of habitat (based on the last 3 sampling trips) was highest in the brackish zone and lowest in the intermediate zone (Fig. 5). Although the main effect of salinity zone was significant, this effect varied by sample date; mean density was usually highest in the saline zone, except for on trip 5 when mean density was higher in the brackish zone than in the saline zone (Fig. 6).

Mortality

We estimated mortality by combining shrimp length-frequency data from the last 3 sampling trips in each salinity zone and conducting 2 catch-curve analyses per zone. Within a salinity zone, no difference in mortality rates could be detected between the results of the 2 catch-curve analyses (Table 4). Among salinity zones, no statistically significant difference in mortality rates was detected between the saline (0.09 [SE

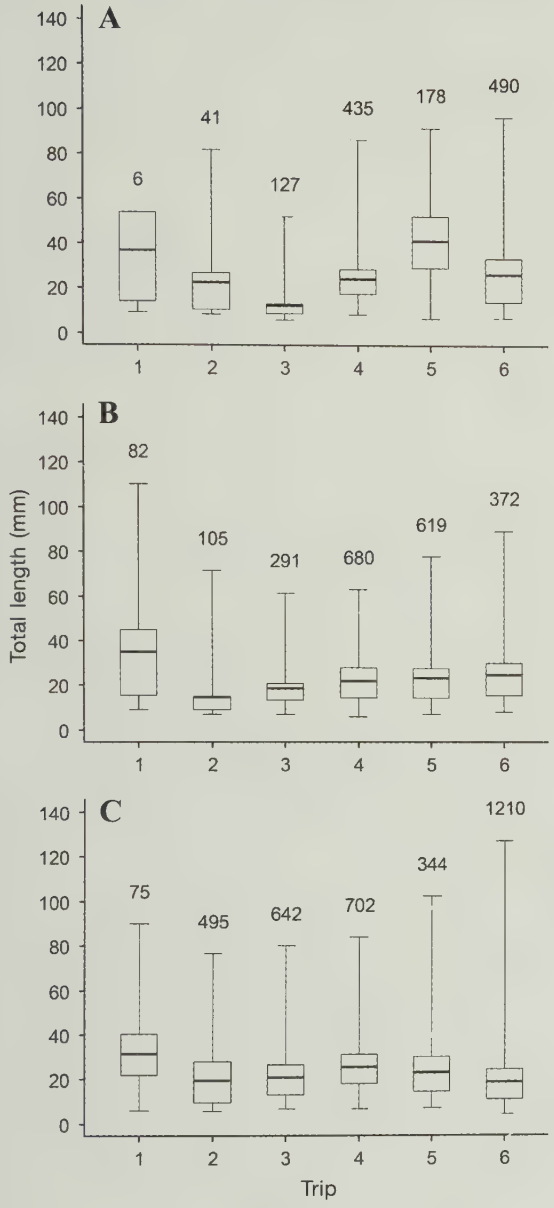

Figure 4

Box plots of the size, measured as total length in millimeters, of juvenile white shrimp (*Litopenaeus setiferus*) collected on 6 sampling trips in 3 salinity zones, (**A**) intermediate, (**B**) brackish, and (**C**) saline zones, in Sabine Lake in 2011. The black line inside boxes represents the mean size, the boxes extend to the 25th and 75th percentiles, and the whiskers extend to the minimum and maximum size. Numbers above each box-and-whisker plot are the sample size for each sampling trip.

0.007] and 0.08 [SE 0.006]) and brackish (0.08 [SE 0.005] and 0.09 [SE 0.006]) zones, but estimates that resulted from the use of both methods showed significantly higher mortality in the brackish zone than in the intermediate zone (0.05 [SE 0.006] and 0.07 [SE 0.008]). Only the linear-regression estimates indicated significantly greater mortality in the saline zone than in the intermediate zone.

Growth

We were unable to consistently track individual cohorts of shrimp over sampling trips in each salinity zone. Identifying individual cohorts on some sample dates was difficult because there were no clear modes that indicated separate cohorts, and the mixdist package could not adequately fit any of the 3 distributions to the data. On most sampling dates when we were able to track individual cohorts, more than 1 model had some support from AIC values; for these dates, we used model-averaged estimates for mean carapace length from models that had a combined AIC weight ≥0.95 (Suppl. Tables 2 and 3, avail. online).

Mean growth rate estimates among all salinity zones and cohorts combined ranged from 0.72 mm TL/d (SE 0.28) to 1.83 mm TL/d (SE 0.23) (Table 5). Among salinity zones, mean growth rates were 1.22 mm TL/d (SE 0.13), 0.99 mm TL/d (SE 0.19), and 1.62 mm TL/d (SE 0.12) in the intermediate, brackish, and saline zones, respectively (Table 5). Mean growth rates were significantly higher in the saline zone than in the brackish and intermediate zones. No significant difference in mean growth rates was detected between the brackish and intermediate zones.

Secondary production

Secondary production of juvenile white shrimp estimated with the conservative approach (i.e., the one based on the same growth rate of 1 mm TL/d in each salinity zone) varied by salinity zone and was significantly higher in the saline than in the intermediate zone (Table 6). Secondary production in the saline zone during the 84-d sampling period was estimated as 382 kg/ha (95% CI, 187 to 577), which was approximately 3 times the value of 116 kg/ha (95% CI, 27 to 205) for the intermediate zone. In the brackish zone, production was estimated as 232 kg/ha (95% CI, 102 to 361), approximately twice that of the intermediate zone. Production-to-biomass ratios over the 84-d sampling period were estimated as 5.0, 6.5, and 7.4 in the intermediate, brackish, and saline zones, respectively (Table 6). When we used the mean growth rates estimated for each salinity zone (Table 5) to compute shrimp age and CPIs, the overall pattern of secondary production during the 84-d sampling period was the same among salinity zones, although some estimates of production were higher (intermediate=142 kg/ha, brackish=227 kg/ha, and saline=614 kg/ha) when compared with results from the conservative approach (Table 6). Differences in production estimates appear to have been driven mainly by differences in shrimp density among salinity zones (Table 2).

Table 2

Mean densities, measured in individuals per square meter, of juvenile white shrimp (*Litopenaeus setiferus*) in Sabine Lake during 6 sampling trips in 2011 in 3 salinity zones (intermediate, brackish, and saline) and 4 habitat types: 1—marsh edge, or marsh vegetation ≤1 m from the interface of marsh and open water (ME); 2—shallow water ≤1 m from the marsh edge (SW1); 3—shallow water 1–5 m from the marsh edge (SW1–5); and 4—shallow water >5 m from the marsh edge (SW>5). A dash indicates that no sample was taken in that habitat on that date. Sample sizes for each mean range from 5 to 10 and are provided in Table 1. Standard errors (SEs) of the means are given in parentheses.

	Zone											
	Intermediate				Brackish				Saline			
Trip	ME	SW1	SW1–5	SW>5	ME	SW1	SW1–5	SW>5	ME	SW1	SW1–5	SW>5
1	–	1.2 (0.8)	0.0 (0.0)	0.0 (0.0)	–	11.2 (5.9)	0.4 (0.4)	2.4 (1.9)	–	6.0 (5.3)	7.6 (4.4)	1.6 (0.7)
2	–	7.8 (4.7)	0.4 (0.4)	0.0 (0.0)	–	13.6 (2.7)	4.6 (4.1)	3.0 (2.0)	63.0 (28.2)	29.4 (26.2)	3.8 (3.1)	4.0 (1.5)
3	–	12.0 (5.3)	1.4 (0.5)	0.0 (0.0)	–	27.7 (10.4)	1.0 (0.8)	2.2 (1.6)	–	46.4 (11.7)	29.4 (12.2)	10.0 (3.2)
4	61.8 (25.4)	25.2 (9.4)	0.4 (0.4)	0.2 (0.2)	74 (22.1)	58.6 (23.1)	2.8 (1.5)	1.8 (0.6)	60.4 (24.4)	65.0 (36.2)	6.2 (3.9)	10.4 (3.4)
5	16.0 (4.7)	19.4 (4.8)	0.4 (0.4)	0.6 (0.6)	64.8 (20.0)	51.0 (15.8)	8.4 (5.1)	1.6 (0.9)	43.0 (9.2)	9.0 (3.9)	10.8 (3.7)	5.6 (2.6)
6	46.8 (12.6)	47.8 (20.7)	4.0 (1.3)	0.6 (0.2)	31.4 (13.4)	28.8 (6.6)	5.8 (2.1)	9.4 (8.4)	174.0 (74.6)	33.0 (16.1)	17.0 (3.8)	22.8 (3.5)
Overall mean	41.5 (10.2)	17.9 (4.2)	1.1 (0.3)	0.2 (0.1)	56.7 (11.2)	31.2 (5.5)	3.8 (1.2)	3.4 (1.5)	85.1 (22.6)	33.6 (7.8)	12.4 (2.8)	9.1 (1.6)

Table 3

Results of 3-way analysis of variance (ANOVA) to examine differences in mean density of juvenile white shrimp (*Litopenaeus setiferus*) among salinity zones, habitat types, and sampling trips in Sabine Lake in 2011. A measure of effect size, omega squared (ω^2), is given for each factor and can be interpreted as an estimate of the proportion of variance accounted for by each source of variation. Data used in this analysis were obtained from trips 4–6.

Factor	df	Sum of squares	*F* ratio	*P*	ω^2
Zone	2	27.90	13.86	<0.0001	0.06
Trip	2	8.80	4.37	0.0143	0.02
Habitat type	3	208.57	69.10	<0.0001	0.45
Zone*Trip	4	13.35	3.32	0.0124	0.02
Zone*Habitat type	6	25.30	4.19	0.0006	0.04
Trip*Habitat type	6	8.92	1.48	0.1899	0.01
Zone*Trip*Habitat type	12	13.70	1.34	0.3373	0.00
Error	144	144.90			

Discussion

The suitability of habitat for juvenile white shrimp varies among salinity zones within Sabine Lake. The saline and brackish zones provide more important nursery habitat for white shrimp than does the intermediate zone, on the basis of our estimates of shrimp density, growth, and secondary production. The intermediate zone contains the least important nursery area, although shrimp mortality rates were lower there than in the 2 other salinity zones. Although growth, mortality, and secondary production, together with density, are considered necessary for a comprehensive assessment of nursery habitat (Beck et al., 2001), and density alone may sometimes be a misleading indicator of habitat quality (Van Horne, 1983), in our study, density appeared to be an accurate indicator of habitat quality for juvenile white shrimp.

Habitat type accounted for most of the variation in density of white shrimp. Density of white shrimp was highest for habitat ≤1 m from the marsh edge and declined with increasing distance into open water in all 3 salinity zones. This general pattern for white shrimp, namely high density near the marsh edge and a decline in density in open water, has been observed in another area of Sabine Lake (Nevins et al., 2014), in Galveston Bay, Texas (Minello et al., 2008), and in Barataria Bay, Louisiana (Rozas and Minello, 2015). Densities of white shrimp at the marsh edge sites in our study area were among the highest densities reported for this species in the northern Gulf of Mexico. This concentration of shrimp may be a response to the short flooding dura-

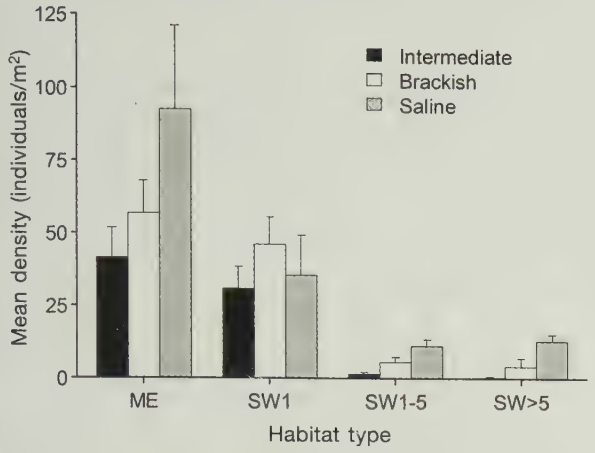

Figure 5

Comparison of mean densities of juvenile white shrimp (*Litopenaeus setiferus*) among 4 habitat types and 3 salinity zones (intermediate, brackish, and saline) within Sabine Lake, based on data from the last 3 sampling trips (trips 4–6) in 2011. Habitat types are 1—marsh edge (ME), or marsh vegetation ≤1 m from the interface of marsh and open water; 2—shallow water ≤1 m from the marsh edge (SW1); 3—shallow water 1–5 m from the marsh edge (SW1–5); and 4—shallow water >5 m from the marsh edge (SW>5). Means and standard errors were computed from 15 replicate samples. Figure represents the significant interaction of habitat type and salinity zone.

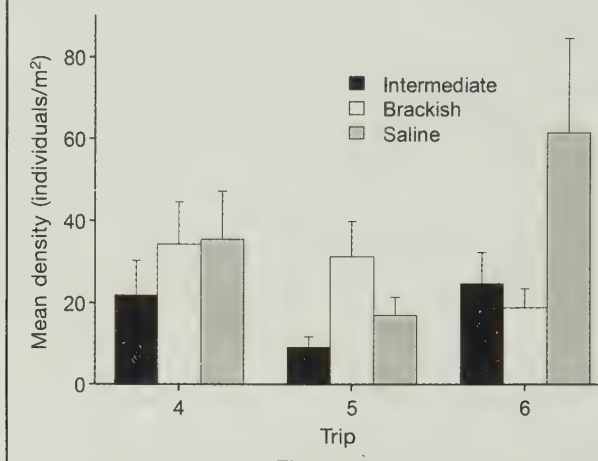

Figure 6

Comparison of mean densities of juvenile white shrimp (*Litopenaeus setiferus*) among 3 sampling trips (trips 4–6) made in 2011 and among 3 salinity zones (intermediate, brackish, and saline) within Sabine Lake. Means and standard errors were computed from 20 replicate samples. Figure represents the significant interaction between sample date and salinity zone.

tion of marsh >1 m from the marsh edge because this short duration limited access to the vegetated marsh surface and concentrated individuals at the marsh edge sites.

Nekton density patterns in shallow water also can be influenced by the distribution of submerged aquatic vegetation (SAV) or other structure (Rozas and Minello, 2010). In our study area in 2011, SAV was absent because of an ongoing drought; however, SAV can be present, especially in the intermediate and brackish zones of estuaries during periods of normal rainfall (Chabreck, 1971). Because densities of juvenile white shrimp are similar in marsh vegetation and SAV (Howe and Wallace, 2000; Rozas and Minello, 2006), we expect that the distribution pattern of shrimp in our intermediate and brackish zones could be quite different in years of normal rainfall, when SAV beds in these locations may be extensive.

The pattern we observed in growth rates of juvenile white shrimp among salinity zones was similar to that reported for the Cape Fear River estuary in North Carolina (Laney and Copeland[4]), but the growth rates we observed in our study area were overall higher than those reported in Barataria Bay (Rozas and Minello, 2011). In laboratory experiments, extremes in salinity have been shown to reduce growth rates of juvenile white shrimp (Zein-Eldin and Griffith, 1969). Salinity may directly influence growth rates through increased metabolic costs for shrimp in low-salinity (e.g., oligohaline) areas (Rozas and Minello, 2011), although this explanation did not likely pertain to our study because salinities in the intermediate zone were elevated by the ongoing drought and more typical of the brackish zone.

Although comparisons of natural mortality rates among salinity zones are rare, results of available studies indicate that mortality may increase with salinity for a variety of species. Mortality of juvenile white shrimp within marsh tidal creeks of the Cape Fear River estuary was lower in low-salinity areas than in high-salinity areas (Laney and Copeland[4]). The mortality rate for juvenile spot (*Leiostomus xanthurus*) in the Cape Fear estuary was lower at a low-salinity site than at a high-salinity site during the first year, although it was similar between the 2 sites in the second year (Weinstein and Walters, 1981). Mortality rates for this species and Atlantic croaker (*Micropogonias undulatus*) were also lower at low-salinity, up-estuary sites than at high-salinity sites near tidal inlets in both the Cape Fear River and Pamlico Sound estuaries of North Carolina (Ross, 2003). Possible explanations given by Weinstein and Walters (1981) and Ross (2003) for this pattern include the following: 1) higher density of predators at high-salinity sites, 2) higher stress on juvenile fish induced by high salinity indirectly increasing mortality, and 3) higher migration rates from saline sites biasing mortality rates upwards in those areas.

[4] Laney, R. W., and B. J. Copeland. 1981. Population dynamics of penaeid shrimp in two North Carolina tidal creeks. Rep. 81-1, 161 p. Carolina Power & Light Co., Raleigh, NC.

Table 4

Daily instantaneous natural mortality estimates (and standard errors) for juvenile white shrimp (*Litopenaeus setiferus*) within intermediate, brackish, and saline zones of Sabine Lake. Mortality rates were estimated with 2 different catch-curve analyses, linear regression and the Chapman-Robson estimator, by using data from trips 4–6 in 2011.

Analysis	Intermediate	Brackish	Saline
Linear regression	0.05 (0.006)	0.08 (0.005)	0.09 (0.007)
Chapman-Robson	0.07 (0.008)	0.09 (0.006)	0.08 (0.006)

Table 5

Absolute growth rate estimates ($G_{absolute}$) and standard errors calculated by following individual cohorts of juvenile white shrimp (*Litopenaeus setiferus*) collected during 3 sampling trips (trips 4–6) in 2011 within intermediate, brackish, and saline zones of Sabine Lake. Growth rates are given in total length in millimeters per day.

Zone	Start	End	$G_{absolute}$
Intermediate	Trip 4	Trip 5	1.22 (0.13)
Brackish	Trip 4	Trip 5	0.77 (0.45)
	Trip 4	Trip 5	0.74 (0.28)
	Trip 5	Trip 6	1.72 (0.50)
	Trip 5	Trip 6	0.72 (0.28)
	mean		0.99 (0.19)
Saline	Trip 2	Trip 3	1.42 (0.07)
	Trip 2	Trip 3	1.83 (0.23)
		Mean	1.62 (0.12)

Although we did not directly address these possible explanations for our results, we know that juvenile white shrimp can survive in a wide range of salinities (Zein-Eldin and Griffith, 1969), and we believe it is unlikely that environmental conditions would be more stressful for juvenile shrimp in a saline zone than in an intermediate zone (Rozas and Minello, 2011). We also tried to minimize any bias due to migration by considering only shrimp ≤60 mm TL in our mortality estimates. White shrimp do not begin to migrate from estuaries into the northern Gulf of Mexico until they reach 60 mm TL (Pullen and Trent, 1969). We, therefore, conclude that increased predation may be responsible for the relatively higher mortality rates we estimated in the saline and brackish zones, compared with the rates in the intermediate zone. We did not quantify the density of all potential predators of juvenile white shrimp in each salinity zone to test this possibility, but previous studies indicate that juvenile penaeid shrimps are more abundant in the diets of fish predators from high-salinity areas of estuaries than in the diets of predators in areas with low salinity (Minello et al., 1989) and in the diets of predators at estuarine sites near the sea than at sites farther up an estuary (Salini et al., 1990). Alternatively, this higher shrimp mortality may have been the result of less access to marsh edge habitat in the brackish and saline zones than in the intermediate zone. In the intermediate zone, marsh edge habitat was flooded for longer periods and, therefore, may have provided more protection from predators than that provided by this type of habitat in the other salinity zones.

Our secondary production estimates for juvenile white shrimp in shallow marsh habitats of Sabine Lake are similar to, and within the range of, production estimates for this species reported elsewhere. Comparisons among published values should be made cautiously, however, because of differences in definitions of the term secondary production and the methods used to estimate it. We know of no other comparisons of white shrimp production among salinity zones, but production (technically *yield*) of white shrimp in aquaculture ponds of different salinities was approximately 3.5 times greater in 4 ponds with high salinity (2 ponds at 15 and 2 ponds at 21) than in 2 low-salinity (7) ponds (Hysmith and Colura, 1976). Our estimate of 382 kg/ha for production during the 84-d sampling period in the saline zone is higher than the estimate of annual production for juvenile white shrimp (109 kg/ha) reported for saline marshes in Galveston Bay (Minello et al., 2008; Table 4). The difference in these 2 estimates of production of juvenile white shrimp is most likely due to the higher densities we documented in our study area than those reported for Galveston Bay. Using shrimp landings data and area of emergent wetlands in the U.S. states bordering the Gulf of Mexico, Engle (2011) estimated mean annual production (technically *yield*) of penaeid shrimps (all species combined) as 241 kg/ha (range: 57–1660 kg/ha).

The intermediate zone contained less valuable habitat than the saline zone on a per-hectare basis during the 84-d sampling period, but the estimated production from the intermediate zone, which occupies a large proportion of coastal marshes within Louisiana, was not trivial (116 kg/ha). Therefore, the production from these low-salinity areas would contribute substantially to the total production of white shrimp in Louisiana estuaries. Multiplying our production estimates in the saline and intermediate zones by the total area of these 2 zones determined for coastal Louisiana in 2013 (Sasser et al.[5]), the total production over the 84-d sampling period from the intermediate zone would equal

[5] Sasser, C. E., J. M. Visser, E. Mouton, J. Linscombe, and S. B. Hartley. 2014. Vegetation types in coastal Louisiana in 2013: U.S. Geological Survey Scientific Investigations Map 3290, 1 sheet, scale 1:550,000. [Available at website.]

Table 6

Estimates of secondary production (with 95% confidence interval and measured as kilograms per hectare), mean biomass (measured as kilograms per hectare), and production-to-biomass ratios for juvenile white shrimp (*Litopenaeus setiferus*) within intermediate, brackish, and saline zones of Sabine Lake. Production (P) and biomass (B) estimates are based on data collected over an 84-d period from July through October 2011 (trips 1–6) and production was estimated by using the size-frequency method (Garman and Waters, 1983).

Salinity zone	Production	Biomass	P:B
Intermediate	115.7 (26.8 to 204.7)	23.3	5.0
Brackish	231.6 (102.4 to 360.8)	35.6	6.5
Saline	382.0 (186.8 to 577.3)	51.7	7.4

44 million kg in comparison with 113 million kg from the saline zone.

Our study was conducted during drought conditions in southwest Louisiana, and the relative habitat value of the 3 salinity zones in our study area may differ during nondrought periods. During years of normal rainfall, the intermediate zone may provide less valuable habitat for white shrimp. For example, the mean density of juvenile white shrimp within the marsh edge habitat of the intermediate zone during September in 2012, a year of normal rainfall, was 80% less than the density we observed there in the same month in 2011 and report here; whereas, shrimp densities in the same habitat type in the brackish and saline zones differed between these 2 years by <20% (senior author, unpubl. data). Juvenile penaeid shrimp abundance and commercial landings may be higher during warm, dry periods with low freshwater inflows to estuaries (Möller et al., 2009; Piazza et al., 2010), although Gunter and Hildebrand (1954), Browder (1985), and Palmer and Montagna (2015) reported examples of a positive relationship between rainfall or freshwater inflow and the abundance or commercial landings of penaeid shrimp. More comparisons of secondary production from other estuaries conducted over several years are needed before definitive conclusions can be drawn about patterns of juvenile white shrimp production among salinity zones.

Inferences from our results are limited to the locations and time period we sampled. Our study was confined to a single year, and sampling sites were replicated in space but drawn from an area limited to 100 ha in each salinity zone. Support for extending the inferences from our study more generally, however, comes from studies of other estuaries that corroborate our results. For example, the spatial distribution and growth rates of juvenile white shrimp among salinity zones that we observed are consistent with the pattern reported from studies of Barataria Bay, Louisiana (Rozas and Minello, 2010, 2011). In a meta-analysis of 5149 samples collected from multiple locations in the northern Gulf of Mexico, mean densities of juvenile white shrimp were highest in mesohaline and polyhaline areas (equivalent to our brackish and saline salinity zones, respectively) (Minello, 1999)—densities that were consistent with our results. Additional comparisons of demographic rates and secondary production from other estuaries of the Gulf of Mexico would allow broader inferences to be drawn in the future.

Our estimates of density, biomass, growth, natural mortality, and secondary production of juvenile white shrimp were generally higher in the saline or brackish zones and lowest in the intermediate zone. To our knowledge, this study is the first attempt to simultaneously estimate and compare population dynamics and secondary production of juvenile penaeid shrimps along an estuarine salinity gradient. Although inference from our work is limited in scope to the 3 locations and the time period we sampled, the saline and brackish zones provided more important nursery habitat for juvenile white shrimp than such habitat in the intermediate zone. The total amount of production from the intermediate zone, however, was not trivial when the area that this zone covers in coastal Louisiana is considered. Nursery habitats that provide a small contribution on a per-area basis, such as the intermediate zone in our study area, may still have a large effect at the population level because the habitat covers a relatively large total area (Dahlgren et al., 2006). Moreover, the relative value of nursery habitats can be dynamic, with variation occurring both spatially (e.g., within as well as among estuaries) and temporally, from year to year (Kraus and Secor, 2005). We documented within-estuary (i.e., among salinity zones) differences in habitat value for white shrimp in Sabine Lake and expect this value, especially in the intermediate zone, to vary interannually. For example, the habitat value of the intermediate zone in our study area likely would be less in a year in which rainfall was greater than or equal to average levels (i.e., in a year of lower salinity) than in the year we documented, 2011, a year of severe drought and relatively high salinity. This dynamic nature of habitat value should be considered when assessing estuarine nursery areas.

Acknowledgments

We thank S. Hillen and J. Salas of the NOAA Southeast Fisheries Science Center's (SEFSC) Galveston Laboratory; L. Broussard, S. Beck, and D. O'Malley of Louisiana State University; A. Cummings of the SEFSC Estuarine Habitats and Coastal Fisheries Center in Lafayette, Louisiana; and J. C. Robichaux and J. Thompson of the University of Louisiana at Lafayette for help collecting and processing samples. We would also like to thank D. Richard at Stream Wetland Services, Lake Charles, Louisiana, for helping to locate sites and for providing lodging, the staff at Murphree

Wildlife Management Area for providing lodging, and the staff of the Texas Point National Wildlife Refuge for access to one of our field sites. We thank P. Caldwell for conducting the GIS analysis needed to weight the length-frequency distributions and for creating Figure 1. A teaching assistantship from the University of Louisiana at Lafayette, the Rockefeller Wildlife Scholarship, the Coastal Conservation Association/Ted Beaulieu Sr. Scholarship, a research grant from the Wetland Foundation, and the SEFSC provided funding for this project. We also thank T. Minello and 3 anonymous reviewers whose comments improved this article.

Literature cited

Anonymous.
1958. Symposium on the classification of brackish waters. Oikos 9:311–312.

Baker, R., and T. J. Minello.
2010. Growth and mortality of juvenile white shrimp *Litopenaeus setiferus* in a marsh pond. Mar. Ecol. Prog. Ser. 413:95–104.

Baker, R., M. Fujiwara, and T. J. Minello.
2014. Juvenile growth and mortality effects on white shrimp *Litopenaeus setiferus* population dynamics in the northern Gulf of Mexico. Fish. Res. 155:74–82.

Baxter, K. N., and W. C. Renfro.
1967. Seasonal occurrence and size distribution of postlarval brown and white shrimp near Galveston, Texas, with notes on species identification. Fish. Bull. 66:149–158.

Beck, M. W., K. L. Heck Jr., K. W. Able, D. L. Childers, D. B. Eggleston, B. M. Gillanders, B. Halpern, C. G. Hays, K. Hoshino, T. J. Minello, et al.
2001. The identification, conservation, and management of estuarine and marine nurseries for fish and invertebrates. BioScience. 51:633–641.

Benke, A. C.
1979. A modification of the Hynes method for estimating secondary production with particular significance for multivoltine populations. Limnol. Oceanogr. 24:168–171.

Boesch, D. F., and R. E. Turner.
1984. Dependence of fishery species on salt marshes: the role of food and refuge. Estuaries 7:460–468.

Browder, J. A.
1985. Relationship between pink shrimp production on the Tortugas Grounds and water flow patterns in the Florida Everglades. Bull. Mar. Sci. 37:839–856.

Burnham, K. P., and D. R. Anderson.
2002. Model selection and multimodel inference: a practical information-theoretic approach, 2nd ed., 488 p. Springer, New York.

Chabreck, R. H.
1970. Marsh zones and vegetation types in the Louisiana coastal marshes. Ph.D. diss., 113 p. Louisiana State Univ., Baton Rouge, LA.
1971. Ponds and lakes of the Louisiana coastal marshes and their value to fish and wildlife. Proc. Annu. Conf. SEAFWA 25:206–215.

Chapman, D. G., and D. S. Robson.
1960. The analysis of a catch curve. Biometrics 16:354–368.

Dahlgren, C. P., G. T. Kellison, A. J. Adams, B. M. Gillanders, M. S. Kendall, C. A. Layman, J. A. Ley, I. Nagelkerken, and J. E. Serafy.
2006. Marine nurseries and effective juvenile habitats: concepts and applications. Mar. Ecol. Prog. Ser. 312:291–295.

Dall, W., B. J. Hill, P. C. Rothlisberg, and D. J. Sharples.
1990. The biology of the Penaeidae. Adv. Mar. Biol. 27:1–484.

Diop, H., W. R. Keithly Jr., R. F. Kazmierczak Jr., and R. F. Shaw.
2007. Predicting the abundance of white shrimp (*Litopenaeus setiferus*) from environmental parameters and previous life stages. Fish. Res. 86:31–41.

Ditty, J. G.
2011. Young of *Litopenaeus setiferus*, *Farfantepenaeus aztecus* and *F. duorarum* (Decapoda: Penaeidae): A reassessment of characters for species discrimination and their variability. J. Crustac. Biol. 31:458–467.

Dolbeth, M., M. Cusson, R. Sousa, and M. A. Pardal.
2012. Secondary production as a tool for better understanding of aquatic ecosystems. Can. J. Fish. Aquat. Sci. 69:1230–1253.

Engle, V. D.
2011. Estimating the provision of ecosystem services by Gulf of Mexico coastal wetlands. Wetlands. 31:179–193.

Garman, G. C., and T. F. Waters.
1983. Use of the size-frequency (Hynes) method to estimate annual production of a stream fish population. Can. J. Fish. Aquat. Sci. 40:2030–2034.

Gunter, G., and H. H. Hildebrand.
1954. The relation of total rainfall of the state and catch of the marine shrimp (*Penaeus setiferus*) in Texas waters. Bull. Mar. Sci. 4:95–103.

Gunter, G., J. Y. Christmas, and R. Killebrew.
1964. Some relations of salinity to population distributions of motile estuarine organisms, with special reference to penaeid shrimp. Ecology (USA) 45:181–185.

Heck, K. L., Jr., G. Hays, and R. J. Orth.
2003. Critical evaluation of the nursery role hypothesis for seagrass meadows. Mar. Ecol. Prog. Ser. 253:123–136.

Howe, J. C., and R. K. Wallace.
2000. Relative abundance of postlarval and juvenile penaeid shrimps in submerged aquatic vegetation and emergent marsh habitats. Gulf Mex. Sci. 18:130–137.

Howe, J. C., R. K. Wallace, and F. Scott Rikard.
1999. Habitat utilization by postlarval and juvenile penaeid shrimps in Mobile Bay, Alabama. Estuaries 22:971–979.

Hysmith, B. T., and R. L. Colura.
1976. Effect of salinity on growth and survival of penaeid shrimp in ponds. J. World Aquat. Soc. 7:289–303.

Kathiresan, K., and B. L. Bingham.
2001. Biology of mangroves and mangrove ecosystems. Adv. Mar. Biol. 40:81–251.

Kneib, R. T.
1997. The role of tidal marshes in the ecology of estuarine nekton. Oceanogr. Mar. Biol. Annu. Rev. 35:163–220.
2003. Bioenergetic and landscape considerations for scaling expectations of nekton production from intertidal marshes. Mar. Ecol. Prog. Ser. 264:279–296.

Kraus, R. T., and D. H. Secor.
2005. Application of the nursery-role hypothesis to an estuarine fish. Mar. Ecol. Prog. Ser. 291:301–305.

Macdonald, P., and J. Du.
2012. Mixdist: finite mixture distribution models. R package vers. 0.5-4. [Available at website, accessed October 2015.]
Mace, M., III, and L. P. Rozas.
2015. Estimating natural mortality rates of juvenile white shrimp *Litopenaeus setiferus*. Estuar. Coasts 38:1580–1592.
Milliken, G. A., and D. E. Johnson.
1992. Analysis of messy data. Vol. 1: designed experiments, 473 p. Chapman and Hall, London.
Minello, T. J.
1999. Nekton densities in shallow estuarine habitats of Texas and Louisiana and the identification of essential fish habitat. Am. Fish. Soc. Symp. 22:43–75.
Minello, T. J., R. J. Zimmerman, and T. E. Czapla.
1989. Habitat-related differences in diets of small fishes in Lavaca Bay, Texas, 1985–1986. NOAA Tech. Memo. SEFC-NMFS-236, 16 p.
Minello, T. J., K. W. Able, M. P. Weinstein, and C. G. Hays.
2003. Salt marshes as nurseries for nekton: testing hypotheses on density, growth and survival through meta-analysis. Mar. Ecol. Prog. Ser. 246:39–59.
Minello, T. J., G. A. Matthews, P. A. Caldwell, and L. P. Rozas.
2008. Population and production estimates for decapod crustaceans in wetlands of Galveston Bay, Texas. Trans. Am. Fish. Soc. 137:129–146.
Minello, T. J., L. P. Rozas, and R. Baker.
2012. Geographic variability in salt marsh flooding patterns may affect nursery value for fishery species. Estuar. Coasts 35:501–514.
Möller, O. O., Jr., J. P. Castello, and A. C. Vaz.
2009. The effect of river discharge and winds on the interannual variability of the pink shrimp *Farfantepenaeus paulensis* production in Patos Lagoon. Estuar. Coasts 32:787–796.
Muncy, R. J.
1984. Species profiles: life histories and environmental requirements of coastal fishes and invertebrates (Gulf of Mexico)—white shrimp. U.S. Fish Wildl. Serv. FWS/OBS-82/11.20. U.S. Army Corps Eng., TR EL-82-4, 19 p.
Nance, J. M., C. W. Caillouet Jr., and R. A. Hart.
2010. Size-composition of annual landings in the white shrimp, *Litopenaeus setiferus*, fishery of the northern Gulf of Mexico, 1960–2006: its trend and relationships with other fishery-dependent variables. Mar. Fish. Rev. 72:1–13.
Nevins, J. A., J. B. Pollack, and G. W. Stunz.
2014. Characterizing nekton use of the largest unfished oyster reef in the United States compared with adjacent estuarine habitats. J. Shellfish Res. 33:227–238.
NMFS (National Marine Fisheries Service).
2010. Marine fisheries habitat assessment improvement plan. Report of the National Marine Fisheries Service Habitat Assessment Improvement Plan Team. NOAA Tech. Memo. NMFS-F/SPO-108, 115 p.
Olejnik, S., and J. Algina.
2003. Generalized eta and omega squared statistics: measures of effect size for some common research designs. Psychol. Methods 8:434–447.
Palmer, T. A., and P. A. Montagna.
2015. Impacts of droughts and low flows on estuarine water quality and benthic fauna. Hydrobiologia 753:111–129.
Piazza, B. P., M. K. La Peyre, and B. D. Keim.
2010. Relating large-scale climate variability to local species abundance: ENSO forcing and shrimp in Breton Sound, Louisiana, USA. Clim. Res. 42:195–207.
Pullen, E. J., and W. L. Trent.
1969. White shrimp emigration in relation to size, sex, temperature and salinity. FAO Fish. Rep. 57:1001–1014.
R Core Team.
2014. R: a language and environment for statistical computing. R Foundation for Statistical Computing, Vienna, Austria. [Available from website, accessed April 2014]
Rakocinski, C. F., D. M. Baltz, and J. W. Fleeger.
1992. Correspondence between environmental gradients and the community structure of marsh-edge fishes in a Louisiana estuary. Mar. Ecol. Prog. Ser. 80:135–148.
Ricker, W. E.
1975. Computation and interpretation of biological statistics of fish populations. Bull. Fish. Res. Board Can. 191, 382 p.
Rose, K. A., H. Huang, D. Justic, and K. de Mutsert.
2014. Simulating fish movement responses to and potential salinity stress from large-scale river diversions. Mar. Coast. Fish. 6:43–61.
Ross, S. W.
2003. The relative value of different estuarine nursery areas in North Carolina for transient juvenile marine fishes. Fish. Bull. 101:384–404.
Rozas, L. P., and T. J. Minello.
2006. Nekton use of *Vallisneria americana* Michx. (Wild celery) beds and adjacent habitats in coastal Louisiana. Estuar. Coasts 29:297–310.
2010. Nekton density patterns in tidal ponds and adjacent wetlands related to pond size and salinity. Estuar. Coasts 33:652–667.
2011. Variation in penaeid shrimp growth rates along an estuarine salinity gradient: implications for managing river diversions. J. Exp. Mar. Biol. Ecol. 397:196–207.
2015. Small-scale nekton density and growth patterns across a saltmarsh landscape in Barataria Bay, Louisiana. Estuar. Coasts 38:2000–2018.
Rozas, L. P., T. J. Minello, and D. D. Dantin.
2012. Use of shallow lagoon habitats by nekton of the northeastern Gulf of Mexico. Estuar. Coasts 35:572–586.
Salini, J. P., S. J. M. Blaber, and D. T. Brewer.
1990. Diets of piscivorous fishes in a tropical Australian estuary, with special reference to predation on penaeid prawns. Mar. Biol. 105:363–374.
Schenker, N., and J. F. Gentleman.
2001. On judging the significance of differences by examining the overlap between confidence intervals. Am. Stat. 55:182–186.
Smith, M. W., A. Y. Then, C. Wor, G. Ralph, K. H. Pollock, and J. M. Hoenig.
2012. Recommendations for catch-curve analysis. North Am. J. Fish. Manage. 32:956–967.
Turner, R. E.
1990. Landscape development and coastal wetland losses in the northern Gulf of Mexico. Am. Zool. 30:89–105.
Van Horne, B.
1983. Density as a misleading indicator of habitat quality. J. Wildl. Manage. 47:893–901.
Vance, D. J., M. D. E. Haywood, D. S. Heales, R. A. Kenyon, and N. R. Loneragan.
1998. Seasonal and annual variation in abundance of

postlarval and juvenile banana prawns *Penaeus merguiensis* and environmental variation in two estuaries in tropical northeastern Australia: a six year study. Mar. Ecol. Prog. Ser. 163:21–36.

Vetter, E. F.
1988. Estimation of natural mortality in fish stocks: a review. Fish. Bull. 86:25–43.

Visser, J. M., C. E. Sasser, R. H. Chabreck, and R. G. Linscombe.
1998. Marsh vegetation types of the Mississippi River Deltaic Plain. Estuaries 21:818–828.

Visser, J. M., C. E. Sasser, R. H. Chabreck, and R. G. Linscombe.
2000. Marsh vegetation types of the Chenier Plain, Louisiana, USA. Estuaries. 23:318–327.

Wagner, C. M., and H. M. Austin.
1999. Correspondence between environmental gradients and summer littoral fish assemblages in low salinity reaches of the Chesapeake Bay, USA. Mar. Ecol. Prog. Ser. 177:197–212.

Weinstein, M. P., and M. P. Walters.
1981. Growth, survival and production in young-of-year populations of *Leiostomus xanthurus* Lacépéde residing in tidal creeks. Estuaries 4:185–197.

Weinstein, M. P., S. L. Weiss, and M. F. Walters.
1980. Multiple determinants of community structure in shallow marsh habitats, Cape Fear River estuary, North Carolina, USA. Mar. Biol. 58:227–243.

Zein-Eldin, Z. P., and G. W. Griffith.
1969. An appraisal of the effects of salinity and temperature on growth and survival of postlarval penaeids. FAO Fish. Rep. 57:1015–1026.

Zimmerman, R. J., T. J. Minello, and G. Zamora Jr.
1984. Selection of vegetated habitat by brown shrimp, *Penaeus aztecus*, in a Galveston Bay salt marsh. Fish. Bull. 82:325–336.

Zimmerman, R. J., T. J. Minello, and L. P. Rozas.
2000. Salt marsh linkages to productivity of penaeid shrimps and blue crabs in the northern Gulf of Mexico. *In* Concepts and controversies in tidal marsh ecology (M. P. Weinstein and D. A. Kreeger, eds.), p. 293–314. Kluwer Academic Publishers, Dordrecht, Netherlands.

National Marine Fisheries Service
NOAA

Fishery Bulletin
established in 1881

Spencer F. Baird
First U.S. Commissioner of Fisheries and founder of *Fishery Bulletin*

Modeling the habitat distribution of spiny dogfish (*Squalus acanthias*), by sex, in coastal waters of the northeastern United States

Andrea Dell'Apa (contact author)[1]
Maria Grazia Pennino[2]
Christopher Bonzek[3]

Email address for contact author: dellapa.andrea@gmail.com

[1] Earth Resources Technology Inc.
1315 East-West Highway
Silver Spring, Maryland 20910

[2] Universidade Federal do Rio Grande do Norte (UFRN)
Department of Ecology
Campus Universitário s/n, Lagoa Nova
CEP 59.098-970 Natal (RN), Brazil

[3] Virginia Institute of Marine Science
College of William and Mary
P.O. Box 1346
Gloucester Point, Virginia 23062-1346

Abstract—A hierarchical Bayesian approach was used to model the spatiotemporal habitat distribution of spiny dogfish (*Squalus acanthias*) of both sexes (adults) caught during trawl surveys conducted by the Northeast Area Monitoring and Assessment Program in inshore coastal waters between New England and North Carolina during 2007–2013. The best model for predicting catch per unit of effort (CPUE) for this species includes the following relevant variables: bathymetry, sea surface temperature, salinity, chlorophyll-*a* (chl-*a*) concentration, season and time of survey, and a random spatial effect for both sexes. Predicted CPUE was related to depth for both sexes; females occurred in shallower waters than those in which males occurred. Also, more females than males were predicted to occur in warmer, less saline and more productive (higher chl-*a* concentration) waters. Seasonality and time of predicted CPUE indicated that the abundance of females was higher in inshore coastal waters in the spring and in the morning, and the abundance of males was greater in the afternoon and in the fall in the same area. Collectively, these results provide information that enhances our understanding of differences in habitat selection and spatiotemporal distribution of the 2 sexes of this species—information that can help to modify present management strategies for the U.S. Atlantic fishery.

Manuscript submitted 15 April 2016.
Manuscript accepted 17 November 2016.
Fish. Bull. 115:89–100 (2017).
Online publication date: 6 December 2016.
doi:10.7755/FB.115.1.8

The views and opinions expressed or implied in this article are those of the author (or authors) and do not necessarily reflect the position of the National Marine Fisheries Service, NOAA.

The spiny dogfish (*Squalus acanthias*) is a small shark commonly found in oceanic and coastal temperate waters throughout the world, at depths less than 900 m (Compagno et al., 2005; Dell'Apa et al., 2015). The species is sexually dimorphic; adult females, on average, are larger than adult males (Nammack et al., 1985). Moreover, aggregations of adult individuals are segregated by sex and size (Ford, 1921; Shepherd et al., 2002; Dell'Apa et al., 2014)—a common occurrence with elasmobranchs (Springer, 1967; Sims, 2005). Sexual segregation can be the effect of social segregation, in which the interaction between the sexes is limited by behavioral differences between the sexes, or it can be the effect of habitat segregation, in which the 2 sexes use habitats with different physical and environmental characteristics. Social segregation and habitat segregation can also occur simultaneously for the two sexes and can lead to differences in spatial distribution and habitat associations between the sexes (Wearmouth and Sims, 2008). Additionally, sexual dimorphism may influence feeding habits in live-bearing elasmobranchs (Sims, 2005), resulting in the 2 sexes having evolved specific physiological requirements that have led to differences in diet and prey preferences (Ruckstuhl and Clutton-Brock, 2005). Consequently, the 2 sexes may occupy different habitats characterized by different prey compositions and thus reduce intraspecific competition (Sims, 2005).

For commercially important species, such as the spiny dogfish (Lack, 2006; Dell'Apa et al., 2013), predicting abundance and identifying habitat associations in response to environmental and spatiotemporal factors can be a valuable approach to the development of sustainable fishery strategies (Perry and Smith, 1994; Pittman et al., 2011; Espinoza et al., 2014). For assessments of many elasmobranchs, understanding habitat associations is complex and

confounded by sexual segregation that can lead to spatial or temporal segregation (Conradt, 2005).

On the northwest Atlantic continental shelf, habitat use and seasonal movements of spiny dogfish have been reported to differ by sex—the key driver being seasonal changes in temperatures (Shepherd et al., 2002; Methratta and Link, 2007; Sagarese et al., 2014a, 2014b). Additionally, it has been suggested that the movement of species is influenced by the distribution of their prey (Overholtz and Tyler, 1985; Sagarese et al., 2014b). In this region, aggregations of mature females are commonly found inshore, in shallower and warmer waters, and aggregations of mature males dominate offshore, deeper and colder waters (Shepherd et al., 2002; Sagarese et al., 2014a). Collectively, the spiny dogfish is characterized by north–south seasonal migrations: fish overwinter off North Carolina and migrate northward during the spring to waters in New England and Gulf of Maine, where they remain between summer and late fall before their southward migration (Rulifson, 2010).

A regional study in which fishery-dependent data were used and that was conducted in inshore coastal waters inside and off the peninsula of Cape Cod, Massachusetts (Dell'Apa et al., 2014), elucidated the local habitat association of spiny dogfish, by sex, and provided information on the potential drivers of sexual segregation in this species. The results of that study indicated that the distribution of the 2 sexes differed by location, season, and time. The highest occurrence of adult males was found early in the day and between spring and early autumn in inshore waters off the eastern side of the sampling area in relatively close proximity to deep water (>100 m), and highest occurrence of adult females was found inshore, in waters (depths <78 m) shallower than the waters in which adult males occurred, and farther inside the Cape Cod peninsula than the other locations surveyed (Dell'Apa et al., 2014). Dell'Apa et al. (2014) suggested that adult females may actively seek shallow waters as a strategy to elude adult males and energy-demanding copulation—a tactic that results in spatial segregation. Alternatively, in deeper coastal areas, where males are usually more abundant, adult females may synchronize their different habitat-selection behavior with that of adult males, resulting in temporal segregation (Dell'Apa et al., 2014).

Overall, the results of that study indicate that sexual segregation in spiny dogfish, in the Cape Cod area, occurs both spatially and temporally and is strongly influenced by depth. Different behavioral choices by each of the sexes are reflected in their preferred habitat associations and indicate that depth and time, but likely not temperature, are potential key drivers for sexual segregation in spiny dogfish (Dell'Apa et al., 2014). However, that study was based on limited data collected through fishery-dependent surveys in a regionally restricted inshore coastal area, and the findings may not be representative of the entire U.S. Atlantic stock of spiny dogfish. Therefore, for fishery management purposes it would be useful to analyze existing data sets from a larger coastal area, one that encompasses the entire range of the current commercial fishery between New England and North Carolina.

In addition, it would be beneficial to analyze comparable regional data from fishery-independent inshore surveys. In this regard, the nearshore trawl surveys conducted by the Northeast Area Monitoring and Assessment Program (NEAMAP) in the mid-Atlantic represent the most suitable data source that is available for completing a more extensive study on the influence of environmental habitat characteristics, season, and time of day on the distribution of spiny dogfish in inshore coastal waters of the northeastern United States.

The aim of this study was to use the NEAMAP survey data to model the abundance of spiny dogfish, by sex, in inshore coastal waters of the U.S. Atlantic, by considering oceanographic (i.e., sea-surface temperature [SST], salinity, and chlorophyll-a [chl-*a*] concentration), topographic (i.e., depth, slope, and distance to land), and temporal (i.e., season and time of day) characteristics as predictive variables for catch per unit of effort (CPUE). This study involved the use of hierarchical Bayesian spatiotemporal models and is the first one to use a large fishery-independent database as a source of data for analysis and prediction of the habitat distribution of spiny dogfish along the northwest Atlantic inshore coastal area, by sex and by time of day. The results of this study provide information on the spatial and temporal distribution of adult spiny dogfish that will be valuable for fishery managers because it will enable the adoption of enhanced management strategies for the fishery for spiny dogfish in the U.S. Atlantic that are based on the sexual segregation exhibited by this species.

Materials and methods

Mid-Atlantic surveys

NEAMAP surveys are conducted in the coastal waters bounded by the western edge of Cape Cod, Massachusetts, and by Cape Hatteras, North Carolina. From Montauk, New York, and southward, sampling is confined within the 18.3-m depth contour. In the deeper nearshore waters off southern New England, the deepest stations extend to about 36.6 m (Fig. 1). NEAMAP conducts 2 cruises per year, one each in spring (April–May) and fall (September–October), timed to roughly coincide with offshore surveys carried out by the NOAA Northeast Fisheries Science Center (NEFSC). Each NEAMAP cruise samples 150 stations distributed among 17 regions and 2 depth strata. To allow comparisons with current NEFSC surveys, NEAMAP adopted the bottom trawl design developed for the NEFSC by the Northeast Trawl Survey Advisory Panel, joint board of the Mid-Atlantic and New England Fishery Management Councils. The NEAMAP conducts surveys by fishing with a 3-bridle, 4-seam bottom trawl with a net of 400 meshes (of 12 cm width) for a total length of 48

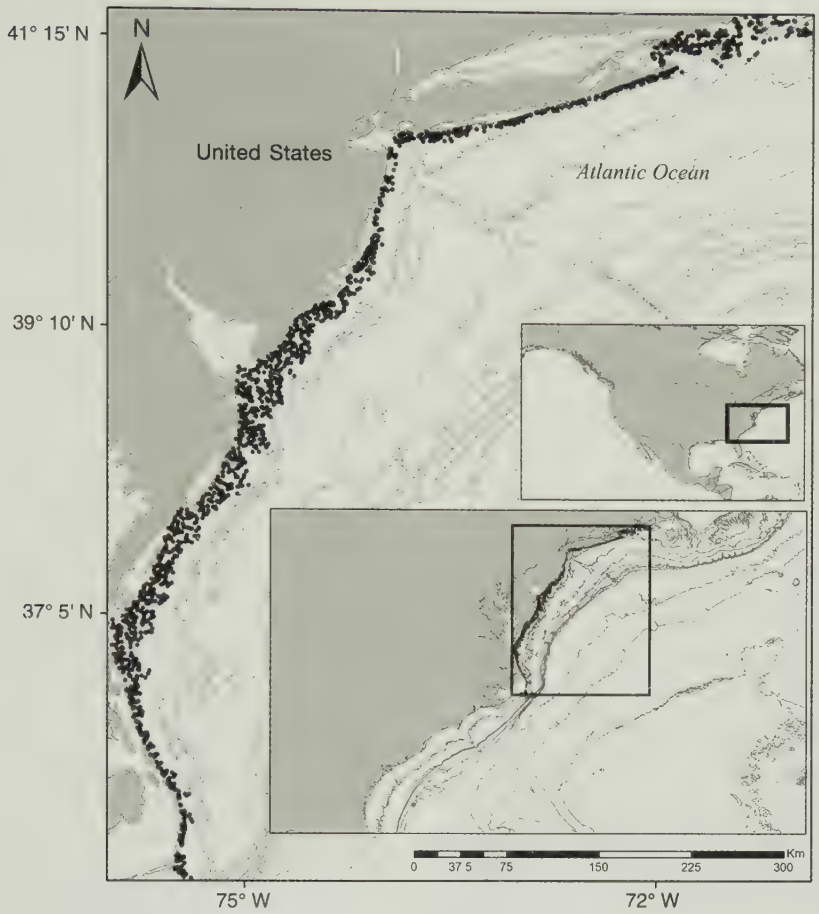

Figure 1

Map of the study area. Black circles represent the locations of 1820 trawl hauls conducted in inshore coastal waters of the mid-Atlantic during surveys by the Northeast Area Monitoring and Assessment Program. Data from these surveys were used to determine the distribution of spiny dogfish (*Squalus acanthias*) between New England and North Carolina in 2007–2013.

m, a 7.6-cm cookie sweep, and a 2.5-cm knotless liner in the codend. The doors are 1.7-m Thyboron Type IV.

Data collection, sources, and analysis

Fishery-independent data on spiny dogfish were collected during the NEAMAP surveys in spring and fall of 2007–2013 on the F/V *Darana R.* As described by Bonzek et al.[1], for each haul, up to approximately 18 spiny dogfish were examined to determine individual length (precaudal length [PCL] in centimeters), weight, sex, and maturity (males only, by external examination of the claspers). All other specimens were weighed in total and measured individually. In rare cases of very large catches, those individuals not processed as described were counted (or weighed) in full without further processing, before being released. When subsampling occurred, the attributes of the subsampled portion (e.g., sex ratios and lengths) were expanded to the total catch (Bonzek et al.[1]). Additionally, for each haul, the date, starting and ending times, and location (latitude and longitude) were recorded.

For the purpose of our analysis, the CPUE for spiny dogfish, by sex, for each trawl haul was calculated as the total number of individuals of each sex for each 20 min of trawling. The length of individuals was converted from PCL to total length (TL) in centimeters by using the conversion factor (*TL=PCL*/0.807) available for this species in FishBase (website). The analysis for this study included only adult females (>80 cm TL) and adult males (>60 cm TL), on the basis of the size at maturity reported for this species in the northwest Atlantic (Nammack et al., 1985). It is worth noting that at the time of the study by Nammack et al.'s (1985),

[1] Bonzek, C. F., J. Gartland, R. A. Johnson, and J. D. Lange Jr. 2008. NEAMAP Near Shore Trawl Survey: peer review documentation. A report to the Atlantic States Marine Fisheries Commission by the Virginia Institute of Marine Science (VIMS), Gloucester Point, VA. [Available from VIMS, P.O. Box 1346, Gloucester Point, VA 23062-1346].

the stock of spiny dogfish was not subjected to the intense exploitation by the domestic commercial fishery that began in the early 1990s. This exploitation caused this stock to be declared overfished in 1998 and resulted in the development of a fishery management plan in 1999 for this species in federal waters (5–322 km offshore) by the New England and Mid-Atlantic Fishery Management Councils (MAFMC[2]). The federal plan was further reinforced by an interstate fishery management plan for state waters (0–5 km offshore) developed by the Atlantic States Marine Fisheries Commission in 2002 (ASMFC[3]; Dell'Apa et al., 2015).

Additionally, the commercial fishery has preferentially targeted adult females because of their larger size. This fishing strategy has resulted in a recent increase in the adult male:female sex ratio in the catch of this species and in a decrease in the average size at maturity for adult females in the U.S. Atlantic stock from the sizes reported by Nammack et al. (1985) (Sosebee, 2005; Rago and Sosebee[4])—a drop from 80 cm TL to about 74.5 cm TL, according to Bubley et al. (2013). Overall, this decline indicates that the actual size at maturity of adult females from the NEAMAP surveys during 2007–2013 was likely to have been smaller than the 80 cm TL used in our analysis. However, because no interannual variability in the predicted CPUE of adult females was found by using the 80-cm-TL size at maturity criterion and because of the inherent difficulties in choosing an alternative size criterion as a result of consistent fluctuation in the annual average size at maturity reported for adult females (Marques da Silva and Ross[5]), we opted to adopt a more conservative approach by using the most commonly accepted size at maturity reported by Nammack et al. (1985).

For statistical purposes, the time of each set was classified into 3 categories: morning (between 6:00 AM and 12:59 PM), afternoon (between 1:00 PM and 6:59 PM), and night (between 7:00 PM and 5:59 AM), according to the time partitioning used by Dell'Apa et al. (2014).

Six environmental variables were included in the analysis: bathymetry (mean depth of each haul in feet and converted to meters for analysis), distance to shore (measured in meters), slope of the seabed (percent grade), monthly mean SST (measured in degrees Celsius), monthly mean chl-*a* concentration (measured in milligrams per cubic meter), and monthly mean values of practical salinity.

Data for 3 variables—SST, chl-*a* concentration, and salinity—were extracted from the NASA Earth Observations website (website) as long-term monthly mean climate data. Bathymetry was derived from the same NASA Earth Observations website by using the General Bathymetric Chart of the Oceans (GEBCO) grid (website). In addition, data for bathymetry were collected at each haul location. These data were used to correct and check the information on final mean depth. When a discrepancy occurred between the GEBCO and survey data, a mean of the values in the 2 data sets was used.

Distances to the coast and slope gradients were derived from the bathymetry map created with the GEBCO grid, by using the Near (World Equidistant Cylindrical coordinate system) and Slope Spatial Analyst tools in ArcGis 9.2[6] (Esri, Redlands, CA).

All the covariates were aggregated at a resolution of 0.25°×0.25° and were transformed into raster layers with the raster package (Hijmans, 2013) in R, vers. 3.1.2 (R Core Team, 2014). To check collinearity between explanatory environmental variables, a draftsman's plot and the Pearson's correlation index were used. Because variables were not correlated highly with coefficients of correlation (r) <0.5, they were considered in further analyses.

Modeling species abundance

For the purpose of our analysis and modeling, we used the spatial distribution approach, which combines observations of species occurrence or abundance with environmental estimates to predict spiny dogfish distribution at locations that were not sampled (Austin, 2007; Elith and Leathwick, 2009). Different approaches and methods can be used to model the spatial distribution of a species. However, most of the common applications do not always provide accurate results when run with traditional prediction methods (i.e., frequentist inference), often because of a large amount of spatiotemporal variability in the data that characterizes dynamic marine ecosystems (Roos et al., 2015). To account for this variability, we used hierarchical Bayesian spatiotemporal models in our study.

Bayesian approaches have several advantages over traditional methods and have been applied successfully to fisheries studies (Colloca et al., 2009; Muñoz et al., 2013; Pennino et al., 2014). Bayesian methods allow the inclusion of both the observed data and model parameters as random variables (Banerjee et al., 2004) and provide more realistic and accurate estimations of uncertainty (Pennino et al., 2014). Additionally, they allow the use of spatial and temporal components as a

[2] MAFMC (Mid-Atlantic Fishery Management Council). 1999. Spiny dogfish fishery management plan, 292 p. Mid-Atlantic Fishery Management Council, Dover, DE. [Available from website.]

[3] ASMFC (Atlantic States Marine Fisheries Commission). 2002. Interstate fishery management plan for spiny dogfish. ASMFC, Fish. Manage. Rep. 40, 98 p. [Available from website.]

[4] Rago, P., and K. Sosebee. 2012. Update on the status of spiny dogfish in 2012 and initial evaluation of harvest at the Fmsy proxy, 43 p. Science and Statistical Committee, Mid-Atlantic Fishery Management Council, Dover, DE.

[5] Marques da Silva, H., and M. R. Ross. 1993. Reproductive strategies of spiny dogfish, *Squalus acanthias*, in the NW Atlantic. ICES Council Meeting (C.M.) Documents 1993/G:51,18 p. [Available from website.]

[6] Mention of trade names or commercial companies is for identification purposes only and does not imply endorsement by the National Marine Fisheries Service, NOAA.

Table 1

Summary of variables as potential fixed effects that influence the distribution of spiny dogfish (*Squalus acanthias*) in the mid-Atlantic and included in Bayesian models. SST=sea-surface temperature; chl-*a*=chlorophyll-*a* concentration; practical salinity is a ratio and does not have physical units.

Variable	Description	Units
Bathymetry	Mean fishing depth of haul	m
Slope	Seabed slope at the sampling station	% grade
Distance to shore	Distance from the coast at the sampling station	m
SST	SST monthly value of haul	°C
Chl-*a*	Chl-*a* monthly value of haul	mg/m^3
Salinity	Salinity of the water	–
Season	Season when haul was sampled	Spring, fall
Time	Time when haul was sampled	Morning, afternoon, night

random-effect term, reducing their influence on the estimation of the habitat variables (Gelfand et al., 2006).

Hierarchical Bayesian spatiotemporal models were used to predict abundance of spiny dogfish, by sex, with respect to explanatory variables, as well as to describe the main spatial distribution changes over time, by sex. These models are extremely applicable to studies characterized by data observed at continuous locations within a defined spatial area, as was the case for the data set used in this study. Values of CPUE from the NEAMAP surveys were considered appropriate proxies for levels of abundance of spiny dogfish.

The spatial variation of the CPUE values for spiny dogfish, by sex, was modeled by using a hierarchical Bayesian spatiotemporal approach, specifically a Poisson point process model with log-linear intensity. It was assumed that the number of spiny dogfish at each station sampled, Y_i, has a Poisson distribution with rate $t_i \lambda_i$, where t_i is the observation time at site i and λ_i is proportional to relative species abundance at station i and measures the survey expectation for a unit observation time, according to this general formulation:

$$\log(\lambda_i)i = \alpha + X_{ij}\beta + Y_j + W_i,$$

where α = the intercept;
X_{ij} = the matrix of covariates at the year j and the station I;
β = the vector of the regression coefficients;
Y_j = the component of the temporal unstructured random effect at the year j; and
W_i = the spatially structured random effect at the station i.

In this model, independence between the sampling locations is assumed. However, some spatial autocorrelation may be present in the data set because the abundance of a species at nearby stations is influenced by similar environmental parameters. Consequently, adjacent, or nearby, stations would be expected to be similar in terms of abundance of spiny dogfish. The W_i accounts for this influence. For each of the models for both sexes, 8 potential fixed-effects were considered: 6 environmental variables and 2 temporal variables (Table 1).

For all the parameters considered in the fixed-effects model, a vague zero-mean Gaussian prior distribution with a variance of 100 was assigned, and a zero-mean Gaussian prior distribution with a Matern covariance structure was assumed for the spatial effect (for more details about the spatial component, see Muñoz et al., 2013). Finally, for the temporal effect, a LogGamma prior distribution with the parameters of shape and scale equal to 1 and 5×10^5, respectively, was assumed for the log-precision parameter λ_j, and j represented the year.

For each parameter, a posterior distribution was obtained. Unlike the mean and confidence interval produced by classical analyses, this type of distribution enables explicit probability statements about the parameter. Therefore, the region bounded by the 0.025 and 0.975 quantiles of the posterior distribution results in an intuitive interpretation: for a specific model, the unknown parameter is 95% likely to fall within this range of values (95% credibility interval [CrI]).

All models obtained by combining environmental, spatial, and temporal variables and the possible interactions were fitted and compared by using the measures of the deviance information criterion (DIC) (Spiegelhalter et al., 2002) and the cross-validated logarithmic score (LCPO) (Roos and Held, 2011). Specifically, smaller DIC and LCPO values indicate better fit and predictive quality.

All the analyses were performed with the integrated nested laplace approximation (INLA) method that is implemented in Rue et al., 2009; Martins et al., 2013 and with the R-INLA package (website) in R software.

Model validation

Two approaches were used to assess the predictive accuracy of the selected model. First, the predicted and observed values from the full data set were compared.

Table 2

Summary of the posterior distributions of the fixed effects for the best model of distribution of spiny dogfish (*Squalus acanthias*), by sex. This summary contains the mean, standard deviation (SD), median ($Q_{0.5}$), and 95% credible interval ($Q_{0.025}$ to $Q_{0.975}$), the latter of which is a central interval containing the 95% of the probability under the posterior distribution. SST=sea-surface temperature; chl-*a*=chlorophyll-*a* concentration.

Sex	Predictors of distribution	Mean	SD	$Q_{0.025}$	$Q_{0.5}$	$Q_{0.975}$
Females	Intercept	0.55	0.94	0.03	0.62	1.22
	Bathymetry	−1.14	0.05	−2.52	−1.05	−0.22
	SST	0.35	0.03	0.08	0.30	1.98
	Chl-*a*	0.25	0.02	0.04	0.19	1.05
	Salinity	−0.94	0.04	−1.65	−0.92	−0.11
	Season (spring)	1.45	0.05	0.34	1.35	2.06
	Time (night)	−0.65	0.03	−1.24	−0.57	−0.12
	Time (morning)	0.88	0.03	0.32	0.67	1.43
Males	Intercept	0.88	0.12	0.24	0.86	1.87
	Bathymetry	1.85	0.05	1.44	1.83	2.36
	SST	−1.02	0.08	−2.33	−0.98	−1.51
	Chl-*a*	−0.15	0.01	−1.56	−0.18	−0.02
	Salinity	0.65	0.03	0.23	0.59	1.43
	Season (spring)	−0.37	0.02	−2.24	−0.32	−0.02
	Time (morning)	−0.43	0.06	−1.52	−0.35	−0.04
	Time (night)	−0.25	0.01	−1.09	−0.23	−0.02

Second, a 50-fold cross-validation based on a random half of the data set was performed to build the model, and the remaining data were used to test the prediction (Fielding and Bell, 1997).

For both of these approaches, 3 statistics were calculated: Pearson's *r*, root mean square error (RMSE), and the average error (avg. error). Pearson's *r* measures the linear dependence between predicted and observed values. It can vary from −1 to 1, with 1 representing a perfect positive correlation between the 2 data sets. The RMSE represents the standard error of the differences between predicted values and observed values, and the avg. error represents the mean error between observed and predicted values. The closer these 2 statistics are to zero, the better the prediction (Potts and Elith, 2006).

Results

Initial results

During 1820 trawl hauls, 2372 adult spiny dogfish were caught, of which 2252 were females and 120 males. Seasonally, 2085 females were caught in spring and 167 females were captured in fall, and 64 and 56 males were caught in spring and in fall, respectively.

The final model with the best fit (based on the lowest DIC and LCPO) for CPUE for each sex includes as relevant covariates bathymetry, SST, salinity, chl-*a* concentration, season and time of the survey, and the random spatial effect for both sexes (Table 2). Slope of the seabed and distance from the coast were not relevant variables for the model of CPUE of spiny dogfish for both sexes. No relevant interannual differences were found in CPUE variability for both the females and males in the sampling area because all models with the yearly temporal effect resulted in higher DIC than those DIC from models without it.

Females

Results for adult females indicated that CPUE had a negative relationship with bathymetry (posterior mean: −1.14; CrI: −2.52 to −0.22), and salinity (posterior mean: −0.94; CrI: −1.65 to −0.11); therefore, higher values for CPUE of females were predicted to be found in shallow, less saline waters compared with CPUE levels predicted for other depths and more saline waters. Conversely, values of SST (posterior mean: 0.35; CrI: 0.08 to 1.98) and chl-*a* concentration (posterior mean: 0.25; CrI: 0.04 to 1.05) indicated a positive relationship with the expected CPUE, indicating that higher CPUE should be expected in warmer waters with higher primary productivity (i.e., higher concentrations of chl-*a*).

Additionally, there was a seasonal effect for the estimated probability of CPUE of adult females; the highest estimated value occurred in spring (posterior mean: 1.45; CrI: 0.34 to 2.06) compared with the reference level (fall season).

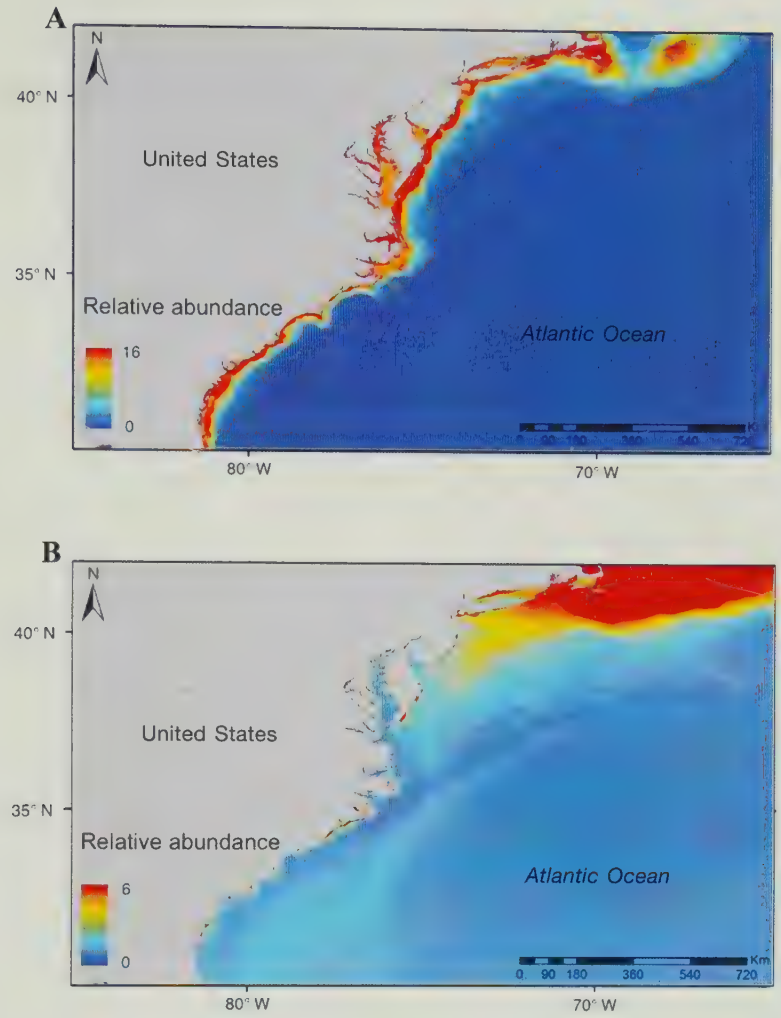

Figure 2

Map of the median of the posterior estimates of the probability of the catch per unit of effort of the mature (**A**) female and (**B**) male spiny dogfish (*Squalus acanthias*) caught during fishery-independent surveys conducted between New England and North Carolina in 2007–2013. Values of CPUE, which ranged from 16 to 0 for females and from 6 to 0 for males, were used as a proxy for relative abundance.

Morning was the period of the day during a survey with the highest estimated probability of CPUE of adult females (posterior mean: 0.88; CrI: 0.32 to 1.43) with respect to the reference level (afternoon). Conversely, hauls conducted at night had the lowest estimated CPUE (posterior mean: −0.65; CrI: −1.24 to −0.12).

Finally, higher estimated values of CPUE for adult females were found for waters off the southern area of the Cape Cod peninsula and off Georges Bank than for CPUE estimates for other areas sampled (Fig. 2A).

Males

For adult males, a positive relationship between bathymetry and CPUE (posterior mean: 1.85; CrI: 1.44 to 2.36) was observed, as well as for salinity and CPUE (posterior mean: 0.65; CrI: 0.23 to 1.43). Predicted values from the model indicated a negative relationship for adult males between expected CPUE and SST (posterior mean: −1.02; CrI: −2.33 to −1.51) and between expected CPUE and chl-*a* concentration (posterior mean: −0.15; CrI: −1.56 to −0.02). We interpret this result as indicating a higher probability of catching adult males as depth and salinity increase and water temperature and chl-*a* concentration decrease.

The estimated probability of CPUE for adult males indicated a seasonal effect, with lower values in spring (posterior mean: −0.37; CrI: −2.24 to −0.02) than in fall, the season of the reference level.

Surveys conducted in the morning had the lowest estimated CPUE of adult males (posterior mean: −0.43;

CrI: −1.52 to −0.04) compared with surveys conducted in the afternoon (the reference level), which was the period of time with the highest CPUE. Night-time surveys also had lower values of CPUE (posterior mean = −0.25; CrI: −1.09 to −0.02) compared with the values from afternoon surveys.

Higher estimated values of CPUE for adult males occurred at higher latitudes, above 40°N, and off Georges Bank, than estimated values of CPUE from other sampled areas (Fig. 2B).

Model performance

For model validation, reasonably high values for Pearson's *r* were obtained for both sexes. In particular, from the model for adult females, an *r* value of ~0.65 was obtained in the cross-validation with the original data set, and an *r* value of ~0.71 was obtained in the cross-validation with half of the data set. For adult males, the *r* value was ~0.68 in the cross-validation with the original data set and was ~0.74 in the cross-validation with half of the data set.

Low values of RMSE and avg. error were achieved for adult females, with an RMSE of 0.98 and an avg. error of 0.045 in the cross-validation with the original data set and with an RMSE of 1.14 and an avg. error of −0.023 in the cross-validation with half of the data set (Table 3). For adult males, low values were also observed, with an RMSE of 1.15 and an avg. error of 0.032 in cross-validation with the original data set and an RMSE of 1.11 and an avg. error of −0.018 in the cross-validation with half of the data set (Table 3). These validation results indicate a good performance of the 2 models.

Table 3

Statistics used in the hierarchical Bayesian spatiotemporal model to estimate abundance of spiny dogfish (*Squalus acanthias*), by sex. The statistics include root mean square error (RMSE) with the original data set, average error (avg. error) with the original data set, root mean square error (RMSE-cross) with half of the data set, and average error (avg. error-cross) with half of the data set.

Sex	RMSE	avg. error	RMSE-cross	avg. error-cross
Females	0.98	0.045	1.14	−0.023
Males	1.15	0.032	1.11	−0.018

Discussion

This study provides predictive information on the habitat distribution of spiny dogfish in U.S. Atlantic coastal waters, by modeling the CPUE in the NEAMAP survey as a proxy for the abundance of this species. The results of this study offer insight into the key environmental and temporal variables that influence the habitat selection for each of the sexes of this species. For our modeling approach, we assumed CPUE is a proxy for species abundance and that CPUE should be the same for both female and male spiny dogfish, although CPUE is not always a viable proxy for species abundance and is not always the same for each sex because of inherent variability in the catchability coefficient (see Hilborn and Walters, 1992; Walters, 2003; Maunder and Punt, 2004; Maunder et al., 2006). However, the lack of linearity between CPUE and fish abundance is largely reduced when data from standardized fishery-independent surveys are used (Maunder and Punt, 2004), as was done in our study.

Another confounding issue in our analysis was that in the NEAMAP survey, female spiny dogfish markedly outnumbered males, by a ratio of 20:1. Ideally, the analysis of data from a simultaneous offshore survey would have been more suitable for determining whether patterns inshore and offshore are the same, but such data were not available. This lack of information points to a need for concurrent offshore sampling to support the extrapolation of our conclusions to the offshore component of and for the generalization of our predictions for the entire U.S. Atlantic stock of spiny dogfish.

Our results related to sex-based segregation and distribution are in line with those reported in other studies. As expected, a higher number of adult females were caught in shallower, inshore, and warmer waters in comparison with adult males, which are more commonly reported in deeper, offshore, and colder waters (Shepherd et al., 2002; Methratta and Link, 2007; Sagarese et al., 2014a).

On the basis of the results of the hierarchical Bayesian spatiotemporal model, abundance of adult female spiny dogfish is predicted to decrease with depth, but abundance of adult males is predicted to increase with depth. In addition, CPUE of adult females is predicted to be higher in warmer, less saline waters and in waters with higher concentrations of chl-*a*, but CPUE of adult males is predicted to be higher in colder, more saline waters, and in waters with lower concentrations of chl-*a*. Nevertheless, adult females occasionally move to deeper waters, mainly in the spring. More studies are needed to understand the drivers for these movements into deeper waters. However, considering that parturition in spiny dogfish is likely to occur in offshore, deeper areas off the edge of the continental shelf and in deep basins (Jensen, 1966; Nammack et al., 1985; Hanchet, 1988; Campana et al., 2009) and that the time of parturition is commonly reported to be between November and January in the northwest Atlantic population (Nammack et al., 1985), despite the observation in a recent study of neonate in more inshore waters off Rhode Island in February (Sulikowski et al., 2013), it is likely that these offshore movements of adult females in the spring are not related to parturition events but might be the result of a strategy to avoid males and

energy-demanding copulation (Pratt and Carrier, 2001; Sims et al., 2001; Dell'Apa et al., 2014, 2015). More studies are needed to test this hypothesis.

That the CPUE predicted in our analysis for adult females was higher in warmer waters than in less warm waters is in accordance with results of Sagarese et al. (2014a), a study in which adult females in the northeastern U.S. continental shelf large marine ecosystem were observed to occupy significantly warmer waters than those occupied by adult males. In regard to adult male abundance, the results of the Bayesian model obtained from our study are also in agreement with results from Sagarese et al. (2014a): results from both studies indicate a higher occurrence of adult males than adult females in deeper, colder waters. In spiny dogfish, gestation lasts for almost 2 years, and it has been hypothesized that this species may have an evolutionary advantage in that adult, pregnant females actively seek inshore, warmer waters because such habitats can maximize the growth rates of embryos (Sagarese et al., 2014a).

Salinity was found to be a relevant environmental variable for predicting the habitat distribution of spiny dogfish for both sexes—a finding that is in agreement with Shepard et al. (2002) and Sagarese et al. (2014a), but we interpret this result and the results of other studies as a possible artifact of the association of salinity with other key environmental habitat characteristics, such as depth and temperature, that better define habitat selection of spiny dogfish. Generally, inshore waters are less saline than offshore environments because of the increased contribution of freshwater runoff.

On the basis of the Bayesian model, we predict that abundance of adult females should be higher in the spring than in the fall and higher in the morning than in the afternoon and night. Conversely, abundance of adult males is predicted to be higher in the fall than in the spring, as well as higher in the afternoon than at other times of day. For adult females, this predicted seasonal pattern of abundance is in agreement with results from the NEFSC survey, which is conducted farther offshore than the NEAMAP survey (Sagarese et al., 2014b). This pattern also indicates that the habitat distribution of adult females in the spring is mainly driven by environmental factors (i.e., temperature and depth) and that habitat distribution in the fall is mainly influenced by ecological factors (i.e., prey abundance) (Sagarese et al., 2014a, 2014b).

For adult males, the results of this study contrast with those reported by Sagarese et al. (2014b), in that we predicted a greater abundance of males in the fall than in the spring. We acknowledge that our analysis is based on fewer males than females, but we are confident that the level of uncertainty that may result from this limited number is included within the parameters analyzed by a Bayesian approach. In combination, however, our results and those of Sagarese et al. (2014b), for inshore and offshore waters, respectively, indicate that abundance of adult males should be higher in the fall than in the spring in inshore coastal waters, although a greater chance for catching larger aggregations of adult males may occur in offshore, deeper waters in the spring. More studies are needed to support this hypothesis and to analyze specific seasonal differences in habitat distribution and abundance of spiny dogfish, by sex, throughout its range. Unfortunately, it was not possible to run the hierarchical Bayesian spatiotemporal model and develop probability distribution maps for each sex, by season, as with the maps obtained for CPUE for each sex, because of the consistent presence in the survey of locations that were sampled multiple times.

This study is the first one to provide a predictive model for the spatial distribution of each sex of spiny dogfish on the basis of time of day, which previously has been suggested to be an important aspect associated with the sexual segregation of this species (Dell'Apa et al., 2014). Such information could be used to enhance fishery sustainability by developing fishery strategies based on the distribution and habitat association of each of the sexes. For example, targeting adult females inshore, in shallower waters, would result in greater pressure on the entire U.S. Atlantic stock of spiny dogfish. Fishery sustainability is measured in terms of fishing mortality and spawning stock biomass, and adult female biomass is used as a biological reference point. Although the spiny dogfish is not currently considered overfished and overfishing is not occurring, low numbers of adult females are expected to be recruiting to the stock over the next few years (Rago and Sosebee[4]; Dell'Apa et al., 2015).

Considering the concentration of chl-*a* as a valid proxy for primary production (de Leiva Moreno et al., 2000), adult females were predicted to associate with habitats characterized by higher productivity, but adult males were predicted to occur in less productive waters. As with our analysis of results for salinity, we interpreted this result for chl-*a* concentration as the direct association of primary productivity with the preferred habitat for females rather than as a driver per se. Because adult females are found most commonly inshore, in shallower and warmer waters where primary production is usually highest, it is likely that chl-*a* concentration and primary production should not be considered as an important predictive variable for abundance of spiny dogfish. However, for coastal elasmobranch species, such as the Atlantic sharpnose shark (*Rhizoprionodon terraenovae*), chl-*a* concentration has been found to be an important environmental variable that affects the abundance and habitat association of that species (Drymon et al., 2013). Papastamatiou et al. (2013) reported that for both sexes of tiger shark (*Galeocerdo cuvier*), immigration across the Hawaiian Archipelago was correlated with chl-*a* concentration—a result that they interpreted to be indicative of a foraging activity. It is, therefore, likely that for large pelagic shark species, such as the blue shark (*Prionace glauca*), primary production is an important variable that influences species habitat distribution (Mitchell et al., 2014).

Our results indicate that adult female spiny dogfish may select warmer inshore habitats not for foraging but to reduce gestation time of embryos, as has been reported to occur in the round stingray (*Urobatis halleri*) and may be common in other elasmobranchs (Jirik and Lowe, 2012). Further research should be focused on understanding the influence of primary productivity on habitat selection in spiny dogfish, by sex, to evaluate the link with gestation and the possible link with foraging success (Dell'Apa et al., 2015).

From a management perspective, the results of this study indicate a higher probability of catching spiny dogfish at higher latitudes, mainly on the Georges Bank shelf area, where the stock of this species is commonly reported to aggregate between spring and fall (Rulifson, 2010). Results also indicate that there is a higher probability of adult male aggregations inshore in coastal waters during the fall. Additionally, a lower abundance of adult females was predicted to be found in the fall in these same waters. Combined, these results indicate that the Georges Bank shelf area may be explored for the development of a male-only directed fishery in the fall. However, further studies are needed to confirm this hypothesis, studies that possibly could combine data analyses of both fishery-independent (e.g., NEFSC surveys) and fishery-dependent surveys in the New England region.

Additionally, the results from this study indicate that a potential male-only directed fishery, mainly in the Georges Bank shelf area, could be limited to fishing in the afternoon, when fewer aggregations of adult females are predicted to be associated with coastal waters, and in the fall, when higher numbers of adult females are predicted to select deeper waters. Sagarese et al. (2014a) noted that during the fall, adult females may move into offshore waters as a strategy to avoid encountering adult males—a suggestion also made by other authors (Verissimo et al., 2011; Dell'Apa et al., 2014). Future research should be undertaken to compare and integrate the spatiotemporal habitat distribution of spiny dogfish, by sex, found in this study with that of fishery-independent surveys, such as the surveys that the NEFSC has conducted in offshore waters and for a longer period of time, and with that of fishery-dependent surveys, which provide less standardized but more direct information on the influence of fishery exploitation of this species between New England and North Carolina. Because temperature and depth are key environmental variables for prediction of the abundance in both sexes, more studies are also needed to understand the influence of climate change in the spatial distribution of spiny dogfish along the northwest Atlantic coast and continental shelf (Nye et al., 2009; Sagarese et al., 2014a).

Acknowledgments

We thank all the people who have worked on the F/V *Darana R* at the Virginia Institute of Marine Science in Gloucester Point, Virginia, from crew members to those people who volunteered to help collect data and samples during the surveys. We are grateful to S. Sagarese and to 3 anonymous reviewers for their valuable inputs and comments that helped to improve the quality of this manuscript.

Literature cited

Austin, M.
2007. Species distribution models and ecological theory: a critical assessment and some possible new approaches. Ecol. Model. 200:1–19.

Banerjee, S., B. P. Carlin, and A. E. Gelfand.
2004. Hierarchical modeling and analysis for spatial data, 474 p. Chapman & Hall/CRC, Boca Raton, FL.

Bubley, W. J., J. A. Sulikowski, D. M. Koester, and P. C. W. Tsang.
2013. Using a multi-parameter approach to reassess maturity of spiny dogfish, *Squalus acanthias*, following increased fishing pressure in the Western North Atlantic. Fish. Res. 147:202–212.

Campana, S. E., D. W. Kulka, and S. Joyce.
2009. Growth and reproduction of spiny dogfish off the eastern coast of Canada, including inferences on stock structure. *In* Biology and management of dogfish sharks (V. F. Gallucci, G. A. McFarlane, and G. G. Bargmann, eds.), p. 195–208. Am. Fish. Soc., Bethesda, MD.

Colloca, F., V. Bartolino, G. J. Lasinio, L. Maiorano, P. Sartor, and G. Ardizzone.
2009. Identifying fish nurseries using density and persistence measures. Mar. Ecol. Prog. Ser. 381:287–296.

Compagno, L., M. Dando, and S. Fowler.
2005. Princeton field guides: sharks of the world, 496 p. Princeton Univ. Press, Princeton, NJ.

Conradt, L.
2005. Definitions, hypotheses, models, and measures in the study of animal segregation. *In* Sexual segregation in vertebrates: ecology of the two sexes (K. E. Ruckstuhl and P. Neuhaus, eds.), p. 11–32. Cambridge Univ. Press, Cambridge, UK.

de Leiva Moreno, J. I., V. N. Agostini, J. F. Caddy, and F. Carocci.
2000. Is the pelagic-demersal ratio from fishery landings a useful proxy for nutrient availability? A preliminary data exploration for the semi-enclosed seas around Europe. ICES J. Mar. Sci. 57:1091–1102.

Dell'Apa, A., J. C. Johnson, D. G. Kimmel, R. A. Rulifson.
2013. The international trade and fishery management of spiny dogfish: a social network approach. Ocean Coast. Manage. 80:65–72.

Dell'Apa, A., J. Cudney-Burch, D. G. Kimmel, and R. A. Rulifson.
2014. Sexual segregation of spiny dogfish in fishery-dependent surveys in Cape Cod, Massachusetts: potential management benefits. Trans. Am. Fish. Soc. 143:833–844.

Dell'Apa, A., C. W. Bangley, and R. A. Rulifson.
2015. Who let the dogfish out? A review of management and socio-economic aspects of spiny dogfish fisheries. Rev. Fish Biol. Fish. 25:273–295.

Drymon, J. M., L. Carassou, S. P. Powers, M. Grace, J. Dindo, and B. Dzwonkowski.
2013. Multiscale analysis of factors that affect the distri-

bution of sharks throughout the northern Gulf of Mexico. Fish. Bull. 111:370–380.

Elith, J., and J. R. Leathwick.
2009. Species distribution models: ecological explanation and prediction across space and time. Annu. Rev. Ecol. Evol. Syst. 40:677–697.

Espinoza, M., M. Cappo, M. R. Heupel, A. J. Tobin, and C. A. Simpfendorfer.
2014. Quantifying shark distribution patterns and species-habitat associations: implications of marine park zoning. PLoS One 9(9):e106885.

Fielding, A. H., and J. F. Bell.
1997. A review of methods for the assessment of prediction errors in conservation presence/absence models. Environ. Conserv. 24:38–49.

Ford, E.
1921. A contribution to our knowledge of the life-histories of the dogfishes landed at Plymouth. J. Mar. Biol. Assoc. U. K. 12:468–505.

Gelfand, A. E., J. A. Silander Jr., S. Wu, A. Latimer, P. O. Lewis, A. G. Rebelo, and M. Holder.
2006. Explaining species distribution patterns through hierarchical modeling. Bayesian Anal. 1:41–92.

Hanchet, S.
1988. Reproductive biology of *Squalus acanthias* from the east coast, South Island, New Zealand. N.Z. J. Mar. Freshw. Res. 22:537–549.

Hijmans, R. J.
2013. Introduction to the "raster" package (version 2.1-25). R Foundation for Statistical Computing, Vienna, Austria.

Hilborn, R., and C. J. Walters (eds).
1992. Quantitative fisheries stock assessment: choice, dynamics and uncertainty, 570 p. Chapman & Hall, New York.

Jensen, A. C.
1966. Life history of the spiny dogfish. Fish. Bull. 65:527–554.

Jirik, K. E., and C. G. Lowe.
2012. An elasmobranch maternity ward: female round stingrays *Urobatis halleri* use warm, restored estuarine habitat during gestation. J. Fish Biol. 80:1227–1245.

Lack, M.
2006. Conservation of spiny dogfish *Squalus acanthias*: a role for CITES?, 40 p. TRAFFIC International, Cambridge, UK. [Available from website.]

Martins, T. G., D. Simpson, F. Lindgren, and H. Rue.
2013. Bayesian computing with INLA: new features. Comput. Stat. Data Anal. 67:68–83.

Maunder, M. N., and A. E. Punt.
2004. Standardizing catch and effort data: a review of recent approaches. Fish. Res. 70:141–159.

Maunder, M. N., J. R. Sibert, A. Fonteneau, J. Hampton, P. Kleiber, and S. J. Harley.
2006. Interpreting catch per unit effort data to assess the status of individual stocks and communities. ICES J. Mar. Sci. 63:1373–1385.

Methratta, E. T., and J. S. Link.
2007. Ontogenetic variation in habitat association for four groundfish species in the Gulf of Maine–Georges Bank region. Mar. Ecol. Prog. Ser. 338:169–181.

Mitchell, J. D., K. J. Collins, P. I. Miller, and L. A. Suberg.
2014. Quantifying the impact of environmental variables upon catch per unit effort of the blue shark *Prionace glauca* in the western English Channel. J. Fish Biol. 85:657–670.

Muñoz, F., M. G. Pennino, D. Conesa, A. López-Quílez, and J. M. Bellido.
2013. Estimation and prediction of the spatial occurrence of fish species using Bayesian latent Gaussian models. Stoch. Environ. Res. Risk Assess. 27:1171–1180.

Nammack, M. F., J. A. Musick, and J. A. Colvocoresses.
1985. Life history of spiny dogfish off the northeastern United States. Trans. Am. Fish. Soc. 114:367–376.

Nye, J. A., J. S. Link, J. A. Hare, and W. J. Overholtz.
2009. Changing spatial distribution of fish stocks in relation to climate and population size on the Northeast United States continental shelf. Mar. Ecol. Prog. Ser. 393:111–129.

Overholtz, W. J., and A. V. Tyler.
1985. Long-term responses of the demersal fish assemblages of Georges Bank. Fish. Bull. 83:507–520.

Papastamatiou, Y. P., C. G. Meyer, F. Carvalho, J. J. Dale, M. R. Hutchinson, and K. N. Holland.
2013. Telemetry and random-walk models reveal complex patterns of partial migration in a large marine predator. Ecology 94:2595–2606.

Pennino, M. G., F. Muñoz, D. Conesa, A. López-Quílez, and J. M. Bellido.
2014. Bayesian spatio-temporal discard model in a demersal trawl fishery. J. Sea Res. 90:44–53.

Perry, R. I., and S. J. Smith.
1994. Identifying habitat associations of marine fishes using survey data: an application to the northwest Atlantic. Can. J. Fish. Aquat. Sci. 51:589–602.

Pittman, S. J., and K. A. Brown.
2011. Multi-scale approach for predicting fish species distributions across coral reef seascapes. PLoS One 6(5): e20583.

Potts, J. M., and J. Elith.
2006. Comparing species abundance models. Ecol. Model. 199:153–163.

Pratt, H. L., Jr., and J. C. Carrier.
2001. A review of elasmobranch reproductive behavior with a case study on the nurse shark, *Ginglymostoma cirratum*. Environ. Biol. Fish. 60(1):157–188.

R Core Team.
2014. R: a language and environment for statistical computing. R Foundation for Statistical Computing, Vienna, Austria. [Available from website, accessed August 2014.]

Roos, M., and L. Held.
2011. Sensitivity analysis in Bayesian generalized linear mixed models for binary data. Bayesian Anal. 6:259–278. [Available from website.]

Roos, N. C., A. R. Carvalho, P. F. Lopes, and M. G. Pennino.
2015. Modeling sensitive parrotfish (Labridae: Scarini) habitats along the Brazilian coast. Mar. Environ. Res. 110:92–100.

Ruckstuhl, K. E., and T. H. Clutton-Brock.
2005. Sexual segregation and the ecology of the two sexes. *In* Sexual segregation in vertebrates: ecology of the two sexes (K. E.Ruckstuhl and P. Neuhaus, eds.), p. 3–10. Cambridge Univ. Press, Cambridge, UK.

Rue, H., S. Martino, and N. Chopin.
2009. Approximate Bayesian inference for latent Gaussian models by using integrated nested Laplace approximations. J. R. Stat. Soc., B 71:319–392.

Rulifson, R. A.
2010. Tagging spiny dogfish overwintering in North Carolina, and summering in Bay of Fundy, Canada. *In* Proceedings of the Transboundary Resources Assessment Committee (TRAC) spiny dogfish review; Woods Hole, MA, 30 March–2 April 2009, p. 15–19. [Available from website.]

Sagarese, S. R., M. G. Frisk, T. J. Miller, K. A. Sosebee, J. A. Musick, and P. J. Rago.
2014a. Influence of environmental, spatial, and ontogenetic variables on habitat selection and management of spiny dogfish in the Northeast (US) shelf large marine ecosystem. Can. J. Fish. Aquat. Sci. 71:567–580.

Sagarese, S. R., M. G. Frisk, R. M. Cerrato, K. A. Sosebee, J. A. Musick, and P. J. Rago.
2014b. Application of generalized additive models to examine ontogenetic and seasonal distributions of spiny dogfish (*Squalus acanthias*) in the Northeast (US) shelf large marine ecosystem. Can. J. Fish. Aquat. Sci. 71:847–877.

Shepherd, T., F. Page, and B. Macdonald.
2002. Length and sex-specific associations between spiny dogfish (*Squalus acanthias*) and hydrographic variables in the Bay of Fundy and Scotian Shelf. Fish. Oceanogr. 11:78–89.

Sims, D. W.
2005. Differences in habitat selection and reproductive strategies of male and female sharks. *In* Sexual segregation in vertebrates: ecology of the two sexes (K. E. Ruckstuhl and P. Neuhaus, eds.), p. 127–147. Cambridge Univ. Press, Cambridge, UK.

Sims, D. W., J. P. Nash, and D. Morritt.
2001 Movements and activity of male and female dogfish in a tidal sea lough: alternative behavioural strategies and apparent sexual segregation. Mar. Biol. 139:1165–1175.

Sosebee, K. A.
2005. Are density-dependent effects on elasmobranch maturity possible? J. Northwest Atl. Fish. Sci. 35:115–124.

Spiegelhalter, D. J., N. G. Best, B. P. Carlin, and A. van der Linde.
2002. Bayesian measures of model complexity and fit. J. R. Stat. Soc., B. 64:583–639.

Springer, S.
1967. Social organization of shark populations. *In* Sharks, skates, and rays (P. W. Gilbert, R. F. Mathewson, and D. P. Rall, eds.), p. 149–174. The Johns Hopkins Press, Baltimore, MD.

Sulikowski, J. A., B. K. Prohaska, A. E. Carlson, A. M. Cicia, C. T. Brown, and A. C. Morgan.
2013. Observations of neonate spiny dogfish, *Squalus acanthias*, in Southern New England: a first account of a potential pupping ground in the Northwestern Atlantic. Fish. Res. 137: 59–62.

Veríssimo, A., D. Grubbs, J. McDowell, J. Musick, and D. Portnoy.
2011. Frequency of multiple paternity in the spiny dogfish *Squalus acanthias* in the Western North Atlantic. J. Hered. 102:88–93.

Walters, C.
2003. Folly and fantasy in the analysis of spatial catch rate data. Can. J. Fish. Aquat. Sci. 60:1433–1436.

Wearmouth, V. J., and D. W. Sims.
2008. Sexual segregation in marine fish, reptiles, birds and mammals: behaviour patterns, mechanisms and conservation implications. Adv. Mar. Biol. 54:107–170.

National Marine
Fisheries Service
NOAA

Fishery Bulletin
established in 1881

Spencer F. Baird
First U.S. Commissioner
of Fisheries and founder
of *Fishery Bulletin*

Horizontal and vertical movements of longfin makos (*Isurus paucus*) tracked with satellite-linked tags in the northwestern Atlantic Ocean

Robert E. Hueter (contact author)[1]
John P. Tyminski[1]
John J. Morris[1]
Alexei Ruiz Abierno[2]
Jorge Angulo Valdes[2,3]

Email address for contact author: rhueter@mote.org

[1] Center for Shark Research
Mote Marine Laboratory
1600 Ken Thompson Parkway
Sarasota, Florida 34236

[2] Centro de Investigaciones Marinas
Universidad de la Habana
Calle 16, No. 114 e/ 1ra y 3ra
Miramar, Playa, La Habana CP 11300, Cuba

[3] School of Natural Resources and Environment
University of Florida
P.O. Box 116455
Gainesville, Florida 32611

Abstract—The longfin mako (*Isurus paucus*) is a poorly studied oceanic shark taken in fisheries throughout its worldwide range in temperate and tropical waters. Satellite-linked tags were deployed to investigate the movements of 2 mature males, one tagged in the northeastern Gulf of Mexico (GOM) and the other off northern Cuba. Horizontal tracks estimated by using likelihood methods were similar for these sharks; comparable movements were documented from the GOM, through the Straits of Florida and the Bahamas, and into the open Atlantic Ocean where they converged on the Mid-Atlantic Bight. Depth and temperature ranges were 0–1767 m and 4.0–28.8°C. A diel pattern of vertical movement was evident for both individuals, along with regular forays from cold daytime depths to warmer near-surface waters, possibly as an adaptation for thermoregulation. The vertical movements of longfin makos allow them to exploit vertically migrating prey but these movements increase their vulnerability to pelagic longlining. The horizontal movements of these sharks reveal the limited benefit of areas currently closed to pelagic longlining off the southeastern United States and also indicate the connectivity of U.S., Cuban, Mexican, and Bahamian waters for this species. Because of the vulnerability of longfin makos to overexploitation, improved biological information is needed for accurate stock assessments and appropriate management and conservation measures.

Manuscript submitted 15 April 2016.
Manuscript accepted 29 November 2016.
Fish. Bull.: 115:101–116 (2017).
Online publication date: 20 December 2016.
doi: 10.7755/FB.115.1.9

The views and opinions expressed or implied in this article are those of the author (or authors) and do not necessarily reflect the position of the National Marine Fisheries Service, NOAA.

The shark genus *Isurus* comprises 2 species with similar morphological features, the shortfin mako (*I. oxyrinchus*) and the longfin mako (*I. paucus*) (Compagno, 2001). The longfin mako is a global oceanic species that inhabits both tropical and subtropical waters (Compagno, 2001) but also ranges into temperate seas (Queiroz et al., 2006; Bustamante et al., 2009; Mucientes et al., 2013). In the western Atlantic Ocean, the longfin mako has been documented in the Gulf Stream off the eastern United States, off Cuba's northern coast, as far south as southern Brazil (Compagno, 2001), and as far north as Georges Bank (Kohler et al., 1998). In the Gulf of Mexico (GOM), longfin makos have been observed infrequently but have been reported in the northern GOM off the Mississippi River and south of Panama City, Florida (Killam and Parsons, 1986) and in the southern GOM off Tabasco, Mexico (Wakida-Kusunoki and de Anda-Fuente, 2012). Despite its large size (to at least 417 cm in total length [TL]; Gilmore, 1983), the longfin mako is an understudied species, partly because of its relative rarity, its pelagic nature, and observers' confusion with its congener, the shortfin mako (Castro, 2011).

The longfin mako is not directly targeted in any fishery, but is taken as bycatch throughout its range in tropical and temperate waters by pelagic longline fisheries that target swordfish (*Xiphias gladius*), tuna species (*Thunnus* spp.), and other shark species (Reardon et al., 2006; Mucientes et al., 2013; Frédou et al., 2015). In a study of shark bycatch in the small-scale, pelagic longline fishery of northwest Cuba, Guitart Manday (1975) reported that the longfin mako was the sixth most common shark by weight of the 11 shark species reported; a more recent study of this fishery ranked the longfin mako higher in landings (Aguilar et al.,

2014). Fins of longfin makos are of desirable quality and have been reported in the Hong Kong (Clarke et al., 2006), Chilean (Sebastian et al., 2008), and Indonesian fin trades (Sembiring et al., 2015). Consequently, in some fisheries but not in the Cuban fishery, this species may be finned and discarded at sea; hence, landings of longfin makos may be underreported (Reardon et al., 2006). Given the apparent declines in some populations of the shortfin mako (Baum et al., 2003; Dulvy et al., 2008), it is likely that populations of the longfin mako have been affected by intensive pelagic longline fisheries (Reardon et al., 2006). Because of its rarity, low reproductive potential, and bycatch-induced mortality, the longfin mako is listed as vulnerable in the IUCN Red List of Threatened Species (Reardon et al., 2006) and in 2008 was added to Appendix II of the Convention on the Conservation of Migratory Species of Wild Animals (Kyne et al., 2012). In U.S. waters, retention of longfin makos has been prohibited for both commercial and recreational fishermen since 2000 under the National Marine Fisheries Service (NMFS) fishery management plan for sharks that inhabit the Atlantic Ocean and adjacent waters (NMFS[1]). In an ecological risk assessment of shark species caught in Atlantic pelagic longline fisheries, Cortés et al. (2015) ranked the vulnerability of the longfin mako among species at highest risk and highlighted the need for better basic biological information for this shark.

Satellite-linked tagging technologies have provided researchers with effective tools for revealing home ranges, movement and migration routes, and habitat-use patterns of marine predators (Hammerschlag et al., 2011). Most lamnid species have been studied by using satellite tracking. These species include the shortfin mako (Loefer et al., 2005; Stevens et al., 2010; Rogers et al., 2015), white shark (*Carcharodon carcharias*) (Bruce et al., 2006; Weng et al., 2007; Nasby-Lucas et al., 2009), porbeagle (*Lamna nasus*) (Pade et al., 2009; Saunders et al., 2011; Francis et al., 2015), and salmon shark (*L. ditropis*) (Weng et al., 2005, 2008). However, there are no detailed reports of satellite-tracked longfin makos from any part of the global range of this species. Conventional tagging results in U.S. waters, although sparse, indicate movement of longfin makos from the eastern GOM into the western North Atlantic Ocean, likely through the Straits of Florida (Kohler et al., 1998). We are the first to use satellite tracking as a means of assessing the behavior, ecology, and vulnerability to fisheries of this species.

Materials and methods

Two specimens of the longfin mako, one from the northeastern GOM and one from the southeastern GOM, were captured and tagged with pop-up satellite archival tags to track their horizontal and vertical movements. In 2012, a male longfin mako (LFM1) was captured during an overnight pelagic longline set deployed on 27 April in the northeastern GOM (28.40°N, 85.84°W) from the RV *Weatherbird II* of the Florida Institute of Oceanography. In 2015, a second male longfin mako (LFM2) was captured during an overnight pelagic longline set deployed from an artisanal Cuban fishing vessel on 13 February off Cojimar in northwest Cuba (23.26°N, 81.98°W).

When LFM1 was captured in 2012, the sea-surface temperature (SST) was 25.3°C and depth to the bottom was approximately 334 m. The gear targeted pelagic fish species and consisted of 26 km of mainline with 30-m gangions composed of 136-kg monofilament connected through a 9/0 nickel-plated swivel to 1 m of 0.8-mm stainless steel cable. The 202 hooks deployed were 18/0 circle hooks with zero offset and were baited with Spanish mackerel (*Scomberomorus maculatus*) or little tunny (*Euthynnus alletteratus*) and were suspended at depths 30–60 m below the surface. Chemical glow sticks (Chemilures,[2] World Plastics, San Carlos, CA) were attached to the gangions approximately 2 m above each baited hook as a fish attractant. Upon haulback of the gear the following morning on 28 April, one longfin mako was among the catch. The captured shark was lifted out of the water and brought on deck with a specially designed cradle to support the shark's body weight (Grace et al., 2007). The animal remained within this cradle for measuring and tagging procedures, during which time its gills were irrigated with seawater from a hose inserted into its mouth.

The shark was tagged with a pop-up satellite archival tag (Mk10; Wildlife Computers, Redmond, WA). The tag archived measurements of ambient temperature, pressure, and light level at 3-s intervals and summarized these data into 8-h periods to facilitate data transmission. The tag was programmed to detach after 90 d on the shark, float to the sea surface, and transmit a summary of its archived data by way of the Argos satellite system with time-at-depth and time-at-temperature histograms in 14 user-defined bins. Black antifouling paint (EP-2000; ePaint Company, East Falmouth, MA) before deployment had been applied to the tag, excluding its sensors and label. At deployment, the tag was inserted into the shark's dorsal musculature just below the first dorsal fin by using a stainless steel dart (Type SSD; 34.0 × 8.5 mm; Hallprint Pty. Ltd., Hindmarsh Valley, Australia) attached to a 15-cm tether composed of 55-kg coated, braided wire (Berkley, Spirit Lake, IA). To avoid tag destruction from extreme depth, a mechanical release device (RD1800; Wildlife Computers), designed to release at a depth of 1800 m, was threaded inline at the midpoint of the tether. The tether, excluding the portion with the RD1800 device,

[1] NMFS (National Marine Fisheries Service). 1999. Final fishery management plan for Atlantic tuna, swordfish, and sharks, 97 p. Natl. Mar. Fish. Serv., Silver Spring, MD. [Available from website.]

[2] Mention of trade names or commercial companies is for identification purposes only and does not imply endorsement by the National Marine Fisheries Service, NOAA.

was protected with heat shrink tubing (3M, Two Harbors, MN). A conventional Rototag (Dalton ID Systems Ltd, Henley-on-Thames, UK) and dart tag (Hallprint Pty. Ltd.) also were applied to the shark's first dorsal fin and dorsal musculature, respectively. The condition of the tagged shark at release was scored as condition 4 (>30 s of revival time, limited swimming on release) according to the release condition categories of Hueter et al. (2006).

In 2015, when LFM2 was captured, the SST was 25.7°C and depth to the bottom was approximately 750 m. The gear targeted pelagic fish species, in particular istiophorids and swordfish, and consisted of 8 km of mainline with gangions of 20–30 m, both composed of 2-mm twisted monofilament. The 66 hooks deployed were either 15/0 or 16/0 J hooks baited with salted clupeid and cyprinid fish species (e.g., silver carp [*Hypophthalmichthys molitrix*]), and suspended approximately 40 m below the surface. The fishermen attached battery-powered light-emitting devices (known locally in Cuba as *lampos*) to the gangions approximately 3 m above each baited hook. During gear retrieval in the early morning of 14 February, the hooked shark was transferred from the fishing vessel to a research boat, secured by tail rope at the stern, and maintained in the water during the process of taking measurements and tagging.

This shark (LFM2) was tagged with a MiniPAT (Wildlife Computers) that archived measurements of temperature, pressure, and light level at 5-s intervals and summarized these data into 6-h periods. The tag was programmed to detach from the shark after 150 d, and the time-at-depth and time-at-temperature histograms of the data were distributed among 12 user-defined bins. Unlike the Mk10 tag, which was deployed on LFM1, the MiniPAT sends time-series data of depth and temperature by way of the Argos satellite system in addition to archiving that data. A clear antifouling coating (Propspeed, Propspeed USA, Miami, FL) had been applied to the tag, excluding its sensors and release pin. At deployment, the tag was inserted into the dorsal musculature of the shark just below the first dorsal fin by using a plastic anchor (Domeier; 20×14 mm; Wildlife Computers) attached to a 15-cm tether composed of stainless steel wire rope with a 23-kg load capacity (type 18-8; McMaster-Carr, Santa Fe Springs, CA). A newer version of the RD1800 device was employed with an internal pin that breaks under pressure at a depth of 1800 m, releasing the tag from the tether. The tether, excluding the portion of the RD1800 device, was protected with heat shrink tubing (3M). No conventional tag was applied to this shark. The condition of the shark at release was classified as condition 2 (no revival time required, slow but strong swimming on release; Hueter et al., 2006).

For both sharks, species identification was determined by the presence of taxonomic characteristics of the genus *Isurus* (Campagno, 2001), together with a first dorsal fin well behind the free rear tip of the pectoral fin, dark coloration on the ventral surface of the snout, and long pectoral fins, all of which collectively distinguish the longfin mako from the shortfin mako (Guitart Manday, 1966; Garrick, 1967; Bustamante et al., 2009). Maturity of the 2 males was assessed by stage of clasper development and its condition.

Compiled data collected through the Argos system were uploaded to the Wildlife Computers Data Portal (website) for processing with GPE3 software (Wildlife Computers). This statistical processing tool runs exclusively on the tag manufacturer's Internet servers. The GPE3 software uses tag data and corresponding SST (NOAA Optimum Interpolation (OI) SST V2 High Resolution) and bathymetry (NOAA ETOP01 global relief model, Bedrock version) reference data as inputs into its gridded hidden Markov model to generate the most likely animal location for a given time, as well as a distribution of likelihoods as an indicator of location quality. This model provides an overall score as an indicator of how well the model fits the observed data. We ran the model with varying inputs for the parameter of animal speed to generate a fit with an optimal score and realistic maximum likelihood track (MLT). Optimal MLTs for LFM1 and LFM2 were generated by using animal speed inputs of 4.5 and 2.5 m/s, respectively. The total distance of the MLT was calculated with GE-Path software (vers. 1.4.5). Likelihood surfaces were generated by using the raster and ncdf packages for statistical software R, vers. 3.2.3 (R Core Team, 2015) and by using the script made available by the tag manufacturer. For comparing the MLT with SST, we produced imagery in R from the Group for High Resolution Sea Surface Temperature (GHRSST) global 1-km SST data set (website) using functions in the fields, maps and raster packages for R.

We assigned a diel period to each record (day, night, dawn, dusk) in the time-series data sent by the MiniPAT. To approximate the times of sunrise and sunset for a given date and location (from the MLT), we consulted an online calculator (website). On the basis of these estimates, dawn was defined as the 30-min period before and after sunrise, and dusk was defined as the 30-min period before and after sunset. To evaluate differences in percent time at depth and percent time at temperature between the 2 sharks and to test differences between day and night, we performed 2-sample Kolmogorov–Smirnov (K–S) tests. Mean depths between diel periods were compared with Welch's unequal variances t-test. These statistical analyses were performed by using the stats package for R (R Core Team, 2015).

To further investigate the environmental drivers of behavior, we used the time-series depth data from the MiniPAT to calculate vertical speed (as a proxy for activity level) for comparison with the corresponding temperature at depth. The difference between sequential depth data points was used to determine vertical velocity. The absolute value of the vertical velocity was considered the vertical speed. We then examined the relationship between daily mean vertical speed and minimum (daytime) and maximum (nighttime) temperatures during that segment of the day, using a linear

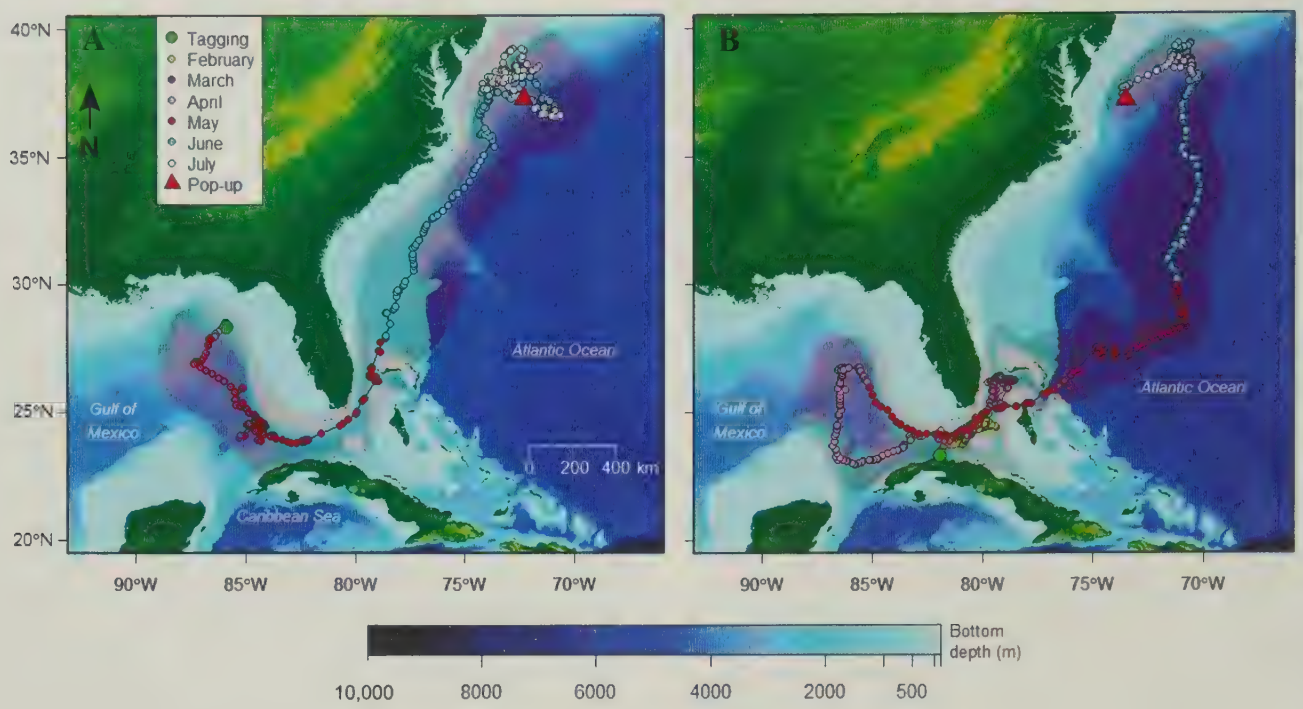

Figure 1

The model-derived maximum likelihood tracks for 2 longfin makos (*Isurus paucus*) and the locations where they were tagged and where their pop-up tags were released: (**A**) the first longfin mako, LFM1, was tagged 28 April 2012 off northwest Florida, and (**B**) the second longfin mako, LFM2, was tagged 14 February 2015 off Cojimar, Cuba. Shaded areas around the tracks represent 99% likelihood surfaces of track locations. The bathymetric scale represents water depth (in meters) to the bottom.

least-squares regression analysis. This analysis was also used to examine the relationship between daytime interforay duration and mean temperature, as well as to test for a possible correlation between mean nighttime depth and moon phase. For the latter analysis, moon illumination data were acquired from the U.S. Naval Meteorology and Oceanography Command (website) and were arcsine-transformed before statistical analysis (Abascal et al., 2010). All regression analyses were performed in SigmaPlot 10.0 (Systat Software Inc., San Jose, CA).

Results

On 28 April 2012, LFM1, a mature male (precaudal length [PCL]=201 cm), was tagged with a Mk10 pop-up satellite archival tag in the northeastern GOM. The 90-d tag was released on schedule and began transmitting on 27 July 2012. The first location recorded through the Argos system (37.46°N, 72.35°W) was 330 km east-northeast of Virginia Beach, Virginia, a minimum at-sea distance of 2233 km from the tagging site (Fig. 1A). Transmitted data were received over a period of 8 d, providing approximately 70% of the summary data. Therefore, although the condition of this shark was judged to be relatively poor (condition 4) when tagged and released, the transmitted data revealed that this animal survived the capture-and-release event.

On 14 February 2015, LFM2, a mature male measuring 190 cm PCL, was tagged with a MiniPAT off the northern coast of Cuba. The 150-d tag was released on schedule and began transmitting on 15 July 2015. The first location recorded through the Argos system (37.21°N, 73.51°W) was 223 km east-northeast of Virginia Beach, Virginia, a minimum at-sea distance of 1762 km from the tagging site (Fig. 1B). The tag transmitted data for 21 days, providing approximately 82% of the summary data.

Horizontal movements

During the first 3 weeks after tagging, LFM1 remained off the continental shelf in the eastern GOM, moving in a southeasterly direction (Fig. 1A). By the third week of May, the shark entered the Straits of Florida and then continued on an easterly path in the waters between Cuba and the Florida Keys. Then LFM1 moved in a northeasterly direction and entered waters of the Bahamas by the end of May, passed to the west of Grand Bahama Island, and moved into the open Atlantic Ocean by early June. During the first 3 weeks of June, the shark maintained a northeasterly direction until reaching continental shelf edge waters offshore of the mouth of Chesapeake Bay. For the rest of its track,

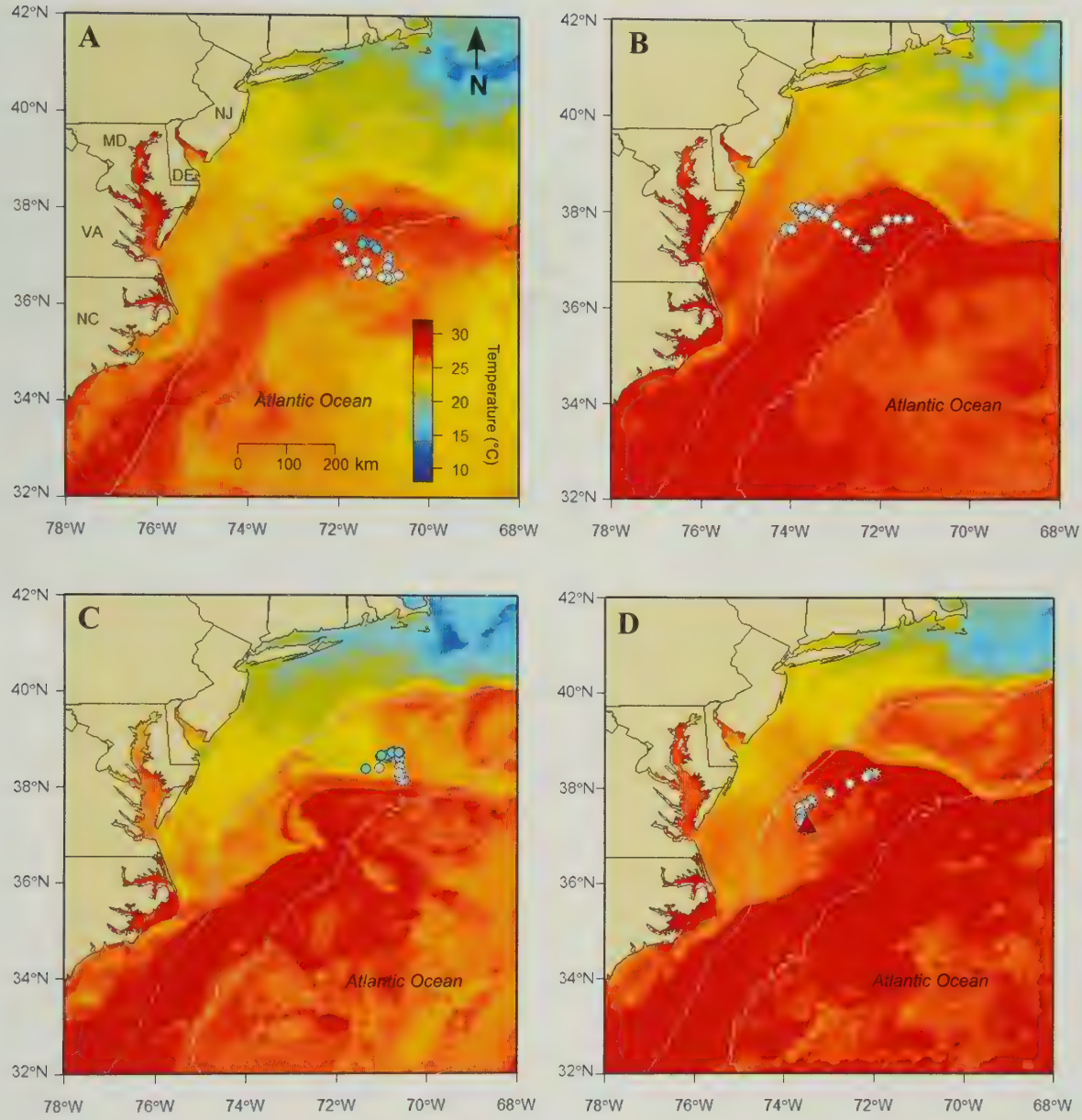

Figure 2

Locations of warm water from the Gulf Stream during late June and July and estimated positions of longfin makos (*Isurus paucus*) tracked with satellite-linked tags in the northwestern Atlantic Ocean. (**A**) Track of the first shark, LFM1, from 29 June to 5 July 2012 in relation to sea-surface temperature (SST) for 2 July 2012. (**B**) Track of LFM1 for the period 21–27 July 2012 in relation to SST for 24 July 2012. (**C**) Track of the second shark, LFM2, from 29 June to 5 July 2015 in relation to SST for 2 July 2015. (**D**) Track of LFM2 for the period 9–15 July 2015 in relation to SST for 12 July 2015. Blue and white circles represent positions in June and July, respectively. Red triangles mark the locations where the pop-up tag was released. The gray lines represent the 1000-m and 4000-m depth contours.

LFM1 remained within warm Gulf Stream waters and largely off the continental shelf 100–400 km from the coasts of Delaware, Maryland, and Virginia (Fig. 1A; Fig. 2, A and B). The northernmost position of the track (39.25°N, 72.83°W) was reached on 11 July. The total distance of the MLT was 6809 km, representing a mean movement rate of 75.7 km/d.

The MLT for LFM2 displayed movement from the northern coast of Cuba into the Straits of Florida in the latter half of February, followed by movements into waters of the Bahamas by early March (Fig. 1B). Then LFM2 remained in Gulf Stream waters between Grand Bahama Island and southeast Florida for a period of about 3 weeks. By late March and early April,

the shark moved back through the Straits of Florida in a westerly direction. After reaching the edge of the Yucatan shelf by mid-April, LFM2 moved northward into the GOM. By the beginning of May, the shark initiated southerly movements and re-entered the Straits of Florida, and it was located south of the Florida Keys by the first week of May. Next, LFM2 continued on an easterly to northeasterly path through the Bahamas (north of Andros Island), into the open Atlantic Ocean, and off the continental shelf. This shark continued in a northeasterly direction during the latter half of May. Then LFM2 remained in pelagic waters and shifted to a northerly direction during the month of June. On 24 June, the shark reached its northernmost position (39.38°N, 70.65°W) before moving in a southwesterly direction during July to the point where its tag was detached (on 15 July). During late June and the first half of July, LFM2 remained within the Gulf Stream and off the continental shelf, approximately 140–330 km from the coasts of New Jersey, Delaware, Maryland, and Virginia (Fig. 2, C and D). The total MLT covered 8826 km, a mean movement rate of 58.8 km/day.

By comparing the 2 tracks for the calendar days they had in common, one in 2012 and the other in 2015, one can observe a high degree of synchronicity in the movements of these sharks in the GOM and Straits of Florida, in their parallel tracks northward in the Atlantic Ocean, and in their convergence in the Mid-Atlantic Bight (MAB) (Fig. 3). In U.S. territorial waters, a broad system of areas in the GOM and off the Atlantic coast are closed year-round or seasonally to pelagic longline fishing (NMFS[3]). Both LFM1 and LFM2 stayed largely outside these protected areas (Fig. 3).

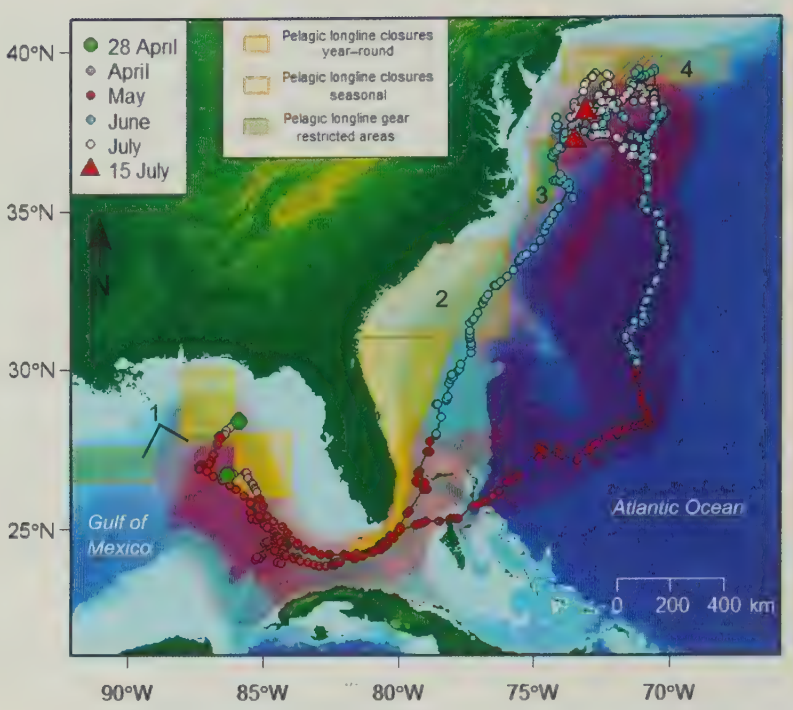

Figure 3

Maximum likelihood tracks for 2 longfin makos (*Isurus paucus*) tracked with satellite-linked tags in different years (2012 and 2015) in the northwestern Atlantic Ocean. Only the common calendar days of tracking (28 April–15 July) are shown, which show a high degree of seasonal synchronicity. Shaded areas around tracks represent 99% likelihood surfaces. Both tracks indicate movement largely outside area closures and gear-restricted areas as mandated by the National Marine Fisheries Service (yellow and green polygons). Areas 1–4 with seasonal fishing restrictions are in effect for 1) 1 April–31 May, 2) 1 Feb–30 April, 3) 1 Dec–30 April, and 4) the month of June.

Vertical movements

Both sharks undertook daily vertical movements and portions of most days were spent near the surface and at depths in excess of 200 m. For LFM1, the depth and temperature ranges experienced during its recorded track were 6–952 m and 4.6–28.8°C. The mean daily vertical range (i.e., difference between minimum and maximum depths) was 494.7 m (standard deviation [SD] 173.8). For LFM2, the ranges in depth and temperature were 0–1767 m and 4.0–28.4°C. The mean daily vertical range of this shark was 435.4 m (SD 147.0). The depth profile for LFM2 indicates a pattern of diel vertical migration (DVM), with the shark spending nighttime toward the surface and daytime at greater depths and with periods of dawn and dusk spent largely at intermediate depths (Fig. 4). We noted evidence of seasonal variation in vertical habitat use; LFM2 remained at shallower depths at night during June and July than during other months (Fig. 4). The mean depth at daytime (321.7 m [SD 107.6]) was significantly deeper for LFM2 than the mean depth at nighttime (94.2 m [SD 90.2]; $P<0.0001$) (Fig. 5). The mean depth at dawn (245.1 m [SD 104.5]) was shallower than the mean depth at dusk (258.7 m [SD 111.9]; $P=0.023$) (Fig. 5).

The results from a comparison of the histogram data for the 2 sharks indicated similar time-at-depth distributions (K–S test: $P=0.575$; Fig. 6A), although some differences were noted. For example, LFM2 spent 26.1% of its time in the depth range of 300–400 m and LFM1 spent 10.0% of its time within that range. The first longfin mako spent more time at depths >500 m (10.3%) than did LFM2 (1.6%; Fig. 6A). Time-at-tem-

[3] NMFS (National Marine Fisheries Service). 2016. Pelagic longline restrictions. *In* HMS commercial compliance guidance: guide for complying with the Atlantic tunas, swordfish, shark, and billfish regulations, p. 17–23. Natl. Mar. Fish. Serv., Silver Spring, MD. [Available from website.]

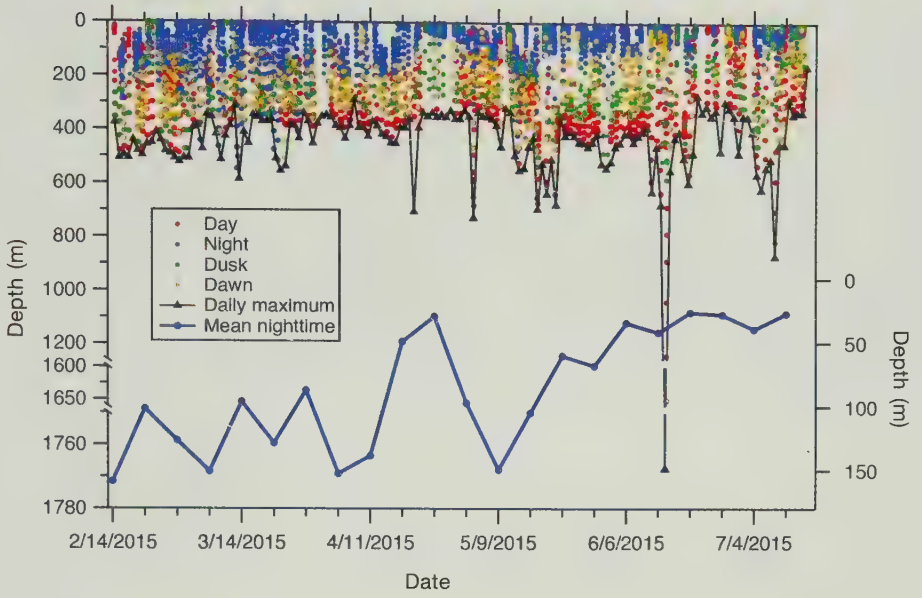

Figure 4

Depth profile for the 150-d track of a longfin mako (*Isurus paucus*; LFM2) tagged with a pop-up satellite archival tag off the northwestern coast of Cuba in 2015. The time-series depth data points are color-coded by diel period. The daily maximum depth is based on all received summary data sources for this shark. The line for weekly mean depth at nighttime corresponds with values on the right axis. Note that the left axis is split in 2 places.

perature distributions were not significantly different for these sharks (K–S test: P=0.989), and both sharks spent the largest proportion of their time in waters with a temperature range of 24–27°C (Fig. 6B). Large proportions of time in cold temperatures were observed; LFM1 and LFM2 spent 19.6% and 14.5% of their time in temperatures ≤12°C, respectively. We separated the binned histogram data for LFM2 into 12-h blocks of time that roughly corresponded to day (0800–2000) and night (2000–0800). The differences between day and night for time at depth (K–S test: P=0.536; Fig. 6C) and time at temperature (K–S test: P=0.9895; Fig. 6D) were not significant but further highlighted the DVM pattern.

Plotting time-series depth and temperature data for LFM2 was useful for visualizing dynamic patterns in vertical movement, although the relatively low resolution of these data (10-min intervals) precluded accurate calculations of ascent and descent rates. This shark spent daytime periods largely at depth (mean daily depth: 321.7 m); however, we noted upward vertical forays during these periods that appeared to be regularly timed and came closer to the surface when the temperature at depth was coldest (Fig. 7). The depth profile in Figure 7D shows that LFM2 experienced a change in temperature as high as 18.8°C during its upward movements but spent a relatively brief period of time in the warmer, near-surface waters (approximately 10–15 min) before initiating descent. When we examined this daytime pattern over LFM2's entire track, we found an inverse linear relationship between temperature and vertical speed (coefficient of multiple determination [R^2]=0.63; Fig. 8A).

In contrast, vertical speed during the night for this shark did not appear to be correlated with temperature (R^2=0.001). For LFM2, mean vertical speed in the daytime (2.3 m/min) was higher than in the nighttime (1.91 m/min; P=0.0133). Mean vertical speed at dawn (3.46 m/min) did not differ from that at dusk (3.48 m/min; P=0.921), although both crepuscular periods showed that this shark traveled at significantly higher speeds than during day and night (P<0.0001). Further, we examined the durations between the upward daytime forays from depths of 250–531 m for the entire track of LFM2 (n=36) and found that they ranged from 1.2 to 3.8 h. The results of a linear regression indicate that the duration between these forays was correlated with the mean temperature experienced by this shark at depth (R^2=0.60; Fig. 8B). Time-series data further revealed that LFM2 did not always remain in near-surface waters during the night because forays to depths >250 m were not uncommon, particularly during the period February–May (Fig. 9). Unlike the regularly timed daytime movements from depth (>250 m) toward the surface, the nighttime dive profiles for this shark were more variable and indicated a period of bottom time

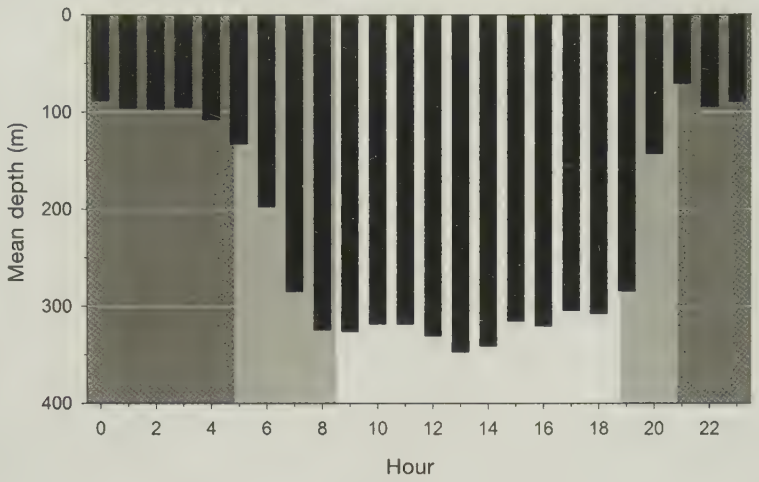

Figure 5

Mean depth by hour of the day for the 150-d track of a longfin mako (*Isurus paucus*; LFM2) tagged with a pop-up satellite archival tag off the northwestern coast of Cuba in 2015. Shading represents nighttime (dark gray), the variable periods of dawn and dusk that are dependent on location and date (light gray), and daytime (white). Hours are in local time (GMT–4 h; 4 hours behind Greenwich Mean Time).

before ascent (20–40 min). Additionally, an examination of lunar phase with mean nighttime depth did not detect any significant correlation (R^2=0.0005).

Discussion

This article is the first published report on the movements and vertical habitat use of the longfin mako, a poorly studied shark species for which our knowledge has largely been based on incidental catches from pelagic fisheries. This study is based on 2 satellite tracks, and the results revealed similar movements of the 2 longfin makos from the GOM to the western North Atlantic Ocean, as well as a diel pattern of vertical movement, a tolerance for extended periods in deep cold water, and dynamic vertical forays.

Horizontal movements and distribution

The MLTs for the 2 longfin makos revealed long-distance movements from the eastern GOM, through the Straits of Florida, and into the open Atlantic Ocean off the northeastern coast of the United States. Although direct comparisons between movement rates are made difficult by differences in tracking or analytical methods, the rates of movement for LFM1 (75.7 km/d) and LFM2 (58.8 km/d) are comparable with those reported for other lamnids. Short-term acoustic tracks of shortfin makos have indicated mean speeds of 53 km/d (2.2 km/h; Sepulveda et al., 2004). Migratory tracks from satellite tagging of white sharks have shown mean movement rates of 74.4 km/d (Bruce et al., 2006) and that individual white sharks travel as fast as 119 km/d (Weng et al., 2007). Data from conventional tagging of longfin makos, although scant, have indicated movements consistent with those observed with our satellite-tracked longfin makos: 2 sharks conventionally tagged in the eastern GOM were recaptured off the coasts of northern Cuba and eastern Florida (Kohler et al., 1998). Data from a more recent return of a conventional tag from a longfin mako indicated movement from the eastern Caribbean to the continental slope off of Delaware Bay (Kohler[4]). Off the U.S. north Atlantic coast, this species has been tagged in waters along the shelf edge (at depths >200 m), and the few recaptures from this area indicate a pattern of movement eastward into deeper pelagic waters (Kohler et al., 1998).

The presence of LFM1 and LFM2 in the Straits of Florida is consistent with fisheries data from this region. In an overview of the landings of large pelagic species along the northern coast of Cuba, Guitart Manday (1975) reported that the longfin mako was captured in nearly every month but noted peaks in abundance in surveys conducted during August–November in 1971 and during April–May and August–November in 1972. Observations from recent studies of the artisanal pelagic longline fishery along the northern coast of Cuba have indicated that the longfin mako continues to be caught year-round and peaks in relative abundance during January–March (J. Angulo Valdes, unpubl. data). Dodrill and Gilmore (1979) documented a beached specimen of longfin mako at Melbourne Beach, along the east coast of Florida, during the month of December (in 1975) and made note in their addendum of 2 additional specimens captured with drift longlines at depths of 200–400 m between Jupiter and Sebastian Inlets during the months of April and May (in 1978). In a 2-year study of the shark bycatch in the swordfish fishery off the east coast of Florida, Berkeley and Campos (1988) recorded 2 longfin makos captured during the months of October and December (in 1982).

In our study, both male longfin makos moved into the MAB during the months of June and July and used outer continental shelf, slope, and oceanic habitats during this period. Conventional tagging data from this area indicated a similar distribution of captures, along with a male:female ratio of 1.9:1.0, for the longfin mako (Kohler et al., 1998). Data provided by the NMFS Pelagic Observer Program (POP) for the period 1992–2014 indicated that 18% of longfin makos documented

[4] Kohler, N. 2015. Personal commun. Northeast Fish. Sci. Cent., Natl. Mar. Fish. Serv., 28 Tarzwell Dr., Narragansett, RI 02882.

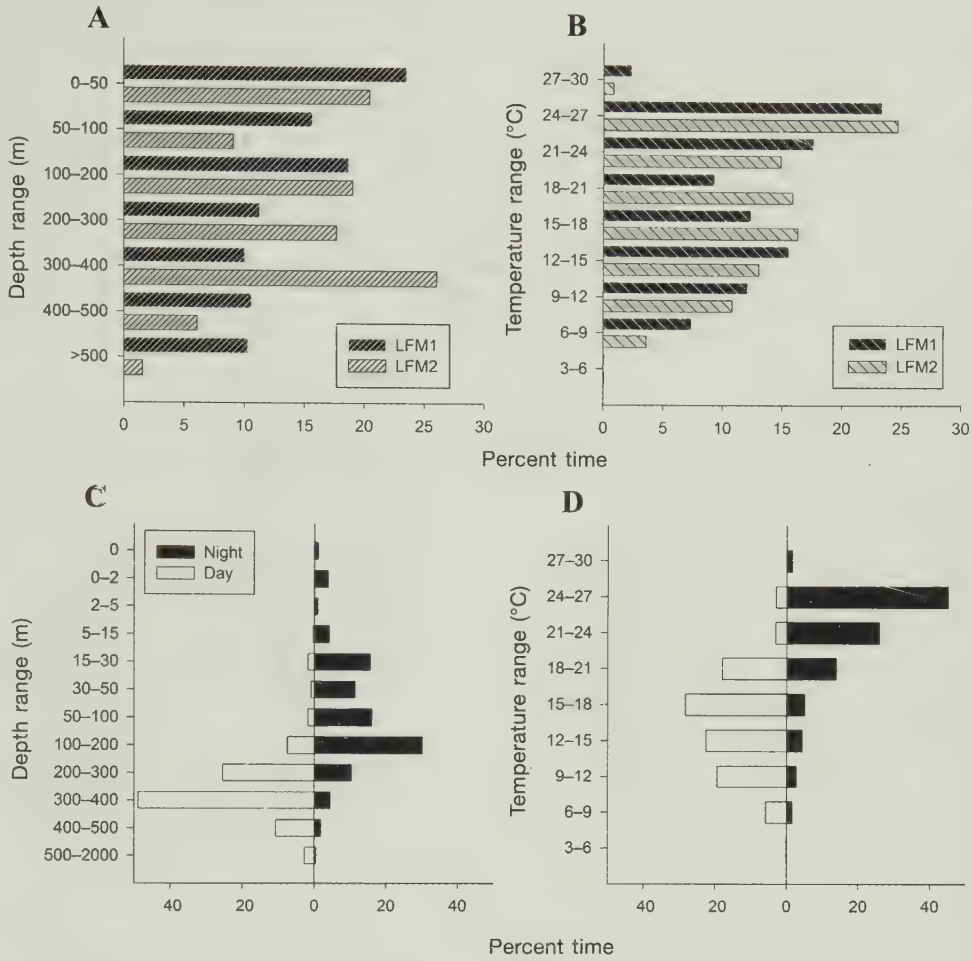

Figure 6

Depth and temperature histograms for 2 longfin makos (*Isurus paucus*) tracked with satellite-linked tags in the northwestern Atlantic Ocean in 2012 and 2015: (**A**) mean time-at-depth comparison for the 2 sharks LFM1 and LFM2, (**B**) time-at-temperature comparison for LFM1 and LFM2, (**C**) day (0800–2000) versus night (2000–0800) comparison of time at depth for LFM2, and (**D**) day versus night comparison of time at temperature for LFM2.

were from the MAB area (delineated as 35–43°N; 71–78°W) and that the greatest proportion were landed in July and August (combined 45%) (Cortés[5]). Of the 11 geographic areas covered by the POP, only the GOM had a larger proportion of longfin mako captures (34%) than the MAB (Cortés[6]).

Diel vertical movement

The depth and temperature data from the tags of LFM1 and LFM2 indicate a daily pattern of vertical movement between near-surface waters and the mesopelagic zone, with overall depth and temperature ranges of 0–1767 m and 4.0–28.8° C. A pattern of DVM was evident with greater time at depth during the day and more time in the mixed layer at night. These observations are consistent with longline catches of longfin makos in that most captures occur during overnight sets with baits set at depths of 0–220 m below the surface (Dodrill and Gilmore, 1979; Queiroz et al., 2006; Hemida and Capapé, 2008; Bustamante et al., 2009). Satellite tracking results for its congener, the shortfin mako, indicate a similar DVM pattern, but shortfin makos do not appear to have as great a tolerance for depth and cold temperatures. In the western North Atlantic Ocean, for example, a tagged shortfin mako had depth and temperature ranges of 0–556 m and 10.4–28.6° C (Loefer et al., 2005), and results from tracking a shortfin mako in the

[5] Cortés, E. 2015. Personal commun. Southeast Fish. Sci. Cent., Natl. Mar. Fish. Serv., 3500 Delwood Beach Rd., Panama City, FL 32408-7403.

[6] Cortés, E. 2015. Personal commun. Southeast Fish. Sci. Cent., Natl. Mar. Fish. Serv., 3500 Delwood Beach Rd., Panama City, FL 32408-7403.

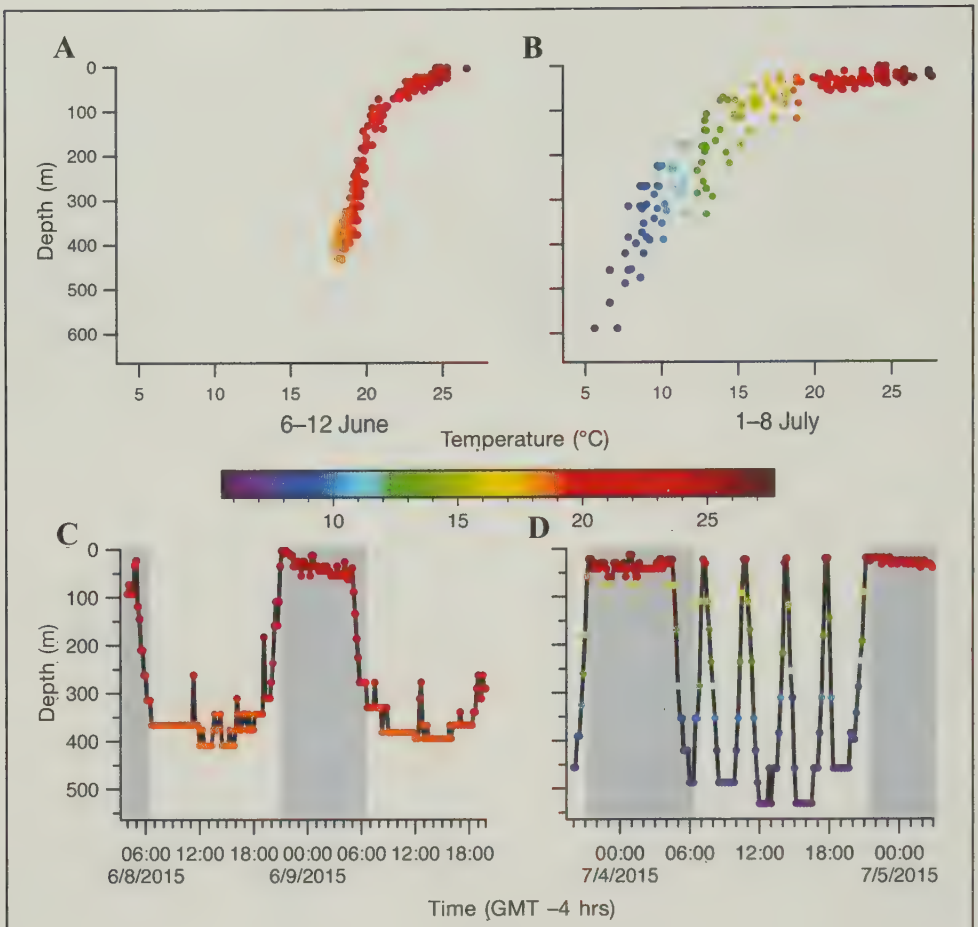

Figure 7

Variability in daytime vertical movements of a longfin mako (*Isurus paucus*; LFM2) tagged off the northwestern coast of Cuba in 2015. (**A**) Temperature–depth profile during a week-long period in June showing limited temperature variability. (**B**) Temperature–depth profile in early July showing movement through a temperature-stratified water column. (**C**) 39-h period beginning 8 June when the shark remained largely at depths of 300–400 m during the day within this relatively unstratified water column. (**D**) 31-h period beginning 3 July showing regular daytime forays from cold depths into warmer surface waters. GMT–4 h=4 hours behind Greenwich Mean Time.

southwest Pacific indicated a comparable vertical movement pattern of shallower depths at night than those during the day, descents to 620 m, and a temperature range of 8.8–23.4°C (Stevens et al., 2010).

Similar DVM behavior has been observed in a number of other pelagic shark species, including the bigeye thresher (*Alopias superciliosus*; Stevens et al., 2010), white shark (Nasby-Lucas et al., 2009), and porbeagle (Saunders et al., 2011), as well as in pelagic teleosts such as the swordfish (Carey and Robison, 1981; Abascal et al., 2010; Sepulveda et al., 2010) and bigeye tuna (*T. obesus*; Musyl et al., 2003), and it often has been suggested that this behavior is a response to the movement of their prey (Musyl et al., 2003; Stevens et al., 2010; Saunders et al., 2011). Although the diet of the longfin mako has not been described fully, the presumed prey of this species includes schooling fish and pelagic squid species (Compagno, 2001). The latter may be the more important dietary component because squid and squid beaks have been identified in the contents of stomachs of longfin makos (Dodril and Gilmore, 1979; Castro, 2011) and are similarly a known component of the shortfin mako diet (Stillwell and Kohler, 1982; Maia et al., 2006). The stomach of a 310-cm-TL female longfin mako from the southeastern Pacific Ocean contained squid remains, most likely from jumbo squid (*Dosidicus gigas*; Bustamante et al., 2009). Pelagic cephalopods also have been shown to be diel vertical migrators (Roper and Young, 1975). A distinct DVM pattern was observed for jumbo squid tagged with satellite tags: they spent most daylight hours at depths >250 m, rose toward the surface at dusk, and spent the majority of time at night at depths <150 m (Gilly et al., 2006). This pattern is similar to

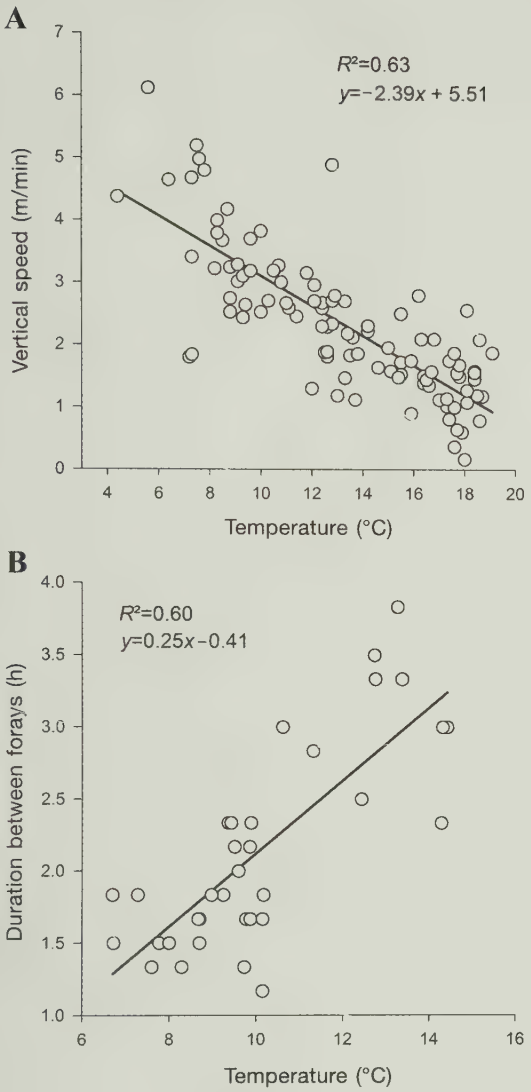

Figure 8

Relationship of daytime vertical movements and water temperature at depth for a longfin mako (*Isurus paucus;* LFM2) tracked with a satellite-linked tag in the northwestern Atlantic Ocean in 2015. (**A**) Mean daytime vertical speed and minimum temperature. (**B**) Daytime interforay duration and mean temperature. R^2=the coefficient of multiple determination.

the pattern of movements of longfin makos observed in our study and indicate that the diel pattern of the longfin mako may be related to a habit of following cephalopod prey.

The importance of the convergence of the tracks of LFM1 and LFM2 in the MAB in summer is unclear, but their movements likely are influenced directly or indirectly by water temperature, given their observed tendency to remain near or within the Gulf Stream (Fig. 2). The water column in this region becomes strongly stratified by mid-summer and is characterized by the formation of a warm, mixed surface layer of about 30 m in depth (Castelao et al., 2008). We noted a shallower mean depth at nighttime (~30 m) for LFM2 during June and July that indicates a nighttime preference for this mixed layer. Similarly, satellite tagging of bluefin tunas (*T. thynnus*) in the Atlantic Ocean has indicated a shallower summertime depth distribution when bluefin tunas occupy well-stratified water in this region (Galuardi and Lutcavage, 2012). The 60-d track of a shortfin mako tagged in Gulf Stream waters off South Carolina also had a decrease in nightly depth range after the summer solstice, indicating that the shark or its prey was tracking a thermal regime at night (Loefer et al., 2005). In a study of the diet of large, pelagic, predatory fish species in this same region of the North Atlantic Ocean, the most common component of stomach contents was cephalopods, and the highest biomass was represented by ommastrephid squid species (Logan et al., 2013).

Taken together, the data from these studies indicate that longfin makos use this area off the MAB as a summer feeding area and adjust their vertical movement patterns in response to seasonal changes in distributions of cephalopod or teleost prey to maximize foraging efficiency. Because both LFM1 and LFM2 were sexually mature males, we cannot discount the possibility that this area may also be a mating ground for this species. Using NMFS POP data from the MAB (Keene[7]), we estimated that 58% of female and 46% of male longfin makos caught in this area are of a sexually mature size. There is evidence that other lamnids, such as the white shark, use the MAB as both feeding and mating grounds (Gilmore, 1993). However, additional information, such as the presence of female longfin makos with fresh mating scars, will be needed to verify that the MAB is a mating ground for this species.

Use of deep, cold habitat and endothermy

Profiles of time at depth and time at temperature for the 2 longfin makos (Fig. 6) indicated that this species is capable of using cold, deepwater habitat for extended periods of time (42–54% of time at depths >200 m; 14–20% of time at temperatures ≤12° C), particularly during daytime hours. This pattern contrasts with that of its congener, the shortfin mako, which appears to make only brief excursions below the thermocline (Abascal et al., 2011) and reportedly spends only 4% of its time at depths greater than 300 m in the southwest Pacific (Stevens et al., 2010) and only about 6–10% of its time at depths exceeding 200 m in the northwestern Atlantic Ocean (Vaudo[8]).

[7] Keene, K., Jr. 2016. Personal commun. Southeast Fish. Sci. Cent., Natl. Mar. Fish. Serv., 75 Virginia Beach Dr., Bldg. 2, Miami, FL 33149-1003.

[8] Vaudo, J. 2013. Personal commun. The Guy Harvey Res. Inst., Nova Southeastern Univ., 8000 N Ocean Dr., Dania Beach, FL 33004.

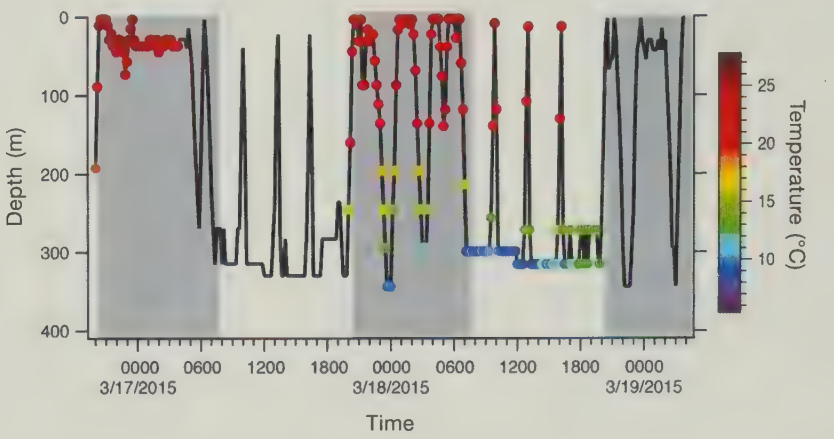

Figure 9

Time and depth profile for a 2-d period in March 2015 for a longfin mako (*Isurus paucus*; LFM2) tracked with a satellite-linked tag in the northwestern Atlantic Ocean, indicating nighttime forays by this shark from warm, near-surface waters to cold waters at depths around 300 m. The shaded areas approximate nighttime. Depth data points are color-coded by temperature where available.

Lamnid shark species have the ability to conserve metabolic heat by means of vascular countercurrent heat exchangers (a complex called the *retia mirabilia*) and can maintain their tissues at temperatures significantly above ambient temperatures, likely as a means for broadening their habitat (Block and Carey, 1985; Goldman, 1997; Goldman et al., 2004). In a study of body temperature measurements and anatomical features related to heat production and conservation for lamnid species, the longfin mako was found to have a relatively small amount of red muscle and poorly developed retia mirabilia and consequently was rated as the least endothermic of the lamnid shark species (Carey et al., 1985). However, these authors suggest that the retia mirabilia of the longfin mako could increase its thermal inertia and prolong cooling time so that this shark species can maintain a body temperature higher than the ambient temperature in cold, deep waters after spending periods of time in warm surface waters. Our findings that daytime vertical activity and interforay duration both are related to temperature at depth (Figs. 7 and 8) are consistent with this hypothesis. Tracked shortfin makos have shown a similar pattern in the southeastern Pacific Ocean in that reduced thermal structure of the water column coincided with a decrease in the vertical activity of these fish (Abascal et al., 2011).

We hypothesize that LFM2 conducted regular forays during daytime from cold depths to surface waters to gain heat lost at depth. A similar daytime movement pattern from depth to surface waters has been described for the blue shark (*Prionace glauca*; Carey et al., 1990), and this movement pattern is a thermoregulatory strategy that is aided by the property of muscle to warm up more quickly than the time it takes to cool down (Carey and Gibson, 1987). In contrast to the blue shark, the endothermic longfin mako may be able to remain warmer than the ambient water temperature for longer periods of time at depth and then re-warm rapidly during relatively brief forays to the surface. This form of behavioral thermoregulation may enable longfin makos to remain active predators in cold water and to exploit agile, vertically migrating prey, such as pelagic squid species that would largely become unavailable (during the day) to competing ectothermic predators.

We also noted nighttime vertical oscillations of LFM2 from near surface waters to depths >300 m (Fig. 9). The subsequent ascents brought this shark within 3 m of the surface, perhaps to regain heat after a period (20–40 min) at cold depths. For the shortfin mako, directed descents into deeper water, followed by rapid ascents (also known as bounce dives), have been associated primarily with daytime hours (Abascal et al., 2011) and have been correlated with successful feeding events at depth (Sepulveda et al., 2004). Although a DVM pattern has been reported for satellite-tracked jumbo squid, a highly variable amount of nighttime diving to depths in excess of 300 m has been observed for this species (Gilly et al., 2006). It is likely that the nighttime forays we observed with LFM2 are related to foraging and may be a response to variable nighttime movement patterns of its pelagic prey. The large size of the longfin mako (second largest of all lamnid species after the white shark, by length) may also be thermally advantageous by further minimizing conductive heat loss to surrounding sea water. Larger shortfin makos have been found to

dive to greater maximum depths than those attained by smaller specimens (Sepulveda et al., 2004). As with all other lamnid shark species, the longfin mako has the capacity to maintain its visceral temperature substantially above ambient sea temperature through a suprahepatic rete (Carey et al., 1985; Bernal et al., 2012), which may be a mechanism for enhancing rates of digestion and food assimilation (Goldman 1997; Newton et al., 2015).

Implications for conservation strategies

Pelagic longline fisheries pose a principal threat to longfin makos (Reardon et al., 2006). Although bycatch data for this species are insufficient, there are published accounts of longfin makos having been captured in gear that targeted swordfish (Dodrill and Gilmore, 1979; Buencuerpo et al., 1998; Queiroz et al., 2006; Mucientes et al., 2013). In a report on the swordfish fishery along the east coast of Florida, Berkeley and Campos (1988) noted that more shark species than target species were captured and that the overall mortality rate was 66% for 13 species of hooked sharks. Furthermore, in a recent 1-year survey (conducted from October 2010 through November 2011) of the pelagic longline fishery along the northwestern coast of Cuba, the longfin mako was the second-most abundant shark species landed (by number), exceeded only by the shortfin mako, out of the 15 different shark species observed (Aguilar et al., 2014). A nearly 5-year (from October 2010 through April 2015) pilot monitoring program of the same fishery documented the longfin mako as the most abundant pelagic shark species landed (MINAL, 2015). Currently, there are no restrictions on catches of longfin makos in the waters of Cuba. In U.S. waters, the year-round or seasonal closing of areas to pelagic longline fisheries in the GOM and Atlantic Ocean appear to offer minimal protection for this species. Although based on only 2 tracks from 2 individuals, our data do not indicate that these sharks spent much time inside these closed areas, where they could have been protected from pelagic longlining.

The effect of this fishing pressure may be profound for the longfin mako, given its lower fecundity (2–8 pups per litter; Guitart Manday, 1975; Compagno, 2001) than that of the shortfin mako (4–25 pups per litter; Mollet et al., 2000; Compagno, 2001). The combination of this low productivity and high susceptibility of longfin makos to longline gear has led to this species being ranked as highly vulnerable in ecological risk assessments of shark species caught in pelagic longline fisheries (Cortés et al., 2010, 2015). With this vulnerability and generally lower abundance in comparison with its conspecific, for which it is often misidentified, the longfin mako is a shark species of special conservation concern in today's oceans.

The depths at which sharks distribute themselves profoundly affect their susceptibility to commercial fisheries (Speed, et al., 2010). The diel vertical movement pattern of the longfin mako contributes to its vulnerability to pelagic longline fisheries, especially to fisheries that target swordfish. Results from a recent study, in which the satellite tracks of sharks were compared with fishing vessel movements in the North Atlantic Ocean, indicate how effectively pelagic longline fleets are exploiting key oceanic shark habitats, almost entirely overlapping fishing effort with preferred habitat of shark species for much of the year (Queiroz et al, 2016). With only 2 satellite tracks of longfin makos that covered periods of 3–5 months, the results of our study reveal connectivity in the range of this species among the territorial waters of 4 countries—the United States, Cuba, Mexico, and the Bahamas—and hence the vulnerability of this species to fishing fleets from multiple nations. More than 75% of species of pelagic sharks and rays have an elevated risk of extinction due to overfishing (Dulvy et al., 2008), and large pelagic shark species, such as the longfin mako, have an approximately 80% probability of being threatened (Dulvy et al., 2014). Effective management and assessment efforts, however, are often impeded by a lack of species-specific fishery and biological data. Although our study contributes new information to the limited knowledge of the longfin mako, continued efforts to improve data collection and the monitoring of pelagic shark catches, particularly in areas of concentrated abundance of longfin makos, such as those off the northern coast of Cuba, are warranted. The recent implementation of the first National Plan of Action for conservation and management of species of sharks and rays by Cuba (MINAL, 2015) is a positive step toward this goal.

Acknowledgments

We are indebted to the captains and crews of Florida Institute of Oceanography's RV *Weatherbird II* and of the MV *Marinabella* and FV *Poco a Poco* in Cuba. We sincerely thank our many Cuban colleagues, including L. Garcia Lopez, A. Alvarez Aleman, and C. Aguilar Betancourt of the Centro de Investigaciones Marinas, Universidad de la Habana, and F. Pina of the Centro de Investigaciones de Ecosistemas Costeros. Special gratitude is extended to Tandem Stills + Motion, Herzog & Co., and Discovery Communications for documenting the work in Cuba. Permission to deploy satellite tags in Cuba was made possible through the dedicated efforts of D. Whittle of the Environmental Defense Fund and of Mundo Latino TV of Cuba. We thank J. Stewart for the R script used to generate likelihood surfaces and B. Galuardi for his helpful advice in constructing figures of sea-surface temperatures. We are grateful to P. Rogers and 2 anonymous reviewers for their input toward improving the manuscript. This work was funded by the Gulf of Mexico Research Initiative through the Florida Institute of Oceanography and by the Guy Harvey Ocean Foundation, Christopher Reynolds Foundation, Environmental Defense Fund, and Discovery Communications.

Literature cited

Abascal, F. J., J. Mejuto, M. Quintans, and A. Ramos-Cartelle.
2010. Horizontal and vertical movements of swordfish in the Southeast Pacific. ICES J. Mar. Sci. 67:466–474.

Abascal, F. J., M. Quintans, A. Ramos-Cartelle, and J. Mejuto.
2011. Movements and environmental preferences of the shortfin mako, *Isurus oxyrinchus*, in the southeastern Pacific Ocean. Mar. Biol. 158:1175–1184.

Aguilar, C., G. González-Sansón, R. Hueter, E. Rojas, Y. Cabrera, A. Briones, R. Borroto, A. Hernández, and P. Baker.
2014. Captura de tiburones en la región noroccidental de Cuba. Lat. Am. J. Aquat. Res. 42:477–487.

Baum, J. K., R. A. Myers, D. G. Kehler, B. Worm, S. J. Harley, and P. A. Doherty.
2003. Collapse and conservation of shark populations in the northwest Atlantic. Science 299:389–392.

Berkeley, S. A., and W. L. Campos.
1988. Relative abundance and fishery potential of pelagic sharks along Florida's east coast. Mar. Fish. Rev. 50(1):9–16.

Bernal, D., J. K. Carlson, K. J. Goldman, and C. G. Lowe.
2012. Energetics, metabolism, and endothermy in sharks and rays. *In* Biology of sharks and their relatives, 2nd ed. (J. C. Carrier, J. A. Musick, and M. R. Heithaus, eds.), p. 211–237. CRC Press, Boca Raton, FL.

Block, B. A., and F. G. Carey.
1985. Warm brain and eye temperatures in sharks. J. Comput. Physiol. B 156:229–236.

Bruce, B. D., J. D. Stevens, and H. Malcom.
2006. Movements and swimming behaviour of white sharks (*Carcharodon carcharias*) in Australian waters. Mar. Biol. 150:161–172.

Buencuerpo, V., S. Rios, and J. Morón.
1998. Pelagic sharks associated with the swordfish, *Xiphias gladius*, fishery in the Eastern North Atlantic Ocean and the Strait of Gibraltar. Fish. Bull. 96:667–685.

Bustamante, C., F. Concha, F. Balbontín, and J. Lamilla.
2009. Southernmost record of *Isurus paucus* Gitart Manday, 1966 (Elasmobranchii: Lamnidae) in the southeast Pacific Ocean. Rev. Biol. Mar. Oceanogr. 44:523–526.

Carey, F. G., and B. H. Robison.
1981. Daily patterns in the activities of swordfish, *Xiphias gladius*, observed by acoustic telemetry. Fish. Bull. 79:277–292.

Carey, F. G., and Q. H. Gibson.
1987. Blood flow in the muscle of free-swimming fish. Physiol. Zool. 60:138–148.

Carey, F.G., J. G. Casey, H. L. Pratt, D. Urquhart, and J. E. McCosker.
1985. Temperature, heat production and heat exchange in lamnid sharks. Mem. Calif. Acad. Sci. 9:92–108.

Carey, F. G., J. V. Scharold, and A. J. Kalmijn.
1990. Movements of blue sharks (*Prionace glauca*) in depth and course. Mar. Biol. 106:329–342.

Castelao, R., S. Glenn, O. Schofield, R. Chant, J. Wilkin, and J. Kohut.
2008. Seasonal evolution of hydrographic fields in the central Middle Atlantic Bight from glider observations. Geophys. Res. Lett. 35:L03617.

Castro, J. I.
2011. The sharks of North America, 613 p. Oxford Univ. Press, New York.

Clarke, S. C., J. E. Magnussen, D. L. Abercrombie, M. K. McAllister, and M. S. Shivji.
2006. Identification of shark species composition and proportion in the Hong Kong shark fin market based on molecular genetics and trade records. Conserv. Biol. 20:201–211.

Compagno, L. J. V.
2001. Sharks of the world: an annotated and illustrated catalogue of shark species known to date. Vol. 2: Bullhead, mackerel and carpet sharks (Heterodontiformes, Lamniformes and Orectolobiformes). FAO Species Catalogue for Fishery Purposes 1, vol. 2, 269 p. FAO, Rome.

Cortés, E., F. Arocha, L. Beerkircher, F. Carvalho, A. Domingo, M. Heupel, H. Holtzhausen, M. N. Santos, M. Ribera, and C. Simpfendorfer.
2010. Ecological risk assessment of pelagic sharks caught in Atlantic pelagic longline fisheries. Aquat. Living Resour. 23:25–34.

Cortés, E., A. Domingo, P. Miller, R. Forselledo, F. Mas, F. Arocha, S. Campana, R. Coelho, C. Da Silva, F. H. V. Hazin, et al.
2015. Expanded ecological risk assessment of pelagic sharks caught in Atlantic pelagic longline fisheries. Collect. Vol. Sci. Pap. ICCAT 71:2637–2688.

Dodrill, J. W, and R. G. Gilmore.
1979. First North American continental record of the longfin mako (*Isurus paucus* Guitart Manday). Fla. Sci. 42:52–58.

Dulvy, N. K., J. K. Baum, S. Clarke, L. J. V. Compagno, E. Cortés, A. Domingo, S. Fordham, S. Fowler, M. P. Francis, C. Gibson, et al.
2008. You can swim but you can't hide: the global status and conservation of oceanic pelagic sharks and rays. Aquat. Conserv: 18:459–482.

Dulvy, N. K., S. L. Fowler, J. A. Musick, R. D. Cavanagh, P. M. Kyne, L. R. Harrison, J. K. Carlson, L. N. K. Davidson, S. V. Fordham, M. P. Francis, et al.
2014. Extinction risk and conservation of the world's sharks and rays. eLife 2014;3:e00590.

Francis, M. P., J. C. Holdsworth, and B. A. Block.
2015. Life in the open ocean: seasonal migration and diel diving behaviour of Southern Hemisphere porbeagle sharks (*Lamna nasus*). Mar. Biol. 162:2305–2323.

Frédou, F. L., M. T. Tolotti, T. Frédou, F. Carvalho, H. Hazin, G. Burgess, R. Coelho, J. D. Waters, P. Travassos, and F. H. V. Hazin.
2015. Sharks caught by the Brazilian tuna longline fleet: an overview. Rev. Fish Biol. Fish. 25:365–377.

Galuardi, B, and M. Lutcavage.
2012. Dispersal routes and habitat utilization of juvenile Atlantic bluefin tuna, *Thunnus thynnus*, tracked with mini PSAT and archival tags. PLoS ONE 7(5):e37829.

Garrick, J. A. F.
1967. Revision of sharks of genus *Isurus* with description of a new species (Galeoidea, Lamnidae). Proc. U.S. Natl. Mus. 118:663–690.

Gilly, W. F., U. Markaida, C. H. Baxter, B. A. Block, A. Boustany, L. Zeidberg, K. Reisenbichler, B. Robison, G. Bazzino, and C. Salinas.
2006. Vertical and horizontal migrations by the jumbo squid *Dosidicus gigas* revealed by electronic tagging. Mar. Ecol. Prog. Ser. 324:1–17.

Gilmore, R. G.
1983. Observations on the embryos of the longfin mako, *Isurus paucus*, and the bigeye thresher, *Alopias superciliosus*. Copeia 1983:375–382.
1993. Reproductive biology of lamnoid sharks. Environ. Biol. Fish. 38:95–114.

Goldman, K. J.
1997. Regulation of body temperature in the white shark, *Carcharodon carcharias*. J. Comput. Physiol. B 167:423–429.

Goldman, K. J., S. D. Anderson, R. J. Latour, and J. A. Musick.
2004. Homeothermy in adult salmon sharks, *Lamna ditropis*. Environ. Biol. Fish. 71:403–411.

Grace, M. A., W. B. Driggers III, J. Forrester, and N. Hopkins.
2007. Landing sling use increases data accuracy and sampling opportunities for large marine fishes captured during fishery-independent longline surveys. Fish. Res. 88:146–149.

Guitart Manday, D.
1966. Nuevo nombre para una especie de tiburón del génereo *Isurus* (Elasmobranchii: Isuridae) de aguas Cubanos. Poeyana (Inst. Biol.), A 15:1–9.
1975. Las pesquerías pelágico-oceánicas de corto radio de acciòn en la regiòn noroccidental de Cuba. Ser. Oceanol. Acad. Cienc. Cuba 31:1–26.

Hammerschlag, N., A. J. Gallagher, and D. M. Lazarre.
2011. A review of shark satellite tagging studies. J. Exp. Mar. Biol. Ecol. 398:1–8.

Hemida, F., and C. Capapé.
2008. On the occurrence of the longfin mako, *Isurus paucus* (Chondrichthyes: Isuridae) off the Algerian coast (southwestern Mediterranean). Acta Adriat. 49(2):185–189.

Hueter, R. E., C. A. Manire, J. P. Tyminski, J. M. Hoenig, and D. A. Hepworth.
2006. Assessing mortality of released or discarded fish using a logistic model of relative survival derived from tagging data. Trans. Am. Fish. Soc. 135:500–508.

Killam, K., and G. Parsons.
1986. First record of the longfin mako, *Isurus paucus*, in the Gulf of Mexico. Fish. Bull. 84:748–749.

Kohler, N. E., J. G. Casey, and P. A. Turner.
1998. NMFS Cooperative Shark Tagging Program, 1962–93: an atlas of shark tag and recapture data. Mar. Fish. Rev. 60(2):1–87.

Kyne, P. M., J. K. Carlson, D. A. Ebert, S. V. Fordham, J. J. Bizzarro, R. T. Graham, D. W. Kulka, E. E. Tewes, L. R. Harrison, and N. K. Dulvy.
2012. The conservation status of North American, Central American, and Caribbean chondrichthyans, 148 p. IUCN Species Survival Commission Shark Specialist Group, Vancouver, Canada.

Loefer, J. K., G. R. Sedberry, and J. C. McGovern.
2005. Vertical movements of a shortfin mako in the western north Atlantic as determined by pop-up satellite tagging. Southeast. Nat. 4:237–246.

Logan, J. M., R. Toppin, S. Smith, B. Galuardi, J. Porter, and M. Lutcavage.
2013. Contribution of cephalopod prey to the diet of large pelagic fish predators in the central North Atlantic Ocean. Deep Sea Res. (Part II: Top. Stud. Oceanogr.) 95:74–82.

Maia, A., N. Queiroz, J. P. Correia, and H. Cabral.
2006. Food habits of the shortfin mako, *Isurus oxyrinchus*, off the southwest coast of Portugal. Environ. Biol. Fish. 77:157–167.

MINAL (Ministry for the Food Industry).
2015. National plan of action for the conservation and management of Chondrichthyes in the Republic of Cuba, 48 p. Ministry for the Food Industry, Havana, Cuba.

Mollet, H. F., G. Cliff, H. L. Pratt Jr., and J. D. Stevens.
2000. Reproductive biology of the female shortfin mako, *Isurus oxyrinchus* Rafinesque, 1810, with comments on the embryonic development of lamnoids. Fish. Bull. 98:299–318.

Mucientes, G., R. Bañón, and N. Queiroz.
2013. Updated distribution range of longfin mako *Isurus paucus* (Lamniformes: Lamnidae) in the North Atlantic. J. Appl. Ichthyol. 29:1163–1165.

Musyl, M. K., R. W. Brill, C. H. Boggs, D. S. Curran, T. K. Kazama, and M. P. Seki.
2003. Vertical movements of bigeye tuna (*Thunnus obesus*) associated with islands, buoys, and seamounts near the main Hawaiian Islands from archival tagging data. Fish. Oceanogr. 12:152–169.

Nasby-Lucas, N., H. Dewar, C. H. Lam, K. J. Goldman, and M. L. Domeier.
2009. White shark offshore habitat: a behavioral and environmental characterization of the eastern Pacific shared offshore foraging area. PLoS ONE 4(12):e8163.

Newton, K. C., J. Wraith, and K. A. Dickson.
2015. Digestive enzyme activities are higher in the shortfin mako shark, *Isurus oxyrinchus*, than in ectothermic sharks as a result of visceral endothermy. Fish Physiol. Biochem. 41:887–898.

Pade, N. G., N. Queiroz, N. E. Humphries, M. J. Witt, C. S. Jones, L. R. Noble, and D. W. Sims.
2009. First results from satellite-linked archival tagging of porbeagle sharks, *Lamna nasus*: area fidelity, wider-scale movements and plasticity in diel depth changes. J. Exp. Mar. Biol. Ecol. 370:64–74.

Queiroz, N., S. Araújo, P. A. Ribeiro, P. Tarroso, R. Xavier, and A. M. Santos.
2006. A first record of longfin mako, *Isurus paucus*, in the mid-North Atlantic. Mar. Biodivers. Rec. 1:e34.

Queiroz, N., N. E. Humphries, G. Mucientes, N. Hammerschlag, F. P. Lima, K. L. Scales, P. I. Miller, L. L. Sousa, R. Seabra, and D. W. Sims.
2016. Ocean-wide tracking of pelagic sharks reveals extent of overlap with longline fishing hotspots. Proc. Natl. Acad. Sci. U.S.A. 113:1582–1587.

R Core Team.
2015. R: a language and environment for statistical computing. R Foundation for Statistical Computing, Vienna, Austria. [Available from website, accessed January 2016.]

Reardon, M. B., L. Gerber, and R. D. Cavanagh.
2006. *Isurus paucus*. The IUCN Red List of Threatened Species 2006: e.T60225A12328101.

Rogers, P. J., C. Huveneers, B. Page, S. D. Goldsworthy, M. Coyne, A. D. Lowther, J. G. Mitchell, and L. Seuront.
2015. Living on the continental shelf edge: habitat use of juvenile shortfin makos *Isurus oxyrinchus* in the Great Australian Bight, southern Australia. Fish. Oceanogr. 24:205–218.

Roper, C. F. E., and R. E. Young.
1975. Vertical distribution of pelagic cephalopods. Smithson. Contrib. Zool. 209, 51 p.

Saunders, R. A., F. Royer, and M. W. Clarke.
2011. Winter migration and diving behaviour of porbeagle shark, *Lamna nasus*, in the Northeast Atlantic. ICES J. Mar. Sci. 68:166–174.

Sebastian, H., P. A. Haye, and M. S. Shivji.
2008. Characterization of the pelagic shark-fin trade in north-central Chile by genetic identification and trader surveys. J. Fish Biol. 73:2293–2304.

Sembiring, A., N. P. D. Pertiwi, A. Mahardini, R. Wulandari, E. M. Kurniasih, A. W. Kuncoro, N. K. D. Cahyani, A. W. Anggoro, M. Ulfa, H. Madduppa, et al.
2015. DNA barcoding reveals targeted fisheries for endangered sharks in Indonesia. Fish. Res. 164:130–134.

Sepulveda, C. A., S. Kohin, C. Chan, R. Vetter, and J. B. Graham.
2004. Movement patterns, depth preferences, and stomach temperatures of free-swimming juvenile mako sharks, *Isurus oxyrinchus*, in the Southern California Bight. Mar. Biol. 145:191–199.

Sepulveda, C. A., A. Knight, N. Nasby-Lucas, and M. L. Domeier.
2010. Fine-scale movements of the swordfish *Xiphias gladius* in the Southern California Bight. Fish. Oceanogr. 19:279–289.

Speed, C. W., I. C. Field, M. G. Meekan, and C. J. A. Bradshaw.
2010. Complexities of coastal shark movements and their implications for management. Mar. Ecol. Prog. Ser. 408:275–293.

Stevens, J. D., R. W. Bradford, and G. J. West.
2010. Satellite tagging of blue sharks (*Prionace glauca*) and other pelagic sharks off eastern Australia: depth behaviour, temperature experience and movements. Mar. Biol. 157:575–591.

Stillwell, C. E., and N. E. Kohler.
1982. Food, feeding habits, and estimates of daily ration of the shortfin mako (*Isurus oxyrinchus*) in the northwest Atlantic. Can. J. Fish. Aquat. Sci. 39:407–414.

Wakida-Kusunoki, A. T., and D. de Anda-Fuente.
2012. Presence of longfin mako shark *Isurus paucus* (Chondrichthyes: Lamnidae) in the south-eastern Gulf of Mexico, Tabasco, Mexico. Mar. Biodivers. Rec. 5:e92.

Weng, K. C., P. C. Castilho, J. M. Morrissette, A. M. Landeira-Fernandez, D. B. Holts, R. J. Schallert, K. J. Goldman, and B. A. Block.
2005. Satellite tagging and cardiac physiology reveal niche expansion in salmon sharks. Science 310:104–106.

Weng, K. C., A. M. Boustany, P. Pyle, S. D. Anderson, A. Brown, and B. A. Block.
2007. Migration and habitat of white sharks (*Carcharodon carcharias*) in the eastern Pacific Ocean. Mar. Biol. 152:877–894.

Weng, K. C., D. G. Foley, J. E. Ganong, C. Perle, G. L. Shillinger, and B. A. Block.
2008. Migration of an upper trophic level predator, the salmon shark *Lamna ditropis*, between distant ecoregions. Mar. Ecol. Prog. Ser. 372:253–264.

National Marine
Fisheries Service
NOAA

Fishery Bulletin
established in 1881

Spencer F. Baird
First U.S. Commissioner
of Fisheries and founder
of *Fishery Bulletin*

Age, growth, and length–weight relationship of roosterfish (*Nematistius pectoralis*) in the eastern Pacific Ocean

Sofia Ortega-Garcia (contact author)[1]
Chugey Sepulveda[2]
Scott Aalbers[2]
Ulianov Jakes-Cota[1]
Ruben Rodriguez-Sanchez[1]

Email address for contact author: sortega@ipn.mx

[1] Instituto Politécnico Nacional
Centro Interdisciplinario de Ciencias Marinas
Avenida Instituto Politécnico Nacional s/n
Colonia Playa Palo de Santa Rita
C.P. 23096 La Paz, Baja California Sur, México

[2] Pfleger Institute of Environmental Research
2110 South Coast Highway
Oceanside, California 92054

Abstract—Growth of roosterfish (*Nematistius pectoralis*) was estimated by analyzing daily growth increments of sagittal otoliths collected from individuals captured in El Golfo Dulce, Costa Rica during 2013–2014 and in southern Baja California Sur, Mexico during 2010–2015. Isometric growth was observed for all individuals and no significant differences were observed in the length–weight relationships between sexes or locations. Age estimates ranged from 18 d (0.05 years) to 545 d (1.5 years), although 26% of otoliths (57–133 cm) were not legible because narrow daily growth increments were difficult to differentiate in older fish. Individual growth parameters indicate that roosterfish grow at a rapid rate during the first year of life, reaching sizes of around 60–70 cm in fork length. Although future field validation is necessary, the results of our study provide insight into the life history of this valuable resource of the eastern Pacific Ocean.

Manuscript submitted 11 March 2016.
Manuscript accepted 30 November 2016.
Fish. Bull. 115:117–124 (2017).
Online publication date: 27 December 2016.
doi: 10.7755/FB.115.1.10

The views and opinions expressed or implied in this article are those of the author (or authors) and do not necessarily reflect the position of the National Marine Fisheries Service, NOAA.

A game fish that inhabits the neritic waters of the subtropical and tropical eastern Pacific Ocean (Eschmeyer et al., 1983), the roosterfish (*Nematistius pectoralis*) is the only species in the genus *Nematistius* (family Nematistiidae). The most notable external feature of this species is the presence of 7 elongated dorsal spines, which give rise to its common name (Rosenblatt and Bell, 1976) and allows it to be easily distinguished from other species (Niem, 1995).

The roosterfish is a coastal species that has been found to occur in the Pacific Ocean from San Clemente, Southern California to San Lorenzo Island, Peru, including the Gulf of California and the Galapagos Islands (Love et al., 2005). Results from work to date indicate that roosterfish reside primarily in warm (23–31°C), shallow waters where they may spend up to 90% of their time between the sea surface and a depth of 12 m (Sepulveda et al., 2015). All age classes are considered neritic; juveniles are often found along the shoreline and larger individuals are commonly associated with both the surf line and complex near shore habitats (i.e., reefs and sand bars) (Niem, 1995; Sepulveda et al., 2015).

Roosterfish can attain sizes up to 191 cm in total length and more than 51.7 kg (Robertson and Allen, 2015). They are active predators that have been reported to feed in shallow waters (i.e., depths of 3–4 m) on schooling fish species, such as species of mojarra (i.e., Pacific spotfin mojarra [*Eucinostomus dowii*] and graceful mojarra [*E. gracilis*]), and species of anchovy (i.e., sharpnose anchovy [*Anchoa ischana*] and *Anchoa* spp.) (Hobson, 1968; Rodríguez-Romero et al., 2009).

The roosterfish is a very important resource for sportfishing industries, especially for those that operate at destinations favored by ecotourists, such as Baja California Sur, mainland Mexico, and the coast of Central America. Roosterfish contribute significantly to the local economy because it is a common target of inshore anglers; in fact, this species is sought out among anglers around the

world (Eschmeyer et al., 1983). To a lesser degree, the roosterfish also supports small-scale artisanal fisheries along the coast of Baja California Sur and Central America; however, because of its limited market value, it is not typically the primary target of such fishing operations (Lindner, 1947; Niem, 1995).

Despite the ecological and economic importance of roosterfish, very few scientific studies have focused on this species and basic biological parameters remain largely unknown. In particular, questions pertaining to age and growth, natural mortality, longevity, and reproductive biology remain unanswered. These parameters are essential for fisheries management and form the basis for most stock assessment models (Goldman, 2005). This information is also essential for understanding other biological and population traits such as productivity, yield per recruit, predator and prey dynamics, and habitat requirements (DeVries and Frie, 1996; Campana, 2001; Robinson and Motta, 2002).

Given the importance of this species to regional fisheries off the coast of Baja California Sur and Central America, we estimated age and growth in our study by counting presumed daily growth increments (DGIs) within the sagittal otolith. The results of our study provide the first estimates of growth for this species and allow intraspecific comparisons of growth between 2 geographically distinct locations along the range of the roosterfish in the eastern Pacific Ocean.

Materials and methods

Collection details

From 2010 through 2015, roosterfish specimens were obtained from the sportfishing fleet in Cabo San Lucas and La Paz, Baja California Sur, Mexico. Similarly, from 2013 through 2014, specimens were collected from commercial and recreational fleets that operated out of the Golfo Dulce, Costa Rica. Each specimen was measured to determine fork length (FL) to the nearest 0.1 cm and weighed to the nearest 0.01 kg. Sex was determined by visual inspection of the gonads, and, when possible, sagittal otolith pairs were removed, cleaned, and stored dry.

Length–weight relationships

Length–weight relationships (LWRs) were estimated by using the allometric equation:

$$W = a\mathrm{FL}^b,$$

where W = the weight; and
a and b = the intercept and the slope of the regression line, respectively (Ricker, 1975).

As with previous works, we assumed that, when b was equal to 3, the relationship was considered to be isometric (Sangun et al., 2007). Similarly, b values $\neq 3$ were associated with allometric growth (Froese, 2006). Estimates of LWRs were calculated independently for both sex (males and females) and location (Baja California Sur and Golfo Dulce) and compared by using a Student's t-test (Zar, 2010). A Student's t-test was also used to evaluate whether b values were significantly different from the null hypothesis for isometric growth (H_0: b=3) (Sangun et al., 2007; Zar, 2010).

Preparation and analysis of otoliths

Preparation of otoliths followed closely the protocol described by Secor et al., 1992. Briefly, the right otolith of each specimen was embedded in crystal polyester resin and allowed to harden and dry for a 24-h period. We created transverse sections (0.6 mm) through each otolith that included the core (Fig. 1) by using an IsoMet Low Speed Saw[1] (model 11-1280-160; Buehler, Lake Bluff, IL) equipped with a diamond wafering blade (series 15HC, Buehler). Because otolith increments (e.g., daily or annual) of many perciform fish species are not deposited in the sagittal plane, the transverse or the frontal planes typically are used for assessing DGIs (Secor et al., 1992).

Most otoliths need some form of preparation before their microstructure can be accurately determined; therefore, a polishing procedure was used to remove material, expose the core region, and reveal the presumed DGIs (Secor et al., 1992). To clearly define DGIs and facilitate readings, transversal sections were mounted on histological slides with Cytoseal mounting medium (Thermo Fisher Scientific, Waltham, MA) and hand polished with a series of micrometric sandpaper of decreasing grit size (15–3 µm, Diamond Lapping Film disc; Buehler). For finishing, sections were polished with 0.3-µm MicroPolish alumina (Buehler) and 0.3-µm MicroCloth micrometric sandpaper (Buehler).

Two readers independently counted presumed DGIs of prepared otolith sections without prior knowledge of fish length and weight. Readers counted DGIs on transverse sections by using a microscope with transmitted light (40–100×). Daily growth increments were counted from the core toward the dorsal edge of the otolith along the same transect (Fig. 1).

The consistency or concordance of counts between readers was estimated by using a coefficient of variation (CV) (Chang, 1982):

$$CV_j = 100\% \times \frac{\sqrt{\sum_{i=1}^{R} \frac{(X_{ij}-X_j)^2}{R-1}}}{X_j}, \quad (1)$$

where CV_j = the age precision estimate for the jth fish;
X_{ij} = the ith age determination of the jth fish;
X_j = the mean age estimate of the jth fish; and
R = the number of times each fish was aged.

Lengths at age derived from otolith readings were used to estimate the 3 parameters of the standard von Bertalanffy growth model:

[1] Mention of trade names or commercial companies is for identification purposes only and does not imply endorsement by the National Marine Fisheries Service, NOAA.

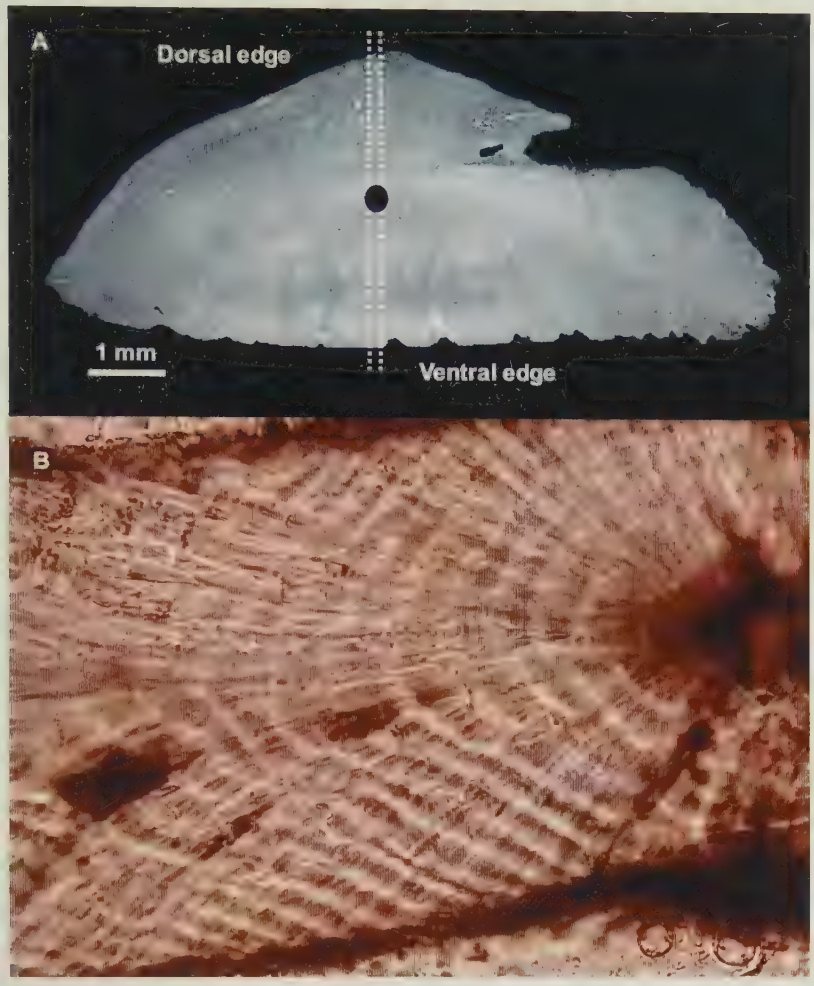

Figure 1

(**A**) Right sagitta of a 63.5-cm-FL roosterfish (*Nematistius pectoralis*) captured in Baja California Sur, Mexico, in 2014. Dotted white lines represent a transverse section through the core, which is indicated by the black circle. (**B**) Sagitta showing daily growth increments (that consists of two rings: gray and white) from a 5.2-cm-FL roosterfish (18 d in age) captured in Baja California Sur in 2014.

$$L_t = L_\infty[1-e^{-k(t-t_0)}], \quad (2)$$

where L_t = length (FL in centimeters) at age t;
L_∞ = average maximum length;
k = the individual growth coefficient;
t_0 = the hypothetical age when the length is equal to 0; and
t = age.

A power function was also tested; however, because our results were similar to those of the von Bertalanffy growth model, only results from the von Bertalanffy growth model were included for consistency and comparison with other growth studies.

Growth parameters were estimated independently for both study areas (Baja California Sur and Costa Rica), and an analysis of the residual sum of squares was used to evaluate the possible differences in parameters between the 2 locations (Ratkowsky, 1983).

Parameters for both the LWR and von Bertalanffy growth model were estimated by using nonlinear least squares by means of an iterative process with the Gauss-Newton algorithm (Bates and Watts, 1988), which allows estimation of nonlinear model parameters without needing to transform the data into a linear function. Statistical analyses were performed with R statistical software, vers. 3.2.3 (R Core Team, 2015). Significance was determined by using a t-test with an alpha level of 0.05.

Results

During the sampling period, 290 roosterfish (190 specimens from Baja California Sur and 100 specimens from Costa Rica) were measured and weighed. Specimens from Baja California Sur (66 males, 74 females, and 50 fish of unknown sex) ranged from 5.2 to 133.0 cm FL and from 0.01 to 25.87 kg in weight. Specimens from Costa Rica (47 males, 18 females, and 35 fish of unknown sex) ranged from 8.3 to 116.0 cm FL and 0.01 to 17.80 kg (Fig. 2).

The estimated parameters of the LWR by area and sex are provided in Table 1. Comparisons of growth parameters (values of the exponent b) revealed that all LWRs were not significantly different from a value of 3 (Student's t-test: $P>0.05$) and indicated that roosterfish growth is isometric (Table 1). Given the finding of isometric growth for both location and sex, the length and weight data were pooled into one representative LWR for this study (Fig. 3, Table 1).

For age estimation, 182 pairs of sagittal otoliths were collected and processed, 103 pairs from fish collected in Baja California Sur (5.2–120.0 cm FL) and 79 pairs from fish collected in Costa Rica (13.5–116.0 cm FL). Of these pairs, 130 pairs or 71.5% (Baja California Sur=68 and Costa Rica=62) were readable and used in the age estimation analyses. The remaining 52 otolith pairs (Baja California Sur=35 and Costa Rica=17) were discarded for one or more of the following reasons: the otoliths were broken, crosscuts did not include the core,

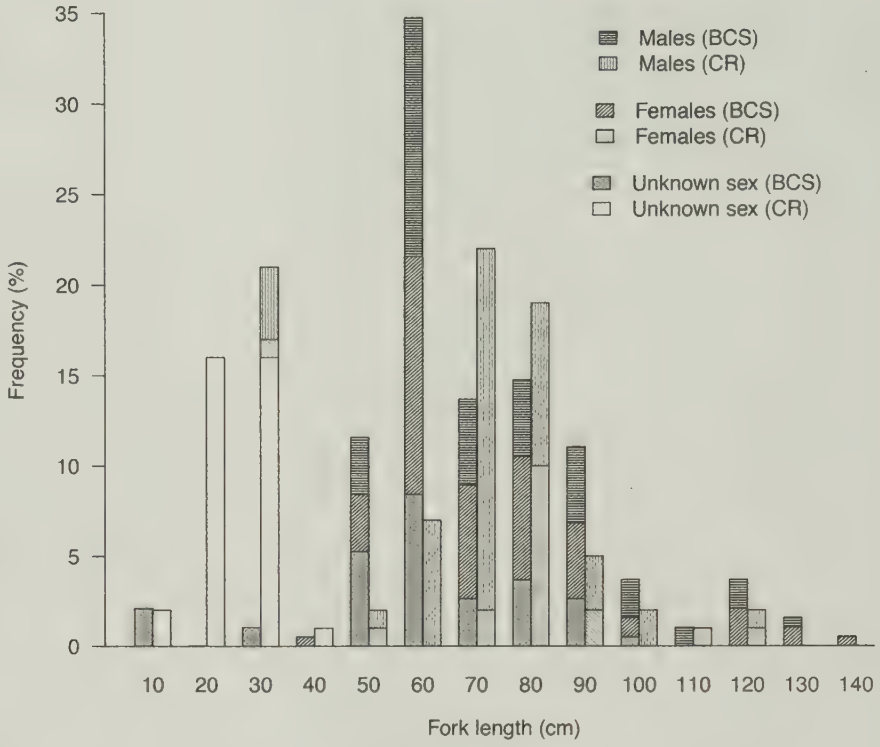

Figure 2

Size distribution (measured in fork length) of roosterfish (*Nematistius pectoralis*) captured in Baja California Sur (BCS), Mexico, during 2010–2015 and in Golfo Dulce, Costa Rica (CR), 2013–2014.

Table 1

Parameters (a and b) of the length–weight relationship of roosterfish (*Nematistius pectoralis*) captured from 2 locations, Baja California Sur (BCS), Mexico, during 2010–2015 and Costa Rica (CR) during 2013–2014, by area and sex, and Student's t-test results for the testing of isometric growth.

Area	Sex	a	b	t	P
BCS	Males	2.4×10^{-5}	2.84	−0.18	0.85
BCS	Females	2.8×10^{-5}	2.81	−0.25	0.80
BCS	Sexes combined	2.7×10^{-5}	2.82	−0.25	0.79
CR	Males	2.7×10^{-5}	2.81	−0.48	0.62
CR	Females	2.8×10^{-5}	2.81	−0.50	0.62
CR	Sexes combined	2.7×10^{-5}	2.81	−0.60	0.54
Combined	Sexes combined	2.6×10^{-5}	2.82	−0.29	0.76

sections were overpolished, and otolith sections were illegible because of increasingly narrow widths of DGIs in older fish.

The estimated ages of the fish assessed from Baja California Sur ranged from 18 d (0.05 years, 5.2 cm FL) to 548 d (1.49 years, 86 cm FL). The range of age estimates from Costa Rica was 32 d (0.08 years, 13.5 cm FL) to 448 d (1.22 years, 78.7 cm FL).

In most cases, it was possible to count DGIs from sagittal otoliths of fish <57 cm FL (the size reached at an age of approximately 1 year). The agreement between the estimated ages assigned independently by the 2 readers revealed a CV of 9.02%, indicating a high consistency. The average CV for different size classes increased from 5.9 for fish with 18–100 DGIs to 6.8 for fish with 101–199 DGIs and 9.5 for fish with 200–

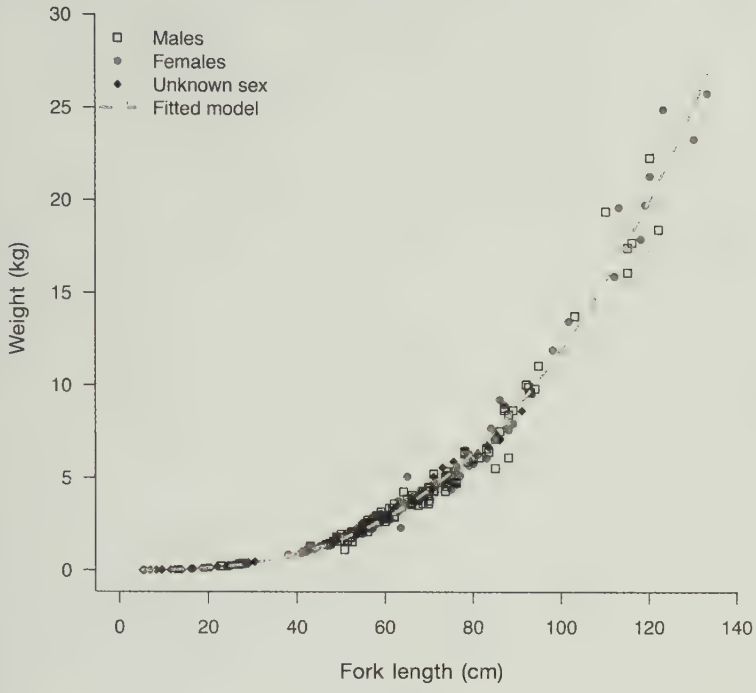

Figure 3

Collective length–weight relationship of all roosterfish (*Nematistius pectoralis*) examined in this study. Specimens were captured in Baja California Sur, Mexico, in 2010–2015 and in Golfo Dulce, Costa Rica, 2013–2014.

549 DGIs. Reader confidence was reduced for samples from fish that ranged from 57 to 86 cm FL, primarily because of the narrowing and softening of DGI edges. Similarly, for roosterfish >86 cm FL, DGIs were not easily differentiated and, therefore, these fish were not included in the age-estimation portion of our study. Annual growth marks were not observed in sagittal otoliths or in cross sections.

The estimated parameters of the von Bertalanffy growth model are given by area in Table 2. The analysis of residual sums of squares did not reveal significant differences in growth parameters between Baja California Sur and Costa Rica (P>0.05). Therefore, the data for both locations was combined into a single growth model (Fig. 4). Estimates of growth parameters indicate that roosterfish grow rapidly during the first year of life, attaining a size of approximately 60–70 cm FL within the first year (40% of L_∞).

Discussion

Our study provides the first estimates of age and growth for the roosterfish, a species that supports a substantial recreational fishery throughout the eastern Pacific Ocean. The growth estimates presented here indicate that roosterfish grow at a rapid rate and that they may reach up to 60–70 cm FL (40% of L_∞) during the first year of life. Accelerated growth in the first year of life has been reported for other warm-water pelagic species, such as the cobia (*Rachycentron canadum*; Franks et al., 1999), dolphinfish (*Coryphaena hippurus*; Schwenke and Buckel, 2008), blue marlin (*Makaira nigricans*; Prince et al., 1991), and sailfish (*Istiophorus platypterus*; Alvarado-Castillo and Félix-Uraga, 1996). As hypothesized previously, rapid early growth is likely advantageous for survival because it is linked to swimming speed, foraging success, and predation (Prince et al., 1991). Although field validation is necessary, our work provides an initial hypothesis regarding the growth of this valuable eastern Pacific Ocean species and increases scientific knowledge of this poorly known species.

Samples of roosterfish were obtained primarily from recreational fisheries that operate seasonally throughout Baja California Sur and Central America. Because roosterfish are typically released in most of these recreational fisheries, acquisition of samples was challenging; specimens from smaller size classes (<50 cm FL) proved to be especially difficult to obtain. In addition, because larger individuals are particularly prized in the catch-and-release fisheries, guides and captains rarely harvest specimens >100 cm FL, a tendency that further inhibited the collection of larger individuals for our study.

Length–weight relationships

The estimated b values (Table 1) were within the normal, expected range for fish (b=2.5–3.5) (Froese, 2006). Bagenal and Tesch (1978) suggested that when the

Table 2

Parameter values from the von Bertalanffy growth model for roosterfish (*Nematistius pectoralis*) captured in Baja California Sur (BCS), Mexico, and Golfo Dulce, Costa Rica (CR), during 2010–2015: average maximum length (L_∞), measured as fork length in centimeters, individual growth coefficient (k), and the hypothetical age when the length is equal to 0 (t_0), measured in years.

Area	L_∞	k	t_0
BCS	166.90	0.48	−0.02
CR	171.72	0.47	−0.08
Areas combined	163.77	0.47	−0.08

value of b is between 2.8 and 3.2, growth is considered to be isometric (i.e., growth of all body parts is consistent and proportional throughout development). Based on t-test results, estimated b values were not significantly different from 3 (Table 1), indicating that isometric growth for roosterfish is independent of location and sex.

Because we did not identify differences in the LWR, samples were pooled and collectively presented (see Froese, 2006). A similar b value was reported by González-Sansón et al. (2014) for roosterfish caught in a coastal lagoon off Barra de Navidad, Jalisco, Mexico. However, the González-Sansón et al. (2014) study was based on a limited sample size and size range of fish (b=2.92, n=8; 7.5–29.3 cm in total length). Values of the exponent b can be influenced by statistical procedure and sample size (Bolger and Connolly, 1989), as well as by variations associated with size range, maturation, sex, and time of year (Cone, 1989). Because the spawning dynamics of this species (i.e., season and time of year) remain unknown and we were unable to obtain samples from exceptionally large individuals, it is possible that differences in LWR exist for larger, mature roosterfish.

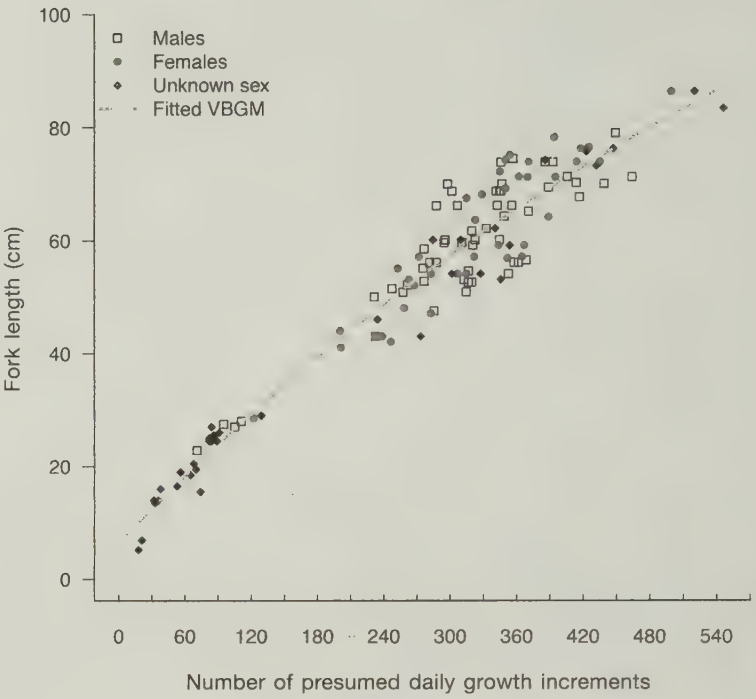

Figure 4

The combined (sex and location) von Bertalanffy growth model (VBGM) of roosterfish (*Nematistius pectoralis*) captured in Baja California Sur, Mexico, in 2010–2015 and in Golfo Dulce, Costa Rica, 2013–2014.

Age and growth

The sagittal otolith is the preferred hard structure for estimating age in fish because deposition occurs continuously throughout life, a scenario that enhances age estimation when compared with the use of other hard structures (Campana and Thorrold, 2001). Otoliths are also preferred for age estimation because the structures are not lost or shed (as they are with scales) or reabsorbed (as with bones and spines) (Ramírez-Peréz et al., 2011). Sectioned and polished otoliths from individuals <57 cm FL provided visible DGIs that were readily distinguishable. However, in otoliths from larger individuals (>57 cm FL), it was difficult to differentiate between recent outer edge DGIs, thus causing increased uncertainty in age estimates. Campana (1999) reported that calcium, oxygen, and carbon dominate the elemental composition of the otolith and that these elements form the calcium carbonate matrix of the otolith. An excess of calcium carbonate in sagittal otoliths may hinder ridge quantification to varying degrees (Hill et al., 1989).

In cross sections, DGIs were counted from the core to the dorsal edge of the otolith. The path of visual counts were not always in a straight line from the core to the outer edge of a sagitta. The optimal reading path that provided the best visual clarity of DGIs typically followed a somewhat circuitous route that shifted from one area of the sagitta to another (Uchiyama et al., 1986).

The precision of age estimates for the 2 readers of this study was high (CV=9.02%) and aligns with CV values from other studies in which counts of annual marks were used (Prince et al., 1991; DeMartini et al., 2007). Campana (2001) proposed that there is no a priori value of CV that can be assigned as a target level for studies of age because it is highly influenced by the species and the nature of the hard structure itself. In addition, the consistency between readings often decreases as fish age increases because growth marks are closer together in older fish (Steward et al., 2009).

We found that the precision of DGI counts decreased with increasing age (18–548 d) and FL (5.2–86.0 cm). Prince et al. (1991) suggested that estimating the age of large or old fish by using DGI counts may result in an underestimation of age and an overestimation of the growth rate. Because it was not possible to count DGIs precisely in roosterfish >86 cm FL (1.5 years old), it is recommended that otolith DGIs be used only for individuals of ages less than 1 year (the age reached at a size of approximately 66 cm FL).

Although it was not possible to detect annual marks on the otoliths of roosterfish in our study, a previous study had focused on assessing the potential use of dorsal spines for aging this species (Chávez-Arellano, 2016). Chávez-Arellano (2016) analyzed roosterfish between 14 and 133 cm FL and found a similar average length (70.61 cm FL) for year-1 individuals. However,

robust comparisons between these studies are not possible because the work of Chávez-Arellano (2016) was not focused on age determination; he assessed only dorsal spine suitability for aging purposes. Despite differences in our study and that of Chávez-Arellano (2016), both works support the hypothesis of rapid growth in this species, especially in the first year of life. As has been reported for others species like the dolphinfish, additional structures (e.g., scales) may prove useful in future age assessments of the roosterfish (Schwenke and Buckel, 2008).

Although field validation is necessary to confirm the proposed growth hypothesis for roosterfish, the inclusion of small size classes (5 cm FL) and a large size range provides support for the use of DGIs for age estimation. Oxenford and Hunte (1983) assumed DGIs for dolphinfish, and Uchiyama et al. (1986) subsequently validated those values with both hatchery-reared and fish caught in the wild. For some species, DGIs have been validated by experiments with fish reared in captivity, otolith marking, radiochemical dating, or various other techniques (Prince et al., 1991; Campana, 2001). Ideally, validation experiments should include the period during which the initial growth ring is formed and should evaluate the regularity of growth-ring formation during all life stages (e.g., spawning, migration, and periods of starvation) because all of these factors may influence the regularity of deposition rates (Uchiyama et al., 1986).

Values of L_∞ estimated from the von Bertalanffy growth equation were greater than the length of the largest roosterfish sampled in our study (133 cm FL) and slightly lower than the maximum length recorded by Robertson and Allen (2015). This difference likely occurred because the estimated parameters were based only on the initial phases of growth for roosterfish (up to 1.49 years).

The relatively rapid growth rate that we report here is similar for both regions (Baja California Sur and Costa Rica), despite differences in oceanographic conditions (e.g., annual sea-surface temperature) or potential prey sources and availability. These similarities may be due to the lack of larger individuals in this study (e.g., readability of fish >86 cm FL), a scenario that may have masked potential ontogenetic differences. It may also be that roosterfish from the 2 regions have deposition rates that differ from each other. If ring formation occurs at a rate that is less than one ring per day, it may be that this study underestimates the actual age of the fish surveyed. Regardless, this work presents the first data supporting a growth hypothesis for this species, and future investigations should focus on the use of field validation techniques.

Acknowledgments

We wish to thank the Pfleger Institute of Environmental Research and the Instituto Politécnico Nacional for the research grant SIP20150861. We also are grateful to C. McCue and M. Gutiérrez for their help during sampling and to the sportfishing fleet at Cabo San Lucas, Baja California Sur, Mexico. The senior author and R. Rodríguez-Sánchez received a Comision de Operacion y Fomento de Actividades Academicas fellowship. We thank the anonymous reviewers for their constructive comments, which helped us to improve the manuscript.

Literature cited

Alvarado-Castillo, R. M., and R. Félix-Uraga.
1996. Determinación de la edad de *Istiophorus platypterus* (Pisces: Istiophoridae) al sur del Golfo de California, México. Rev. Biol. Trop. 44(1):233–239.

Bagenal, T. B., and F. W. Tesch.
1978. Age and growth. *In* Methods for assessment of fish production in freshwater (T. B. Bagenal, ed.), p. 101–136. Blackwell Scientific Publications, Oxford, UK.

Bates, D. M., and D. G. Watts.
1988. Nonlinear regression analysis and its applications, 365 p. John Wiley and Sons Inc., New York.

Bolger, T., and P. L Connolly.
1989. The selection of suitable indices for the measurement and analysis of fish condition. J. Fish Biol.

Campana, S. E.
1999. Chemistry and composition of fish otoliths: pathways, mechanisms and applications. Mar. Ecol. Prog. Ser. 188: 263–297.
2001. Accuracy, precision and quality control in age determination, including a review of the use and abuse of age validation methods. J. Fish Biol. 59:197–242.

Campana, S. E., and S. R. Thorrold.
2001. Otoliths, increments, and elements: keys to a comprehensive understanding of fish population. Can. J. Fish. Aquat. Sci. 58:30–38.

Chang, W. Y. B.
1982. A statistical method for evaluating the reproducibility of age determination. Can. J. Fish. Aquat. Sci. 39:1208–1210.

Chávez-Arellano, R.
2016. Uso potencial de las espinas de la aleta dorsal del pez gallo, *Nematistius pectoralis* Gill, 1862, para la determinación de edad. Bachelor's thesis, 48 p. Universidad Autonoma de Baja California Sur, La Paz, Baja California Sur, Mexico.

Cone, R. S.
1989. The need to reconsider the use of condition indices in fisheries science. Trans. Am. Fish. Soc. 118:510–514.

DeMartini, E. E., J. H. Uchiyama, R. L. Humphreys Jr., J. D. Sampaga, and H. A. Williams.
2007. Age and growth of swordfish (*Xiphias gladius*) caught by the Hawaii-based pelagic longline fishery. Fish. Bull. 105:356–367.

DeVries, D. R., and R. V. Frie.
1996. Determination of age and growth. *In* Fisheries techniques, 2nd ed. (B. R. Murphy and D. W. Willis, eds.), p. 483–512. Am. Fish. Soc., Bethesda, MD.

Eschmeyer, W. N., E. S. Herald, and H. Hammann.
1983. A field guide to Pacific coast fishes of North America, 336 p. Houghton Mifflin Co., Boston, MA.

Franks, J. S, J. R. Warren, and M. V. Buchanan.
1999. Age and growth of cobia, *Rachycentron canadum*,

from the northeastern Gulf of Mexico. Fish. Bull. 97:459–471.

Froese, R.
2006. Cube law, condition factor and weight–length relationships: history, meta-analysis and recommendations. J. Appl. Ichthyol. 22:241–253.

Goldman, K. J.
2005. Age and growth of elasmobranch fishes. *In* Management techniques for elasmobranch fisheries (J. A. Musick and R. Bonfil, eds.), p. 76–102. FAO Fish. Tech. Pap. 474, Rome.

González-Sansón, G., C. Aguilar-Betancourt, D. Kosonoy-Aceves, G. Lucano-Ramírez, S. Ruiz-Ramírez, J. R. Flores-Ortega, and F. Silva-Bátiz.
2014. Weight–length relationships for 38 fish species of Barra de Navidad coastal lagoon, Jalisco, Mexico. J. Appl. Ichthyol. 30:428–430.

Hill, K. T., G. M. Cailliet and R. L. Radtke.
1989. A comparative analysis of growth zones in four calcified structures of Pacific blue marlin, *Makaira nigricans*. Fish. Bull. 87: 829–843.

Hobson, E. S.
1968. Predatory behavior of some shore fishes in the Gulf of California. U.S. Fish Wildl. Serv., Res. Rep. 73, 92 p.

Lindner, M. J.
1947. The commercial marine fishes, crustaceans and molluscs of the west coast of Mexico. Trans. Am. Fish. Soc. 74:71–80.

Love, M. S., C. W. Mecklenburg, T. A. Mecklenburg, and L. K. Thorsteinson.
2005. Resource inventory of marine and estuarine fishes of the West Coast and Alaska: a checklist of North Pacific and Arctic Ocean species from Baja California to the Alaska–Yukon border, 276 p. U.S. Dep. Interior, U.S. Geol. Surv., Biol. Res. Div., Seattle, WA.

Niem, V. H.
1995. Nematistiidae. *In* Pacífico centro-oriental. Volumen III. Vertebrados—Parte 2 (W. Fischer, F. Krupp, W. Schneider, C. Sommer, K. E. Carpenter, and V. H. Niem, eds.), p. 1322. Guía FAO para la identificación de especies para los fines de la pesca. FAO, Rome.

Oxenford, H. A., and W. Hunte.
1983. Age and growth of dolphin, *Coryphaena hippurus*, as determined by growth rings in otoliths. Fish. Bull. 81:906–909.

Prince, E. D., D. W. Lee, and J. R. Zwelfel.
1991. Estimating age and growth of young Atlantic blue marlin, *Makaira nigricans* from otolith microstructure. Fish. Bull. 89:441–459.

R Core Team.
2015. R: a language and environment for statistical computing. R Foundation for Statistical Computing, Vienna, Austria. [Available from website, accessed December 2015.]

Ramírez-Peréz, J. S., F. N. Melo-Barrera, and L. E. Ayala-Bobadilla.
2011. Age and growth of Pacific golden-eye tilefish (*Caulolatilus affinis*) in the central region of the Gulf of California. Cienc. Mar. 37:71–85.

Ratkowsky, D. A.
1983. Nonlinear regression modeling: a unified practical approach, 288 p. Marcel Dekker Inc., New York.

Ricker, W. E.
1975. Computation and interpretation of biological statistics of fish populations. Bull. Fish. Res. Board Can. 191, 382 p.

Robertson, D. R., and G. R. Allen.
2015. Shorefishes of the tropical eastern Pacific: online information system: online information system. Version 2.0. Smithsonian Tropical Research Institute, Balboa, Panama.

Robinson, M. P., and P. J Motta.
2002. Patterns of growth and the effects of scale on the feeding kinematics of the nurse shark (*Ginglymostoma cirratum*). J. Zool. 256:449–462.

Rodríguez-Romero, J., X. G. Moreno-Sanchez, L. A. Abitia-Cárdenas, and D. S. Palacios-Salgado.
2009. Trophic spectrum of the juvenile roosterfish, *Nematistius pectoralis* Gill, 1862 (Perciformes: Nematistiidae), in Almejas Bay, Baja California Sur, Mexico. Rev. Biol. Mar. Oceanogr. 44:803–807.

Rosenblatt, R. H. and M. A. Bell.
1976. Osteology and relationships of the roosterfish, *Nematistius pectoralis* Gill. Nat. Hist. Mus. Los Ang. Cty., Contrib. Sci. 279, 23 p.

Sangun, L., E. Akamca, and M. Akar.
2007. Weight–length relationships for 39 fish species from the north-eastern Mediterranean coast of Turkey. Turkish J. Fish. Aquat. Sci. 7:37–40.

Schwenke, K. L., and J. A. Buckel.
2008. Age, growth, and reproduction of dolphinfish (*Coryphaena hippurus*) caught off the coast of North Carolina. Fish. Bull. 106:82–92.

Secor, D. H., J. M. Dean, and E. H. Laban.
1992. Otolith removal and preparation for microstructural examination. *In* Otolith microstructure examination and analysis (D. K. Stevenson and S. E. Campana, eds.), p. 19–57. Can. Spec. Publ. Fish. Aquat. Sci. 117.

Sepulveda, C. A., S. A. Aalbers, and D. Bernal.
2015. Post-release survival and movements patterns of roosterfish (*Nematistius pectoralis*) off the Central American coastline. Lat. Am. J. Aquat. Res. 43:162–175.

Steward, C. A., K. D. DeMaria, and J. M. Shenker.
2009. Using otolith morphometrics to quickly and inexpensively predict age in the gray angelfish (*Pomacanthus arcuatus*). Fish. Res. 99:123–129.

Uchiyama, J. H., R. K. Burch, and S. A. Kraul Jr.
1986. Growth of dolphins, *Coryphaena hippurus* and *C. equiselis*, in Hawaiian waters as determined by daily increments on otoliths. Fish. Bull. 84:186–191.

Zar, J. H.
2010. Biostatistical analysis, 5th ed., 944 p. Prentice Hall, Upper Saddle River, NJ.

Fishery Bulletin

Guidelines for authors

Contributions published in *Fishery Bulletin* describe original research in marine fishery science, fishery engineering and economics, as well as the areas of marine environmental and ecological sciences (including modeling). Preference will be given to manuscripts that examine processes and underlying patterns. Descriptive reports, surveys, and observational papers may occasionally be published but should appeal to an audience outside the locale in which the study was conducted.

Although all contributions are subject to peer review, responsibility for the contents of papers rests upon the authors and not on the editor or publisher. *Submission of an article implies that the article is original and is not being considered for publication elsewhere.*

Plagiarism and double publication are considered serious breaches of publication ethics. To verify the originality of the research in papers and to identify possible previous publication, manuscripts may be screened with plagiarism-detection software.

Manuscripts must be written in English; authors whose native language is not English are strongly advised to have their manuscripts checked by English-speaking colleagues before submission.

Once a paper has been accepted for publication, online publication takes approximately 3 weeks.

There is no cost for publication in *Fishery Bulletin.*

Types of manuscripts accepted by the journal

Articles generally range from 20 to 30 double-spaced typed pages (12-point font) and describe an original contribution to fisheries science, engineering, or economics. Tables and figures are not included in this page count, but the number of figures should not exceed one figure for every four pages of text. Articles contain the following divisions: **abstract, introduction, methods, results, and discussion.**

Short contributions are generally less than 20 double spaced typed pages (12-point font) and, like articles, describe an original contribution to fisheries science. They follow the same format as that for articles: **abstract, introduction, results and discussion, but the results and discussion sections may be combined**. They are distinguished from full articles in that they report a noteworthy new observation or discovery—such as the first report of a new species, a unique finding, condition, or event that expands our knowledge of fisheries science, engineering or economics—and do not require a lengthy discussion.

Companion articles are presented together and published together as a scientific contribution. Both articles address a closely related topic and may be articles that result from a workshop or conference. They must be submitted to the journal at the same time.

Review articles generally range from 40 to 60 double-spaced typed pages (12-point font) and address a timely topic that is relevant to all aspects of fisheries science. They should be forward thinking and address novel views or interpretations of information that encourage new avenues of research. They can be reviews based on the outcome from thematic workshops, or contributions by groups of authors who want to focus on a particular topic, or a contribution by an individual who chooses to review a research theme of broad interest to the fisheries science community. **A review article will include an abstract, but the format of the article *per se* will be up to the authors**. Please contact the Scientific Editor to discuss your ideas regarding a review article before embarking on such a project.

Preparation of manuscript

Title page should include authors' full names, mailing addresses, and the senior author's e-mail address.

Abstract should be limited to 200 words (one-half typed page), state the main scope of the research, and emphasize the authors conclusions and relevant findings. Do not review the methods of the study or list the contents of the paper. Because abstracts are circulated by abstracting agencies, it is important that they represent the research clearly and concisely.

General text must be typed in 12-point Times New Roman font throughout. A brief introduction should convey the broad significance of the paper; the remainder of the paper should be divided into the following sections: Materials and methods, Results, Discussion, and Acknowledgments. Headings within each section must be short, reflect a logical sequence, and follow the rules of subdivision (i.e., there can be no subdivision without at least two subheadings). The entire text should be intelligible to interdisciplinary readers; therefore, all acronyms, abbreviations, and technical terms should be written out in full the first time they are mentioned. Abbreviations should be used sparingly because they are not carried over to indexing databases and slow readability for those readers outside a discipline. They should never be used for the main subject (species, method) of a paper.

For general style, follow the U.S. *Government Printing Office Style Manual* (2008) [available at website] and *Scientific Style and Format: the CSE Manual for Authors, Editors, and Publishers* (2014, 8th ed.) published by the Council of Science Editors. For scientific nomenclature, use the current edition of the American Fisheries Society's *Common and Scientific Names of*

Fishes from the United States, Canada, and Mexico and its companion volumes (*Decapod Crustaceans, Mollusks, Cnidaria and Ctenophora*, and *World Fishes Important to North Americans*). For species not found in the above mentioned AFS publications and for more recent changes in nomenclature, use the Integrated Taxonomic Information System (ITIS) (available at website), or, secondarily, the California Academy of Sciences *Catalog* of *Fishes* (available at website) for species names not included in ITIS. Common (vernacular) names of species should be lowercase. Citations must be given of taxonomic references used for the identification of specimens. For example, "Fishes were identified according to Collette and Klein-MacPhee (2002); sponges were identified according to Stone et al. (2011)."

Dates should be written as follows: 11 November 2000. Measurements should be expressed in metric units, e.g., 58 metric tons (t); if other units of measurement are used, please make this fact explicit to the reader. Use numerals, not words, to express whole and decimal numbers in the general text, tables, and figure captions (except at the beginning of a sentence). For example: We considered 3 hypotheses. We collected 7 samples in this location. Use American spelling. Refrain from using the shorthand slash (/), an ambiguous symbol, in the general text.

Word usage and grammar that may be useful are the following:

- *Aging* For our journal the word *aging* is used to mean both age determination and the aging process (senescence). Authors should make clear which meaning is intended where ambiguity may arise.

- *Fish and fishes* For papers on taxonomy and biodiversity, the plural of *fish* is *fishes,* by convention. In all other instances, the plural is *fish.*

  Examples:
  The fishes of Puget Sound [biodiversity is indicated];
  The number of fish caught that season [no emphasis on biodiversity];
  The fish were caught in trawl nets [no emphasis on biodiversity].
  The same logic applies to the use of the words *crab* and *crabs, squid* and *squids,* etc.

- *Sex* For the meaning of male and female, use the word *sex*, not *gender.*

- *Participles* As adjectives, participles must modify a specific noun or pronoun and make sense with that noun or pronoun.

  Incorrect:
  Using the recruitment model, estimates of age-1 recruitment were determined. [Estimates were not using the recruitment model.]

  Correct:
  Using the recruitment model, we determined age-1 estimates of recruitment. [The participle now modifies the word *we,* i.e., those who were using the model.]

  Incorrect:
  Based on the collected data, we concluded that the mortality rate for these fish had increased. [*We* were not based on the collected data.]

  Correct:
  We concluded on the basis of the collected data that the mortality rate for these fish had increased. [Eliminate the participle and replace it with the adverbial phrase *on the basis of.*]

Equations and mathematical symbols should be set from a standard mathematical program (MathType) and tool (Equation Editor in MS Word). LaTex is acceptable for more advanced computations. For mathematical symbols in the general text (α, χ^2, π, $\pm$, etc.), use the symbols provided by the MS Word program and italicize all variables, except those variables represented by Greek letters. Do not use photo mode when creating these symbols in the general text and do not cut and paste equations and letters or symbols of variables from a different software program.

Number equations (if there are more than 1) for future reference by scientists; place the number within parentheses at the end of the first line of the equation.

Literature cited section comprises published works and those accepted for publication in peer-reviewed journals (in press). Follow the name and year system for citation format in the "Literature cited" section (that is to say, citations should be listed alphabetically by the authors' last names, and then by year if there is more than one citation with the same authorship. A list of abbreviations for citing journal names can be found at website.

Authors are responsible for the accuracy and completeness of all citations. Literature citation format: Author (last name, followed by first-name initials). Year. Title of article. Abbreviated title of the journal in which it was published. Always include number of pages. For a sequence of citations in the general text, list chronologically: (Smith, 1932: Green. 1947; Smith and Jones, 1985).

Acknowledgments should be no more than 6 lines of text. Only those who have contributed in an outstanding way should be acknowledged by name. For recognition of other persons or groups, use a general term, such as "crew," "observers," "research coordinators," and do not include names with these terms.

Digital object identifier (doi) code ensures that a publication has a permanent location online. Doi code should be included at the end of citations of published literature. Authors are responsible for submitting ac-

curate doi codes. Faulty codes will be deleted at the page-proof stage.

Cite all software, special equipment, and chemical solutions used in the study within parentheses in the general text: e.g., SAS, vers. 6.03 (SAS Inst., Inc., Cary, NC).

Footnotes are used for all documents that have not been formally peer reviewed and for observations and personal communications. These types of references should be cited sparingly in manuscripts submitted to the journal.

All reference documents, administrative reports, internal reports, progress reports, project reports, contract reports, personal observations, personal communications, unpublished data, manuscripts in review, and council meeting notes are footnoted in 9 pt font and placed at the bottom of the page on which they are first cited. Footnote format is the same as that for formal literature citations. A link to the online source (e.g., [http://www/..... , accessed July 2007.]), or the mailing address of the agency or department holding the document, should be provided so that readers may obtain a copy of the document.

Tables are often overused in scientific papers; it is seldom necessary to present all the data associated with a study. Tables should not be excessive in size and must be cited in numerical order in the text. Headings should be short but ample enough to allow the table to be intelligible on its own.

All abbreviations and unusual symbols must be explained in the table legend. Other incidental comments may be footnoted with italic numeral footnote markers. Use asterisks only to indicate significance in statistical data. Do not type table legends on a separate page; place them above the table data. *Do not submit tables in photo mode.*

- Notate probability with a capital, italic *P*.
- Provide a zero before all decimal points for values less than one (e.g., 0.07).
- Round all values to 2 decimal points.
- Use a comma in numbers of five digits or more (e.g., 13,000 but 3000).

Figures must be cited in numerical order in the text. Graphics should aid in the comprehension of the text, but they should be limited to presenting patterns rather than raw data. Figures should not exceed one figure for every four pages of text and must be labeled with the number of the figure. Place labels **A, B, C,** etc. within the upper left area of graphs and photos. Avoid placing labels vertically (except for the y axis).

Figure legends should explain all symbols and abbreviations seen in the figure and should be double-spaced on a separate page at the end of the manuscript.

Line art and halftone figures should be submitted as pdf files with >800 dpi and >300 dpi, respectively. Color is allowed in figures to show morphological differences among species (for species identification), to show stain reactions, and to show gradations in temperature contours within maps. Color is discouraged in graphs, and for the few instances where color may be allowed, the use of color will be determined by the Managing Editor. Approved color figures should be submitted as TIFF or JPG files in CMYK format.

- Capitalize the first letter of the first word in all labels within figures.
- Do not use overly large font sizes in maps and for axis labels in graphs.
- Do not use bold fonts or bold lines in figures.
- Do not place outline rules around graphs.
- Place a North arrow and label degrees latitude and longitude (e.g., 170°E) in all maps.
- Use symbols, shadings, or patterns (not clip art) in maps and graphs.

Supplementary materials that are considered essential, but are too large or impractical for inclusion in a paper (e.g., metadata, figures, tables, videos, websites), may be provided at the end of an article. These materials are subject to the editorial standards of the journal. A URL to the supplementary material and a brief explanation for including such material should be sent at the time of initial submission of the paper to the journal.

- **Metadata, figures, and tables** should be submitted in standard digital format (Word docx) and should be cited in the general text as (Suppl. Table, Suppl. Fig., etc.).
- **Websites** should be cited as (Suppl. website) in the general text and be made available with doi code (if possible) at the end of the article.
- **Videos** must not be larger than 30 MB to allow a swift technical response for viewing the video. Authors should consider whether a short video uniquely captures what text alone cannot capture for the understanding of a process or behavior under examination in the article. Supply an online link to the location of the video.

Copyright law does not apply to *Fishery Bulletin,* which falls within the public domain. However, if an author reproduces any part of an article from *Fishery Bulletin,* reference to source is considered correct form (e.g., Source: Fish. Bull. 97:105).

Failure to follow these guidelines and failure to correspond with editors in a timely manner will delay publication of a manuscript.

Submission of manuscript

Submit manuscript online at the ScholarOne website. Commerce Department authors should submit papers under a completed NOAA Form 25-700. For further details on electronic submission, please contact the Associate Editor, Kathryn Dennis, at

kathryn.dennis@noaa.gov

When requested, the text and tables should be submitted in Word format. Figures should be sent as separate PDF files (preferred), TIFF files, or JPG files. Send a copy of figures in the original software if conversion to any of these formats yields a degraded version of the figure.

Questions? If you have questions regarding these guidelines, please contact the Managing Editor, Sharyn Matriotti, at

sharyn.matriotti@noaa.gov

Questions regarding manuscripts under review should be addressed to Kathryn Dennis, Associate Editor.

Fishery Bulletin

Subscription form

Superintendent of Documents **Publications** Order Form

*5178

☐ YES, please send me the following publications:

____ Subscriptions to *Fishery Bulletin*
for $32.00 per year ($44.80 foreign)

The total cost of my order is $ _____ . Prices include regular domestic postage and handling and are subject to change.

_____
(Company or Personal Name) (Please type or print)

_____
(Additional address/attention line)

_____
(Street address)

_____
(City, State, ZIP Code)

_____
(Daytime phone including area code)

_____
(Purchase Order No.)

Charge your order. IT'S EASY!

VISA

MasterCard

Please Choose Method of Payment:

☐ Check payable to the Superintendent of Documents

☐ GPO Deposit Account ☐☐☐☐☐☐☐–☐

☐ VISA or MasterCard Account

☐☐☐☐☐☐☐☐☐☐☐☐☐☐☐☐

☐☐☐☐ (Credit card expiration date)

To fax your orders (202) 512-2104

_____
(Authorizing Signature)

Mail to: Superintendent of Documents
P.O. Box 979050, St. Louis, Missouri 63197
Tel. no. (U.S. callers): 866-512-1800
Tel. no. (International callers): 1-202-512-1800

Thank you for your order!

Also available online at
http://bookstore.gpo.gov/actions/GetPublication.do?stocknumber=703-023-00000-2
email: ContactCenter@gpo.gov